

# UC Berkeley

## UC Berkeley Electronic Theses and Dissertations

### Title

Cranial Morphology, Variation, and Integration in Homo sapiens

### Permalink

<https://escholarship.org/uc/item/8sw0b1kj>

### Author

Reiner, Whitney B

### Publication Date

2017

Peer reviewed|Thesis/dissertation

Cranial Morphology, Variation, and Integration in *Homo sapiens*

By

Whitney Brooke Reiner

A dissertation submitted in partial satisfaction of the

requirements for the degree of

Doctor of Philosophy

in

Integrative Biology

in the

Graduate Division

of the

University of California, Berkeley

Committee in charge:

Professor Leslea J. Hlusko, Chair

Professor Thomas Carlson

Professor Craig Miller

Summer 2017

Cranial Morphology, Variation, and Integration in *Homo sapiens*

Copyright © 2017

by

Whitney Brooke Reiner

## Abstract

### Cranial Morphology, Variation, and Integration in *Homo sapiens*

by

Whitney Brooke Reiner,

Doctor of Philosophy in Integrative Biology

University of California, Berkeley

Professor Leslea Hlusko, Chair

Herein I present three separate manuscripts pertaining to cranial morphology, variation, and integration in humans. The first manuscript introduces a newly recovered partial calvaria, OH 83, from the upper Ndutu Beds of Olduvai Gorge, Tanzania. I present the geological context of its discovery, a comparative analysis of its morphology, and place OH 83 within the context of our current understanding of the origins and evolution of *Homo sapiens*. The morphology of OH 83 was analyzed using quantitative and qualitative data from penecontemporaneous fossils and the W.W. Howells modern human craniometric dataset.

OH 83 is geologically dated to ca. 60–32 ka. Its morphology is indicative of an early modern human, falling at the low end of the range of variation for post-orbital cranial breadth, the high end of the range for bifrontal breadth, and near average in frontal length.

There have been numerous attempts to use cranial anatomy to define the species *Homo sapiens* and identify it in the fossil record. These efforts have not met wide agreement by the scientific community due, in part, to the mosaic patterns of cranial variation represented by the fossils. The variable, mosaic pattern of trait expression in the crania of Middle and Late Pleistocene fossils implies that morphological modernity did not occur at once. However, OH 83 demonstrates that by ca. 60–32 ka modern humans in Africa included individuals that are at the fairly small and gracile range of modern human variation.

In the second manuscript I provide craniometric data from Early Period (ca. 5000 B.P.) hunter-gatherers from the Sacramento Valley and the San Francisco Bay Area that represent some of the earliest indigenous Californians. I compare these data to the published worldwide human craniometric data set to provide perspectives on the range of human variation and the inter-relatedness of that variation.

I collected 76 cranial measurements and five indices from 59 adult crania collected using a three-dimensional (3D) digitizer (MicroScribe G2, Immersion Corporation), following published protocols associated with the comparative data set.

I conducted two sets of analyses exploring the range of variation, and calculating correlations. My analyses reveal that the Early Period Native Californians extends the known range of variation for 20 measurements. For six of the measurements, the smaller end of the range is extended, while the higher end of the range is extended for 14 measurements. For Native Americans, the Early Period Native Californians extend the range for 53 measurements, four of which are extended at both ends of the range. Correlation matrices for these data suggest the face is an integrated region of the cranium across modern humans, but specific patterns of correlation within and between regions of the cranium varied across populations. The early Native Californian crania exhibited the strongest overall correlations, differing significantly from the other samples (Mantel test,  $p < .0001$ ).

Bringing the Early Period Native California morphologies into the published W.W. Howells data set provides an improved appreciation of the range of cranial variation in modern humans. While the message of Howells' assessment that modern human crania vary widely was well-established by Howells, the Early Period data underscore this point. The evidence for integration within the facial skeleton revealed by the correlation matrices observed across all populations corroborates previous research demonstrating that the mammalian facial skeleton is an integrated region that varies fairly independently from the rest of the cranium.

In the third and final manuscript, I explore the influence of sample composition on the patterns of correlation for modern human crania by assessing correlation patterns at the level of the species, geographic regions, and populations, and the variation in sexual dimorphism at each of these levels.

I analyzed patterns of correlation for craniometric traits using the W.W. Howells' worldwide human craniometric data set, and data I collected from 59 adult Early Period Native Californian crania (ca. 5000 B.P.) using a three-dimensional (3D) digitizer (MicroScribe G2, Immersion Corporation) following Howells' definitions to locate all anatomical landmarks and collect all measurements. Using these data, I generated correlation matrices for samples of varying composition to test three hypotheses for cranial integration. I test these hypotheses at the level of the species, then divided by geographic region, and at the population level, and further decompose each of these samples by sex.

I found that patterns of correlation varied the most at the population level. Patterns of correlation did not persist at all levels below the species. Thus, sample composition does influence patterns of correlation, but is inversely proportional to the sample's level of composition, such that variation between samples is greater between populations than it is between geographic regions.

Studies investigating human cranial integration are often interpreted at the species level, even when based on analyses of below-species level data. Because the influence of sample composition on these analyses is not well-known, it is unclear if this broad application of the data is merited. My results demonstrate that patterns of correlation may reveal signals of the underlying mechanisms responsible for generating sexual dimorphism and inter-population variation in cranial morphology as a dataset becomes more specific. These patterns of variation may stem from environmental pressures that could influence cranial shape, and even development via epigenetic interactions. While the use of pooled-sex samples of multiple populations could reduce population-specific noise, by design, it could also temper signals of biologically interesting and informative patterns within and between populations. Furthermore, understanding the way patterns of correlation vary at the level of the population could benefit researchers seeking to combine data from multiple populations into a single sample with the least amount of population-specific environmental pressures or epigenetic interactions that could bias the data. This study represents an initial effort to begin to understand this variation.

I dedicate this dissertation to my family, including the quadrupedal family members, who have been there for throughout my time as a doctoral student, and my advisor, Leslea J. Hlusko.



## Table of Contents

ABSTRACT .....	1
DEDICATION .....	i
TABLE OF CONTENTS .....	ii
ACKNOWLEDGEMENTS .....	vi
<b>CHAPTER 1: Introduction .....</b>	<b>1</b>
<b>CHAPTER 2: OH 83: A new early modern human fossil cranium from the Ndotu Beds of Olduvai Gorge, Tanzania .....</b>	<b>6</b>
2.1 INTRODUCTION .....	7
2.2 GEOLOGICAL AND GEOCHRONOLOGICAL CONTEXT OF OH 83 .....	8
2.3 ANATOMICAL DESCRIPTION .....	9
2.4 MATERIALS AND METHODS .....	10
2.4.1 <i>Comparative samples</i> .....	10
2.4.2 <i>Craniometric measurements</i> .....	11
2.4.2.A <i>Three-dimensional laser scanning</i> .....	11
2.4.2.B <i>Data collection</i> .....	11
2.4.2.C <i>Data validation</i> .....	12
2.4.2.D <i>Quantitative comparisons</i> .....	12
2.5 RESULTS .....	13
2.5.1 <i>Morphological trait comparison</i> .....	13
2.5.2 <i>Craniometric comparison</i> .....	13
2.6 DISCUSSION AND CONCLUSIONS .....	14
2.7 ACKNOWLEDGEMENTS .....	16
2.8 REFERENCES .....	17
FIGURES .....	24
<i>Figure 1</i> .....	24
<i>Figure 2</i> .....	25
<i>Figure 3</i> .....	25
<i>Figure 4</i> .....	26
<i>Figure 5</i> .....	27
TABLES .....	29
<i>Table 1</i> .....	29
<i>Table 2</i> .....	30
<i>Table 3</i> .....	31
<b>CHAPTER 3: Cranial variation in Early Period Native Californians: A new perspective on the W.W. Howells Craniometric Dataset .....</b>	<b>32</b>
3.1 INTRODUCTION .....	33
3.2 HYPOTHESES .....	36
3.2.1 <i>First set of hypotheses (<math>H_{1A-B}</math>)</i> .....	36
3.2.2 <i>Second set of hypotheses (<math>H_{2A-B}</math>)</i> .....	36
3.2.3 <i>Third set of hypotheses (<math>H_{3A-C}</math>)</i> .....	37
3.3 MATERIALS AND METHODS .....	38

3.3.1 Materials .....	38
3.3.1.A Native Californian data set .....	38
3.3.1.A.i Inclusion criteria .....	38
3.3.1.A.ii Age and sex estimation .....	38
3.3.1.B Comparative data .....	39
3.3.1.B.i Native American subset and hunter gatherer subset of Howells' data .....	39
3.3.2 Methods .....	39
3.3.2.A Linear measurements .....	39
3.3.2.B Data collection .....	40
3.3.2.C Analyses .....	41
3.3.2.C.i Univariate analyses for first set of hypotheses .....	41
3.3.2.C.ii Correlations .....	41
3.4 RESULTS.....	42
3.4.1 Range of variation ( $H_{1A-B}$ ) .....	43
3.4.1.A Range of Variation compared to Howells' Native Americans .....	43
3.4.2 Patterns of correlation .....	44
3.4.2.A Correlation patterns of Early Period Native Californian crania .....	44
3.4.2.B Patterns of correlation for the Howells data .....	46
3.4.2.B.i Howells' complete data set .....	46
3.4.2.B.ii Native American and hunter gatherer subsets of Howells' data ...	47
3.4.2.B.iii Second set of hypotheses ( $H_{2A-B}$ ).....	47
3.4.2.B.iv Third set of hypotheses ( $H_{3A-C}$ ).....	47
3.5 DISCUSSION AND CONCLUSIONS.....	48
3.5.1 Range of variation for measurements .....	48
3.5.2 Patterns of correlation .....	49
3.6 ACKNOWLEDGEMENTS.....	51
3.7 REFERENCES.....	52
FIGURES .....	57
Figure 1 .....	57
Figure 2 .....	58
Figure 3a–b .....	59
Figure 4 .....	61
Figure 5 .....	62
TABLES .....	63
Table 1 .....	63
Table 2 .....	64
Table 3 .....	65
Table 4 .....	66

**CHAPTER 4: Cranial variation in Early Period Native Californians: A new perspective on the W.W. Howells Craniometric Dataset ..... 77**

4.1 INTRODUCTION .....	78
4.2 HYPOTHESES .....	80

4.2.1 Hypothesis 1.....	80
4.2.2 Hypotheses 2 and 3 .....	81
4.2.2.A Hypothesis 2 .....	81
4.2.2.B Hypothesis 3 .....	81
4.3 MATERIALS AND METHODS .....	82
4.3.1 Craniometric data .....	82
4.3.1.A Howells data set.....	82
4.3.1.B Early Period Native Californian data set.....	82
4.3.1.B.i Inclusion criteria .....	83
4.3.1.B.ii Age and sex estimation .....	83
4.3.1.B.iii Linear measurements .....	83
4.3.1.B.iv Data collection .....	83
4.3.2. Analyses .....	84
4.3.2.A Correlations .....	84
4.3.2.B Hypothesis 1 methods .....	85
4.3.2.C Hypothesis 2 methods .....	86
4.3.2.D Hypothesis 3 methods .....	86
4.4 RESULTS.....	86
4.4.1 Hypothesis 1 .....	86
4.4.2 Hypothesis 2 .....	88
4.4.3 Hypothesis 3 .....	88
4.4.4 Sexual dimorphism .....	90
4.5 DISCUSSION AND CONCLUSIONS.....	90
4.6 ACKNOWLEDGEMENTS.....	93
4.7 REFERENCES.....	94
FIGURES .....	97
Figure 1 .....	97
Figure 2 .....	98
Figure 3 .....	101
Figure 4 .....	110
TABLES .....	119
Table 1 .....	119
Table 2 .....	120
Table 3 .....	125
<b>CHAPTER 5: Discussion and conclusions .....</b>	<b>126</b>
5.1 DISCUSSION AND CONCLUSIONS .....	127
5.2 REFERENCES CITED WITHIN CHAPTERS 1 AND 5 .....	132
<b>APPENDICES .....</b>	<b>135</b>
APPENDIX 1 .....	135
APPENDIX 2 .....	136
APPENDIX 3 .....	137
APPENDIX 4 .....	151
APPENDIX 5 .....	152

<b>SUPPLEMENTARY TABLES</b> .....	<b>154</b>
SUPPLEMENTARY TABLE 1 .....	154
SUPPLEMENTARY TABLE 2 .....	155

## Acknowledgements:

I thank the members of my dissertation committee for the support they have provided throughout the dissertation process, for the encouragement they have given me, and for the confidence in me that they have had throughout the various stages of this work, some of which were more challenging than others. It was during these most challenging times that their confidence in me, their continued interest in my progress, and their words of encouragement, made the most significant impact on my success and which I am most grateful for. It is impossible to fully express my gratitude for my advisor and dissertation committee chair Leslea Hlusko, who has been supportive, encouraging, and enthusiastic from day-one of my graduate studies at UC Berkeley. The things she has taught me reach far beyond the walls of Berkeley – from the outcrops of Olduvai Gorge, to the museums of Dar es Salaam and London – she has provided me with invaluable experiences, advice, and support. Throughout all these experiences, her continued confidence in my abilities and potential have also been invaluable to me, as have the opportunities and resources she has made available to me. Most of all, I am grateful for the confidence she has inspired and taught me to have in myself, which I will take with me as I proceed onward and begin the next chapter of my life. I am also grateful for her ability to communicate to me that she has been proud of my achievements every step of the way as I finalized my dissertation and completed my doctoral degree. I am so fortunate to have had such a wonderful advisor, mentor, and teacher through her and I am extremely fortunate to be part of her “academic family”. I hope to be able to show the enthusiasm and passion she has for teaching and research in the next academic or professional challenge I take on. Tom Carlson and Craig Miller generously provided their time and energy to read my thesis and to provide suggestions to help me improve it immensely. To my entire committee, I thank you so much for your efforts and patience along the way and will be forever grateful.

I must also thank Sabrina Sholts and Tim White, who also fulfilled advisory-type roles during my graduate career at Berkeley, providing me with invaluable advice and support on the research and writing processes of this dissertation, and throughout the trials and tribulations of graduate school, all of which I am very grateful for.

I am very grateful for the help of Korshid Tarin, who helped me navigate the final few years of this program as I sought funding and filed this dissertation. I also thank Mei Griebenow for her help in the first few semesters of this program.

I would also like to thank Lucy Chang, Helen Kurkijian, and Jennifer Hoffmeister for their advice and assistance on statistical analyses and graphics processing, along with all those who taught and organized the 2017 Integrative Biology workshop in R.

My graduate experience was also enhanced by the members of my cohort and by Theresa Grieco, who provided me with advice and encouragement not only while she was part of the Hlusko lab, but also following her graduation. I also thank the members

of the Human Evolution Research center, and Joshua Carlson for his kindness and support, and the members of the Hlusko lab for their feedback along the way. I am very grateful for the support of my close friends in the Department of Integrative Biology, especially Phillip Skipwith, Ashley Poust, Lucy Chang, Melinda Yang, Jenna Judge, Sarah Hykin, as well as many other friends and colleagues from the department who I have been honored to have as my fellow graduate students and share these past six years with.

Outside of Berkeley, I thank my close friends for their support and continued interest in my progress: Mia Marek, Stevie Jablonski, Audra Johnson, JD Delgado, Caroline Brady, Andie and Lucy Vas, Quinn-Monique Ogden, Claudia Astorino, Allison Sharplin, Christopher Rainwater, Shannon Lavelle, and Christopher Schmitt.

I also must thank my family; Dad, Mom, and Wade: I am so grateful for your support and for your messages of encouragement and perseverance, and for always being there for me. And to Patricia and Stephen Reiner, you have always put so much confidence in my abilities and shown so much interest in my success, I am so grateful to have your support.

Last and certainly not least, I thank my girlfriend Jess Reed, for being such a wonderful and supportive partner. Jess has helped me in innumerable ways and has applied her professional expertise in production to help me organize my thoughts and goals, and to communicate science on a more “human” level. She has helped me proofread and outline my ideas when I was most challenged or felt overwhelmed, has provided constructive critiques and suggestions for optimal data visualization, and has been so generous with her time, even letting me practice presenting my research at 10 PM in VLSB on a Sunday night. She has helped to keep me motivated, and her dedication and the self-discipline she has for her own work been inspiring to me. I am so fortunate. Thank you for keeping me motivated and making it all worth it.

## **Chapter 1**

### **Introduction**

## Introduction:

That there is no *Homo sapiens* holotype (Tattersall and Schwartz 2008), or formal definition for the species, is perhaps to some, ironic, but to the anthropologist not in the least, especially to one who is well-versed in human skeletal variation. Phenotypic traits of the human cranium are morphologically heterogeneous and cover a wide range of variation (Howells 1973, 1989, 1995). It is this characteristic of human cranial morphology that both facilitates and inhibits our understanding of the species. Biological anthropologists including forensic anthropologists, bioarcheologists, and paleoanthropologists use what is known about the sources of human cranial variation – sex, ontogeny, ancestry, and idiosyncrasies – and what is known about the way variation is patterned by these sources to estimate sex and ancestry of human remains. In paleoanthropology, cranial morphological variation is of primary importance in the assessment and taxonomic placement of hominid fossils and phylogenetics. However, there is much that remains to be understood about the patterns by which human crania vary and the etiologies of these patterns.

Cranial anatomy is integral to the characterization of morphology among fossil hominids (Day and Stringer, 1982; Stringer et al. 1984; Tattersall and Schwartz 2008). Although the known patterns by which human crania vary are exploited to glean information about skeletal remains, what we know and what we do not yet understand about these patterns have both led to disagreement over the cranial traits that define modern *Homo sapiens*. Disagreement over the defining cranial traits of modern *Homo sapiens* is due in part to the mosaic patterns of variation observed in the fossil record (Bräuer and Leakey 1986; Lieberman et al. 2002; Pearson 2008), and in (an arguably larger) part, a result of the morphological heterogeneity present in Holocene modern humans (Howells, 1973; 1989; Lahr, 1996; Haile-Selassie et al., 2004). One way to improve our understanding of the etiologies driving human cranial morphologies and patterns of morphological variation is to learn more about the evolutionary forces unique to populations that potentially play a role, by studying patterns of variation between and within populations throughout human evolutionary history.

The objective of my dissertation research is to study human cranial variation throughout the history of the species, and to analyze this variation with the goal of adding to what is known about the intraspecific patterns of human cranial variation. I present three studies which altogether represent three major moments in the evolutionary history of *Homo sapiens*, one spanning the time around which modern humans originated ca. 250 ky through the Late Pleistocene (ca 60–32 ky), one focusing on prehistoric hunter gatherers living ca. 5000 BP, and finally, one concentrated primarily on humans living within the later parts of the Holocene to around the present day.

In the first chapter I present an initial description of OH 83, an early modern human fossil calvaria from Olduvai Gorge, Tanzania, a fossil site that documents the last two million years of hominid evolution. I use traditional methods of morphological trait description to describe and analyze the cranial morphology of this specimen and geochronological assessments of the excavation site to place the specimen within a geological context and estimate its age. In addition, I place OH 83 within an

evolutionary context using qualitative morphological and quantitative craniometric comparisons to other spatiotemporally relevant fossils and the range of cranial variation found in extant modern humans, using the W.W. Howells worldwide craniometric data set (Howells 1973, 1989, 1995).

My analyses of OH 83 underscore that there is wide range of variation among human crania. However, throughout the process of studying OH 83, I observed gaps in the scientific knowledge on the range of human cranial variation and the way this variation is patterned, both of which inhibit interpretations of the fossil record. I also found that a lack of appreciation for the wide range of human cranial variation was common in the scientific literature. Chapter three was inspired by these observations.

In the third chapter, I delve deeper into the study of human cranial variation in an attempt to begin to fill the gaps in the scientific knowledge base of the range of human cranial variation. There are three main scientific contributions I aim to make in this study. First, I present craniometric data for prehistoric Native Californian hunter gatherers dated to the Early Period, ca. 5000 BP, to document the cranial morphology and variation of these individuals. Second, I compare the range of variation for this data set with the range of human cranial variation assessed by Howells (1963, 1989, 1995) using the range for linear measurements and cranial indices, as well as the variation in the relationships between craniometric traits, which I analyze using correlation matrices. There is a relatively wide range of variation among Native Americans (González-José et al. 2001), and the Early Period Native Californian crania are generally quite robust. The third main scientific contribution I anticipate is from my focus on the range of variation among Native Americans, by providing data that essentially quantifies the robusticity of Native Americans ca. 5000 BP along with expands the spatio-temporal range of quantitative data on the range of variation among Native Americans. I compare the range of variation among Howells Native Americans to the range observed when I add my Early Period Native Californian data. Because it is unclear if the robusticity observed among Early Period Native Californian skeletal remains is related to ancestry, functional requirements of a hunter-gather subsistence strategy and a reliance on tough food items, and/or systemic effects, I assess phenotypic variation of the correlations between traits of the Early Period Native Californians comparatively to populations with shared ancestry, represented by the Howells Native American data, and to populations with similar subsistence strategies, using a different subset of the Howells data composed of hunter gatherer populations. Finally, I compare the correlation matrices for these four samples (Early Period Native Californians, Howells complete data, Howells' Native Americans, Howells' hunter gatherers) to analyze patterns of correlation that may signal morphological integration and modularity.

Studies on human crania provide evidence for the influence of genetic effects on the cranial vault (Susanne, 1977; Sherwood et al., 2008; 2011; Sherwood and Duren, 2013; Šešel et al., 2015), but when it comes to the genetic architecture underlying the development of cranial traits and the underlying mechanisms driving variation in cranial anatomy, relatively little is known. The fourth chapter represents an attempt to contribute to the scientific understanding of the mechanisms driving cranial variation, and to reconcile the variation I observed among correlation matrices in the third

chapter. In this study, I further explore correlations between phenotypic traits of the human cranium to investigate how population level variation in the relationships between traits could influence interpretations of evidence for morphological integration. I fulfill this objective by analyzing the influence of sample composition on patterns of correlation.

Principles of integration and modularity are often tested and/or interpreted at the species level. However, the sample composition may not merit such a wide application of the data, when sample composition is actually below the species level. The data are often assessed in a vacuum without regard to how the patterns may deviate from the average patterns for the species, and from other groups within the species, or are even interpreted as representative of the species (e.g., Martinez-Abadias et al. 2009 and Ackermann 2005). Ackermann (2005) used a sample from sub-Saharan Africa to represent the range of modern human variation, although the author noted that the sample does not strictly represent diversity of humans across the globe, she also stated that because of the high levels of genetic variation demonstrated for this region (Lewontin 1972, Barbujani et al. 1997), most of the cranial variation among humans is likely represented by the sub-Saharan African sample used in the study (Ackermann 2005). However, this assumption implies that genetic variation directly mirrors cranial variation and that cranial morphological variation is driven purely by genetics. The relationship between cranial variation and genetic variation is likely much less direct. Studies that do comparatively assess patterns of correlation below the species level are often restricted to testing functional or adaptive hypotheses, regarding mechanisms that directly physically interact with the environment, like the masticatory region of the skull (e.g., González-Jose et al. 2005).

Morphological integration is defined as a set of features that are developmentally, structurally, or functionally inter-related (Olson & Miller 1958) and is a concept that continues to be useful as we work towards a better understanding of the relationship between genotype and phenotype (Pigliucci & Preston 2004). There is evidence for strong integration in the human skull (Martinez-Abadias et al. 2009). But with the wide range of variation among human crania (Howells 1973, 1995), and the large, nearly world-wide geographic distribution of humans, it would be expected that factors unique to populations influence biological differences in the levels of integration among different populations. As such, understanding the effects of sample composition on patterns of correlation is necessary to establish the potential differential influences on population-level variation. Shedding light on the influence of different evolutionary pressures on cranial integration at the population level could ultimately advance our understanding of cranial integration and modularity across humans. Doing so may have eventual applications to human biology in general, in the ways by which known environmental pressures unique to a population can be tied to patterns of correlation that deviate from other populations or the species-wide average.

To investigate sample composition's influence on patterns of correlation, I examine patterns of correlation at increasingly decomposed intraspecific levels, and assess how these patterns vary between samples at the regional and population level. In addition, I explore the variation in sexually-dimorphic patterns of correlation at each of these levels. As the dataset becomes more specific, the patterns of correlation could

be signaling underlying mechanisms responsible for intersex and interpopulation variation in cranial morphology.

In chapter four, I analyze variation using three hypotheses of morphological integration. The first hypothesis is based on theoretical levels at which morphological integration is expected to act, which ranges from the most basic, cellular level, through the interspecific level (Strait 2001). I compare correlation matrices comprising large sets of phenotypic traits. Testing hypotheses focused on small sets of traits is a useful method to effectively model variation. Hypotheses two and three use smaller sets of traits to test a traditional hypothesis for human cranial integration (Enlow and Hans 1996) and a developmental hypothesis for integration across mammalian crania (Hallgrímsson et al. 2007). Overall, this last study (Chapter 4) applies some of the observations from the third chapter, but tests them within a broader context.

Chapters three and four present research that is relevant to the first chapter. Patterns of correlation in modern human crania are often used as extant reference samples. Extant analogs can be used to approximate patterns of covariation for close relatives (Ackermann 2002). In studies on morphological integration of fossil crania extant analogs are often used as a method to reduce biases that can be introduced by small sample sizes, that are not atypical of the hominid fossil record. While researchers have noted the importance of exercising caution in choosing extant reference samples, there is little that is known about the biological factors unique to populations that can potentially influence correlations and could introduce their own sources of bias to these studies. This dissertation research enhances our understanding of variation among modern humans and within the hominid fossil record.

## Chapter 2

### **OH 83: A new early modern human fossil cranium from the Ndotu Beds of Olduvai Gorge, Tanzania**

The following chapter is in-press as an article in the American Journal of Physical Anthropology.

Whitney B. Reiner<sup>1</sup>

Fidelis Masao<sup>2,3</sup>, Sabrina B. Sholts<sup>4</sup>, Agustino Venance Songita<sup>3</sup>, Ian Stanistreet<sup>5,6</sup>, Harald Stollhofen<sup>7</sup>, R.E. Taylor<sup>8</sup>, Leslea J. Hlusko<sup>1</sup>

<sup>1</sup>Department of Integrative Biology, University of California Berkeley, Berkeley, CA 94720

<sup>2</sup>University of Dar es Salaam, Dar es Salaam, 35091 TZ

<sup>3</sup>Conservation Olduvai Project, Dar es Salaam, 35091 TZ

<sup>4</sup>Department of Anthropology, National Museum of Natural History, Smithsonian Institution, Washington, DC 20560

<sup>5</sup>University of Liverpool, Liverpool L69 3GP UK

<sup>6</sup>The Stone Age Institute, Bloomington, Indiana 47407

<sup>7</sup>GeoZentrum Nordbayern, Universität Erlangen-Nürnberg, Schlossgarten 5, 91054 Erlangen, Germany

<sup>8</sup>University of California Riverside, Riverside, CA 92521

## 2.1 Introduction:

Hominid crania from the Middle and Late Pleistocene are characterized by a mosaic of primitive traits shared with *Homo erectus* combined with derived morphologies of anatomically modern *Homo sapiens*, with a general shift from the earlier species to the later (Reed and Tishkoff, 2006; Bruner, 2007; Rightmire, 2008, 2009). The general pattern of changes that mark the evolution of anatomically modern cranial morphologies from *H. erectus* include overall reductions in the size and robusticity of the cranial superstructures (crests and tori) (Rightmire, 2008), as well as increased parietal expansion and globularity of the brain case, frontal bone expansion in both the dimensions of breadth and along the sagittal plane, and retraction and size reduction of the facial skeleton (Lieberman, 1998; Rightmire, 2008). The specific combination of these derived and ancestral traits observed on different specimens is variable (Crevecoeur et al., 2009), revealing a mosaic pattern in the mode and tempo of human evolution. The morphological heterogeneity among present-day modern humans further complicates this matter (Haile-Selassie et al. 2004).

Fossil, archaeological, and genetic evidence indicate an African origin for anatomically modern *H. sapiens* (AMHS) around 200 ka, followed by a range expansion beyond Africa between 190–70 ka (Day and Stringer, 1982; Cann et al., 1987; Kocher and Wilson, 1991; Stoneking et al., 1993; McDermott et al. 1996; Tishkoff et al., 1996; Relethford and Jorde, 1999; McBrearty and Brooks, 2000; Cann, 2001; Relethford, 2001; Stringer, 2002; Clark et al., 2003; Henshilwood and Marean, 2003; White et al., 2003; Haile-Selassie et al., 2004; Trinkaus, 2005; Llorente et al., 2015). Skeletal remains from the Middle Pleistocene (ca. 780–120 ka, Cohen et al., 2013) have been differentiated at the subspecies level (*Homo sapiens idaltu*) on the basis of robust craniofacial morphology and a number of cranial vault dimensions exceeding the modern human range of variation in length (White et al., 2003). Newly discovered fossil crania from the Late Pleistocene (ca. 120–11 ka (Cohen et al., 2013)) of Africa increase the morphological information for the time period following *H. s. idaltu*, thereby improving our understanding of intra- and interspecific variation for *Homo* and the origins and early diversification of our species (White et al., 2003; Haile-Selassie et al., 2004; Crevecoeur et al., 2009; Stojanowski, 2014; Tryon et al., 2015).

With this in mind, we announce the discovery of a fossil calvaria recovered from Olduvai Gorge, Tanzania (Figure 1). Here, we present the initial description and metric data for OH 83, along with a morphological description of the fossil and preliminary analyses.

In 2009, as part of the Conservation Olduvai Project (COP) directed by F.M., A.V.S. found a few small fragments of a hominid fossil eroding from Ndotu Beds on the northern side of Olduvai Gorge. The University of Dar es Salaam's archaeology field school and COP ran a controlled excavation under the direction of F.M. during which additional, larger fragments (see Figure 2) were recovered *in situ* 110–280 cm below the surface. The larger pieces of the partial crania, and the majority of the smaller fragments were recovered through excavation. We associated the few surficial fragments with those recovered through excavation because there is no clear evidence

that they are not from the same individual (i.e., there are no duplicated identifiable elements and size and preservation are in accord). Hereafter designated “OH 83”, the specimen and associated fragments are housed in the Natural History Museum (NHM) in Arusha, Tanzania.

## 2.2 Geological and geochronological context of OH 83:

The sediments naturally exposed at Olduvai Gorge are approximately 100 m thick and divided into seven beds, numbered sequentially from oldest to youngest, with the base of Bed I dated to ~ 2 mya and the uppermost part of Bed IV dated to ~600,000 ka (Hay, 1976) (Figure 3). The stratigraphic units younger than Bed IV (the Masek, Ndotu and Naisiusiu Beds) have been the subject of considerably less geological research than the lower stratigraphic units (Beds I–IV) (Skinner et al., 2003). OH 83 was discovered eroding from sediments of the Ndotu Beds, near archeological locality PLK (Hay, 1976) and geological locality 23 (Hay, 1976), situated on the downthrown side of FLK Fault between the Fourth and Fifth Faults on the north side of the main gorge (Figure 3). Based on our field observations, the sediments at locality 23 compare best to the massive “eolian tuff” facies (Hay, 1976) of the upper unit of the Ndotu Beds.

Although multiple attempts to date the Ndotu Beds have been made with varying success (Hay, 1976) (see references in Millard, 2008, and also Leakey et al., 1972; Bada and Protsch, 1973; Macintyre et al., 1974; Bada, 1981), altogether the results suggest that the upper unit represents the period from about 60–32 ka and the lower unit spans from about 400–60 ka (Hay, 1976). While these age estimations for the Ndotu Beds are still debated to some extent, in part because distinguishing between sediments of the upper and lower units of Ndotu Beds exposures can be especially difficult along the rim of the gorge, Hay’s age estimates for the upper and lower units of the Ndotu Beds are provisionally accepted (Hay, 1976; Manega, 1993; Skinner et al., 2003; Eren et al., 2014). Recent archaeological survey of the upper unit of the Ndotu Beds has confirmed the presence of lithic technology from the Middle Stone Age (MSA) (Eren et al., 2014), which indicates an absolute lower age boundary of ~200 ka that is far below the older date for the upper Ndotu.

Radiocarbon ( $^{14}\text{C}$ ) dating was attempted on an equid molar discovered in the excavation of OH 83. Attempts to isolate >30 kDa molecular weight organics were made on tooth material taken from three different points on the molar. Unfortunately, all organic constituents of the molar were degraded beyond use for this method. It is unclear whether the degradation is a factor of age, depositional setting, or a combination of both, due to the complex manner by which environmentally related biogeochemical processes are compounded. It is possible that the lack of organic matter is exclusively a result of the molar’s age having surpassed the limits of the  $^{14}\text{C}$  dating method, as accurate  $^{14}\text{C}$  age determinations are difficult to obtain on materials older than 30 ka (Wood, 2015) and the maximum effective measurement limit is around 40 ka (Taylor and Bar-Josef, 2014). However, this does not rule out that these

sediments represent the upper unit of the Ndutu Beds, since this unit extends to 60 ka (Hay, 1976).

While the age of OH 83 remains to be more definitively determined, we place OH 83 within the age range of the upper unit of the Ndutu Beds, between 60 and 32 ka based on the available evidence. OH 83 is now the fourth hominid cranial fossil discovered in the uppermost beds of Olduvai Gorge, following three previously described specimens (OH 11 (Rightmire, 1980); OH 23 (Leakey, 1971); OH 1968 (Von Zieten, 2009)).

### 2.3 Anatomical description:

OH 83 is composed mainly of the frontal and left parietal bones; neither the facial skeleton nor the basicranium is preserved (Figure 1). The right half of the neurocranium is almost entirely absent. As the occiput is not preserved, maximum cranial length cannot be measured, but the maximum length of the preserved cranial vault is 179.8 mm. Similarly, OH 83's preservation precludes the measurement of maximum cranial breadth, but the maximum width of preserved left half of the cranial vault is 57.4 mm.

The OH 83 frontal preserves the glabellar region, the superior half of the orbital region, and the majority of the squamous portion. The orbital region is broken superior to the level of nasion so that only about one-third of the superior-most portion of the orbit is preserved. The width of the preserved frontal between the medial-most extent of the orbital rims is 26.5 mm. The right side of the frontal squama is preserved near bregma at its superior-most extent, and it extends inferolaterally towards the level of supraglabella to the partially preserved right orbit. The left half of the frontal squama is present and complete. The supraorbital region's supraciliary arches are moderately pronounced and medially divided by a bilaterally arched glabella that is somewhat prominent, but only projects minimally beyond the superomedial corners of the orbits. The medial and lateral segments of the brow ridges are clearly differentiated from one another. In addition to its vertically oriented frontal squama at the region of the forehead, the supraorbital morphology of OH 83 is characteristic of the derived condition within recent *Homo* that is seen in AMHS (Rightmire, 1996).

For the right parietal, OH 83 preserves only a small fragment that articulates with the left parietal along the sagittal plane near the vertex. Although nearly complete, the left parietal around the midline is not preserved in the posterior region, but the inferolateral portion that would have articulated with the left posterior half of the occipital bone is present. The lateral side of the left parietal is broken inferior to the temporal line. The border of the break follows the squamous suture that would have been present during life, and a small portion of the left temporal bone preserving the supramastoid crest is preserved.

Most of OH 83's surface anatomy is not well preserved, most likely due to post-depositional processes leading to compaction, or erosion by windblown sands (Stojanowski, 2013). Two meningeal grooves are visible on the endocranial vault surface of the left parietal. On the ectocranial surface, parietal striae are visible on the

inferolateral extension of the left parietal and the superior temporal line is clearly demarcated. Enough of the coronal suture is preserved to allow for the estimation of bregma at the midline, but unlike the frontal, the left parietal is only preserved lateral to the midsagittal plane. As a result, the sagittal suture is not preserved. However, OH 83 appears to preserve a metopic suture remnant, a feature only seen in 1–10% of adult modern humans worldwide (Byers, 2005).

The OH 83 partial calvarium bears clear indications of post-mortem distortion. On the left lateral side of the calvarium a posterior portion of parietal overhangs the vault (see arrow in Figure 1), which is an obvious artifact of preservational distortion that does not reflect the biology of the individual during life. White (2003) provides a cautionary tale that demonstrates post-mortem distortion in hominid fossils should be carefully considered. We interpret distortion in OH 83 as primarily affecting the cranial breadth dimension, but cannot rule out possible effects on other dimensions, such as the relatively long anteroposterior dimension of the preserved cranial vault in comparison to breadth.

OH 83 represents a mature adult, on the basis of overall cranial size and closure of the preserved coronal suture. The preservational state of OH 83 prohibits a confident estimation of sex for this individual. However, its small overall vault size and gracility of the preserved superstructures may indicate that it is female.

Although limited in number due to poor preservation, OH 83's traits are morphologically characteristic of AMHS. The frontal bone of OH 83 is characterized by a weakly developed torus with clear differentiation of its medial and lateral aspects, the frontal squama is high and vertically oriented, and bossed, and its weak glabellar prominence and broad upper face are all modern and expressed within the range of variation seen in living people. The cranial vault of OH 83 is modern in its long, generally globular form and overall morphology, aligning it with anatomically modern humans.

## 2.4 Materials and methods:

### 2.4.1 Comparative samples:

The fossil sample used for comparative analyses are crania from the Middle Pleistocene to the Early Holocene in Africa and the Levant, a spatio-temporal context that subsumes OH 83 (Table 1). Measurements for the fossils were taken from published literature, and when available, compared to physical measurements we collected from research quality casts at the Human Evolution Research Center at the University of California, Berkeley (Table 2).

The modern human samples used for comparative analyses are the archaeological and historic populations represented in the Howells craniometric dataset (1973; 1989; <http://web.utk.edu/~auerbach/HOWL.htm>). This dataset compiles cranial measurements of over 2500 adult individuals from 28 Late Holocene populations worldwide. For our comparative analyses, we parsed the total dataset into groups according to geographic region: Americas, Asia, Australasia, Europe, North

Africa, Polynesia, and Sub-Saharan Africa (Table 3).

Sexual dimorphism almost certainly contributes to the range of variation in the comparative fossil sample. While sex may be estimated for some of the more complete fossils, it would be untenable to estimate sex for others and risk increasing potential error in the comparative analyses. Consequently, although the Howells dataset includes sex estimations for all individuals, the males and females were combined as a pooled sex sample of modern humans to mirror the fossil sample.

#### 2.4.2 Cranial measurements:

Twenty-seven cranial fragments and three teeth were found in association with the main calvarial pieces of OH 83. While the main calvarial pieces and associated cranial fragments are similar in preservational state, they do not conjoin (Figures 1 and 2). We focus our analysis here on the larger elements of the OH 83 calvaria.

##### 2.4.2.A Three-dimensional laser scanning:

Given OH 83's fragile state of preservation, we used a three-dimensional (3D) laser scanner to facilitate measurement (Kuzminsky and Gardiner, 2012). We created a digital 3D model of OH 83 using a NextEngine Desktop 3D laser scanner (NextEngine Inc., Santa Monica, CA) at the National Museum of Natural History, Arusha, Tanzania. The NextEngine scanner uses lasers and a camera to capture surface geometry and full-color photo data from the scanned object, which is then rendered and measurable as a digital 3D model. The scanner was set to the standard capture settings for larger objects, e.g., a human cranium (Sholts et al., 2010), with a geometric point resolution of 75 dots per inch (DPI) and 150 DPI color. The fossil was scanned multiple times at different angles. Following scanning, we manually aligned the images via common points and removed overlapping meshes using ScanStudio PRO 1.6.3 software (NextEngine Inc. 2006–2008), and following data processing, the completed 3D model (Figure 4) was imported into RapidWorks 2.3.2 software (Rapidform, Sunnyvale, CA, 2006). Using digital tools to create geometric points and measure distances on 3D models, we placed points at craniometric landmarks and recorded the linear distances between them. To facilitate accurate point placement, high-resolution photographs of the specimen were used to identify sutures and topographic anatomy when they were not easily discernible, which is especially common in 3D laser scanned models of crania exhibiting deterioration or discoloration (Sholts et al., 2011).

##### 2.4.2.B Data collection:

We collected seven linear distance measurements from six craniometric landmarks preserved on OH 83 (Table 4). For each distance, one of us (W.B.R.) collected at least three repeated measurements based on iterations of point placement. Intraobserver error ranged between 0.5–4.9%. Due to the lack of preservation of the right side of the cranial vault, we relied on the bilateral symmetry of

the skull for all breadth measurements requiring paired osteometric points. These measurements (BFM, FMB, STB, XFB, WFB) were calculated by measuring the distance from the preserved (left) paired craniometric point to the mid-sagittal plane, and doubling the result. The mid-sagittal plane was identified in the 3D model as corresponding with the midline of the metopic suture remnant. The frontal (nasion-bregma) chord was measured, although the location of nasion was estimated at the most inferior midline point on the frontal bone; however small, there is potential for error introduced by this estimation. Opisthocranium could not be estimated without significant potential error. In consequence, glabello-occipital length (GOL) was not included in the comparative analyses, but the anteroposterior length of the preserved remains was included in the morphological description. Eurion could not be located on the lateral portion of the parietal or the squama of the temporal bone, due to the poor preservation of OH 83, preventing a confident estimation of maximum cranial breadth (XCB). For this reason, XCB is also omitted from the comparative analyses. Instead, the maximum width of the left half of the cranial vault, measured from the lateral-most preserved part of the left side of the vault to the midline was included in the morphological description.

#### 2.4.2.C Data validation:

As the comparative datasets for the fossil and modern human samples are composed of direct measurements on the physical specimens with calipers rather than indirect measurements on digital 3D models, we performed a validation study to assess potential measurement error in the comparative analyses. Eleven modern human crania from the Phoebe A. Hearst Museum of Anthropology (PAHMA) were selected on the basis of preservation and measured by W.B.R. with calipers following Howells (1973) protocols and with digital 3D methods as outlined for OH 83 above (Supplementary Table 1). Evaluations of measurement error comparing direct anthropometry and indirect measurement of digital models produced by laser scanning and other 3D surface capture systems have indicated that 3D systems-based measurements are accurate and reliable for research and clinical use (Fourie et al. 2011). Following Fourie et al. (2011), we calculated average error (AE) and average percentage error (APE) for caliper and 3D-model based measurements (Supplementary Table 2). Mean AE for all cranial measurements was 0.76 mm, and ranged from 0.18–1.44 mm. Mean APE was 0.69% and ranged from 0.1–1.7%. Mean error values were comparable to those reported by Fourie et al.'s (2011) measurements on laser scanner models for AE (0.89 mm) and APE (1.48%), indicating they are sufficiently reliable for use in our comparative analyses of OH 83.

#### 2.4.2.D Quantitative comparisons:

Descriptive statistics were calculated in RStudio (2015. RStudio: Integrated Development for R. RStudio, Inc., Boston, MA URL <http://www.rstudio.com/>) and GGPlot2 (H. Wickham. ggplot2: Elegant Graphics for Data Springer-Verlag New York,

2009). We compared the four linear distances measurable on OH 83 that are also included in the Howells dataset (1973, 1989): Bifrontal breadth (FMB), bistephanic breadth (STB), frontal chord (FRC), and maximum frontal breadth (XFB). The Howells data and OH 83 are also compared to a sample of other fossil data from roughly penecontemporaneous sites across the Old World.

## 2.5 Results:

### 2.5.1 Morphological trait comparison:

The Ndutu cranium (distinct from OH 83 from the Ndutu Bed at Olduvai Gorge) was found less than 50 km from Olduvai Gorge near Lake Ndutu. This cranium has an estimated age of ca. 600–300 ka (Clarke, 1976; Millard, 2008), securely placing it in the Middle Pleistocene. Both OH 83 and the Ndutu crania are relatively small; estimated cranial capacity for the Ndutu cranium is 1110 cm<sup>3</sup> (Clarke, 1976). Due to the preservation of OH 83, further comparison on the cranial size of these two fossils is limited. Similar to other Middle Pleistocene hominid crania including Kabwe 1 (Woodward, 1921) and Herto (BOU-VP-16/1) (White et al., 2003), the Ndutu cranium (Clarke, 1976; 1990) is more robust in the supraorbital and glabellar regions than OH 83, which is similarly gracile to the Omo I reconstruction (Day, 1969) and Eliye Springs. In comparison to the dimensions of the frontal squama of the Ndutu cranium (Clarke, 1976), Dar es Soltane II, and the preserved squama on Iwo Eleru (Harvati et al. 2011), the frontal squama of OH 83 is more vertical and thus more modern in its appearance. The frontal squama of Omo I (Day, 1969), Zuttiyeh (Freidline et al., 2012) are also morphologically modern in this way, although less so than OH 83. The Skhul and Qafzeh hominid crania, for the most part, appear to have slightly higher, more modern frontal squama, but larger brow ridges than OH 83. The Saldanha specimen from South Africa exhibits a supraorbital region that is quite robust with an almost inflated appearance over the orbits, morphology which is not present on the relatively gracile supraorbital region of OH 83. The moderate angle of the parietals toward the sagittal suture and vertically-oriented lateral walls of the cranial vault expressed in the Manot 1 specimen from Israel (Hershkovitz et al., 2015), as well as the Skhul and Qafzeh hominids, are morphologies that are also expressed in OH 83.

Compared with Holocene populations of *H. sapiens*, OH 83 shows an overall pattern of modern human cranial morphology. OH 83 is gracile in almost all respects, and the slight glabellar prominence and slight rugosity of the supraorbital region are well within the expected range of variation for modern humans. While the cranial vault appears to be low and long relative to its breadth, this is likely (?) an artifact of preservation and distortion due to post-depositional processes and is not likely (?) representative of what the cranium looked like during its life.

### 2.5.2 Craniometric comparison:

Box plots showing the distribution of measurements, mean, and 95% confidence interval of the median for the modern human comparative sample, with OH 83 and the comparative fossil sample superimposed are shown in Figure 5. Mean and standard deviation values for the modern human sample by geographic region are reported in Appendix 1. For STB (90.71 mm) and XFB (95.58 mm), OH 83 falls at the lower end of the range compared to the fossil and modern data, and outside the 95% confidence interval. Two of the East African specimens, Herto and LH 18, also fall at the low end of the range for STB, but for XFB, OH 83 falls nearest Qafzeh 2 from Israel. For FMB (120.57 mm), OH 83 falls at the upper end of the range for modern humans. For FRC (114.94 mm), OH 83 fits well within the range for modern human variation, and is nested within the comparative fossil specimens.

## 2.6 Discussion and conclusions:

The Middle and Early-Late Pleistocene represents the transition between *H. erectus* and the earliest appearances of *H. sapiens* ca. 200 ka (Magori, 1980; McBrearty and Brooks, 2000; Henshilwood & Marean, 2003; White et al., 2003; McDougall et al., 2005; Trinkaus, 2005; Rightmire, 2008; Fu et al., 2013; Poznik et al., 2013; Scozzari et al., 2014). Specimens from <200 ka tend to exhibit traits more similar to recent modern humans (Rightmire, 2009), such as the Herto crania (*H. s. idaltu*, dated to 160–154 ka). This specimen, while being robust, is more similar to the anatomically modern end of the *H. erectus*–*H. sapiens* spectrum with respect to its occipital flexion, anteriorly projecting supraorbital region, and parietal curvature (White et al., 2003).

There have been numerous attempts to biologically define *H. sapiens* (Day and Stringer, 1982; Stringer et al., 1984; Lieberman et al., 2002; Tattersall and Schwartz, 2008). Attempts to characterize morphological traits that define humans in the fossil record rely heavily on cranial anatomy (Day and Stringer, 1982; Stringer et al. 1984; Tattersall and Schwartz, 2008). These efforts have not met wide agreement by the scientific community due, in part, to the mosaic patterns of cranial variation represented by the fossils (Bräuer and Leakey, 1986; Lieberman et al., 2002) and the morphological heterogeneity present in living modern humans (Howells, 1973; 1989; Lahr, 1996; Haile-Selassie et al., 2004). The irregular, mosaic pattern of trait expression in the crania of Middle and Late Pleistocene fossils implies that morphological modernity did not occur at once (McBrearty and Brooks, 2000; Trinkaus, 2005; Reed and Tishkoff, 2006).

OH 83 adds to the current understanding of early modern humans by adding to the fossil record, and by expanding the dataset for Late Pleistocene hominid crania. The initial description we present here demonstrates that *Homo sapiens* in Africa exhibited morphologically modern cranial characters by 60–32 ka. But, that said, the metric data for OH 83 do not specifically cluster with the Africans sampled by Howells (1973; 1989). The early fossils of *H. sapiens* demonstrate that the patterns of ancestry that characterize present-day human cranial variation were not present as of 160 ka (White et al., 2003). Perhaps these geographic clusters of cranial variation still had not

coalesced by the time of OH 83, as this specimen does not cluster with the Africans sampled by Howells. However, the data available to adequately explore this possibility are quite limited due to the fragmentary nature of OH 83, and much further research on additional fossil material is needed to say anything more conclusive.

While we know that many aspects of the cranial vault bones are influenced by genetic effects (Susanne, 1977; Sherwood et al., 2008; 2011; Sherwood and Duren, 2013; Šešel et al., 2015), we still know very little about the genetic architecture that underlies the development of, or variation in, cranial features such as glabellar prominence or overall cranial vault shape (Boas, 1912; 1928; Kohn, 1991; Sherwood and Duren, 2013; Šešel et al., 2015). Until we have a better grasp of the biological etiology of these morphologies, a cautious interpretation of the skeletal evidence is that the morphological variation of Middle and Late Pleistocene African hominid crania signifies population-level, rather than species-level differences.

Given the genetic evidence for small population sizes for the lineage ancestral to humans over the past million years, which is estimated to have fluctuated between 40,000 to 100,000 individuals (Rogers and Jorde, 1995; Takahata et al., 1995; Sherry et al., 1997; Lahr and Foley, 1998), it is likely that the demography of African *Homo* fluctuated considerably. Some of the morphological variation at this time would be the result of adaptation to local environments, leading to morphological divergence between populations. However, Lahr and Foley (1998) note that this population structure also leads to variation that is not the result of genetic effects, or which is genetic in origin but not necessarily adaptive to the environment (i.e. genetic drift and gene flow). Because of its morphological overlap with non-African humans (Figure 5), OH 83 provides support for this observation.

Our study demonstrates that morphologically and metrically, OH 83 falls within the range of variation observed in *Homo sapiens*. The metric data alone are less convincing than are the morphological data, but we reiterate that the crania shows clear evidence of taphonomic distortion and as such, standard linear metrics should not be considered in isolation. Our interpretation of the cranial morphology of OH 83 is that it should be placed taxonomically within anatomically modern humans. As is always the case in a historical science such as paleoanthropology, only fieldwork and the discovery of more hominid remains will elucidate the transition from *H. erectus* to *H. sapiens*, and how population variation was patterned as our species evolved. For now, the discovery of OH 83 demonstrates that a fully anatomically modern human, indistinguishable from living people, died in northern Tanzania ca. 60–32 ka

## 2.7 Acknowledgements:

This project would not have been possible without the support and assistance of: Dr. H. Mshinda, Director General, Commission for Science and Technology; Mr. J. Paresso and Mr. J. Temba, Tanzanian Department of Antiquities; Ms. V. Ufunguo, Ngorongoro Conservation Area Authority; Mrs. F. Mangalu, Director of the National Natural History Museum, Arusha; J. Njau; T. White, and the Human Evolution Research Center. We also acknowledge the collaboration of J. R. Southon, Keck Carbon Cycle Accelerator Mass Spectrometry Laboratory, University of California, Irvine, and support from the Gabrielle R. Vierra Memorial Fund. Thanks to J. Hofmeister, M. Brasil, and T. Monson for assistance with, and in some cases for providing the backbone of RStudio code. Special thanks to colleagues in the Department of Integrative biology for their feedback: J. Carlson, M. Huffman, M. Yang, H. Kurkjian, and C. Jennings; and to J. Reed, A. Johnson, and W. Reiner for providing invaluable feedback and support. This article was greatly improved by comments from the associate editor and two anonymous reviewers. This research is based upon work supported by the National Science Foundation under Grant No. BCS 1025263 to LJH, and based upon work supported by the Palaeontological and Scientific Trust to HS and IS. This material will be submitted as partial fulfillment of Reiner W.B.'s doctoral dissertation at the University of California Berkeley.

## 2.8 References:

- Bada JL. 1981. Racemization of amino acids in fossil bones and teeth from the Olduvai Gorge region, Tanzania, East Africa. *Earth Planet Sci Lett* 55(2): 292–298.
- Bada JL, Protsch R. 1973. Racemization reaction of aspartic acid and its use in dating fossil bones. *PNAS* 70: 1331–34.
- Boas F. 1912. Changes in the bodily form of descendants of immigrants. *Am Anthropol* 14(3):530–562.
- Boas F. 1928. *Materials for the study of inheritance in man*. Vol 6. New York: Columbia University Press.
- Bräuer G. 2008. The origin of modern anatomy: By speciation or intraspecific evolution? *Evol Anthropol* 17:22–37.
- Bräuer G, Groden C, Delling G, Kupczik K, Mbua E, & Schultz M. 2003. Pathological alterations in the archaic *Homo sapiens* cranium from Eliye Springs, Kenya. *Am J Phys Anthropol* 120(2):200–4.
- Bräuer G & Leakey RE. 1986. The ES-11693 cranium from Eliye Springs, West Turkana, Kenya. *J Hum Evol* 15(4): 289–312.
- Bruner E. 2007. Cranial shape and size variation in human evolution: Structural and functional perspectives. *Childs Nerv Syst* 23:1357–1365.
- Byers, SN. 2005. *Introduction to forensic anthropology: A textbook*. Boston, MA: Pearson.
- Cann RL, Stoneking M, & Wilson AC. 1987. Mitochondrial DNA and human evolution. *Nature* 325(6099):1–7.
- Cann RL. 2001. Genetic clues to dispersal in human populations: Retracing the past from the present. *Science* 291(5509):1742–1748.
- Clark JD, Beyene Y, WoldeGabriel G, Hart WK, Renne PR, Gilbert H, Boisserie JR. 2003. Stratigraphic, chronological and behavioural contexts of Pleistocene *Homo sapiens* from Middle Awash, Ethiopia. *Nature* 423(6941):747–752.
- Clarke RJ. 1976. A new cranium of *Homo erectus* from Lake Ndutu, Tanzania. *Nature* 262 :485–487.
- Clarke RJ. 1990. The Ndutu cranium and the origin of *Homo sapiens*. *J Hum Evol* 19:699–736.
- Cohen KM, Finney SC, Gibbard PL, & Fan JX. 2013. The ICS international chronostratigraphic chart. *Episodes* 363:199–204.
- Crevecoeur I. 2008. Étude anthropologique du squelette du Paléolithique supérieur de Nazlet Khater 2 (Égypte). Apport à la compréhension de la variabilité passée des hommes modernes. Leuven: Egyptian Prehistory Monographs 8.
- Crevecoeur I, Rougier H, Grine F, & Froment A. 2009. Modern human cranial diversity in the Late Pleistocene of Africa and Eurasia: Evidence from Nazlet Khater, Peştera cu Oase, and Hofmeyr. *Am J Phys Anthropol* 140:347–358.
- Crevecoeur I & Vilotte S. 2006. Evidence of pathology on the Nazlet Khater 2 skeleton and mining activity at the beginning of the early Upper Palaeolithic in Egypt. 2006. *Bull Mém Soc Anthropol Paris* 18:165–175.
- Day MH. 1969. Omo human skeletal remains. *Nature*. 222(5199):1135.

- Day MH & Stringer CB. 1982. A reconsideration of the Omo Kibish remains and the *erectus-sapiens* transition. In: de Lumley MA, editor. *Homo erectus et la Place de l'Homme de Tautavel parmi les Hominidés Fossiles*. Première Congrès International de Paléontologie Humaine. UNESCO Colloque International du Centre National de la Recherche Scientifique Vol. 2, Prétirages, Nice:814–846.
- Dean D, Hublin JJ, Holloway R, & Ziegler R. 1998. On the phylogenetic position of the pre-Neandertal specimen from Reilingen, Germany. *J Hum Evol* 34:485–508.
- Dreyer TF. 1935. A human skull from Florisbad, Orange Free State, with a note on the endocranial cast, by CU Ariens Kappers. *Proc Kon Ned Akad Wetensch* 38:3–12.
- Eren MI, Durant AJ, Prendergast M, & Mabulla AZ. 2014. Middle Stone Age archaeology at Olduvai Gorge, Tanzania. *Quat Intl* 322:292–313.
- Feibel CS. 2008. Microstratigraphy of the Kibish hominin sites KHS and PHS, Lower Omo Valley, Ethiopia. *J Hum Evol* 55:404–408.
- Fourie Z, Damstra J, Gerrits PO, & Ren Y. 2011. Evaluation of anthropometric accuracy and reliability using different three-dimensional scanning systems. *Forensic Sci Int* 207(1): 127–34.
- Freidline SE, Gunz P, Janković I, Harvati K, & Hublin JJ. 2012. A comprehensive morphometric analysis of the frontal and zygomatic bone of the Zuttiyeh fossil from Israel. *J Hum Evol* 62:225–241.
- Fu Q, Mittnik A, Johnson PL, Bos K, Lari M, Bollongino R, Sun C, Giemsch L, Schmitz R, Burger J, & Ronchitelli AM. 2013. A revised timescale for human evolution based on ancient mitochondrial genomes. *Curr Biol* 23(7):553–559.
- Grine FE, Bailey RM, Harvati K, Nathan RP, Morris AG, Henderson GM, Ribot I, & Pike AWG. 2007. Late Pleistocene human skull from Hofmeyr, South Africa, and modern human origins. *Science* 315:226–229.
- Grün R, Brink JS, Spooner NA, Taylor L, Stringer CB, Franciscus RG, & Murray AS. 1996. Direct dating of Florisbad hominid. *Nature* 382:500–501.
- Grün R, Stringer C, McDermott F, Nathan R, Porat N, Robertson S, Taylor L, Mortimer G, Eggins S, & McCulloch M. 2005. U-series and ESR analyses of bones and teeth relating to the human burials from Skhul. *J Hum Evol* 49:316–334.
- Grün R & Beaumont P. 2001. Border Cave revisited: a revised ESR chronology. *J Hum Evol* 40(6):467–482.
- Grün R & Stringer CB. 1991. Electron spin resonance dating and the evolution of modern humans. *Archaeometry* 33:153–199.
- Haile-Selassie Y, Asfaw B, & White TD. 2004. Hominid cranial remains from upper Pleistocene deposits at Aduma, Middle Awash, Ethiopia. *Am J Phys Anthropol* 123:1–10.
- Harvati K, Stringer C, Grün R, Aubert M, Allsworth-Jones P, & Folorunso CA. 2011. The Later Stone Age calvaria from Iwo Eleru, Nigeria: morphology and chronology. *PLoS ONE* 6:e24024.
- Hay RL. 1976. *Geology of the Olduvai Gorge: A study of sedimentation in a semiarid basin*. Berkeley: University of California Press.

- Henshilwood CS & Marean CW. 2003. The Origin of modern human behavior: Critique of the models and their test implications. *Curr Anthropol* 44:627–651.
- Hershkovitz I, Marder O, Ayalon A, Bar-Matthews M, Yasur G, Boaretto E, Caracuta V, Alex B, Frumkin A, Goder-Goldberger M, & Gunz P. 2015. Levantine cranium from Manot Cave (Israel) foreshadows the first European modern humans. *Nature* 520: 216–219.
- Howell FC. 1994. A Chronostratigraphic and taxonomic framework of the origins of modern humans. In: Nitecki MH & Nitecki DR, editors. *Origins of anatomically modern humans*. New York: Plenum Press. p 253–319.
- Howells WW. 1973. *Cranial Variation in Man. A Study by multivariate analysis of patterns of differences among recent human populations*. Peabody Mus Amer Arch Ethnol 67.
- Howells WW. 1989. Skull shapes and the map. Craniometric analyses in the dispersion of modern *Homo*. *Peabody Mus Amer Arch Ethnol* 79.
- Hublin JJ. 1991. *L'émergence des Homo sapiens archaïques: Afrique du Nord-Ouest et Europe occidentale* [dissertation]. Université Bordeaux 1, France.
- Hublin JJ. 1992. Recent human evolution in northwestern Africa. *Philos Trans R Soc Lond B Biol Sci* 337:185–191.
- Huxtable J. 1990. Burnt flint date for Yabrud shelter I ancient TL date. *Lists No 4 Entry* 43.
- Keith A. 1931. *New discoveries relating to the antiquity of man*. London: Williams and Newgate.
- Klein RG, Avery G, Cruz-Uribe K, & Steele TE. 2007. The mammalian fauna associated with an archaic hominin skullcap and later Acheulean artifacts at Elandsfontein, Western Cape Province, South Africa. *J Hum Evol* 52(2):164–186.
- Kocher TD & Wilson AC. 1991. Sequence evolution of mitochondrial DNA in humans and chimpanzees: Control region and a protein-coding region. In: Osawa S & Honjo T, editors. *Evolution of life: fossils, molecules and culture*. Tokyo: Springer. pp 391–413.
- Kohn LAP. 1991. The Role of genetics in craniofacial morphology and growth. *Ann Rev Anthropol* 20:261–278.
- Kuzminsky SC & Gardiner MS. 2012. Three-dimensional laser scanning: potential uses for museum conservation and scientific research. *J Archaeol Sci* 39(8):2744–2751.
- Lahr MM. 1996. *The evolution of modern human diversity: a study of cranial variation*. Vol. 18. Cambridge: Cambridge University Press.
- Lahr MM. 2013. Genetic and fossil evidence for modern human origins. In: Mitchell P & Lane P, editors. *The Oxford Handbook of African Archaeology*. Oxford: Oxford University Press. p 325–340.
- Lahr MM & Foley RA. 1998. Towards a theory of modern human origins: Geography, demography, and diversity in recent human evolution. *Am J Phys Anthropol Suppl* 27:137–176.
- Leakey RE. 1969. Early *Homo sapiens* remains from the Omo River region of Southwest Ethiopia. *Nature* 222:1132–1133.

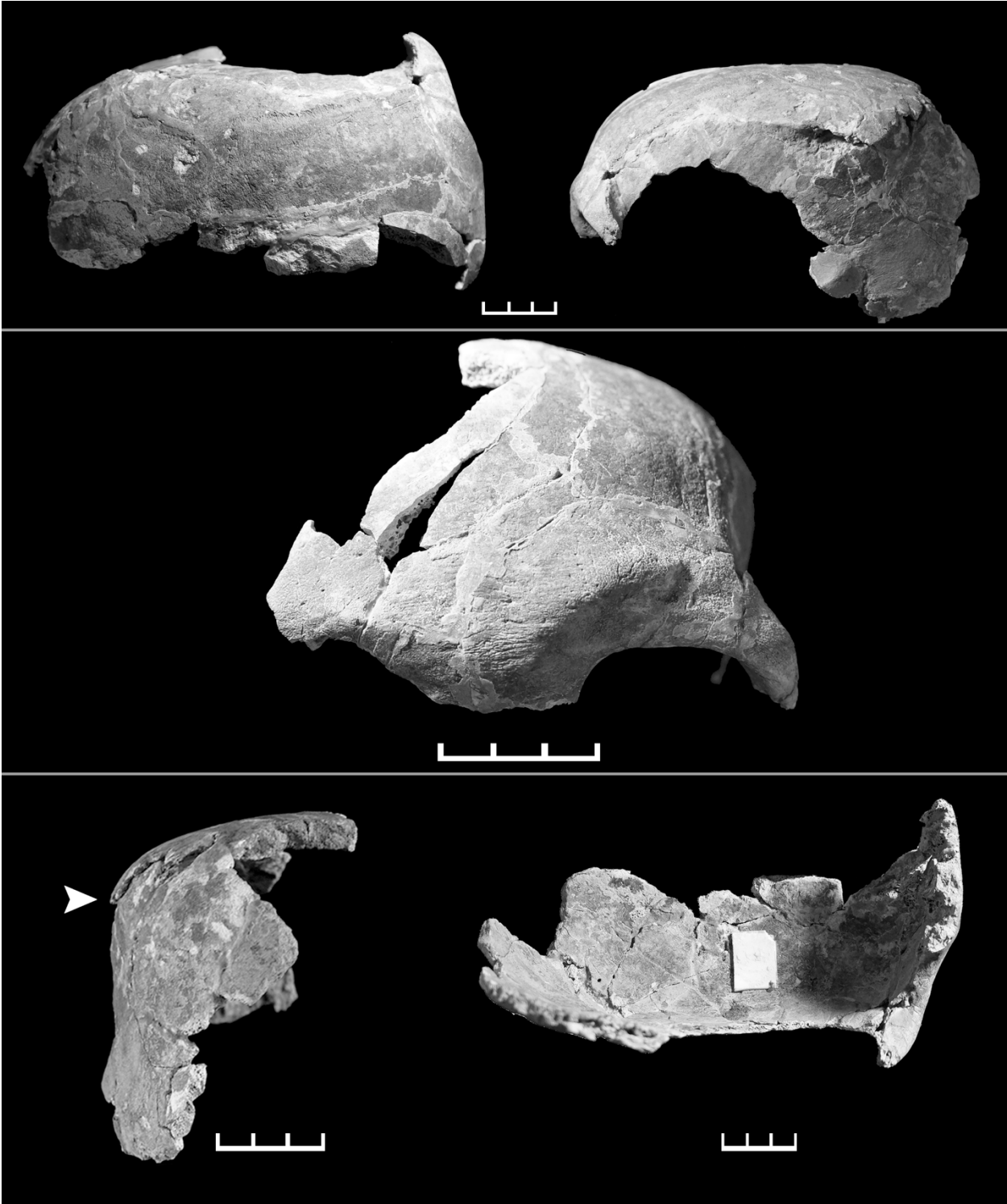
- Leakey MD. 1971. Olduvai Gorge: Volume 3, Excavations in Beds I and II, 1960-1963. Cambridge: Cambridge University Press.
- Leakey MD, Hay RL, Thurber DL, Protsch R, & Berger R. 1972. Stratigraphy, archaeology, and age of the Ndotu and Naisiusiu beds, Olduvai Gorge, Tanzania. *World Archaeol* 3(3): 328–341.
- Lieberman, DE. 1998. Sphenoid shortening and the evolution of modern human cranial shape. *Nature* 393(6681): 158–162.
- Lieberman DE, McBratney BM, & Krovitz G. 2002. The evolution and development of cranial form in *Homo sapiens*. *PNAS* 3:1134–1139 doi:10.1073/pnas.022440799
- Llorente GM, Jones ER, Eriksson A, Siska V, Arthur KW, Arthur JW, Curtis MC, Stock JT, Coltorti M, Pieruccini P, Stretton S, Brock F, Higham T, Park Y, Hofreiter M, Bradley DG, Bhak J, Pinhasi R, & Manica A. 2015. Ancient Ethiopian genome reveals extensive Eurasian admixture throughout the African continent. *Science* 350(6262):820–822.
- Macintyre RM, Mitchell JG, & Dawson JB. 1974. Age of fault movements in Tanzanian sector of East African rift system. *Nature* 247:354–56.
- Magori CC. 1980. Laetoli hominid 18: Studies on a Pleistocene fossil human skull from northern Tanzania [dissertation]. London: University of London.
- Magori CC, Day MH. 1983. Laetoli Hominid 18: An Early *Homo sapiens* skull. *J Hum Evol* 12:747–753.
- Manega PC. 1993. Geochronology, geochemistry and isotopic study of the Plio-Pleistocene hominid sites and the Ngorongoro Volcanic Highland in Northern Tanzania [dissertation]. Boulder: University of Colorado, Boulder.
- Manega PC. 1995. New geochronological results from the Ndotu, Naisiusiu and Ngoloba Beds at Olduvai and Laetoli in northern Tanzania: their significance for evolution of modern humans. Bellagio Conference, Italy.
- McBrearty S & Brooks AS. 2000. The revolution that wasn't: A New interpretation of the origin of modern human behavior. *J Hum Evol* 39:453–563.
- McDermott F, Stringer C, Grün R, Williams CT, Din VK, & Hawkesworth CJ. 1996. New Late Pleistocene uranium-thorium and ESR dates for the Singa hominid Sudan. *J Hum Evol.* 31(6):507–16.
- McDougall I, Brown FH, & Fleagle JG. 2005. Stratigraphic placement and age of modern humans from Kibish, Ethiopia. *Nature.* 433:733–736.
- Mercier N, Valladas H, Valladas G, Reyss JL, Jelinek A, Meignen L, & Joron JL. 1995. TL dates of burnt flints from Jelinek's excavations at Tabun and their implications. *J Archaeol Sci* 22:495–509.
- Mercier N & Valladas H. 2003. Reassessment of TL age estimates of burnt flints from the Paleolithic site of Tabun Cave Israel. *J Hum Evol* 45:401–9.
- Millard AR. 2008. A critique of the chronometric evidence for hominid fossils: I. Africa and the Near East 500–50ka. *J Hum Evol* 54:848–874.
- Pinhasi R & Semal P. 2000. The position of the Nazlet Khater specimen among prehistoric and modern African and Levantine populations. *J Hum Evol* 39(3):269–288.

- Poznik GD, Henn BM, Yee MC, Sliwerska E, Euskirchen GM, Lin AA, Snyder M, Quintana-Murci L, Kidd JM, Underhill PA, & Bustamante CD. 2013. Sequencing Y chromosomes resolves discrepancy in time to common ancestor of males versus females. *Science* 341(6145):562–5.
- Reed FA & Tishkoff SA. 2006. African human diversity, origins and migrations. *Curr Opin Genet Dev* 16:597–605.
- Relethford DJH. 2001. Ancient DNA and the origin of modern humans. *Proc Nat Acad Sci* 982:390–391.
- Relethford DJH & Jorde LB. 1999. Genetic evidence for larger African population size during recent human evolution. *Am J Phys Anthropol* 108:251–260.
- Rightmire GP. 1980. Middle Pleistocene hominids from Olduvai Gorge, northern Tanzania. *Am J Phys Anthropol* 53(2):225–241.
- Rightmire PG. 1996. The human cranium from Bodo, Ethiopia: evidence for speciation in the Middle Pleistocene? *J Hum Evol* 31:21–39.
- Rightmire GP. 2008. Homo in the Middle Pleistocene: Hypodigms, variation, and species recognition. *Evol. Anthropol* 17:8–21.
- Rightmire GP. 2009. Middle and later Pleistocene hominins in Africa and Southwest Asia. *Proc Nat Acad Sci* 106:16046–16050.
- Rogers AR & Jorde LB. 1995. Genetic evidence on modern human origins. *Hum Biol* 67(1): 1–36.
- Szwarcz HP, Grün, R, Vandermeersch B, Bar-Yosef O, Valladas H, & Tchernov E. 1988. ESR dates for the hominid burial site of Qafzeh in Israel. *J Hum Evol* 17(8):733–737.
- Scozzari R, Massaia A, Trombetta B, Bellusci G, Myres NM, Novelletto A, & Cruciani F. 2014. An unbiased resource of novel SNP markers provides a new chronology for the human Y chromosome and reveals a deep phylogenetic structure in Africa. *Genome Res* 24(3):535–44.
- Šešelj M, Duren DL, & Sherwood RJ. 2015. Heritability of the human craniofacial complex. *Anat Rec* 298(9):1535–47.
- Sherry ST, Harpending HC, Batzer MA, & Stoneking M. 1997. Alu evolution in human populations: Using the coalescent to estimate effective population size. *Genetics* 147(4): 1977–82
- Sherwood RJ & Duren DL. 2013. The genetics of morphology. In: Begun DR, editor. *A companion to paleoanthropology*. Malden, MA: Wiley-Blackwell. p 306–320.
- Sherwood RJ, Duren DL, Demerath EW, Czerwinski SA, Siervogel RM, & Towne B. 2008. Quantitative genetics of modern human cranial variation. *J Hum Evol* 54:909–914.
- Sherwood RJ, Duren DL, Mahaney MC, Blangero J, Dyer TD, Cole SA, Czerwinski SA, Chumlea WC, Siervogel RM, Choh AC, Nahhas RW, Lee M, & Towne B. 2011. A genome-wide linkage scan for quantitative trait loci influencing the craniofacial complex in humans (*Homo sapiens sapiens*). *Anat Rec* 294(4):664–675.
- Sholts SB, Flores L, Walker PL, & Wärmländer SKTS. 2011. Comparison of coordinate measurement precision of different landmark types on human crania using a 3D

- laser scanner and a 3D digitiser: Implications for applications of digital morphometrics. *Int J Osteoarchaeol* 21(5): 535–543.
- Sholts SB, Wärmländer SKTS, Flores LM, Miller KW, & Walker PL. 2010. Variation in the measurement of cranial volume and surface area using 3D laser scanning technology. *J Forensic Sci* 55(4):871–876.
- Singer R. 1954. The Saldanha skull from Hopefield, South Africa. *Am J Phys Anthropol* 12:345–362.
- Skinner AR, Hay RL, Masao F, & Blackwell BA. 2003. Dating the Naisiusiu Beds, Olduvai Gorge, by electron spin resonance. *Quat Sci Rev* 22:1361–1366.
- Smith FH. 1992. Models and realities in modern human origins: The African fossil evidence. *Phil Trans Roy Soc B* 337: 243–250.
- Smith TM, Tafforeau P, Reid DJ, Grün R, Eggins S, Boutakiout M, & Hublin JJ. 2007. Earliest evidence of modern human life history in North African early *Homo sapiens*. *Proc Nat Acad Sci* 104:6128–6133.
- Stojanowski CM. 2013. An archaeological perspective on the burial record at Gobero. In: *Gobero: The No Return frontier. Archaeology and landscape at the Saharo-Sahelian borderland*. Garcea EAA, editor. *J Afr Archaeol Monograph series number 9*. Frankfurt: Africa Magna Verlag, p 44–64.
- Stojanowski CM. 2014. Iwo Eleru's place among Late Pleistocene and Early Holocene populations of North and East Africa. *J Hum Evol* 75:80–89.
- Stoneking M, Sherry ST, Redd AJ, & Vigilant L. 1993. New approach to dating suggests a recent age for the human mtDNA ancestor. In: Aitken MJ, Stringer CB, & Mellars PA, editors. *The Origin of modern humans and the impact of chronometric dating*. Princeton: Princeton University Press, p 84–103.
- Stringer CB. 1974. Population relationships of later Pleistocene hominids: A Multivariate study of available crania. *J Archaeol Sci* 1(4): 317–342.
- Stringer CB. 2002. Modern human origins: Progress and prospects. *Phil Trans Roy Soc B* 357:563–579.
- Stringer CB, Hublin JJ, & Vandermeersch B. 1984. The Origins of modern humans: A World survey of the fossil evidence. In: Smith FH & Spencer F, editors. *The Origins of modern humans: A World survey of the fossil evidence*. Liss: New York. p 51–135.
- Susanne C. 1977. Heritability of Anthropological Characters. *Hum Biol* 49(4): 573–580.
- Takahata N, Satta Y, & Klein J. 1995. Divergence time and population size in the lineage leading to modern humans. *Theor Popul Biol* 48(2): 198–221.
- Tattersall I & Schwartz JH. 2008. The morphological distinctiveness of *Homo sapiens* and its recognition in the fossil record: Clarifying the problem. *Evol Anthropol* 17(1): 49–54.
- Taylor RE & Bar-Yosef O. 2014. *Radiocarbon dating: An Archaeological perspective*. 2nd edition. Walnut Creek: Left Coast Press/London: Routledge.
- Thoma A. 1984. Morphology and affinities of the Nazlet Khater man. *J Hum Evol* 13(3): 287–296.
- Tishkoff SA, Dietzsch E, Speed W, Pakstis AJ, Kidd JR, Cheung K, Bonn -Tamir B, Santachiara-Benerecetti AS, Moral P, & Krings M. 1996. Global patterns of

- linkage disequilibrium at the CD4 locus and modern human origins. *Science* 271:1380–1387.
- Trinkaus E. 2005. Early modern humans. *Annu Rev Anthropol* 34:207–230.
- Tryon CA, Crevecoeur I, Faith JT, Ekshtain R, Nivens J, Patterson D, Mbua EN, & Spoor F. 2015. Late Pleistocene age and archaeological context for the hominin calvaria from GvJm-22 (Lukenya Hill, Kenya). *Proc Natl Acad Sci* 112:2682–2687.
- Valladas H, Reyss JL, Joron JL, Valladas G, Bar-Yosef O, & Vandermeersch B. 1988. Thermoluminescence dating of Mousterian “Proto-Cro-Magnon” remains from Israel and the origin of modern man. *Nature* 331:614–6.
- Vandermeersch B. 1981. *Les hommes fossiles de Qafzeh Israël*. Paris: Editions du CNRS
- Vermeersch P. 2010. Middle and upper palaeolithic in the Egyptian Nile Valley. In: Garcia EAA, editor. *South-eastern Mediterranean Peoples between 130,000 and 10,000 years ago*. Oxford: Oxbow Books. p 66–88
- Von Zieten RRR. 2009. Preliminary report on a new Olduvai hominid from 1968—an “anatomically-modern-man” from Upper Ndutu Bed. Retrieved from [www1.uni-hamburg.de/helmut-ziegert](http://www1.uni-hamburg.de/helmut-ziegert).
- Wells LH. 1951. The fossil human skull from Singa. In: *Fossil mammals of Africa 2*. London: British Museum of Natural History. p 29–42.
- White TD, Asfaw B, DeGusta D, Gilbert H, Richards GD, Suwa G, & Howell FC. 2003. Pleistocene *Homo sapiens* from Middle Awash, Ethiopia. *Nature* 423:742–747.
- White TD. 2014. Delimitating species in paleoanthropology. *Evol Anthropol* 23:30–32.
- Wood R. 2015. From Revolution to convention: The Past, present and future of radiocarbon dating. *J Arch Sci* 56:61–72.
- Woodward AS. 1921. A new cave man from Rhodesia, South Africa. *Nature* 108:371–372.

Figure 1. OH 83 rearticulated calvaria recovered from the surface.



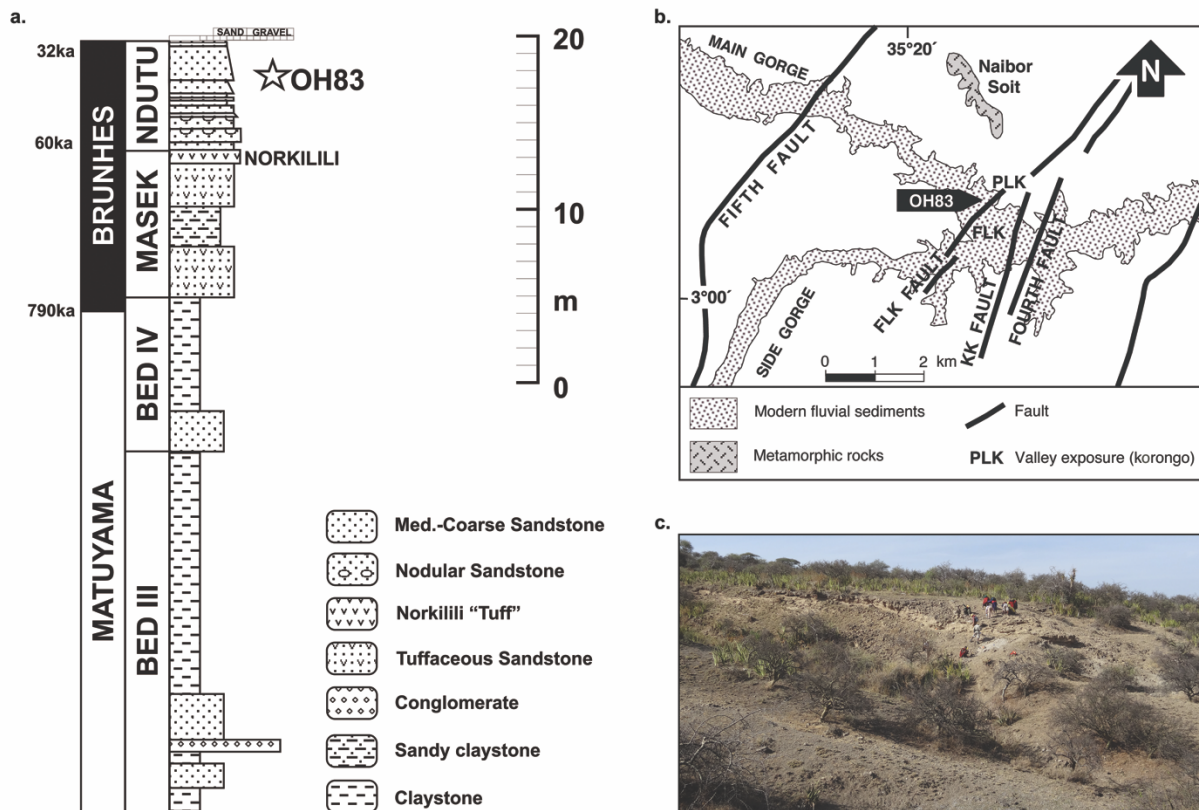
Center: OH 83 in norma frontalis. From top-right, and then clockwise: Norma lateralis, norma basalis, norma occipitalis, and norma verticalis. Arrow points to the left portion of the parietal that overhangs the vault, a clear indication of distortion. All scale bars are 3 cm length.

Figure 2. OH 83 cranial and dental fragments recovered in situ.



Length of scale bar for cranial fragments is 6 cm length. Length of scale bar for teeth is 3 cm.

Figure 3. Geological context of OH 83.



a. Generalized stratigraphic column of the area on the downthrown side of the FLK Fault where OH 83 was found. Incorporates data from measured section of Loc. 23 of Hay (1976), b. Depiction of geology at PLK (Loc. 23 of Hay, 1976), c. photograph showing topography of OH 83's site of discovery.

Figure 4. Image of three-dimensional scan depicting OH 83 in norma frontalis. Length of scale bar is 10 mm.



Figure 5. Box plots representing the range of modern human variation for four cranial measurements (see Appendix 1 for summary data).

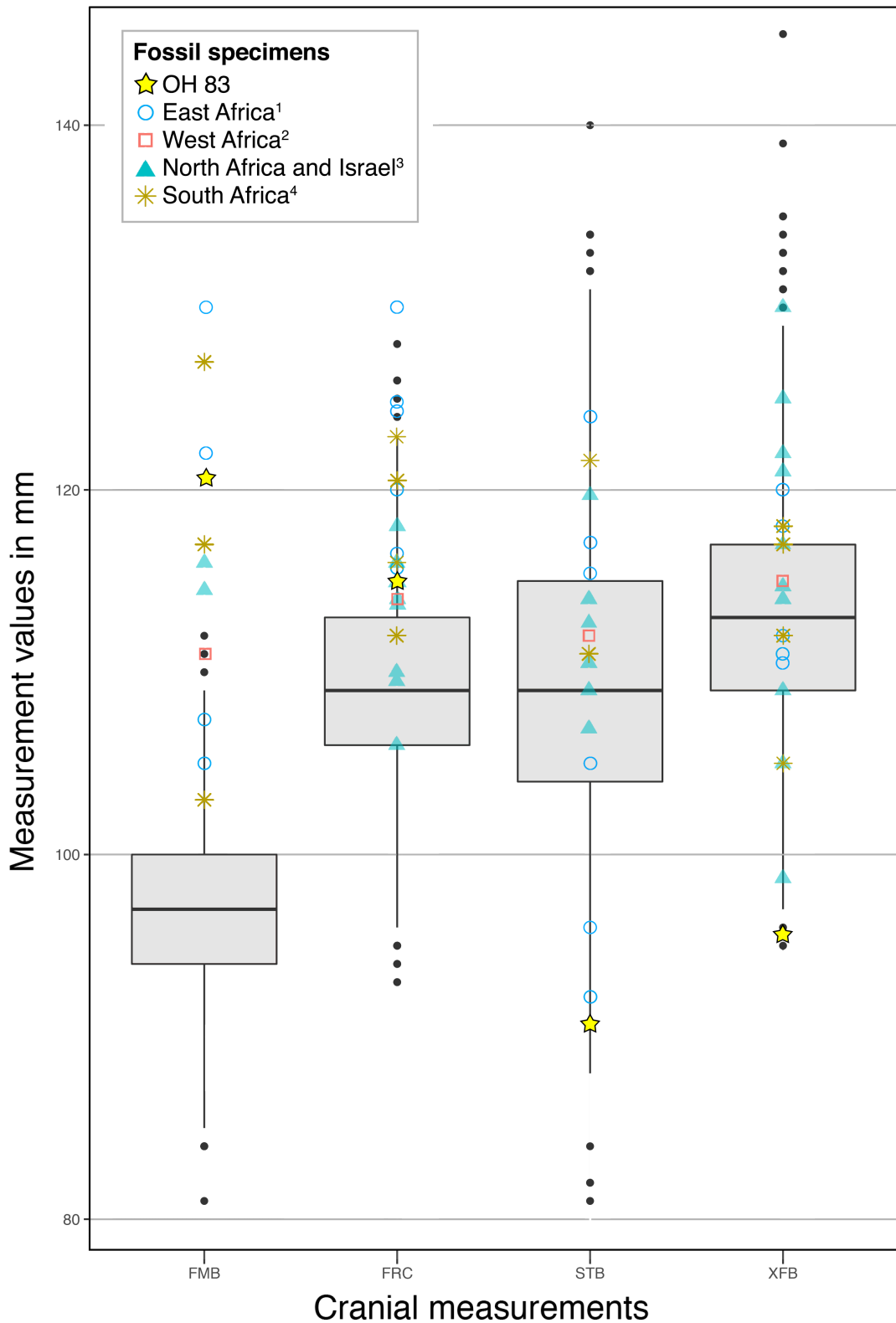


Figure 5 (continued). Box and whisker plots indicate 95% confidence limits of the distribution of Howells' data (1973, 1989, 1995) for four cranial measurements. Superimposed on these box plots are OH 83 and a sample of penecontemporaneous fossils (see Tables 1-3). All data are reported in mm. Shapes refer to the fossil specimens, the yellow stars refer to OH 83. Individual measurements are plotted for the comparative fossils, but specimens are depicted by shapes that refer to the fossil's geographic region: <sup>1</sup>Eastern Africa: Omo I and II, Herto, Eliye Springs, LH 1, LH 18, Ndotu Lake; <sup>2</sup>Western Africa: Iwo Eleru; <sup>3</sup>Northern Africa and Israel: Dar es Soltane II, Jebel Irhoud 1, Singa, Nazlet Khater 2, Skhul IV and V, Qafzeh 1, 2, 6, and 9, Zuttiyeh; <sup>4</sup>Southern Africa: Kabwe 1, Border Cave 2, Fish Hoek, Hofmeyr, Florisbad, Saldanha. Individual specimen measurements are listed in Table 2.

Table 1. List of comparative fossil material with estimated geologic ages.

Country	Specimen	Age	References
Ethiopia	Omo I, II <sup>1</sup>	195 kya	Day and Stringer, 1991; McDougal et al., 2005.; Feibel, 2008.
	Herto (BOU-VP/16-1)	160–154 kya	Clark et al., 2003; White et al., 2003.
Kenya	Eliye Springs (ES-11693)	> 200 kya <sup>2</sup>	Bräuer and Leakey, 1986; Bräuer, 2008; Cieri et al., 2014.
	LH 1	> 46 kya	Tryon et al., 2015.
Egypt	Nazlet Khater 2	40–35 kya	Thoma, 1984; Pinhasi and Semal, 2000; Crevecoeur and Vilotte, 2006; Crevecoeur, 2008; Crevecoeur et al., 2009; Vermeersch, 2010.
Nigeria	Iwo Eleru	~11.7–16.3 kya	Harvati et al., 2013.
Morocco	Dar es Soltane II	150-8 kya	Millard et al., 2008.
	Jebel Iroud 1	190-90 kya	Grün and Stringer, 1991; Hublin, 1991; Smith et al., 2007.
S. Africa	Border Cave 2	115-90 kya	Grün and Beaumont, 2001.
	Fish Hoek	35 kya	Clark, 1982; Protsch, 1974.
	Hofmeyr	36.2 ± 3.3 kya	Grine et al., 2007.
	Florisbad	290-230 kya	Grün et al., 1996.
	Saldanha	1 mya < 600 kya	Klein et al., 2006.
Sudan	Singa	145.5 ± 7.5 – 89 ± 9.3 kya	McDermott et al., 1996.
Tanzania	LH 18	3–200 kya	Magori and Day, 1983; Manega, 1995.
	Ndutu	400 kya	Manega, 1995.
Zambia	Kabwe 1	4–300 kya <sup>2</sup>	Klein, 1999.
Israel	Manot 1	54.7 ± 5.5 kya	Hershkovitz et al., 2015
	Skhul IV, V	135–100 kya	Grün et al., 2005.
	Qafzeh 1,2,6,9	115–92 kya	Vandermeersch, 1981; Schwarcz et al., 1988; Valladas et al., 1988.
	Zuttiyeh	5-200 kya	Huxtable, 1990; Bar-Yosef, 1992; Mercier et al., 1995; Mercier and Valladas, 2003; Friedline et al., 2012.

<sup>1</sup>Omo I was recovered *in situ* during excavation. Omo II was found on the surface. Its age is estimated on the basis of stratigraphic correlation with Omo I (Leakey, 1969; McDougal et al., 2005; Fleagle et al., 2008).

<sup>2</sup>Indicates age is estimated due to absence of context for stratigraphic location of the fossil when discovered (Woodward, 1921; Bräuer and Leakey, 1986).

Table 2. Cranial measurements of the fossils used in comparative analysis.

<b>Specimens</b>	<b>STB</b>	<b>XFB</b>	<b>FRC</b>	<b>FMB</b>
<i>Border Cave 2</i>	—	—	116.3 <sup>1</sup>	105.0 <sup>1</sup>
<i>Dar es Soltane II</i>	—	132.0 <sup>1</sup>	—	—
<i>Eliye Springs</i> <sup>2</sup> <i>ES-11693</i>	105.0 <sup>3</sup>	118.0 <sup>3</sup>	116.5 <sup>3</sup>	—
<i>Fish Hoek</i>	121.6 <sup>1</sup>	105.0 <sup>4</sup>	122.9 <sup>1</sup>	103.0 <sup>1</sup>
<i>Florisbad</i>	—	137.0 <sup>5</sup>	117.0 <sup>5</sup>	130.0 <sup>6</sup>
<i>Herto</i> <i>BOU-VP-16/1</i>	96.0±3.0 <sup>7</sup>	120.0±5 <sup>7</sup>	124.8 <sup>1</sup>	130.0±2 <sup>7</sup>
<i>Hofmeyr</i>	—	117.0 <sup>8</sup>	112.0 <sup>8</sup>	—
<i>Iwo Eleru</i>	112.0 <sup>9</sup>	115.0 <sup>10</sup>	114.0 <sup>10</sup>	111.0 <sup>10</sup>
<i>Jebel Irhoud 1</i>	113.0 <sup>10</sup>	120.0 <sup>11</sup>	109.5 <sup>1</sup>	116.0 <sup>1</sup>
<i>Kabwe 1</i>	111.0 <sup>1</sup>	118.0 <sup>1</sup>	120.5 <sup>1</sup>	127.0 <sup>6</sup>
<i>LH 1</i>	—	111.0 <sup>12</sup>	120.0 <sup>12</sup>	107.4 <sup>12</sup>
<i>LH 18</i>	92.2 <sup>6</sup>	112.7 <sup>1</sup>	115.7 <sup>1</sup>	105.0 <sup>6</sup>
<i>Ndutu Lake</i>	115.4 <sup>13</sup>	112.0 <sup>14</sup>	—	—
<i>Nzalet Khater 2</i>	—	122.0 <sup>8</sup>	116.0 <sup>8</sup>	—
<i>Omo I</i>	124.0 <sup>9</sup>	110.5 <sup>13</sup>	130.0 <sup>9</sup>	122.0 <sup>9</sup>
<i>Omo II</i>	117.1 <sup>1</sup>	120.0 <sup>1</sup>	124.3 <sup>6</sup>	—
<i>Qafzeh 1</i>	114.0 <sup>1</sup>	114.7 <sup>1</sup>	—	114.5 <sup>1</sup>
<i>Qafzeh 2</i>	110.5 <sup>1</sup>	98.7 <sup>1</sup>	113.7 <sup>1</sup>	—
<i>Qafzeh 6</i>	109.0 <sup>1</sup>	125.0 <sup>15</sup>	114.0 <sup>15</sup>	—
<i>Qafzeh 9</i>	112.7 <sup>6</sup>	117.0 <sup>15</sup>	115.0 <sup>15</sup>	—
<i>Saldanha</i>	—	112.0 <sup>14</sup>	116.0 <sup>14</sup>	117.0 <sup>16</sup>
<i>Singa</i>	—	105.0 <sup>17</sup>	—	—
<i>Skhul IV</i>	—	121.0 <sup>15</sup>	118.0 <sup>15</sup>	—
<i>Skhul V</i>	—	114.0 <sup>15</sup>	106.0 <sup>15</sup>	—
<i>Zuttiyeh</i>	106.9 <sup>1</sup>	109.0 <sup>1</sup>	110.0 <sup>1</sup>	—

All measurements in mm. “—” indicates that measurement could not be collected either because the specimen is incomplete or deformed in that region.

<sup>1</sup>Measurement collected by one of the authors (WBR) using research quality cast at HERC, University of California Berkeley.

<sup>2</sup>Specimen has a pathology that may affect its measurements (Bräuer et al., 2003).

<sup>3</sup>Bräuer & Leakey, 1986.

<sup>4</sup>Keith, 1931.

<sup>5</sup>Dreyer, 1935.

<sup>6</sup>Magori, 1980.

<sup>7</sup>White et al., 2003.

<sup>8</sup>Crevecoeur et al., 2009.

<sup>9</sup>Measurement in parentheses (Stringer, 1974).

Table 3. Regional divisions used for the Howells (1973, 1989) comparative modern human dataset.

<b>Geographic Region</b>	<b>Population</b>
<b>Asia</b> N=665	Ainu Andaman Anyang Atayal Buriat Hainan N. Japan Philippines S. Japan
<b>Americas</b> N=389	Arikara Eskimo Peru Santa Cruz
<b>Australasia</b> N=298	Australia Tasmania Tolai
<b>Europe</b> N=317	Berg Norse Zalavar
<b>North Africa</b> N=111	Egypt
<b>Sub-Saharan Africa</b> N=373	Bushman Dogon Teita Zulu
<b>Polynesia/ Micronesia</b> N=371	Easter Island Guam S. Maori N. Maori Mori Mokapu
<b>Total N=2,524</b>	

## **Chapter 3**

### **Cranial variation in Early Period Native Californians: A new perspective on the W.W. Howells Craniometric Dataset**

### 3.1 Introduction

Among modern humans, there is a wide range of cranial variation (Howells 1973, 1989, 1995). The morphological heterogeneity of human crania facilitates the endeavors of forensic anthropologists and bioarcheologists to estimate sex and ancestry from the human cranium, and paleoanthropologists who must also use cranial morphology to assess the phylogeny of hominid fossils. Furthermore, characterizing the morphological traits of fossil humans relies heavily on cranial anatomy (Day and Stringer, 1982; Stringer et al. 1984; Tattersall and Schwartz, 2008). Although the known patterns by which human crania vary can be exploited in order to study skeletal remains, there is much about human cranial variation that remains to be understood. Thus far, the unknown has led to disagreement over the defining traits of modern *Homo sapiens* crania, due in part to the mosaic patterns of variation observed in the fossil record (Bräuer and Leakey 1986; Lieberman et al. 2002; Pearson 2008), and in (an arguably larger) part, a result of the morphological heterogeneity present in Holocene modern humans (Howells 1973, 1989; Lahr 1996; Haile-Selassie et al. 2004).

Relatively little is known about the biological etiology of human cranial morphologies and their variation. One way to improve our understanding of these etiologies is to better understand the evolutionary forces that could be influencing the variation observed between and within populations. As a first step in fulfilling that objective, this variation can be analyzed with the goal of adding to what is known about the intraspecific patterns of human cranial variation.

There are two main ways I analyze cranial variation: (1) assessing the range of metric variation and (2) comparing the correlation matrices to assess the relationships among measurements of the cranium. In addition to comparing the cranial variation of Early Period Native Californians to the complete Howells data set, I also distilled two subsets from the Howells data. One subset is composed of Native American populations from the Howells data set, thus allowing for comparisons between the Early Period data and populations with shared ancestry. The other subset is composed of the hunter gatherer populations, representing a sample of individuals with subsistence patterns similar to the Early Period Native Californians.

The W.W. Howells data set (1973, 1989, 1995) provides 82 craniometric measurements and five indices of over 2,500 individuals from 28 Holocene populations worldwide, and is freely and publically available on the internet (<http://web.utk.edu/~auerbach/HOWL.htm>). For analyses of skeletal variation in humans, this data set is currently the best research tool available, due to the robusticity of the data and the detailed manner by which Howells defined anatomical landmarks he used and the measurements he collected, as well as its ease of accessibility. This data set is frequently used to represent the range of modern human cranial variation, to test and to generate hypotheses, to study variation within modern humans, and to study the hominid fossil record. In the majority of paleoanthropological studies, this data set is utilized in comparative analyses of Middle and Late Pleistocene fossil *Homo* to assess morphological affinities to modern humans, and to generate hypotheses relating to the reconstruction of human origins (e.g., Chapter 2; White et al.

2003; Roseman 2016), and is one of the two main comparative data sets used in forensic investigations. Although the Howells data set is the largest publically-available dataset of its kind to provide a quantitative representation of human cranial variation using standard measurements, it is unlikely that the entirety of human cranial variation is captured by these data. The addition of craniometric data from populations that are not represented in the dataset could expand the range of human cranial variation (Howells 1995).

Of the populations included in the Howells data, three are Native American, two of these are from North America, and one is from South America; these samples represent individuals living as recently as the past few centuries and as long ago as ca. 2000 BP (Howells 1973, 1995; Stone et al. 2005). How the range of variation of early Central Californians from ca. 5000 BP compares with that of other modern humans is not well known. Studying these individuals will add to what is known about the biology of early American Indian populations in California, provide a better understanding of the cranial variability within Native Americans, and could add more perspective to variation across modern humans (González-José et al. 2005; Jantz and Ousley 2001).

The Central Californian middle to late Holocene archaeological record is divided into three chronological periods, the earliest of which is the prehistoric Early Period (ca. 4500-2500 BP) (Bartelink 2006). The individuals in this study are from two geographically proximate sites dated to this period (Bartelink 2006). The Native Californians populating the San Francisco Bay area sites during this time belonged to the ethnographically-known Ohlone (Costanoan) tribes of the Windmill culture (Ragir 1972), and Plains Miwok (Interior Miwok) Indians occupied the lower Sacramento Valley (Moratto 1984; Bartelink 2006). Both the Ohlone and Miwok belong to the Utian language family (Bartelink 2006) and lived in tribelets (Kroeber 1925), autonomous, self-governed political groups of around 20 to a few hundred individuals, a social organization that is distinct to Californian Indians. Shell mound faunal records in the Bay Area indicate these sites were occupied year-round (Bartelink 2006, and see Howard 1929; Broughton 1994a, b, 1997, 1999, 2002a, 2002b).

These Native Californians were hunter-gatherers, subsisting on the array of resources that were abundant in mid-late Holocene California, including fish, marine mammals, shellfish, and vegetation, including the seeds and acorns prevalent in the region (Kroeber 1939; Bean and Lawton 1976; Bartelink 2006). The archeological record provides evidence that mortar and pestle technology, likely used to process tougher plant foods, was commonplace beginning ca. 4500 BP, as artifacts of this technology were commonly recovered from Early Period sites (Ragir 1972; Basgall 1987; Wohlgemuth 2004; Bartelink 2006). Isotopic data indicate a substantial component of C<sup>3</sup> plant carbohydrates in the diet (Bartelink 2006). These lines of evidence suggest that acorns and seeds (C<sup>3</sup> plant carbohydrates) likely represented a significant portion of diet, alongside meat proteins from freshwater fish and terrestrial herbivores (Bartelink 2006).

Native American populations display a wide range of skeletal variation (González-José et al. 2001), and the Early Period Native Californian crania are generally quite robust.

However, it is unclear if this feature is related to ancestry, functional requirements of a hunter-gather subsistence strategy and a reliance on tough food items, or systemic factors such as body size, sexual dimorphism, and metabolic rates. While the assessment of variation using the metric range of cranial measurements can provide important information about biological variation, comparing differences between measurements does not reveal as much about the shape of the cranium as the relationship between measurements, which provide a broader picture of cranial shape (Howells 1973). The relationship between measurements can thus provide an additional perspective to biological variation, by elucidating patterns within humans at and below the species level. Furthermore, the principles of integration and modularity necessitate an assessment of the relationships between traits.

Morphological integration or modularity, is a conceptual framework positing that anatomical features that are developmentally, structurally, or functionally related will be strongly correlated (Olson and Miller 1958; Von Dassow and Munro 1999; Hlusko 2004) and theoretically evolve as a unit (Olson and Miller 1958). In other words, a change in one feature is expected to be accompanied by changes in other features that strongly correlate (Smith 1996; Strait 2001). Research on morphological integration of the primate cranium has demonstrated integration among traits related by function and developmental origin (Cheverud 1982, 1995).

Modularity can be defined as relatively independent or dissociated morphological traits or sets of traits; to understand the specific biological or evolutionary processes that engender them, morphologically independent units must be delineated (Klingenberg et al., 2003; Hlusko 2004). In fact, Chernoff and Magwene (1999) define morphological integration as the patterns of correlation among traits to hypothesized modules using *a priori* or *posteriori* hypotheses for the developmental and functional determinants of modularity (Chernoff and Magwene 1999). Research has already provided results in support of the hypothesis that the mammalian skull is comprised of regions of tightly integrated modules, and has demonstrated the presence of strong integration within the hominoid cranium (Leamy et al. 1999; Cheverud 1982, 1996; Martínez-Abadías et al. 2009, 2016). Three major regions, the facial skeleton, basicranium, and neurocranium, are hypothesized modules of the mammalian cranium, hypothesized as such due to their independent evolutionary history and developmental origins (Ackermann and Cheverud 2004; Goswami 2006; 2007; Martínez-Abadías et al 2009). However, there is disagreement as to which regions of the cranium are integrated modules separate from others (Martínez-Abadías et al. 2009). Some disagreement over the basicranium as an integrated cranial module exists, with some researchers arguing that it is not a module (Bastir 2008), while others argue that the basicranium and neurocranium, which together comprise the cranial vault, function collectively as a single integrated unit sometimes called the neuro-basicranial complex (Lieberman et al. 2000 a, b), that is separate from the face. The human cranium has been proposed to be composed only of these two modular regions (Lieberman et al. 2000a, b; Bastir and Rosas 2006; Hallgrímsson et al. 2007). Overall, there seems to be agreement that the human facial skeleton is integrated, but whether there are tightly integrated modules within the facial skeleton, and whether the cranial vault is composed of one or more cranial modules necessitates further research.

The objective of this study is to examine cranial morphological variation in Native Californians from the Early Period (ca 5000 BP) from the Sacramento Valley and the San Francisco Bay Area, which represent hunter gatherers and some of the earliest indigenous Californians, and to compare these data to the W.W. Howells data set (1973, 1989, 1995) to provide additional perspective to the range of cranial variation characterized by a widely-published data set by W.W. Howells (1973, 1989, 1995). By comparing Early Period Native Californian craniometric data to the Howells data set, effectively an assessment of modern human variation, I provide additional perspectives to the range of variation among Native Americans and across *Homo sapiens*. I also take a comparative approach to look at the patterns of correlation, because this approach tends to be more informative and consistent than exploratory approaches like cluster analyses, when considering integration and modularity (Goswami and Polly 2010).

### 3.2 Hypotheses:

#### 3.2.1 First set of hypotheses ( $H_{1A-B}$ ):

$H_{1A}$ : The craniometric variation observed in Early Period Native Californians will be subsumed within the range of variation already reported in the Howells data set.

$H_{1B}$ : The craniometric variation observed in Early Period Native Californians will be subsumed within the range of variation already reported for the Native American populations in the Howells data set.

I first compare the range of variation represented by the complete Howells data set to the Early Period Native Californians ( $H_{1A}$ ). Furthermore, I compare the Native American subset of the Howells data set to the Early Period data to assess how the Early Period Native Californians compare to the Native American range of variation assessed by Howells ( $H_{1B}$ ). As such, the null hypothesis for  $H_{1A}$  and  $H_{1B}$  will be rejected if the range of metric variation for any of the craniometric measurements analyzed in this study is extended by the Early Period Native Californian data.

#### 3.2.2 Second set of hypotheses ( $H_{2A-B}$ ):

$H_{2A}$ : Patterns of correlation for the Early Period Native Californians are more similar to patterns of correlation for populations with shared ancestry (Howells Native American subset) than the complete Howells data.

$H_{2B}$ : Patterns of correlation for the Early Period Native Californians are more similar to patterns of correlation for populations with similar subsistence strategies (hunter gatherer subset of the Howells data) than the complete Howells data.

Subsets of the Howells data representing the hunter gatherer populations, and the Native American populations are of particular relevance to the Early Period Native Californians. The hunter gatherer subset represents populations with similar subsistence patterns, while the Native American populations from the Howells data are relevant due to shared ancestry among Native American populations.

Using patterns of correlation, I compare the Early Period Native Californians to the complete Howells data set, which includes 28 populations of varying ancestry and subsistence strategies, and then to each subset of the Howells data. I hypothesize that patterns of correlation for the Early Period Californians will be more similar to patterns of correlation for the Howells Native American subset than to patterns of correlation for the complete Howells data ( $H_{2A}$ ), and more similar to patterns of correlation for the subset of hunter-gatherers than to patterns of correlation for the complete Howells data ( $H_{2B}$ ). The null hypothesis will be rejected if the patterns of correlation for the Early Period Native Californian sample are not significantly more different from the Native American subset ( $H_{2A}$ ), and the hunter gather subset ( $H_{2B}$ ) than they are from the complete Howells data.

### 3.2.3 Third set of hypotheses ( $H_{3A-C}$ ):

- $H_{3A}$ : The pattern of high correlations within the face relative to the other regions of the cranium observed in the Early Period Native Californian sample will also be characteristic of complete Howells data set.
- $H_{3B}$ : The pattern of high correlations within the face relative to the other regions of the cranium observed in the Early Period Native Californian sample will be characteristic among the populations with shared ancestry (Howells Native American subset).
- $H_{3C}$ : The pattern of high correlations within the face relative to the other regions of the cranium observed in the Early Period Native Californian sample will also be characteristic of populations with similar subsistence strategies (hunter gatherer subset of the Howells data).

Integration and modularity observed at the species level is expected to exist at the intraspecific level (Strait 2001). The Early Period Native Californian sample showed strong, distinct correlations within the facial skeleton, and altogether, the facial skeleton demonstrated stronger within-region correlations relative to the neurocranium and basicranium. Based on the theoretical expectations for integration hypothesized by Strait (2001), I predict that the evidence for integration demonstrated by patterns of correlation for the Early Period Native Californians will also be observed in the correlation matrices for the complete Howells data set ( $H_{3A}$ ), in correlation matrices for populations with a common ancestry shared with the Early Period Native Californians ( $H_{3B}$ ), and for populations whose subsistence strategies were similar to the Early Period

Native Californians (H<sub>3C</sub>).

### 3.3 Materials and methods

I collected craniometric measurements from a sample of middle Holocene Californians dated to the Early Period (ca. 5000 B.P.) using three-dimensional digitization following Howells definitions, and performed statistical analyses to assess metric variation and patterns of correlation.

#### 3.3.1. Materials

##### 3.3.1.A Native Californian data set

My data is composed of prehistoric Native Californians from Central California. All individuals are part of the Native Californian skeletal collection at the Phoebe A. Hearst Museum of Anthropology (PAHMA) at the University of California Berkeley, where all data were collected. Only remains that have been reported to the Department of Interior and Tribal groups as Culturally Unidentifiable under NAGPRA statute were the subjects of this research, in accordance with UCOP skeletal remains policy.

The individuals I studied are from two middle Holocene populations (N=59; 36 males, 23 females) of Early Period Native Californians from the Sacramento Valley (San Joaquin County) and the San Francisco Bay Area (Alameda County). Museum accession numbers preceded by SJO-68, SJO-142, and SJO-56 are from the lower Sacramento Valley excavation sites, and remains with accession numbers preceded by ALA-208, ALA-307, and ALA-308 are from excavations in the San Francisco Bay Area.

##### 3.3.1.A.i Inclusion criteria:

I selected specimens found only at excavation sites dated to the Early Period. Within that subset of specimens, my selection criteria included sex, age, and preservation. I only selected specimens for which the cranium was present and the individual was an adult at the time of death. I also tried to equally represent sex in my sample.

##### 3.3.1.A.ii Age and sex estimation:

I used standard methods to assess the skull and pelvis of each specimen to estimate sex and age. For this study, specific estimation of age was not recorded.

Skeletal changes mediated by normal development and ontogeny provide criteria by which the age at death of a skeletal specimen can be estimated. These criteria include assessment of long bone epiphyseal fusion, eruption of the third molars (Buikstra and Ubelaker 1994), and ectocranial suture closure, especially the basilar suture (Meindl and Lovejoy 1985), as well as age-related changes of the pelvis (Lovejoy et al. 1985; Suchey and Katz 1986; Brooks and Suchey 1990). The overall condition of

the skeleton (Bass 1971; White et al. 2011) and dental attrition (Smith 1984) were also considered.

Sex was estimated using anatomy of the skeleton known to display sexual dimorphism in modern *Homo sapiens*, this includes morphological aspects of the cranium and mandible (Bass 1971; Buikstra and Ubelaker 1994; White et al. 2011), and pelvis (Phenice 1969; Bass 1971; Buikstra and Ubelaker 1994; White et al. 2011).

### 3.3.1.B Comparative data:

For comparative analysis I used the archaeological and historic populations represented in the Howells craniometric dataset (1973, 1989, 1995; <http://web.utk.edu/~auerbach/HOWL.htm>), which includes cranial measurements of over 2,500 adults from 28 Holocene populations across the globe. See Appendix 2 for sample composition of the comparative data.

#### 3.3.1.B.i Native American subset and hunter gatherer subset of Howells' data:

I also compared my data with two subsets of the Howells data (1973, 1989, 1995) in order to sample Native populations from the Americas (N=3), and hunter gatherer populations (N=2) (Huxley 1870; Howells 1974; Stock and Pfeiffer 2001; Thangaraj et al. 2003; Stock 2006; Stock 2013; Pozzi and Belcastro 2015) (Table 1). The hunter gatherer subset is comprised of the Andaman Islanders of Southeast Asia and Bushmen, from South Africa (Howells 1973). The Native American subset is comprised of two populations from North America, one from South Dakota (Howells 1973, 1995) and the other from Santa Cruz Island, California (Howells 1995), in addition to the Yauyos Indians from the Yauyos District of Peru, South America (Howells 1973) (Figure 1).

The South Dakota sample derives from a single village site and the individuals are thought to represent a group of proto-historic Arikara, a Plains Indian tribe that occupied this central South Dakota site between ca. 1600 to 1750 (Howells 1973, 1995). The Santa Cruz Island sample represents a somewhat isolated population thought to be the Chumash tribe, from the last few centuries (Howells 1995). The Peruvian Native American sample is a Pre-Contact sample of individuals from the central Highlands in the Yauyos District of Peru (Howells 1973, 1995), this sample is from the Middle to Late Period, but no more specific or conclusive dates for the material exist (Stone et al. 2015).

### 3.3.2 Methods:

#### 3.3.2.A Linear measurements:

I collected 82 total measurements (76 measurements, 5 indices) of the 88 measurements (82 measurements, 6 indices) in the Howells data (1973) (Auerbach <http://web.utk.edu/~auerbach/HOWL.htm>), and one additional index not included,

Total Facial Index (TFI), which represents the ratio between total facial height and bizygomatic breadth (Bharati et al. 2005). Cranial indices utilize ratios between measurements, and can provide a view into the variation of size and shape of morphology that may indicate population differences (Bharati et al. 2005). The measurements I did not collect were those for which either the measurement or anatomical landmarks involved could not be reproduced with confidence based on Howells' published descriptions and definitions (Howells 1973, 1995). Total Facial Index aside, I followed Howells' protocols and definitions (Howells 1973, 1995) for all anatomical landmarks and measurements I collected, and indices I calculated. Measurements and calculated indices are listed in Tables 2 and 3.

### 3.3.2.B Data collection:

All data were collected using a three-dimensional (3D) digitizer (MicroScribe G2, Immersion Corporation) that has an accuracy of  $\pm 0.38$  mm. This technology is widely used in anthropometric data collection and is also used in forensic departments. I used this technology because it is efficient and it reduces some sources of measurement error: when measurements are collected manually with calipers, anatomical landmarks that are involved in multiple measurements must be located by the researcher each time a measurement involving the landmark is collected. Since 3D coordinates for a landmark will be used to calculate all associated linear measurements, landmarks mutual to numerous measurements need only to be located once per round of measurements. In this way, the 3D digitizer reduces potential measurement error.

All landmark coordinates and measurements were recorded using 3Skull software 2.0.77 (Ousley 2004). The database management software Advantage Data Architect 11.1 (Sybase Advantage Data Architect™) was used to store landmark coordinates and measurements. Because 3Skull is designed to be used in tandem with a 3D digitizer, I followed Ousley's protocols for data collection (2004, and see: <http://math.mercyhurst.edu/~sousley/Videos/3Skull-Ousley.mp4>), with additional guidance from protocols developed and used by the Department of Forensic Anthropology at the New York City Office of the Chief Medical Examiner (NYC OCME, New York, NY) (personal communication, C. Rainwater).

When using a MicroScribe, anatomical landmarks must be located prior to digital data collection for all instrumentally-determined measurements. For these measurements, I used digital calipers to locate anatomical landmarks and marked them using removable, weak adhesive indicators that were not hazardous to the skeletal remains, which were removed immediately following data collection. Each cranium was aligned in the Frankfurt horizontal plane (FHP), and the digitizer and the cranium oriented in FHP were stabilized to prevent them from shifting during data collection.

For each individual, I calculated the average of each cranial measurement. If the values of the repeated trials for a craniometric measurement differed from each other by  $> 5\%$ , I dropped them, rather than averaging them, deeming it an unreliably replicable craniometric measurement for that individual cranium. Twenty-eight of the

traits had measurements dropped. I included measurements with 5% error and set the cut-off at > 5% because the error was exactly 5% in three instances, once for each measurement (BAA, BAR, NAS). These traits represent small parts of the cranium such that the largest recorded value for any of these measurements was 42 mm (NAS). For measurements this small, a difference of one millimeter can return a high percentage error, even though the range of the actual measurements can be small.

After removing measurements for individuals that had > 5% error, the calculated, population-level intraobserver error for all measurements in my dataset averaged  $1.09 \pm 1.2\%$  (min. = 0.0%, max. = 5.00%, median = 0.75%). See Appendix 3 for these craniometric data.

### 3.3.2.C Analyses:

Most statistical analyses were performed in RStudio version 1.0.136 (RStudio Team 2016) using R version 3.3.2 (R Core Team 2016) using APE (Paradis et al. 2004) corrplot (Wei et al. 2016), ggplot2 (Wickham 2009), Hmisc (Harrell 2006), and plyr (Wickham 2011) packages. Descriptive statistics for intra-observer error and quantitative comparisons were performed in Excel version 15.28.

#### 3.3.2.C.i Univariate analyses for first set of hypotheses

To test the first set of hypotheses, I first determined which of the Early Period Native Californian measurements had a range that exceeded that of the comparative samples, the Howells data set ( $H_{1A}$ ) and the Native American subset of the Howells data ( $H_{1B}$ ). For each of these measurements, t-tests were used to compare distributions and determine whether they were significantly different between the Early Period Native Californians and the comparative samples ( $p < 0.25$ ). Because the t-test assumes data are normally distributed, I first assessed the distribution of the data using quantile-quantile (q-q) plots, scatterplots that can be used as a graphical tool to evaluate distribution. All but one measurement (JUB) definitively passed this test for normality, with no indication that distributions were not normal. Following this step, a Welch Two Sample t-test was performed ( $p < 0.25$ ). For the one case where the q-q plot suggested a non-normal distribution, a Wilcoxon rank sum test was used instead. This non-parametric test does not rely on the assumption that data are normally distributed. Both the t-test and the Wilcoxon rank-sum test indicated that the distribution of the Early Period Native Californians data for JUB was not significantly ( $p > 0.25$ ) different from the distribution of this measurement for either comparative sample.

#### 3.3.2.C.ii Correlations:

I built correlation matrices with quantitative phenotypic data to analyze relationships within and among parts of the cranial skeleton. Prior to calculating correlations and constructing correlation matrices, I standardized the data. All linear measurements including those from the Howells data set, were scaled and centered to

the mean, for each population, and for each sex within populations. I chose to use population-specific parameters for this step to preserve biological similarities within populations and differences from other populations captured by raw measurement data. Within populations, measurements were also scaled and centered according to sex to preserve the relative sexual dimorphism within each population. Using population and sex-specific parameters to scale and center the data addresses the problem of size-related shape variation by minimizing the contribution of allometry to correlations (Goswami and Polly 2010). Following Goswami and Polly (2010), I did partition size out of my analyses, but by normalizing the data for relatively similarly-sized individuals separately, which minimizes the relative allometric contribution. This was determined to be the best option because it effectively minimizes relative allometric contribution within each dataset, population and sex specific, while preserving the differences between datasets and the variation within populations. Allometry poses real problems for correlations, both options- removing and keeping some form of allometric contribution, have the potential to create issues (see: Goswami and Polly 2010 for more detail).

I used the Hmisc (Harrell 2006) package to calculate Pearson's correlation coefficient, and used corrplot (Wei et al. 2016) to construct correlation matrices for each sample. The matrices include correlation coefficients for 33 of the cranial measurements I collected (Appendix 4). These measurements were chosen because they assess a particular aspect or trait within one of the regions of the cranium hypothesized to act as a module (Cheverud 1982, 1989, 1995; Lieberman et al. 2000a, b; Ackermann and Cheverud 2004; Hallgrímsson et al. 2004; Bastir and Rosas 2006; Goswami 2006, 2007), and arranged them in anatomical clusters, measurements of the facial skeleton are grouped, as are vault and basicranium measurements, and contained within these cranial regions are clusters of measurements of adjacent anatomical features. While some measurements may represent overlapping regions of the cranium because they measure different aspects of its shape and size, I tried to limit this. A Bonferroni correction was used to adjust the confidence intervals for the pairwise correlations in the matrices. I programmed my code so that any correlation coefficients that are insignificant would be removed from the matrices; none were insignificant. For the purposes of effective data visualization, all weak correlations (ranging from  $-0.3$  to  $0.3$ ) are shown in white and nearly-white colors in the figures. The intention and result of which was to place the focus on the most informative correlations and to provide a better, more easily discernable representation of patterns of correlation while reducing the noise created by the weaker correlations.

### 3.4 Results

Here I describe my observations and results for each of my hypotheses, first comparing the range of variation for the craniometric measurements for the Early Period Californians to the Howells data set, and second, by describing patterns of correlation computed for these data sets.

### 3.4.1 Range of variation ( $H_{1A-B}$ )

Bringing the Early Period Native Californian data into the Howells assessment of worldwide human cranial variation (1973, 1989, 1995) expands the range of human cranial variation, as such, my first hypothesis ( $H_{1A}$ ) is rejected. (See Appendix 5 for photos illustrating the variation and robusticity of the Early Period sample.) This hypothesis was tested by comparing the range of metric variation for each of the 82 cranial measurements collected for the Early Period Native Californians to the range for each of those measurements in the Howells data. I observed that the total range of variation is extended for 20 measurements, 13 of which are significantly different when distributions are compared between data sets (Figure 2).

The range is extended at the maximum end for fifteen (75%) of these measurements, and five measurements extend the minimum end of the range. Of the measurements that extend the maximum end of the range, six are measurements of cranial breadth (ASB, AUB, DKB, JUB, MAB, XCB), one measures cranial height (BBH), one measures anteroposterior length of the frontal bone (FRC), and the remainder measure projections or angles (PAS, AVR, OSR, NBA, NDA, RPA). Four of the measurements that extend the minimum end of the range also assess projection and angulation (OCF, BBA, PAA, SBA), and one measures orbital breadth (OBB). All but one of the measurements are less than 4 mm beyond the extent of the range of measurements for Howells data. This measurement, the radio-parietal angle (RPA), measures the angle at the transmeatal axis where the side opposite the angle is the bregma-lambda or parietal chord (PAC) (Howells 1973). As such, RPA is dependent on the anatomical landmarks bregma and lambda, and the auditory meati that the transmeatal cord runs through, and also to some extent, on the shape of the parietals along the sagittal plane. This measurement characterizes the relative positions of bregma and lambda, where a longer parietal chord, a result of increased distance between the two landmarks either will return a higher RPA. That the PAC is not also a measurement for which our data extends the maximum end of the range is probably a reflection of RPA's reflecting the relative position of these landmarks to each other and relative to the transmeatal axis, whereas PAC is descriptive only of the direct distance between the landmarks.

#### 3.4.1.A Range of Variation compared to Howells' Native Americans

When only the Howells' Native American populations (Arikara, Peru, and Santa Cruz) are considered, the Early Period Native Californians extend the range of variation for 53 different measurements. The maximum end of the range is extended for 43 measurements, while the range for 14 of the measurements is extended at the minimum end, and for four measurements the range is extended at both ends. Of these 53 measurements, 42 of the measurements for Early Period Native Californians are significantly ( $p < 0.25$ ) different from the Howells Native Americans in their relative distribution (Figure 3a–b). Based on these results,  $H_{1B}$  is also rejected.

The maximum end of the range is extended by 1 to 19 mm, while the minimum end of the range is extended at smaller increments, between 0. < 0.5 and 7 mm. Both ends of the range were extended for four measurements (Table 4), including maximum alveolar breadth (MAB), orbital breadth (OBB), maximum cranial breadth (XCB), and cranial index (LBI), an index calculated using cranial height (BBH), breadth (XCB), and length (NOL), Early Period Native Californians are craniometrically most similar to the Santa Cruz population of the Native American populations in the Howells database.

### 3.4.2 Patterns of correlation

Hypotheses two and three tested another perspective on morphological variation, the relationships between traits within and between three main regions of the cranium (Figure 4). By considering these relationships within and between regions of the cranium hypothesized to be integrated and behave as modular units within the cranial complex, I study variation in the patterns of correlation among and between sample sets. Prior to testing my hypotheses, I analyzed the patterns of correlation for the Early Period Native Californians, and describe these results first. Following these results, I apply them to a broader context, comparing them to the correlations for the Howells data to test the second hypothesis. Finally, I compare the Howells Native American and the hunter gatherer subsets to the Early Period Native Californian sample to test the third hypothesis.

#### 3.4.2.A Correlation patterns of Early Period Native Californian crania

The correlation matrix for Native Californians (N = 59) shown in Figure 5 demonstrated strong relationships between a number of craniometric traits within the subsets of measurements that correspond with the cranium, which are organized by region: the facial skeleton, neurocranium, and basicranium. The strongest relationships occurred within the facial skeleton. Some of the correlations between the face and breadth of the neurocranium (XCB, STB, XFB, AUB) were also high (0.5 – 0.9). However, this occurred only for measurements of facial breadth, maximum cheek length, and mastoid height, implying that for the most part, the high correlations observed between the face and neurocranium could have been a result of the overall correlations among traits when accounting for breadth, the integration of mastoid height with the face, and the integration of maximum cheek length with the neurocranium. Nonetheless, correlations within the face were relatively stronger than correlations between the face and the other cranial region subsets, implying that the face is an integrated module for this population.

Within the face, measurements of the cheek and maxillary region (ZMB through MAB, and PRR) were strongly correlated, and these measurements correlated more strongly with each other than measurements of the face. Here correlations ranged from 0.3 to 0.9, and the majority ranged between 0.6 and 0.9. This implies that the maxillary region and the cheek region are integrated within the face, and suggests that this integrated group may behave as a module within the face.

Similar to that observed within the face, there was a highly correlated sub-region within the neurocranium, located at the anterior portion of the frontal bone. There were high correlations among frontal length (FRC), and projection at glabella (GLS) and bregma (BRR), all of which assess forehead size and shape. The strong correlations among these traits suggest that this may be an integrated sub-region of the neurocranium for Early Period Native Californians. Patterns observed within the neurocranium also indicated a strong relationship between measurements of cranial breadth (XCB and AUB) and mastoid height (MDH). As mentioned above, strong correlations for these traits extend throughout the other regions of the cranium. In fact, measurements of the face were more highly correlated overall to MDH than to measurements of the neurocranium, the anatomical region of the cranium in which MDH is located. The majority of correlations between MDH and the neurocranium were weak ( $\leq 0.3$ ). This result suggests that this trait is more integrated with the face even though its anatomical location is elsewhere. While there were some regions of high correlations within the neurocranium, these were not as strong as the those within the face, and correlations within the neurocranium were weaker than those between parts of the neurocranium and the other cranial regions. But if the correlations between the face and maximum cranial breadth (XCB), bi-auricular breadth (AUB), and mastoid height (MDH) can be explained by the strength of correlations between measurements of breadth rather than integration of the neurocranium, and if mastoid height is integrated with the face, this implies the neurocranium is not a modular unit of the cranium. At most, the neurocranium may be weakly integrated. Overall, these results do not provide strong support that the neurocranium is a module within the cranium for this sample.

Overall, weak correlations within the basicranium, and between the basicranium and the other regions of the cranium, were observed. Within the basicranium, the only strong correlations observed were among the occipital angle (OCA) and basion projection (BAR) (-0.5). Correlations between the basicranium and neurocranium were overall weakly patterned, but among the correlations ranging from  $\leq -0.3$  or  $\geq 0.3$ , there was patterning indicative of some integration between occipital breadth (ASB) within the basicranium. The strongest of the correlations between ASB and the neurocranium also measure breadth (XCB, XFB, AUB, STB), and these correlations were  $\leq -0.6$  or  $\geq 0.6$ . Interestingly, occipital length as measured from lambda to opisthocranium (OCC) was highly correlated with nasal height (NLH), glabella projection, and parietal angle (PAA), while the occipital angle (OCA), a measurement that accounts for the flatness of the occipital bone in the sagittal plane, was highly negatively correlated (-0.6 to -0.8) with alveolar breath (MAB), bijugal breadth (JUB), and maximum cheek length (XML), all of which are part of the highly correlated sub-region of the face (mid-face through maxillary region) described above. This sub-region also had the strongest correlations within the face. However, because a larger angle represents a flatter surface, high negative correlations for OCA and other angular measurements indicate the occipital angle was smaller, which translates to a more angular anatomical morphology, when the aforementioned measurements of facial breadth and cheek length increased. Additionally, basion projection (BAR) was highly negatively correlated (-0.7 to -0.8) with

frontal subtense (FRS), a measurement that assesses the prominence of the frontal bone and is indicative of frontal bone curvature along the midsagittal plane (Howells 1973). Occipital breadth was more integrated with the face and neurocranium than within the basicranium. The low correlations within the basicranium relative to those observed between the basicranium and other regions imply that the cranial base does not behave as a module within the cranium for this sample. Furthermore, correlations among the neurocranium and basicranium do not support the presence of a highly integrated neuro-basicranial complex (Lieberman et al. 2000a, b) in these Native Californians.

#### 3.4.2.B Patterns of correlation for the Howells data

Before describing the results of hypotheses two and three, I describe the patterns of correlation for the Howells data and subsets of the Howells data, and compare them to the Early Period Native Californian sample.

##### 3.4.2.B.i Howells' complete data set:

Overall, the correlations for the Howells data were weak, and there were few similarities to the correlations for Early Period Native Californians. Within regions of the cranium, there were few regions exhibiting strong relationships, but aside from a few similarities in the general patterning of correlations between the Howells data and the Early Period Native Californian data, correlations of the Howells' complete data varied significantly from the Early Period Native Californians for all cranial regions.

Of the cranial regions, the face had the strongest correlations. Within the face, correlations  $r > 0.5$  were the minority, but the correlations  $> 0.5$  that were observed were between maximum facial breadth (FMB) and other breadth measurements within the upper face. The higher correlations ( $r > 0.5$ ) were related to the orbital region, including orbital breadth and inter-orbital breadth (DKB), and the breadth of the mid-facial (cheek) region, including zygomatic breadth and bijugal breadth, both of which were highly correlated with each other, and correlated with orbital breadth and zygomaxillary breadth. Facial height measured from nasion to prosthion (NPH) is strongly correlated to nasal height. A strong pattern of correlation was also observed among measurements of radius of the nasal bones (nasion radius), zygomatic radius, and prosthion radius, all of which are measurements that assess projection. A relatively strong relationship between the cheek region the frontal bone of the neurocranium was also observed. Similar patterns were observed for Early Period Native Californians, but in the Native Californian sample the strength of these relationships was stronger. For both samples, traits for cranial breadth within the neurocranium exhibited high correlations with other measurements of breadth throughout the cranium, and mastoid height strongly correlated with the cheek region of the face. Correlations within the neurocranium for mastoid height were lower than those between mastoid height and the face in both samples, which supports that mastoid height is integrated with the face more than the neurocranium across human populations. On the basis of

qualitative observations these matrices differ. These matrices also differ quantitatively: the results of a Mantel test performed to compare the correlations for Early Period Native Californians to those for the complete Howells data indicate that these matrices differ significantly (Mantel test,  $r = 70$ ,  $p = < .0001$ ).

#### 3.4.2.B.ii Native American and hunter gatherer subsets of Howells' data

In addition to comparing the Early Period Native Californian correlation matrix to the Howells dataset, I compared it to two subsets of the Howells data. One subset is comprised of the three Native American populations (Arikara, Santa Cruz, Peru) Howells measured, while the other is comprised of two hunter gatherer populations (Andaman and Bushman).

For both the hunter-gatherers and Native Americans, correlations (Figure 5) within the face were strongest relative to the other regions. For these two samples, patterns of correlations within the face were similar. Compared to the Early Period Native Californians, the relationships were weaker, but stronger than the correlations observed for Howells complete data set.

#### 3.4.2.B.iii Second set of hypotheses ( $H_{2A-B}$ ):

On the basis of qualitative observations, the correlations for the Howells complete data differ from the Early Period Native Californian matrix. Quantitatively, these matrices also differ; the results of a Mantel test performed to compare correlation matrices indicated that the correlations for Early Period Native Californians and the Howells complete data set differ significantly (Mantel test,  $r = 70$ ,  $p = < .0001$ ).

The matrix for the hunter gatherers does not correlate significantly with Early Period Native Californians either (Mantel test,  $r = 71$ ,  $p = < .0001$ ), nor does the matrix for the Howells Native American subset (Mantel test,  $r = 72$ ,  $p = < .0001$ ). As such, on a quantitative basis,  $H_{2A}$  and  $H_{2B}$  are rejected. However, results of the Mantel tests comparing the Early Period Native Californian correlation matrix to the matrices for Howells' complete data and two subsets were similar, implying that the patterns of correlation for the Early Period sample are not significantly more similar to any one of the comparative samples. The same result is observed when these matrices are assessed qualitatively.

#### 3.4.2.B.iv Third set of hypotheses ( $H_{3A-C}$ ):

Based on the highly correlated facial skeleton observed in the Early Period Native Californian sample, I predicted the third set of hypotheses, which proposed that this pattern would also be observed among all modern humans as represented by the Howells data set ( $H_{3A}$ ), and that it would also be observed in the Native American ( $H_{3B}$ ) and hunter gatherer ( $H_{3C}$ ) subsets of the Howells data. For all sample sets of the Howells data, the face was the most strongly correlated region of the cranium. As such, all three parts of the third hypothesis ( $H_{3A-C}$ ) are supported. For the Howells

samples, the correlations within the face were also stronger than those between measurements of the face and measurements within other regions of the cranium, which was also observed in the Early Period Native Californians.

### 3.5 Discussion and conclusions:

#### 3.5.1 Range of variation for measurements:

Bringing craniometric data from Early Period Californians into the range of human cranial variation assessed by Howells (1973, 1989, 1995) extends the range of human cranial variation for 20 of 84 measurements, but does so in small (< 4mm) increments. For the Native American subset of data, the range is extended more dramatically than for the complete Howells dataset. Early Period Californians extend the range of Native American cranial variation for almost half of the cranial measurements, and the increments by which the ranges are extended are relatively larger.

Overall, these observations imply that Early Period Native Californians have on average, wider crania, and the projections and angulation of a variety of regions throughout the cranium are more pronounced. While the Early Period Native Californian craniometric data extend the range of human cranial variation represented by Howells data, 95% of these measurements extend the Howells range by < 4 mm, which was less than the standard deviation of each of the measurements for the Howells data. So, while the range of variation is extended by the addition of the Early Period Native Californians, as Howells himself would have hypothesized (1995), the magnitude by which the range is extended is small and in most cases, less than the within-geographic region standard deviation of the measurement.

There are two main patterns by which the Early Period Native Californians extend the range of variation. The primary pattern observed was the extension at the maximum end of the range for measurements of breadth throughout the cranium. In the facial skeleton, this included the upper facial measurement interorbital breadth, and in the masticatory and cheek region of the mid and lower face, alveolar breadth and bijugal breadth. Within the cranial vault, the range for maximum cranial breadth (XCB) and bi-auricular breadth (AUB), both within the neurocranium, and biasterionic breadth (ASB) within the basicranium, were also extended at the upper end. The secondary pattern observed was the extension of the range for measurements that assess shape via projection and angulation throughout the cranium.

When Early Period Native Californians are brought into a subset for Howells' Native American data, the range of variation for metric measurements was extended more significantly. The Early Period Native Californians extend the range of Native American variation across a range of cranial traits. Forty-three measurements extend the range of variation at the maximum end, and 14 measurements extend the minimum end of the range.

The measurements that extend the maximum end of the range by an average of 6 mm (range = 1 to 19 mm). While the measurements that extend the minimum end of

the range do so by 3 mm on average, ranging from < 0.5 to 7 mm beyond the minimum end of the range for the Howells Native Americans. The Early Period Native Americans extend both ends of the range for the standard cranial index (LBI), but not for LBI2, which takes into account nasio-occipital length and maximum cranial breadth, instead of glabello-occipital length and maximum cranial breadth, as is the standard (LBI), for which supraorbital development is a factor (Howells, 1973). That the Early Period Native American data extends the range at both ends for LBI and maximum cranial breadth, but extends only the minimum end of the range for LBI2, implies that there is more variation in supraorbital development in the Early Period Native Americans than in the later Native American populations sampled by Howells. While the range for cranial length (NOL and GOL) are both extended at the maximum end, that the measurement reliant on glabella (GOL) is extended by a larger magnitude (9 mm) than nasio-occipital length, which does not (extends range by 5 mm), provides further support to this conclusion. The maximum extent of the range for the cranial module (CRM), which is calculated by averaging cranial length (GOL), breadth (XCB), and height (BBH), is also extended by the Early Period Native Californians. Altogether, these results demonstrate that the Early Period Native Californians were not only more craniometrically variable than the later Holocene Native Americans assessed by Howells, but some individuals also had larger crania overall. Although the Native Americans in the Howells database represent three geographically disparate populations (Santa Cruz, South Dakota, and Peru), the Early Period Native Americans widen the range of craniometric variation across all three of the Howells Native American groups.

Overall, the range of human cranial variation is extended by the Early Period Native Californian data but in small increments. For the Native American populations however, it is extended more dramatically, demonstrating that there is a wide range of cranial variation among Native American populations, corroborating previous research stating that Native groups from the Americas are highly polymorphic and have high levels of heterogeneity (González-José et al. 2001).

My results demonstrate that the study of other living and extinct Native American populations, using Howells measurement definitions so that this widely-used data set can be expanded may extend the range of variation further and provide other important perspectives on the range of variation in these indigenous groups. This research would apply to a number of fields of study including, but not limited to archaeology, human biology and evolution, and in forensics.

### 3.5.2 Patterns of correlation:

Across all samples, the facial skeleton demonstrated the strongest evidence of morphological integration. This study demonstrates integration of the facial skeleton occurs in humans across geographic regions (Howells' complete data set), shared ancestry (Native American subset) and subsistence strategy (hunter gatherers), including populations from ca. 5000 B.P. While the Early Period Native Americans may be more closely related to each other than the Native American groups measured by Howells, save for the relatively isolated (Howells 1995) Santa Cruz Island population,

that the face shows the highest integration across all samples suggests that pattern is most likely underlain by genetic effects. This evidence for integration within the facial skeleton corroborates previous research demonstrating that the mammalian facial skeleton is an integrated region that varies fairly independently from the rest of the cranium

(Cheverud 1982; 1989; 1995; Lieberman et al. 2000a,b; Ackermann and Cheverud 2004; Hallgrímsson et al. 2004; Goswami 2006). I also observed regions of higher correlation within the face among measurements of the mid-face (cheek) and maxilla, which could imply that these traits are more tightly integrated with each other and act as a module within the facial skeleton that other parts of the face are dissociated with, to some degree. When traits were dissociated in the face, they tended to do so around the nasal and orbital regions, specifically, orbital height, interorbital breadth, and nasal breadth and height, suggesting that these traits of the upper face are not tightly integrated within this region of the cranium, as demonstrated by Lieberman et al. (2000a,b) and Bastir (2008). For the Early Period Native Californians, there is evidence that the mid-face and the forehead regions of the facial and neurocranium, respectively, act as integrated modules within the larger integrated regions of the facial skeleton and neurocranium.

The basicranium demonstrated the least integration across all samples. While the basicranium was observed to have low correlations, of the samples analyzed, the strongest within-basicranium correlations were observed in the Early Period sample. The traits included for the basicranium represent angle of the occiput (OCA), occipital breadth (ASB) and length (OCC), and basion projection (BAR), fewer than the number of traits for the facial skeleton (N=17) and the neurocranium (N=12). Although fewer craniometric traits were included in the analysis of correlations within the basicranium, the measurements I included sufficiently describe the shape and dimensions of the majority of the basicranium. As such, the lack of integration demonstrated within the basicranium for the Native Californians is unlikely a result of not having included enough basicranial traits. As such, these results lend support to previous research suggesting the basicranium is not an integrated unit (Bastir 2008). Across all samples, I did not observe strong correlations among measurements of the neurocranium and basicranium that support the hypothesis that these two regions are integrated and behave as a single cranial module (Lieberman et al. 2000a,b; Bastir and Rosas 2006; Hallgrímsson et al. 2007). Insofar as modularity, that the face exhibits such strong integration across samples not observed in the other regions could be interpreted as evidence for a neuro-basicranial complex in humans, but this interpretation must be rejected when weak correlations I observed among measurements of the neurocranium and basicranium are taken into account. Overall, this study demonstrates integration of the facial skeleton occurs in humans across geographic regions (Howells complete data set (Howells 1973, 1989, 1995), shared ancestry (Native American subset) and subsistence strategy (hunter gatherers) among humans including populations from ca. 5000 B.P.

### 3.6 Acknowledgements

This project would not have been possible without the support and assistance of the following people and institutions: C. Rainwater; S. Sholts, Department of Anthropology, National Museum of Natural History, Smithsonian Institution; T. White, and the Human Evolution Research Center; and Natasha Johnson and Benjamin W. Porter, Director, of the Phoebe A. Hearst Museum of Anthropology. Many thanks also to Stephanie DeGraaf, Department of Statistics, University of California Berkeley. Special thanks to colleagues in the Department of Integrative biology for their feedback: J. Carlson, M. Brasil, T. Monson. And to J. L. Reed for providing invaluable feedback and support. This research was supported in part by the Beim Scholarship through the Department of Integrative Biology, University of California, Berkeley.

### 3.7 References:

- Ackermann RR, Cheverud JM. 2004. Morphological integration in primate evolution. In: Pigliucci M, Preston K, editors. Phenotypic integration. Oxford: Oxford University Press. pp. 302–319.
- Bartelink EJ. 2006. Resource Intensification in Pre-Contact Central California: A Bioarchaeological perspective on diet and health patterns among hunter-gatherers from the Lower Sacramento Valley and San Francisco Bay. Ph.D. dissertation, Department of Anthropology, Texas A&M University.
- Basgall ME. 1987 Resource intensification among hunter-gatherers: Acorn economies in prehistoric California. *Res Econ Anthropol* 9:21–52.
- Bass WM. 1971. Human osteology: A laboratory and field manual of the human skeleton. Columbia, MO: Missouri Archaeological Society.
- Bastir M, Rosas A. 2006. Correlated variation between the lateral basicranium and the face: A Geometric morphometric study in different human groups. *Arch Oral Biol* 51:814–824.
- Bastir M. 2008. A systems-model for the morphological analysis of integration and modularity in human craniofacial evolution. *J Anthropol Sci* 86:37–58.
- Bean LJ, Lawton H. 1976. Some explanations for the rise of cultural complexity in Native California with comments on proto-agriculture and agriculture. In: LJ Bean and TC Blackburn, editors. *Native Californians: A Theoretical Retrospective*, New Mexico: Ballena Press. pp. 19–48.
- Bharati S, Demarchi DA, Mukherji D, Vasulu TS, Bharati P. 2005. Spatial patterns of anthropometric variation in India with reference to geographic, climatic, ethnic and linguistic backgrounds. *Ann Hum Biol* 32:407–444.
- Brooks ST, Suchey JM. 1990. Skeletal age determination based on the os pubis: A Comparison of the Acsadi-Nemerskeri and Suchey-Brooks methods. *Hum Evol* 5:227–238.
- Broughton JM. 1994a Declines in Mammalian Foraging Efficiency during the Late Holocene, San Francisco Bay, California. *Journal of Anthropological Archaeology* 13:371–401.
- Broughton JM. 1994b Late Holocene Resource Intensification in the Sacramento Valley, California: The Vertebrate Evidence. *Journal of Archaeological Science* 21:501–514.
- Broughton JM. 1997. Widening Diet Breadth, Declining Foraging Efficiency, and Prehistoric Harvest Pressure: Ichthyofaunal Evidence from the Emeryville Shellmound, California. *Antiquity* 71(274):845–862.
- Broughton JM. 1999. Resource Depression and Intensification During the Late Holocene, San Francisco Bay. University of California Publications: Anthropological Records 32. University of California Press, Berkeley.
- Broughton JM. 2002a. Pre-Columbian Human Impact on California Vertebrates: Evidence from Old Bones and Implications for Wilderness Policy. In: CE Kay and RT Simmons, editors. *Wilderness and Political Ecology: Aboriginal Influences*

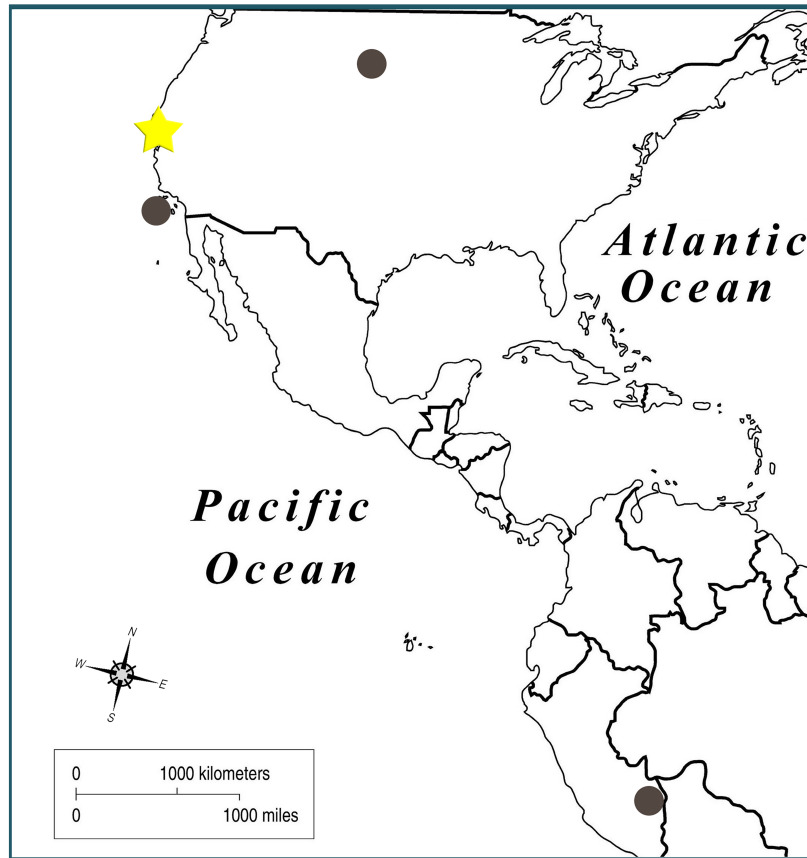
- and the Original State of Nature Salt Lake City: University of Utah Press. pp. 44–71.
- Broughton JM. 2002b. Prey Spatial Structure and Behavior Affect Archaeological Tests of Optimal Foraging Models: Examples from the Emeryville Shellmound Vertebrate Fauna. *World Archaeol* 34:60–83.
- Buikstra JE, Ubelaker DH. 1994. Standards for data collection from human skeletal remains: Proceedings of a seminar at the Field Museum of Natural History. Fayetteville: Arkansas Archaeological Research Series No. 44. Fayetteville: Arkansas Archaeological Survey.
- Chernoff B, Magwene PM. 1999. Afterword. In: Olson EC, Miller PL, editors. *Morphological Integration*. Chicago: University of Chicago. pp. 319–353.
- Cheverud JM. 1982. Phenotypic, genetic, and environmental morphological integration in the cranium. *Evolution* 36:499–516.
- Cheverud JM. 1989. A comparative analysis of morphological variation patterns in the papionins. *Evolution* 43:1737–1747.
- Cheverud JM. 1995. Morphological integration in the saddle-back tamarin (*Saguinus fuscicollis*) cranium. *Am Nat* 145:63–89.
- Cheverud JM. 1996. Developmental integration and the evolution of pleiotropy. *Am Zool* 36:44–50.
- González-José R, Ramírez-Rozzi F, Sardi M, Martínez-Abadías N, Hernández M, Pucciarelli H. 2005. Functional-craniology approach to the influence of economic strategy on skull morphology. *Am J Phys Anthropol* 128:757–771.
- González-José R, Dahinten SL, Luis MA, Hernández M, Pucciarelli HM. 2001. Craniometric variation and the settlement of the Americas: Testing hypotheses by means of R-matrix and matrix correlation analyses. *Am J Phys Anthropol* 116(2):154–165.
- Goswami A. 2006. Cranial modularity shifts during mammalian evolution. *Am Nat* 168:270–280.
- Goswami A. 2007. Cranial modularity and sequence heterochrony in mammals. *Evol Dev*, 9:290–298.
- Goswami A, Polly PD. 2010. Methods for Studying Morphological Integration and Modularity. *Paleontological Society Papers* 16:213–244.
- Hallgrímsson B, Lieberman DE, Liu W, Ford-Hutchinson AF, Jirik FR. 2007. Epigenetic interactions and the structure of phenotypic variation in the cranium. *Evol Dev* 9:76–91.
- Hallgrímsson B, Willmore K, Dorval C, Cooper DM. 2004. Craniofacial variability and modularity in macaques and mice. *J Exp Zool B: Mol Dev Evol* 302:207–225.
- Harrell FE. 2006. Hmisc package. Available online at [http:// biostat.mc.vanderbilt.edu/twiki/ bin/ view/ Main/ Hmisc](http://biostat.mc.vanderbilt.edu/twiki/bin/view/Main/Hmisc).
- Hlusko LJ. 2004. Integrating the genotype and phenotype in hominid paleontology. *P Natl Acad Sci USA* 101(9): 2653–2657.
- Howard H. 1929 *The Avifauna of Emeryville Shellmound*. University of California Press, Berkeley.

- Howells WW. 1973. Cranial Variation in Man. A Study by multivariate analysis of patterns of differences among recent human populations. *Peabody Mus Amer Arch Ethnol* 67.
- Howells WW. 1974. *The Pacific Islanders* (Vol. 2). Scribner Book Company.
- Howells WW. 1989. Skull shapes and the map. Craniometric analyses in the dispersion of modern Homo. *Peabody Mus Amer Arch Ethnol* 79.
- Howells WW. 1995. Who's Who in Skulls. Ethnic identification of crania from measurements. *Peabody Mus Amer Arch Ethnol* 82.
- Huxley TH. 1870. On the geographical distribution of the chief modifications of mankind. *The Journal of the Ethnological Society of London (1869–1870)* 2(4): 404–412.
- Jantz RL, Owsley DW. 2001. Variation among early North American crania. *Am J Phys Anthropol* 114(2):146–155.
- Klingenberg CP, Mebus K, Auffray J-C. 2003. Developmental integration in a complex morphological structure: How distinct are the modules in the mouse mandible? *Evol Dev* 5:522–531.
- Kroeber AL. 1925. *Handbook of the Indians of California*. Washington, D.C.: Smithsonian Institution, Bureau of American Ethnology Bulletin 78.
- Kroeber AL. 1939 *Cultural and Natural Areas of Native North America*. In: University of California Publications in American Archaeology and Ethnology, pp. 1–240, Berkeley.
- Leamy LJ, Routman EJ, Cheverud JM. 1999. Quantitative trait loci for early-and late-developing skull characters in mice: A Test of the genetic independence model of morphological integration. *Am Nat* 153(2):201–214.
- Lieberman DE, Mowbray KM, Pearson OM 2000a Basicranial influences on overall cranial shape. *J Hum Evol* 38:291–315.
- Lieberman DE, Ross CR, Ravosa M 2000b The primate cranial base: Ontogeny, function and integration. *Ybk Phys Anthropol* 43:117–169.
- Lovejoy CO, Meindl RS, Pryzbeck TR, Mensforth RP. 1985. Chronological metamorphosis of the auricular surface of the ilium: A New method for the determination of adult skeletal age at death. *Am J Phys Anthropol* 68:15–28.
- Martínez-Abadías N, Esparza M, Sjøvold T, González-José R, Santos M., Hernández M. 2009. Heritability of human cranial dimensions: Comparing the evolvability of different cranial regions. *J Anat* 214:19–35.
- Martínez-Abadías, N., Esparza, M., Sjøvold, T., & Hallgrímsson, B. 2016. Chondrocranial Growth, Developmental Integration and Evolvability in the Human Skull. In: Boughner J.C. and Rolian C., editors. *Developmental Approaches to Human Evolution*. Hoboken, NJ: John Wiley & Sons. pp. 17–34.
- Meindl RS, Lovejoy CO. 1985. Ectocranial suture closure: A Revised method for the determination of skeletal age at death based on the lateral-anterior sutures. *Am J Phys Anthropol* 68:57–66.
- Moratto M. 1984. *California Archaeology*. Orlando: Academic Press, Inc.
- Olson EC, Miller RL. 1958. *Morphological Integration*. Chicago: University of Chicago Press.

- Ousley S. 2004. Threeskull 2.0.77 [Computer Program]
- Paradis E, Claude J, Strimmer K. 2004. APE: Analyses of phylogenetics and evolution in R language. *Bioinformatics* 20:289–290.
- Pearson OM. 2008. Statistical and biological definitions of “anatomically modern” humans: suggestions for a unified approach to modern morphology. *Evol Anthropol* 17: 38–48.
- Phenice TW. 1969 A Newly Developed Visual Method of Sexing the Os Pubis. *Am J Phys Anthropol* 30:297–301.
- Pozzi A, Belcastro MG. 2015. A global study of sex dimorphism variability in modern humans' crania. 21st Congress Italian Anthropological Association, Next-Generation Anthropology: Challenges and synergies Bologna/Ravenna.
- Ragir S. 1972. The Early Horizon in Central California Prehistory. Contributions of the University of California Archaeological Research Facility 15. Berkeley: University of California Press.
- R Core Team 2016. R: A Language and environment for statistical computing. R Foundation for Statistical Computing, Vienna, Austria. URL <https://www.R-project.org/>.
- Roseman CC. 2016. Random genetic drift, natural selection, and noise in human cranial evolution. *Am J Phys Anthropol* 160:582–592.
- RStudio Team 2016. RStudio 1.0.136: Integrated Development for R. RStudio, Inc., Boston, MA URL <http://www.rstudio.com/>.
- Smith BH. 1984. Patterns of molar wear in hunter-gatherers and agriculturalists. *Am J Phys Anthropol* 63:39–56.
- Smith KK. 1996. Integration of craniofacial structures during development in mammals. *Am Zool* 36:70–79.
- Stock JT. 2006. Hunter-gatherer postcranial robusticity relative to patterns of mobility, climatic adaptation, and selection for tissue economy. *Am J Phys Anthropol* 131:194–204.
- Stock JT. 2013. The skeletal phenotype of “Negritos” from the Andaman Islands and Philippines relative to global variation among hunter-gatherers. *Hum Biol* 85:67–94.
- Stock JT, Pfeiffer S. 2001. Linking the structural variability in long bone diaphyses to habitual behaviors: Foragers from southern African Later Stone Age and the Andaman Islands. *Am J Phys Anthropol* 115:337–348.
- Stone JH, Chew K, Ross AH, Verano JW. 2015. Craniofacial plasticity in ancient Peru. *Anthropologischer Anzeiger* 72:169–183.
- Strait DS. 2001. Integration, phylogeny, and the hominid cranial base. *Am J Phys Anthropol* 114:273–297.
- Suchey J, Katz D. 1986. Skeletal age standards derived from an extensive multiracial sample of modern Americans. *Am J Phys Anthropol* 69:269.
- Thangaraj K, Singh L, Reddy AG, Rao VR, Sehgal SC, Underhill PA, Pierson M, Frame IG, Hagelberg E. 2003. Genetic affinities of the Andaman Islanders, a vanishing human population. *Curr Biol* 13:86–93.

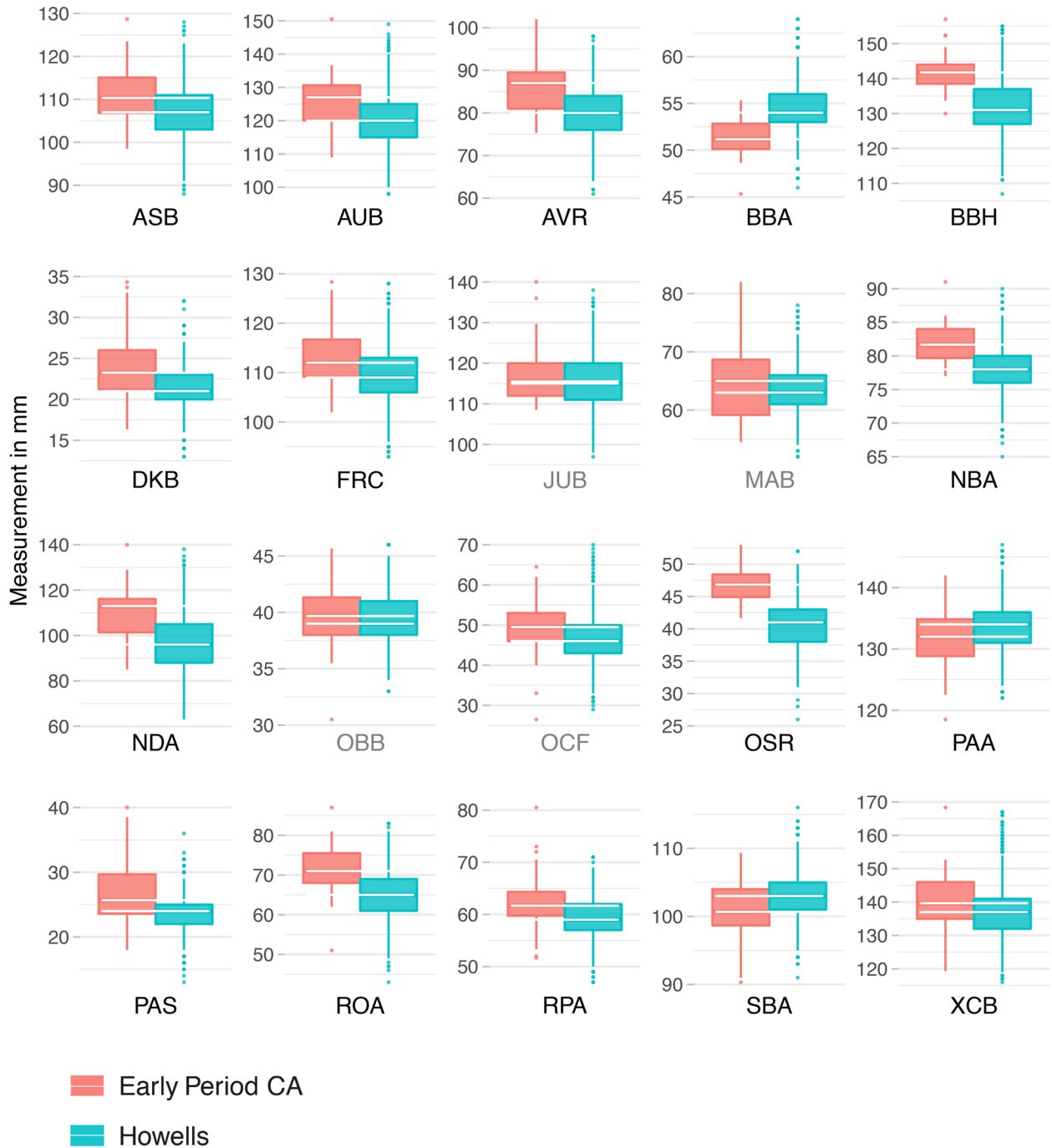
- von Dassow G, Munro E. 1999. Modularity in animal development and evolution: Elements of a conceptual framework for EvoDevo. *J Exp Zool* 285:307–325.
- Wei T, Simko V, Wei MT. 2016. Package ‘corrplot’. *Statistician* 56:316–324.
- White TD, Asfaw B, DeGusta D, Gilbert H, Richards GD, Suwa G, and Howell FC. 2003. Pleistocene *Homo sapiens* from Middle Awash, Ethiopia. *Nature* 423:742–747.
- White TD, Black MT, Folkens PA. 2011. *Human osteology*. San Diego, CA: Academic press.
- Wickham H. 2009. *ggplot2: Elegant graphics for data analysis*. Springer: New York.
- Wohlgemuth, E. 2004 *The Course of Plant Food Intensification in Native Central California*. Ph.D. dissertation, University of California, Davis.

Figure 1. Geographic locations of Howells Native American populations and Early Period Native Californians.



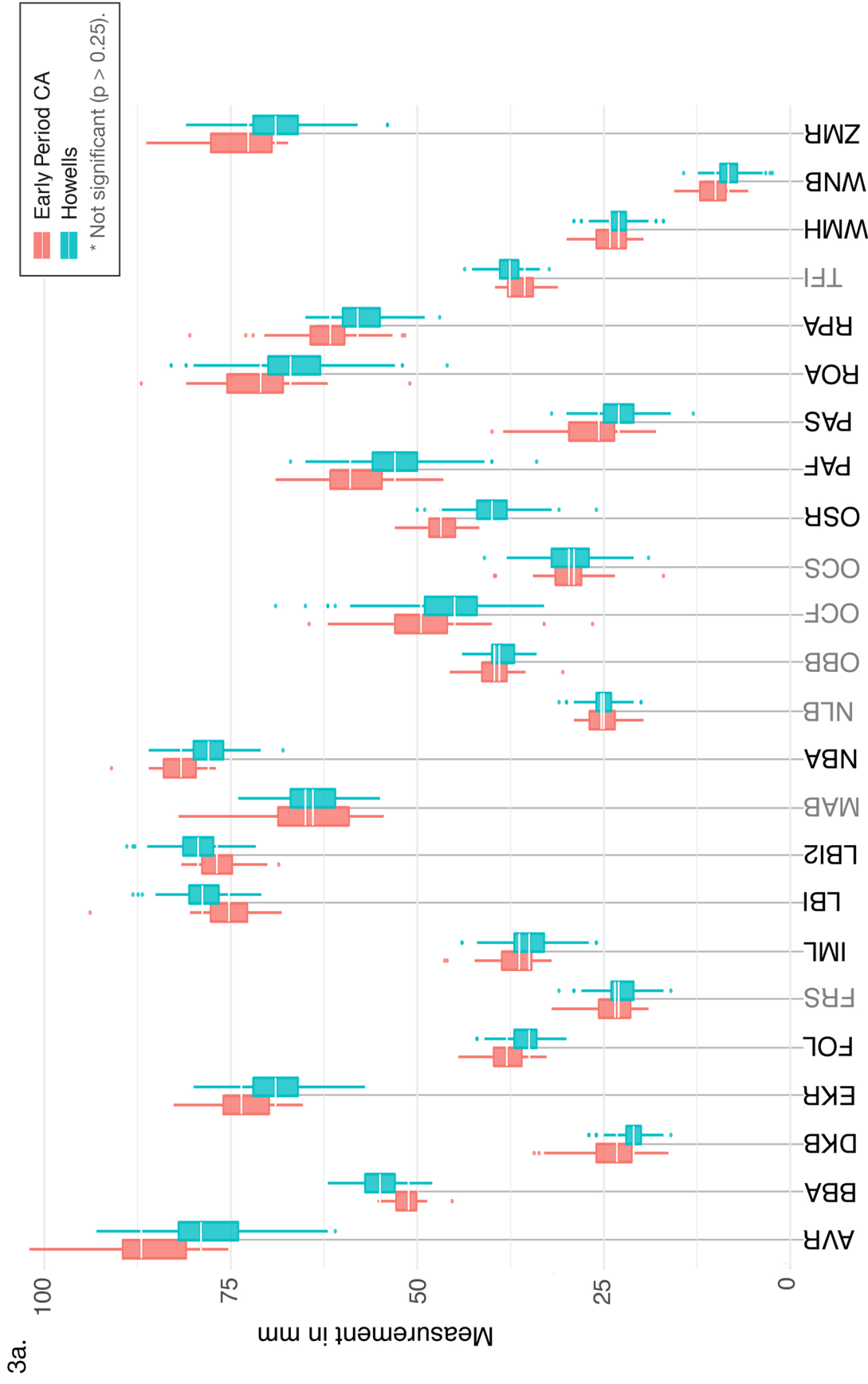
Map with circles indicating the geographic locations of Native Americans in the Howells data (1973, 1989, 1995). From top, clockwise: Early Arikara, South Dakota; Yauyos, Peru; Chumash, Santa Cruz Island, CA. The Early Period Native Californian (Plains Miwok and Ohlone) data presented in this study are from the geographic area indicated by the yellow star.

Figure 2. Measurements for which the Early Period CA data extend the range of variation for all the Howells data.\*



\*Gray headings indicate the Early Period Native Californian was not significantly different from the range of Howells variation for that measurement. For all other measurements  $p < 0.25$ .

Figure 3a,b. Measurements for which the Early Period CA data extend the range for Howells' Native Americans.



\*Gray headings indicate the Early Period Native Californian was not significantly different from the range of Howells variation for that measurement. For all other measurements  $p < 0.25$ . The outlier for LBI and XCB among the Native Californian data is explained by the wide cranial breadth (168.3 mm) of SJO-142-5808. The outlier for OBB is explained by the narrow orbital breadth (OBB) of SJO-142-5679 (30.5 mm).

3b.

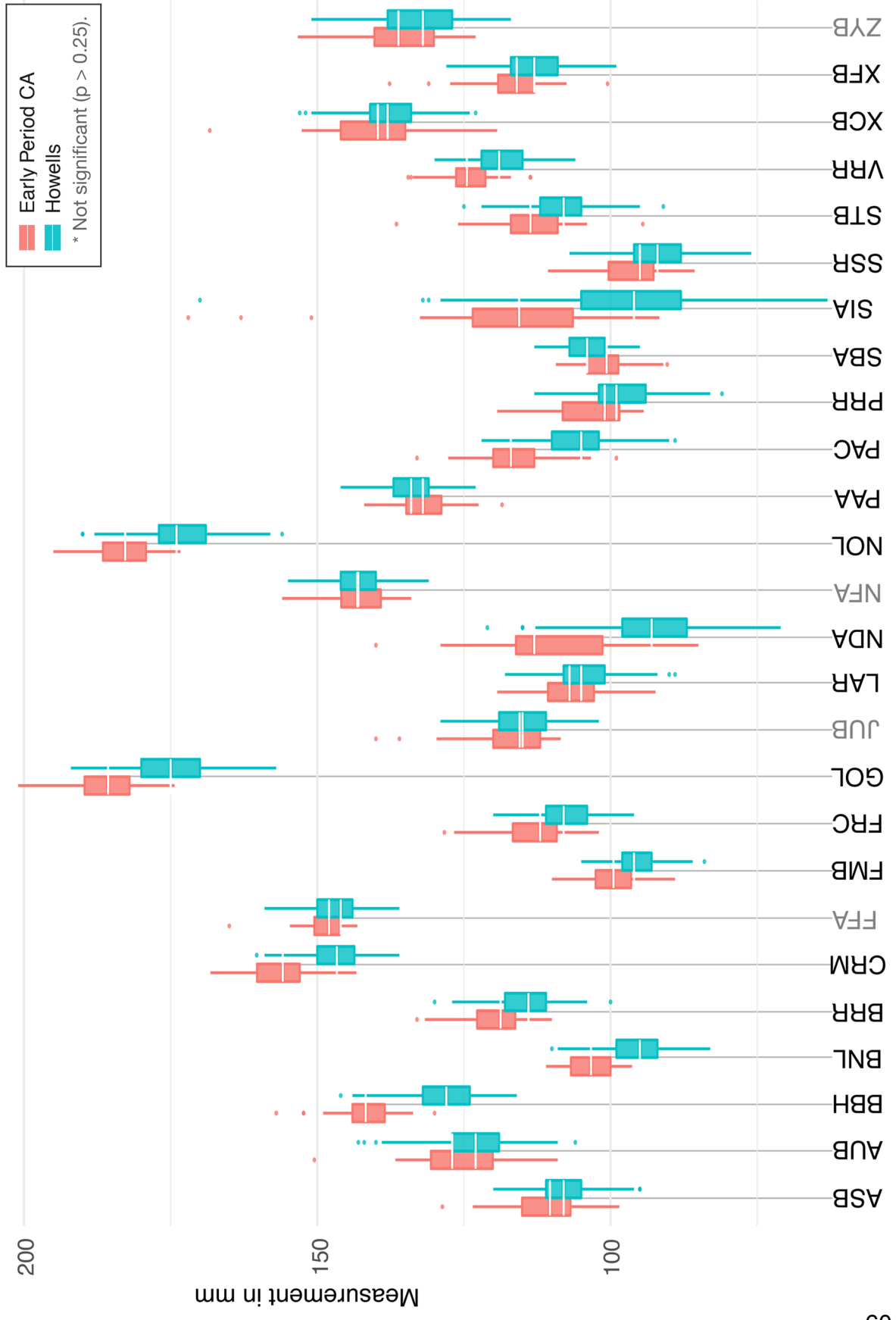


Figure 4. Guide to correlation matrices used in craniometric analyses.

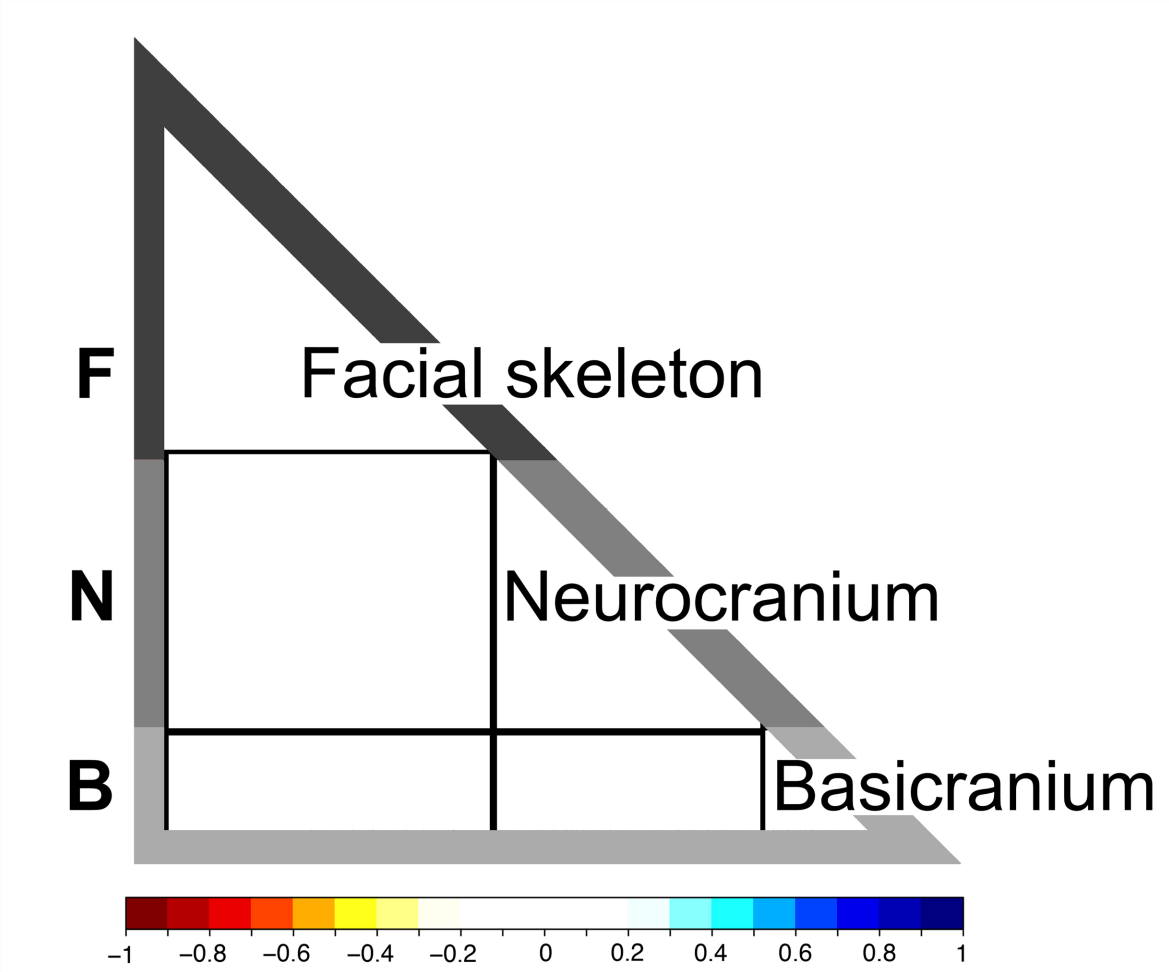


Figure 5. Correlation matrices for all samples tested.

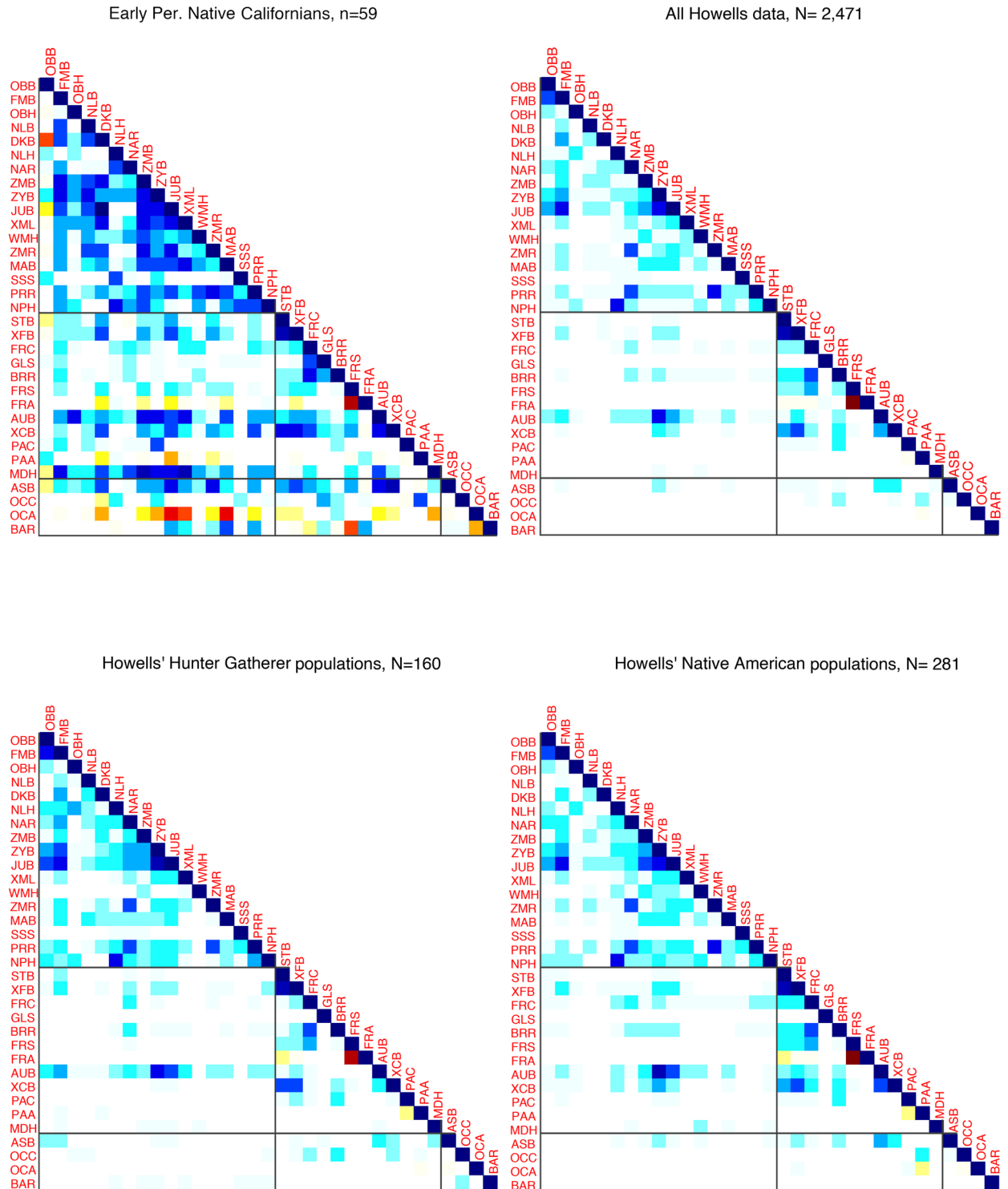


Table 1. Descriptive statistics of samples.

<b>Howells' data</b>	<b>M</b>	<b>F</b>	<b>Total</b>	
<i>26 populations</i>	1368	1156	2524	
<hr/>				
<b>Howells' data subsets</b>	<b>Geographic region</b>	<b>M</b>	<b>F</b>	<b>Total</b>
<i>Native American</i>				
Early Arikara, SD	Americas	42	27	69
Peru, Yauyos District	"	55	55	110
Santa Cruz Island, CA	"	51	51	102
				<b>281</b>
<i>Hunter gatherer</i>				
Andaman Islands	Asia	35	35	70
Bushman, South Africa	Sub-Saharan Africa	41	49	90
				<b>160</b>

Table 2. List of craniometric measurements collected.\*

Abbreviation Name		Abbreviation Name	
ASB	biasterionic breadth	NLH	nasal height
AUB	biauricular breadth	NOL	nasik-occipital length
AVR	molar alveolus radius	NPH	nasion-prosthion height
BAA	basion angle (nasion-prosthion)	OBB	orbit breadth
BAR	basion radius	OBH	orbital height
BBA	basion angle (nasion-bregma)	OCA	occipital angle
BBH	basion-bregma height	OCC	lambda-opisthion chord (occipital chord)
BNL	basin-nasion length	OCF	l-subtense fraction
BPL	basion-prosthion length	OCS	occipital subtense (lambda-opisthion subtense)
BRA	bregma angle (basion-nasion)	OSR	opisthion radius
BRR	bregma radius	PAA	parietal angle
DKB	interorbital breadth	PAC	bregma-lambda (parietal) chord
DKR	dacryon radius	PAF	bregma-subtense fraction
EKB	biorbital breadth	PAS	bregma-lambda subtense
EKR	ectoconchion radius	PRA	prosthion angle
FFA	fronto-facial Angle	PRR	prosthion radius
FMB	bifrontal breadth	RFA	radio-frontal angle (nasion-bregma)
FMR	frontomale radius	ROA	radio-occipital angle (lambda-opisthion)
FOL	foramen magnum length	RPA	radio-parietal angle (bregma-lambda)
FRA	frontal angle	SBA	sub-bregma angle
FRC	frontal chord	SIA	simotic angle
FRF	nasion-subtense fraction	SIS	simotic subtense
FRS	frontal subtense	SLA	sub-lambda angle
GLS	glabella projection	SSA	zygomaxillary angle
GOL	glabella-occipital length	SSR	subspinale radius
IML	malar length, inferior	SSS	zygomaxillary subtense
JUB	bijugal breadth	STB	bistephanic breadth
LAR	lambda radius	TBA	transverse biporial arc
MAB	palate breadth	VRR	vertex radius
MDH	mastoid height	WMH	cheek height
NAA	nasion angle (basion-prosthion)	WNB	minimum nasal breadth
NAR	nasion radius	XCB	maximum cranial breadth
NAS	nasion-frontal subtense	XFB	maximum frontal breadth
NBA	nasion angle (basion, bregma)	XML	malar length, maximum
NDA	naso-dacryal angle	ZMB	bimaxillary breadth
NDS	naso-dacryal subtense	ZMR	zygomaxillare radius
NFA	nasion-frontal angle	ZOR	zygoorbitale radius
NLB	nasal breadth	ZYB	bizygomatic breadth

\*All measurements listed follow Howells (1973, 1995) descriptions and definitions and were collected accordingly.

Table 3. List of cranial indices.

<b>Abbrev.</b>	<b>Name</b>	<b>Formula</b>	<b>Description</b>
CRM	Cranial module	$(GOL + XCB + BBH) \div 3$	Average cranial height, length, and breadth.
LBI	Cranial index	$(XCB \div GOL) \times 100$	Ratio of maximum vault breadth and length (includes glabellar projection).
LBI2	Cranial index 2	$(XCB \div NOL) \times 100$	Supraorbital is not a factor in this index.
NLI	Nasal index	$(NLH \div NLB) \times 100$	Ratio of nasal height to breadth.
TFI	Total facial index	$(NPH \div ZYB) \times 100$	Ratio of facial height to breadth.
UFI	Upper facial index	$(NPH \div ZMB) \times 100$	Ratio of upper facial height to mid-facial breadth.

---

\*All following Howells (1973; 1995), except TFI. IDP is an instrumentally-determined

Table 4. Descriptive statistics of hunter gatherer and Native American subsets of the Howells data.

Meas.	Population	Avg.	Max.	Min.	Std. dev.	Var.
ASB	Andaman	98.00	112.00	88.00	4.66	21.68
	Arikara	107.61	120.00	95.00	5.64	31.86
	Bushman	104.20	117.00	90.00	5.50	30.27
	Early Period CA	111.04	128.67	98.50	6.65	44.23
	Peru	106.71	116.00	97.00	4.47	19.97
	Santa Cruz Is.	109.08	117.00	95.00	4.60	21.14
AUB	Andaman	110.93	126.00	100.00	4.86	23.60
	Arikara	128.42	143.00	118.00	5.98	35.75
	Bushman	110.16	125.00	98.00	5.51	30.40
	Early Period CA	126.08	150.50	109.00	7.72	59.62
	Peru	120.54	134.00	106.00	5.21	27.13
	Santa Cruz Is.	122.77	137.00	112.00	5.41	29.25
AVR	Andaman	73.03	83.00	62.00	3.84	14.72
	Arikara	81.58	91.00	72.00	4.36	19.01
	Bushman	75.93	87.00	67.00	4.19	17.55
	Early Period CA	85.60	102.00	75.33	6.48	41.94
	Peru	73.89	89.00	61.00	4.86	23.64
	Santa Cruz Is.	80.73	93.00	71.00	4.28	18.30
BAA	Andaman	37.17	45.00	33.00	2.13	4.52
	Arikara	41.38	48.00	36.00	2.30	5.30
	Bushman	35.66	44.00	28.00	2.66	7.06
	Early Period CA	38.74	42.00	36.00	1.88	3.53
	Peru	41.55	47.00	36.00	2.26	5.11
	Santa Cruz Is.	40.64	46.00	36.00	2.37	5.64
BAR	Andaman	13.55	22.00	6.00	3.14	9.84
	Arikara	15.36	22.00	10.00	3.38	11.41
	Bushman	13.31	19.00	7.00	2.65	7.05
	Early Period CA	22.03	31.33	15.00	4.25	18.04
	Peru	13.21	22.00	8.00	2.57	6.59
	Santa Cruz Is.	14.48	50.00	7.00	4.50	20.27
BBA	Andaman	54.20	59.00	50.00	2.01	4.05
	Arikara	53.70	62.00	48.00	2.61	6.80
	Bushman	58.23	64.00	49.00	2.71	7.35
	Early Period CA	51.45	55.33	45.33	2.19	4.81
	Peru	55.55	60.00	49.00	2.36	5.55
	Santa Cruz Is.	55.79	61.00	51.00	2.10	4.42
BBH	Andaman	126.46	138.00	116.00	5.59	31.21
	Arikara	130.80	141.00	118.00	5.42	29.43
	Bushman	120.89	134.00	107.00	5.10	25.97
	Early Period CA	142.14	157.00	130.00	5.97	35.61
	Peru	127.72	146.00	117.00	5.44	29.58
	Santa Cruz Is.	126.48	141.00	116.00	4.83	23.30
BNL	Andaman	91.64	102.00	85.00	3.68	13.54

Meas.	Population	Avg.	Max.	Min.	Std. dev.	Var.
	Arikara	100.75	110.00	90.00	4.21	17.69
	Bushman	93.08	104.00	84.00	4.51	20.36
	Early Period CA	103.49	111.00	96.33	4.36	18.98
	Peru	93.29	105.00	83.00	4.50	20.26
	Santa Cruz Is.	95.05	105.00	84.00	3.98	15.81
BPL	Andaman	91.84	100.00	82.00	3.57	12.77
	Arikara	97.25	106.00	87.00	4.38	19.16
	Bushman	92.00	106.00	81.00	5.04	25.44
	Early Period CA	98.25	107.67	89.00	4.73	22.36
	Peru	91.57	104.00	80.00	4.88	23.77
	Santa Cruz Is.	97.03	109.00	86.00	4.42	19.55
BRA	Andaman	45.60	49.00	41.00	1.97	3.90
	Arikara	48.75	55.00	44.00	1.81	3.28
	Bushman	47.76	53.00	42.00	2.04	4.16
	Early Period CA	46.52	51.33	41.00	2.82	7.98
	Peru	45.73	50.00	41.00	1.76	3.10
	Santa Cruz Is.	47.05	52.00	42.00	1.77	3.14
BRR	Andaman	114.65	123.00	107.00	3.87	14.95
	Arikara	116.30	127.00	107.00	4.42	19.51
	Bushman	108.03	120.00	98.00	4.31	18.57
	Early Period CA	119.41	133.00	110.00	5.61	31.45
	Peru	114.95	130.00	106.00	4.36	19.00
	Santa Cruz Is.	112.74	124.00	100.00	4.71	22.14
DKB	Andaman	21.06	27.00	16.00	2.13	4.55
	Arikara	20.74	26.00	17.00	2.01	4.05
	Bushman	21.73	27.00	17.00	2.18	4.76
	Early Period CA	23.95	34.33	16.33	4.77	22.78
	Peru	20.28	27.00	16.00	2.08	4.33
	Santa Cruz Is.	21.39	26.00	18.00	1.67	2.78
DKR	Andaman	74.91	82.00	69.00	3.14	9.85
	Arikara	83.49	94.00	72.00	4.05	16.40
	Bushman	78.89	89.00	70.00	4.01	16.08
	Early Period CA	83.06	91.50	70.67	4.39	19.30
	Peru	76.36	85.00	67.00	3.85	14.84
	Santa Cruz Is.	78.46	91.00	71.00	3.49	12.15
EKB	Andaman	91.86	99.00	83.00	3.15	9.89
	Arikara	97.91	106.00	91.00	3.39	11.46
	Bushman	95.32	107.00	86.00	4.32	18.69
	Early Period CA	94.18	101.67	88.33	3.44	11.82
	Peru	93.12	104.00	84.00	3.75	14.09
	Santa Cruz Is.	97.02	106.00	89.00	3.65	13.33
EKR	Andaman	65.04	72.00	58.00	2.90	8.42
	Arikara	72.97	80.00	66.00	3.24	10.50
	Bushman	68.53	79.00	62.00	3.56	12.68
	Early Period CA	73.42	82.67	65.33	4.28	18.34

Meas.	Population	Avg.	Max.	Min.	Std. dev.	Var.
	Peru	67.03	75.00	57.00	3.28	10.78
	Santa Cruz Is.	68.53	76.00	62.00	3.05	9.32
FFA	Andaman	151.73	164.00	142.00	4.58	21.01
	Arikara	144.22	156.00	136.00	3.92	15.38
	Bushman	145.12	155.00	133.00	3.86	14.92
	Early Period CA	149.15	165.00	143.17	4.99	24.86
	Peru	146.56	154.00	139.00	3.71	13.75
	Santa Cruz Is.	148.58	159.00	140.00	3.97	15.73
FMB	Andaman	90.81	99.00	81.00	3.59	12.91
	Arikara	97.38	105.00	89.00	3.67	13.44
	Bushman	95.43	108.00	86.00	4.37	19.08
	Early Period CA	99.29	110.00	89.00	4.02	16.17
	Peru	93.62	105.00	84.00	3.90	15.25
	Santa Cruz Is.	96.93	105.00	88.00	3.93	15.41
FMR	Andaman	71.06	79.00	63.00	3.45	11.88
	Arikara	78.84	86.00	71.00	3.61	13.05
	Bushman	72.63	82.00	64.00	3.83	14.64
	Early Period CA	75.83	85.50	70.00	4.17	17.36
	Peru	72.31	83.00	63.00	3.39	11.52
	Santa Cruz Is.	73.53	83.00	66.00	3.42	11.70
FOL	Andaman	32.89	39.00	27.00	2.11	4.45
	Arikara	36.91	42.00	32.00	2.47	6.08
	Bushman	35.87	42.00	27.00	2.92	8.50
	Early Period CA	38.12	44.50	32.67	2.85	8.13
	Peru	34.51	40.00	30.00	2.23	4.99
	Santa Cruz Is.	35.52	42.00	31.00	2.12	4.51
FRA	Andaman	129.66	138.00	121.00	3.71	13.79
	Arikara	135.03	145.00	125.00	4.59	21.03
	Bushman	123.44	134.00	114.00	3.83	14.68
	Early Period CA	134.04	145.00	115.00	5.02	25.18
	Peru	132.77	143.00	122.00	3.90	15.20
	Santa Cruz Is.	133.25	143.00	124.00	3.82	14.57
FRC	Andaman	104.11	119.00	95.00	5.02	25.20
	Arikara	107.86	117.00	97.00	4.76	22.66
	Bushman	106.96	124.00	93.00	5.37	28.87
	Early Period CA	112.79	128.33	102.00	6.00	35.95
	Peru	107.40	118.00	96.00	4.80	23.07
	Santa Cruz Is.	107.32	120.00	96.00	4.73	22.36
FRF	Andaman	47.36	56.00	41.00	3.31	10.93
	Arikara	49.17	60.00	39.00	4.84	23.47
	Bushman	46.22	57.00	36.00	3.69	13.64
	Early Period CA	49.89	58.00	40.00	4.28	18.28
	Peru	46.79	55.00	39.00	3.64	13.27
	Santa Cruz Is.	50.50	61.00	40.00	4.24	17.96
FRS	Andaman	24.27	32.00	19.00	2.56	6.58

Meas.	Population	Avg.	Max.	Min.	Std. dev.	Var.
	Arikara	22.12	29.00	16.00	2.79	7.78
	Bushman	28.33	35.00	23.00	2.58	6.65
	Early Period CA	23.87	32.00	19.00	2.92	8.55
	Peru	23.13	31.00	18.00	2.33	5.41
	Santa Cruz Is.	23.06	28.00	18.00	2.29	5.26
GLS	Andaman	2.04	5.00	1.00	0.89	0.80
	Arikara	2.97	5.00	1.00	1.18	1.40
	Bushman	1.96	5.00	1.00	0.89	0.79
	Early Period CA	3.44	7.00	1.00	1.46	2.13
	Peru	2.59	7.00	1.00	1.06	1.12
	Santa Cruz Is.	3.75	7.00	1.00	1.19	1.42
GOL	Andaman	164.49	182.00	151.00	6.71	45.04
	Arikara	176.20	190.00	162.00	7.17	51.34
	Bushman	174.74	191.00	161.00	6.77	45.88
	Early Period CA	186.34	201.00	174.33	6.63	44.00
	Peru	173.48	192.00	157.00	6.87	47.21
	Santa Cruz Is.	176.00	192.00	160.00	6.12	37.49
IML	Andaman	34.81	40.00	25.00	3.22	10.36
	Arikara	36.96	44.00	28.00	3.08	9.48
	Bushman	32.54	43.00	23.00	3.72	13.80
	Early Period CA	37.29	46.33	32.00	3.77	14.21
	Peru	33.66	42.00	26.00	3.66	13.40
	Santa Cruz Is.	35.25	41.00	28.00	2.70	7.28
JUB	Andaman	109.07	124.00	98.00	4.46	19.89
	Arikara	119.46	129.00	108.00	5.48	30.05
	Bushman	108.27	125.00	97.00	5.39	29.01
	Early Period CA	117.96	140.00	108.50	8.40	70.57
	Peru	112.34	126.00	102.00	5.26	27.66
	Santa Cruz Is.	114.73	127.00	104.00	5.56	30.93
LAR	Andaman	102.78	112.00	95.00	4.00	15.97
	Arikara	100.80	118.00	90.00	5.36	28.75
	Bushman	100.43	110.00	88.00	4.40	19.35
	Early Period CA	106.73	119.33	92.33	5.91	34.92
	Peru	105.89	116.00	89.00	4.63	21.47
	Santa Cruz Is.	104.71	116.00	92.00	4.54	20.59
MAB	Andaman	59.46	66.00	54.00	2.57	6.60
	Arikara	65.00	74.00	55.00	3.70	13.71
	Bushman	58.91	70.00	52.00	3.19	10.17
	Early Period CA	64.19	82.00	54.50	6.46	41.69
	Peru	62.85	72.00	55.00	3.62	13.12
	Santa Cruz Is.	65.03	74.00	58.00	4.04	16.31
MDH	Andaman	24.17	30.00	17.00	3.04	9.22
	Arikara	26.93	34.00	19.00	3.08	9.51
	Bushman	23.27	31.00	16.00	4.10	16.80
	Early Period CA	29.41	36.50	24.00	3.32	11.01

Meas.	Population	Avg.	Max.	Min.	Std. dev.	Var.
	Peru	28.14	38.00	21.00	3.53	12.47
	Santa Cruz Is.	27.03	35.00	18.00	3.42	11.71
NAA	Andaman	71.57	83.00	62.00	3.80	14.42
	Arikara	66.62	73.00	60.00	3.05	9.30
	Bushman	71.10	79.00	63.00	3.64	13.21
	Early Period CA	66.71	74.00	61.00	3.11	9.69
	Peru	67.80	75.00	60.00	2.90	8.40
	Santa Cruz Is.	71.38	81.00	64.00	3.52	12.36
NAR	Andaman	85.19	95.00	75.00	3.59	12.91
	Arikara	95.07	106.00	86.00	4.51	20.30
	Bushman	88.09	99.00	78.00	4.27	18.19
	Early Period CA	92.91	102.00	84.00	4.61	21.26
	Peru	87.02	97.00	78.00	4.35	18.95
	Santa Cruz Is.	89.02	103.00	79.00	4.23	17.88
NAS	Andaman	15.31	22.00	11.00	2.07	4.31
	Arikara	17.03	22.00	11.00	2.18	4.73
	Bushman	15.77	21.00	11.00	2.35	5.51
	Early Period CA	16.78	22.00	11.00	2.60	6.78
	Peru	15.14	20.00	10.00	2.17	4.72
	Santa Cruz Is.	16.54	21.00	11.00	1.98	3.91
NBA	Andaman	80.16	86.00	74.00	2.57	6.63
	Arikara	77.59	85.00	68.00	2.72	7.42
	Bushman	74.02	81.00	68.00	2.59	6.72
	Early Period CA	82.01	91.00	77.00	3.08	9.48
	Peru	78.76	86.00	73.00	2.93	8.60
	Santa Cruz Is.	77.20	84.00	71.00	2.37	5.60
NDA	Andaman	97.50	115.00	75.00	9.48	89.91
	Arikara	91.33	115.00	75.00	8.63	74.43
	Bushman	110.40	131.00	90.00	9.73	94.62
	Early Period CA	110.06	140.00	85.00	14.15	200.12
	Peru	91.15	115.00	71.00	8.06	65.03
	Santa Cruz Is.	95.09	121.00	75.00	9.48	89.82
NDS	Andaman	9.27	13.00	7.00	1.35	1.82
	Arikara	10.17	14.00	7.00	1.35	1.82
	Bushman	7.58	11.00	5.00	1.29	1.66
	Early Period CA	9.17	13.00	6.00	2.31	5.34
	Peru	9.97	14.00	7.00	1.27	1.60
	Santa Cruz Is.	9.87	14.00	6.00	1.60	2.57
NFA	Andaman	142.80	151.00	128.00	4.11	16.89
	Arikara	141.46	153.00	131.00	4.25	18.08
	Bushman	143.44	154.00	132.00	4.56	20.79
	Early Period CA	142.76	156.00	134.00	4.93	24.32
	Peru	144.25	155.00	136.00	4.21	17.75
	Santa Cruz Is.	142.29	153.00	133.00	4.01	16.07
NLB	Andaman	24.43	29.00	21.00	1.64	2.68

Meas.	Population	Avg.	Max.	Min.	Std. dev.	Var.
	Arikara	26.59	31.00	23.00	1.79	3.22
	Bushman	26.49	33.00	21.00	2.25	5.08
	Early Period CA	25.10	29.00	19.67	2.26	5.12
	Peru	24.60	30.00	20.00	1.80	3.25
	Santa Cruz Is.	24.22	28.00	20.00	1.74	3.02
NLH	Andaman	45.29	51.00	40.00	2.70	7.31
	Arikara	52.91	61.00	46.00	3.05	9.32
	Bushman	43.27	50.00	36.00	2.95	8.71
	Early Period CA	49.57	56.00	43.00	3.50	12.25
	Peru	49.00	55.00	42.00	2.72	7.41
	Santa Cruz Is.	48.71	55.00	41.00	3.05	9.32
NOL	Andaman	163.49	181.00	151.00	6.26	39.21
	Arikara	174.77	190.00	161.00	6.91	47.80
	Bushman	172.97	190.00	160.00	6.61	43.67
	Early Period CA	183.10	195.00	173.33	5.51	30.33
	Peru	172.15	190.00	156.00	6.57	43.21
	Santa Cruz Is.	173.90	188.00	159.00	5.65	31.93
NPH	Andaman	58.66	68.00	50.00	3.81	14.52
	Arikara	70.10	80.00	60.00	4.31	18.59
	Bushman	56.76	72.00	48.00	4.79	22.95
	Early Period CA	67.14	74.00	59.33	4.26	18.12
	Peru	65.72	76.00	56.00	4.17	17.36
	Santa Cruz Is.	66.78	78.00	57.00	4.16	17.32
OBB	Andaman	36.99	42.00	33.00	1.40	1.96
	Arikara	40.03	43.00	37.00	1.37	1.88
	Bushman	38.40	43.00	34.00	1.95	3.79
	Early Period CA	39.69	45.67	30.50	3.08	9.49
	Peru	37.54	41.00	34.00	1.53	2.34
	Santa Cruz Is.	39.26	44.00	35.00	1.75	3.07
OBH	Andaman	32.46	37.00	29.00	1.37	1.87
	Arikara	34.83	38.00	29.00	1.81	3.26
	Bushman	30.90	37.00	26.00	2.24	5.03
	Early Period CA	34.74	37.33	31.00	1.68	2.83
	Peru	34.21	38.00	31.00	1.43	2.04
	Santa Cruz Is.	34.73	39.00	30.00	1.78	3.17
OCA	Andaman	125.04	133.00	110.00	4.77	22.80
	Arikara	119.64	132.00	104.00	5.54	30.68
	Bushman	114.56	125.00	102.00	4.43	19.67
	Early Period CA	118.26	131.00	104.67	6.26	39.17
	Peru	116.55	131.00	107.00	4.62	21.31
	Santa Cruz Is.	115.01	125.00	104.00	4.46	19.87
OCC	Andaman	90.64	100.00	81.00	4.12	16.96
	Arikara	93.54	113.00	82.00	6.17	38.08
	Bushman	88.51	104.00	79.00	4.73	22.39
	Early Period CA	100.60	113.50	82.00	7.16	51.22

Meas.	Population	Avg.	Max.	Min.	Std. dev.	Var.
	Peru	96.82	115.00	81.00	6.32	40.00
	Santa Cruz Is.	96.39	109.00	85.00	5.05	25.47
OCF	Andaman	43.00	55.00	32.00	4.63	21.45
	Arikara	44.97	62.00	33.00	5.40	29.18
	Bushman	44.50	54.00	34.00	4.52	20.46
	Early Period CA	49.07	64.50	26.50	8.34	69.58
	Peru	46.57	69.00	36.00	5.65	31.88
	Santa Cruz Is.	45.25	61.00	34.00	5.15	26.53
OCS	Andaman	23.40	30.00	18.00	2.62	6.88
	Arikara	27.16	38.00	21.00	3.95	15.64
	Bushman	28.34	36.00	21.00	2.62	6.86
	Early Period CA	29.93	39.67	17.00	4.34	18.84
	Peru	29.82	38.00	19.00	3.70	13.67
	Santa Cruz Is.	30.53	41.00	23.00	3.20	10.25
OSR	Andaman	37.88	47.00	34.00	3.16	10.01
	Arikara	40.20	49.00	26.00	3.99	15.93
	Bushman	39.41	48.00	32.00	3.17	10.02
	Early Period CA	46.96	53.00	41.67	2.78	7.75
	Peru	39.28	47.00	32.00	2.99	8.92
	Santa Cruz Is.	40.86	50.00	35.00	2.70	7.31
PAA	Andaman	130.77	139.00	124.00	3.31	10.93
	Arikara	132.41	142.00	125.00	3.92	15.33
	Bushman	136.26	145.00	126.00	4.19	17.56
	Early Period CA	131.75	142.00	118.50	4.69	21.98
	Peru	132.86	144.00	123.00	4.34	18.80
	Santa Cruz Is.	135.26	146.00	124.00	4.18	17.46
PAC	Andaman	104.94	117.00	91.00	5.71	32.63
	Arikara	107.03	116.00	96.00	4.55	20.68
	Bushman	107.20	120.00	91.00	5.87	34.50
	Early Period CA	116.25	133.00	99.00	7.03	49.36
	Peru	106.53	121.00	90.00	6.51	42.32
	Santa Cruz Is.	103.41	122.00	89.00	5.49	30.11
PAF	Andaman	56.59	70.00	44.00	5.05	25.46
	Arikara	54.19	61.00	40.00	4.42	19.54
	Bushman	56.31	69.00	47.00	4.47	19.95
	Early Period CA	58.18	69.00	46.50	5.39	29.09
	Peru	53.06	67.00	40.00	5.09	25.86
	Santa Cruz Is.	52.02	63.00	34.00	4.68	21.86
PAS	Andaman	23.87	29.00	17.00	2.52	6.35
	Arikara	23.51	29.00	17.00	2.49	6.19
	Bushman	21.44	29.00	15.00	2.85	8.14
	Early Period CA	26.64	40.00	18.00	4.71	22.22
	Peru	23.24	32.00	16.00	3.30	10.86
	Santa Cruz Is.	21.25	29.00	13.00	2.87	8.25
PRA	Andaman	71.21	84.00	62.00	3.57	12.75

Meas.	Population	Avg.	Max.	Min.	Std. dev.	Var.
	Arikara	71.99	80.00	65.00	3.22	10.40
	Bushman	73.22	81.00	67.00	3.58	12.78
	Early Period CA	74.56	79.50	68.67	2.70	7.30
	Peru	70.63	79.00	65.00	2.65	7.04
	Santa Cruz Is.	68.00	75.00	62.00	2.71	7.33
PRR	Andaman	93.21	103.00	83.00	3.77	14.23
	Arikara	101.97	113.00	90.00	4.84	23.44
	Bushman	94.83	107.00	83.00	4.95	24.50
	Early Period CA	103.10	119.33	94.33	6.52	42.46
	Peru	93.98	111.00	81.00	5.13	26.35
	Santa Cruz Is.	100.25	111.00	88.00	4.36	18.98
RFA	Andaman	61.53	69.00	57.00	2.17	4.72
	Arikara	60.32	65.00	56.00	2.03	4.13
	Bushman	65.18	71.00	58.00	2.58	6.64
	Early Period CA	62.55	68.67	58.67	2.34	5.49
	Peru	62.42	67.00	56.00	2.12	4.48
	Santa Cruz Is.	62.96	69.00	59.00	1.93	3.72
ROA	Andaman	62.63	70.00	49.00	4.65	21.63
	Arikara	67.78	83.00	56.00	5.18	26.79
	Bushman	61.24	73.00	47.00	5.32	28.34
	Early Period CA	70.99	87.00	51.00	6.58	43.24
	Peru	65.97	83.00	52.00	6.06	36.72
	Santa Cruz Is.	66.93	78.00	46.00	5.31	28.24
RPA	Andaman	57.85	64.00	51.00	2.62	6.85
	Arikara	58.52	63.00	53.00	2.60	6.75
	Bushman	61.78	69.00	54.00	3.19	10.20
	Early Period CA	62.22	80.50	51.67	5.50	30.22
	Peru	57.52	65.00	49.00	3.60	12.97
	Santa Cruz Is.	56.64	64.00	47.00	2.76	7.60
SBA	Andaman	101.33	108.00	95.00	3.16	9.97
	Arikara	103.46	110.00	97.00	3.34	11.13
	Bushman	103.99	110.00	97.00	2.87	8.26
	Early Period CA	100.80	109.33	90.33	4.46	19.89
	Peru	102.89	110.00	95.00	3.39	11.49
	Santa Cruz Is.	105.48	113.00	97.00	3.76	14.11
SIA	Andaman	126.50	173.00	87.00	16.27	264.80
	Arikara	95.97	132.00	63.00	16.04	257.35
	Bushman	141.27	178.00	94.00	18.85	355.23
	Early Period CA	120.17	172.00	91.67	23.33	544.49
	Peru	95.38	129.00	75.00	11.95	142.86
	Santa Cruz Is.	98.97	170.00	71.00	13.33	177.57
SIS	Andaman	2.25	4.90	0.10	0.95	0.90
	Arikara	3.94	6.20	0.60	1.15	1.32
	Bushman	1.28	4.30	0.10	0.84	0.70
	Early Period CA	3.72	5.47	3.00	0.87	0.76

Meas.	Population	Avg.	Max.	Min.	Std. dev.	Var.
	Peru	4.07	6.20	2.40	0.92	0.85
	Santa Cruz Is.	3.12	5.50	0.10	0.83	0.70
SLA	Andaman	88.18	95.00	82.00	2.72	7.38
	Arikara	91.39	101.00	83.00	3.85	14.80
	Bushman	85.51	97.00	77.00	3.54	12.50
	Early Period CA	89.59	96.33	80.50	3.78	14.28
	Peru	87.17	95.00	81.00	3.04	9.23
	Santa Cruz Is.	88.43	96.00	79.00	3.32	11.02
SSA	Andaman	126.14	137.00	115.00	5.10	25.98
	Arikara	126.32	138.00	117.00	4.74	22.46
	Bushman	132.93	144.00	118.00	5.09	25.95
	Early Period CA	129.60	141.33	119.00	5.95	35.45
	Peru	129.55	139.00	118.00	4.27	18.21
	Santa Cruz Is.	126.48	136.00	115.00	4.40	19.38
SSR	Andaman	87.90	98.00	80.00	3.67	13.48
	Arikara	96.71	106.00	87.00	4.83	23.33
	Bushman	88.10	97.00	78.00	4.34	18.83
	Early Period CA	96.13	110.67	85.67	5.78	33.37
	Peru	87.94	102.00	76.00	4.63	21.44
	Santa Cruz Is.	93.53	107.00	82.00	4.44	19.72
SSS	Andaman	23.29	29.00	18.00	2.58	6.64
	Arikara	24.99	30.00	19.00	2.75	7.57
	Bushman	19.69	28.00	15.00	2.46	6.04
	Early Period CA	24.05	29.33	18.33	2.97	8.81
	Peru	22.21	29.00	17.00	2.15	4.63
	Santa Cruz Is.	24.29	31.00	19.00	2.38	5.68
STB	Andaman	105.74	120.00	93.00	5.85	34.16
	Arikara	108.23	125.00	91.00	6.44	41.42
	Bushman	105.63	120.00	84.00	5.74	32.91
	Early Period CA	113.33	136.50	94.50	6.87	47.24
	Peru	109.65	122.00	97.00	5.02	25.22
	Santa Cruz Is.	106.52	121.00	96.00	5.15	26.51
TBA	Andaman	152.88	167.00	138.00	5.77	33.34
	Arikara	153.14	163.00	141.00	5.62	31.63
	Bushman	152.84	165.00	141.00	5.29	28.02
	Early Period CA	139.81	152.00	128.25	5.96	35.48
	Peru	155.32	165.00	143.00	4.58	21.01
	Santa Cruz Is.	153.59	167.00	101.00	7.20	51.91
VRR	Andaman	117.51	129.00	109.00	4.32	18.66
	Arikara	118.93	130.00	109.00	4.47	19.95
	Bushman	110.90	123.00	101.00	4.55	20.72
	Early Period CA	124.35	134.50	113.67	5.08	25.80
	Peru	120.16	130.00	109.00	4.44	19.70
	Santa Cruz Is.	116.85	127.00	106.00	4.34	18.86
WMH	Andaman	19.40	23.00	16.00	1.81	3.29

Meas.	Population	Avg.	Max.	Min.	Std. dev.	Var.
	Arikara	23.58	28.00	19.00	2.23	4.95
	Bushman	20.33	29.00	15.00	2.23	4.97
	Early Period CA	24.16	30.00	19.67	2.61	6.81
	Peru	23.25	28.00	18.00	2.41	5.82
	Santa Cruz Is.	22.35	29.00	17.00	2.30	5.30
WNB	Andaman	8.58	13.80	1.40	2.26	5.12
	Arikara	8.56	14.30	2.70	1.89	3.58
	Bushman	7.05	12.10	2.20	2.36	5.57
	Early Period CA	10.52	15.55	5.63	2.95	8.68
	Peru	8.85	12.00	5.40	1.42	2.02
	Santa Cruz Is.	7.25	11.90	2.40	1.76	3.10
XCB	Andaman	133.37	146.00	118.00	4.73	22.35
	Arikara	139.57	153.00	126.00	5.73	32.78
	Bushman	130.86	146.00	121.00	5.07	25.68
	Early Period CA	140.50	168.33	119.33	8.04	64.61
	Peru	136.44	149.00	123.00	4.48	20.08
	Santa Cruz Is.	137.46	151.00	124.00	5.22	27.28
XFB	Andaman	108.33	120.00	97.00	5.12	26.22
	Arikara	115.01	128.00	103.00	4.82	23.19
	Bushman	108.22	120.00	98.00	4.89	23.88
	Early Period CA	116.31	137.67	100.50	6.03	36.32
	Peru	113.65	126.00	105.00	4.57	20.93
	Santa Cruz Is.	111.27	125.00	99.00	4.92	24.22
XML	Andaman	49.60	60.00	40.00	3.59	12.91
	Arikara	53.87	62.00	45.00	3.93	15.44
	Bushman	48.01	60.00	40.00	4.15	17.22
	Early Period CA	53.03	60.67	46.50	4.04	16.34
	Peru	50.29	59.00	42.00	3.92	15.40
	Santa Cruz Is.	52.30	61.00	45.00	3.34	11.12
ZMB	Andaman	91.60	101.00	82.00	4.18	17.43
	Arikara	98.70	107.00	88.00	5.00	25.04
	Bushman	90.33	104.00	81.00	4.89	23.87
	Early Period CA	100.75	111.00	90.67	5.87	34.50
	Peru	94.35	109.00	82.00	4.79	22.96
	Santa Cruz Is.	96.44	111.00	83.00	5.47	29.87
ZMR	Andaman	65.34	72.00	58.00	2.96	8.75
	Arikara	72.62	81.00	66.00	3.43	11.74
	Bushman	68.73	77.00	61.00	4.08	16.65
	Early Period CA	73.76	86.33	67.33	4.86	23.63
	Peru	66.00	80.00	54.00	4.38	19.21
	Santa Cruz Is.	70.15	79.00	61.00	3.66	13.37
ZOR	Andaman	72.66	78.00	65.00	3.01	9.04
	Arikara	79.65	88.00	72.00	3.58	12.85
	Bushman	77.54	89.00	69.00	4.07	16.57
	Early Period CA	79.75	88.00	72.33	4.06	16.47

Meas.	Population	Avg.	Max.	Min.	Std. dev.	Var.
	Peru	72.78	81.00	61.00	3.76	14.15
	Santa Cruz Is.	76.54	85.00	68.00	3.37	11.36
ZYB	Andaman	120.71	136.00	106.00	5.07	25.74
	Arikara	136.88	151.00	122.00	7.09	50.28
	Bushman	119.73	136.00	105.00	6.12	37.41
	Early Period CA	136.00	153.33	123.00	8.29	68.72
	Peru	130.26	149.00	117.00	6.27	39.32
	Santa Cruz Is.	131.79	149.00	120.00	6.82	46.56
CRM	Andaman	141.44	152.67	130.33	4.77	22.76
	Arikara	148.86	160.33	138.33	4.86	23.59
	Bushman	142.16	155.67	131.67	4.51	20.36
	Early Period CA	156.29	168.22	143.33	6.09	37.06
	Peru	145.88	159.00	136.00	4.58	20.94
	Santa Cruz Is.	146.65	156.67	136.33	4.42	19.58
LBI	Andaman	81.15	88.68	74.16	2.77	7.65
	Arikara	79.27	87.43	70.90	2.86	8.17
	Bushman	74.94	82.49	69.10	3.35	11.20
	Early Period CA	75.54	93.87	68.19	3.26	10.64
	Peru	78.73	88.13	71.35	3.04	9.24
	Santa Cruz Is.	78.14	84.75	71.58	3.01	9.05
LBI2	Andaman	81.63	88.68	75.29	3.40	11.59
	Arikara	79.92	88.95	71.66	4.85	23.53
	Bushman	75.71	83.85	69.49	3.07	9.43
	Early Period CA	76.33	81.64	68.58	3.13	9.80
	Peru	79.33	88.13	72.11	2.79	7.81
	Santa Cruz Is.	79.08	86.21	73.18	2.78	7.71
NLI	Andaman	54.07	67.50	46.81	4.19	17.52
	Arikara	50.35	58.00	42.37	3.44	11.87
	Bushman	61.37	72.50	50.00	5.26	27.71
	Early Period CA	50.80	60.14	42.14	5.13	26.34
	Peru	50.34	59.09	37.04	4.36	18.98
	Santa Cruz Is.	49.85	60.98	42.31	4.04	16.33
TFI*	Andaman	37.53	42.15	32.79	1.91	3.66
	Arikara	38.68	43.65	34.44	1.69	2.85
	Bushman	36.17	41.67	31.40	2.19	4.78
	Early Period CA	35.86	39.58	31.16	2.51	6.31
	Peru	37.64	41.67	32.31	1.74	3.03
	Santa Cruz Is.	36.96	41.35	33.57	1.45	2.11
UFI	Andaman	48.61	54.84	40.98	2.76	7.63
	Arikara	51.26	60.32	45.70	2.78	7.74
	Bushman	47.42	58.06	39.34	3.36	11.26
	Early Period CA	48.78	56.15	42.99	3.59	12.91
	Peru	50.48	56.35	43.75	2.64	6.99
	Santa Cruz Is.	50.70	56.12	44.76	2.40	5.75

## Chapter 4

**Variation in the patterns of correlation of the human cranium: Exploring the influence of sample composition on patterns of correlation using regional, population-specific, and sex-specific samples.**

## 4.1 Introduction:

Anatomical structures or phenotypic traits are considered to be morphologically integrated when they evolve as a unit due to common function, structure, or developmental origins (Olson and Miller 1958). Thus, when one structure or trait within a unit changes, the other structures within that unit also change (Strait 2001). Modularity accounts for the phenotypic traits that are dissociated from integrated units, both integrated units and modules can be assessed by analyzing patterns of correlation among subsets of craniometric landmarks, since they indicate the interdependence or dissociation among variables (Cheverud 1982; Shea 1985; Cheverud et al. 1989; Klingenberg 2008, 2009).

Not all traits vary and evolve independently, but it is standard practice in phylogenetic analyses to treat them that way, and assign equal weight to each trait named (Martínez-Abadías et al 2009; Lieberman et al. 2000a,b; McCarthy and Lieberman, 2001; González-José et al. 2004; Bastir et al. 2004; Bastir and Rosas, 2004, 2005, 2006; Hlusko 2004; Goswami and Polly 2010). Studies that have re-analyzed cladistic and phylogenetic data using sets of morphological characters have demonstrated that different results are observed when morphological integration is accounted for, and in some cases, have found these results are less ambiguous (Lovejoy et al. 1999; Strait 2001; Hlusko 2004). The conventional model for phylogenetic analyses and assessments of hominid fossil crania, whereby traits are essentially modular until proven integrated, in which traits and not biologically-informed morphological sets are analyzed, is likely to remain the standard practice until the relationships between traits are more clearly resolved.

Studies of modularity and integration of the cranium are of particular importance to biological research, especially within disciplines where the analysis of unknown skeletal remains in paleoanthropological, archaeological, and forensic contexts, is required. The skull is relatively more resilient to taphonomic changes over time, and as a result, parts of the skull are some of the most common anatomical structures recovered among skeletal remains. Gaining a better understanding of patterns of phenotypic integration in human crania could have implications beyond the biology of living humans, by improving the methods by which we study the paleoanthropological record, and potentially impacting our understanding of the most recent ancestors of humans and the evolution of cranial morphology across hominid species.

There is evidence for strong integration in the human skull (Martínez-Abadías et al. 2009). But there is also a wide range of variation among human crania (Howells 1973, 1995) and the nearly world-wide, geographic distribution of the species ultimately results in wide range of variation in population structure. At the intraspecific level, sexual dimorphism is a key source of variation in the human cranial skeleton (Rosas and Bastir 2002; Martínez-Abadías et al. 2009). Genetic analyses have found a considerable level of genetic variation among traits of the facial skeleton, and that these traits are significantly affected by non-genetic factors including sexual dimorphism (Martínez-Abadías et al. 2009).

Understanding how sample composition influences patterns of correlation is a necessary endeavor in the interest of advancing our understanding of cranial

integration and modularity in human skulls. Doing so may reveal more about the biology of the sample analyzed, and may have applications to human biology in general if the ways in which the environmental pressures unique to that population and patterns of correlation deviate from other populations or the species-wide average, are compared.

Previous research (Chapter 3) on cranial integration observed integration in the facial skeleton that was relatively independent from the neurocranium and basicranium. These results were observed across all samples tested: one sample used to represent species-wide correlations the complete W.W. Howells data (1973, 1989, 1995), a population-level sample composed Early Period (ca. 5000 BP) Native Californians, and two subsets of the Howells data, one representative of Native American populations, and the other of hunter gatherer populations. These results corroborate the results of previous studies that found evidence for integration of the craniofacial region of the skull (Cheverud 1982, 1989, 1995; Lieberman et al. 2000a, b; Ackermann and Cheverud 2004; Hallgrímsson et al. 2004; Goswami 2006). However, significant levels of variation in patterns of correlation between samples were also observed. Following these observations, the objective of this study is to provide a more in-depth examination of this variation.

Theoretically, integrated structures or units of multiple structures, should persist at all levels of integration (Strait 2001). These levels are hierarchical in nature and best represented by an inverted pyramid that places the gene at the base, followed by the cellular, individual, and intraspecific or population levels, and at the top, the species (Figure 1) (following Strait 2001). The principle of morphological integration should apply to the all hierarchical levels below the level it is hypothesized to occur at, and should therefore be detectable at each of these levels (Strait 2001). The population level is critical to studies of integration because it is the level at which evolutionary forces act (Strait 2001). While patterns at the interspecific level have the greatest influence on phylogenetic reconstructions (Strait 2001), without knowing how integration patterns vary at and below the species level, it is more difficult to identify conclusive patterns of integration that persist at the species level, and at the intra-specific levels. Mechanisms for population-level morphological variation influence higher taxonomic levels (Hlusko 2004) and, as such, a better understanding of integration patterns between populations is important for the progression of understanding integration at higher levels.

However, at the level of the population, co-selected genetically independent traits can also lead to integration. Therefore, integration without a genetic basis can exist within populations, and integration can deviate from the inverted pyramid scheme because it needn't be present at all underlying levels (Cheverud 1996; Strait 2001). While Jernvall et al. (2000) suggest that a comprehensive study of integration would be one that analyzes many of the levels, studies of human crania have often used analyses of data from a single population and applied the results to an entire geographic region or species-wide, or applied regional data to the species level (Relethford 1994; Relethford and Harpending 1994; Roseman 2004; Roseman and Weaver 2004; in Stone et al. 2015; Ackermann 2005; Martínez-Abadías et al. 2009). Sex specific samples are rarely analyzed in studies of cranial integration in humans

unless they are focused on sexual dimorphism. Because the basis of morphological integration is genetic integration, integration occurring within individuals can be passed to future generations within a breeding population (Cheverud 1996; Wagner 1996, Strait 2001). Sexually dimorphic patterns can be passed on, and thus, population-specific sexual dimorphism could influence patterns of correlation.

The influence of sample composition on patterns of correlation for phenotypic traits of human crania is not well known. The use of a pooled-sex sample of individuals from a variety of populations with varying ancestry is expected to lessen sample bias by washing out the microevolutionary pressures, sexual dimorphism, and patterns of gene flow unique to individual populations. However, since most studies select data from one or a few populations to analyze, it is necessary to determine whether different populations can influence patterns of correlation differently. By decomposing a species-level data set down to incrementally narrower subsets, comparisons can be made between the species and below-species level to investigate the dependence patterns of integration have on the level and sample of the data. To test whether there are populations with unique patterns of correlation that could influence the species-level sample, and if they are present, to determine if they are washed out in the species-level sample.

Here I compare a sample representing species-wide patterns of correlation for human crania and divide this sample into subsets that represent individual geographic regions and populations, and further decompose samples according to sex, to assess the influence of sexual dimorphism on patterns of correlation. I will then test two hypotheses for cranial integration to model the variation among *Homo sapiens* for all populations and geographic regions represented by the Howells data with the addition of the Native Californian data.

## 4.2 Hypotheses:

### 4.2.1 Hypothesis 1:

H<sub>1</sub>: The patterns of correlation for humans at the level of the species do not differ significantly from patterns observed below the species-level.

The first hypothesis tests whether patterns of correlation vary according to sample composition. Following the expectation that morphological integration will persist throughout all levels described by Strait (2001), H<sub>1</sub> predicts that the patterns of correlation will be similar among the samples as sample composition is decomposed from the global level, to the regional, and finally, the population-specific level. In consideration of sexual dimorphism and its potential power to drive patterns of correlation, I also generated sex-specific correlation matrices for each sample.

To test H<sub>1</sub>, I analyze patterns of correlation at the uppermost hierarchical levels of morphological integration (following Strait 2001, see Figure 1), to test how patterns of correlation vary as the samples become more exclusive, by decomposing the Howells' data set into geographic regions and use one geographic region, the Americas, to decompose into population-specific samples, to analyze how sexual

dimorphism could be driving patterns of correlation. I use the Americas because it is a geographic region represented in the Howells data by a variety of populations from North and South America, and represents individuals who lived in a variety of environments. To add to the time-depth of this sample set, I will also include my own craniometric data from the Americas, which represents Native Californians from ca. 5000 BP.

#### 4.2.2 Hypotheses 2 and 3:

I also test two hypotheses for cranial integration, one specific to humans (Enlow and Hans 1996), and the other posited to apply across mammalian species (Hallgrímsson et al. 2007).

##### 4.2.2.A Hypothesis 2:

H<sub>2</sub>: The patterns of correlation at the species, geographic region, population, and sex-specific levels all follow the pattern of human cranial integration predicted by Enlow and Hans (1996), where there is a positive correlation between maximum cranial breadth and facial breadth, and a negative correlation between maximum cranial breadth and cranial height, cranial length, and facial height.

Enlow and Hans (1996) hypothesized the human cranium is integrated along the dimensions of length, breadth, and height, such that maximum cranial breadth has a direct relationship with facial breadth, and an inverse relationship with facial height, and overall height and length of the cranium. If correlations between maximum cranial breadth and facial breadth are not positive, and negative correlations between maximum cranial breadth and facial height, and cranial vault length and height are not observed, the null hypothesis is rejected.

##### 4.2.2.B Hypothesis 3:

H<sub>3</sub>: Correlations between width of the basicranium, neurocranium, and face will be high and statistically significant, with higher correlations observed between the basicranium and neurocranium than between face and neurocranium, and the face and the basicranium (Hallgrímsson et al. 2007).

Research on the influence of epigenetic factors to the patterns of morphological integration in the skulls of mice found strong correlations between measurements of neurocranial and basicranial width, and to a lesser degree, between width measurements of the face and neurocranium, and the face and the basicranium, suggesting that phenotypic variation of the cranium is a result of a few main processes of development that guide underlying genetic variation, and which is phenotypically expressed in ways that maintains the functional integration of the skull (Hallgrímsson et

al. 2007). On the basis of these results, Hallgrímsson et al. (2007) concluded that mammalian skulls are highly structured following this hierarchy.

Hypothesis 3 tests Hallgrímsson et al.'s (2007) hypothesis that the width of the main developmental regions of the skull govern the structure of cranial integration, but that this structure is dominated by strong correlations between the basicranium and neurocranium, thus correlations between breadth of the neurocranium and the face, and the basicranium and the face, will be weaker than correlations between neurocranial and basicranial breadth. The hypothesis is rejected under two mutually exclusive conditions, if correlations between maximum width of the three regions of the skull are not high and significant, and if correlations between basicranial and neurocranial width are weaker than correlations between neurocranial width and facial breadth, and basicranial width and facial breadth. As in  $H_2$ ,  $H_3$  tests Hallgrímsson et al.'s (2007) hypothesis on sample sets at and below the species level.

#### 4.3 Materials and methods:

##### 4.3.1 Craniometric data:

##### 4.3.1.A Howells data set:

Cranial data from the archaeological and historic populations represented in the Howells craniometric dataset (1973, 1989, 1995; and <http://web.utk.edu/~auerbach/HOWL.htm>), which includes cranial measurements of over 2,500 adults from 28 Holocene populations across the globe, were analyzed in this study. Four populations (Anyang, Philippines, North Maori, and South Maori) were omitted from all analyses below the species level because they include only male individuals. Descriptive statistics of sample composition of the Howells data are listed in Appendix 2.

##### 4.3.1.B Early Period Native Californian Sample:

To broaden the range of human variation represented in the samples analyzed in this study, craniometric data from Early Period Native Californians were included in addition to the Howells data. These individuals are part of the Native Californian skeletal collection at the Phoebe A. Hearst Museum of Anthropology (PAHMA) at the University of California Berkeley. These craniometric data were collected from two middle Holocene populations of Native Californians (N=59; 36 males, 23 females) dating to the Early Period (ca. 5000 B.P.) from Central California's Sacramento Valley and the San Francisco Bay Area. Museum accession numbers preceded by SJO-68, SJO-142, and SJO-56 are from the lower Sacramento Valley excavation sites in San Joaquin County, and remains with accession numbers preceded by ALA-208, ALA-307, and ALA-308 are from excavations in the San Francisco Bay Area in Alameda County. A summary describing these archaeological remains can be found in Chapter 3 (3.1).

#### 4.3.1.B.i Inclusion criteria:

I selected specimens found only at excavation sites dated to the Early Period. Within that subset of specimens, my selection criteria included sex, age, and preservation. I only selected specimens for which the cranium was present and the individual was an adult at the time of death. I also tried to equally represent sex in my sample.

#### 4.3.1.B.ii Age and sex estimation:

I used standard methods to assess the skull and pelvis of each specimen to estimate sex and age. For this study, specific estimation of age was not recorded. Skeletal changes mediated by normal development and ontogeny provide criteria by which the age at death of a skeletal specimen can be estimated. These criteria include assessment of long bone epiphyseal fusion, eruption of the third molars (Buikstra and Ubelaker 1994), and ectocranial suture closure, especially the basilar suture (Meindl and Lovejoy 1985), as well as age-related changes of the pelvis (Lovejoy et al. 1985; Suchey and Katz 1986; Brooks and Suchey 1990). The overall condition of the skeleton (Bass 1971; White et al. 2011) and dental attrition (Smith 1984) were also considered.

Sex was estimated using anatomy of the skeleton known to display sexual dimorphism in modern *Homo sapiens*, this includes morphological aspects of the cranium and mandible (Bass 1971; Buikstra and Ubelaker 1994; White et al. 2011), and pelvis (Phenice 1969; Bass 1971; Buikstra and Ubelaker 1994; White et al. 2011).

#### 4.3.B.iii Linear measurements:

I followed Howells' protocols and definitions (Howells 1973, 1995) for all anatomical landmarks and measurements I collected for the Early Period Native Californians. All craniometric data are listed in Appendix 3 and all measurements used in this study are listed in Appendix 4.

#### 4.3.1.B.iv Data collection:

All data were collected using a three-dimensional (3D) digitizer (MicroScribe G2, Immersion Corporation) that has an accuracy of  $\pm 0.38$  mm. This technology is widely used in anthropometric data collection and is also used in forensic departments. I used this technology because it is efficient and it reduces some sources of measurement error: When measurements are collected manually with calipers, anatomical landmarks that are involved in multiple measurements must be located by the researcher each time a measurement involving the landmark is collected. Since 3D coordinates for a landmark will be used to calculate all associated linear measurements, landmarks mutual to numerous measurements need only to be located once per round of measurements. In this way, the 3D digitizer reduces potential measurement error.

All landmark coordinates and measurements were recorded using 3Skull software 2.0.77 (Ousley 2004). The database management software Advantage Data

Architect 11.1 (Sybase Advantage Data Architect™) was used to store landmark coordinates and measurements. Because 3Skull is designed to be used in tandem with a 3D digitizer, I followed Ousley's protocols for data collection (2004, and see: <http://math.mercyhurst.edu/~sousley/Videos/3Skull-Ousley.mp4>), with additional guidance from protocols developed and used by the Department of Forensic Anthropology at the New York City Office of the Chief Medical Examiner (NYC OCME, New York, NY) (personal communication, C. Rainwater).

When using a MicroScribe, anatomical landmarks must be located prior to digital data collection for all instrumentally-determined measurements. For these measurements, I used digital calipers to locate anatomical landmarks and marked them using removable, weak adhesive indicators that were not hazardous to the skeletal remains, which were removed immediately following data collection. Each cranium was aligned in the Frankfurt horizontal plane (FHP), and the digitizer and the cranium oriented in FHP were stabilized to prevent them from shifting during data collection.

For each individual, I calculated the average of each cranial measurement. If the values of the repeated trials for a craniometric measurement differed from each other by > 5%, I dropped them, rather than averaging them, deeming it an unreliably replicable craniometric measurement for that individual cranium. Twenty-eight of the traits had measurements dropped. I included measurements with 5% error and set the cut-off at > 5% because the error was exactly 5% in three instances, once for each measurement (BAA, BAR, NAS). These traits represent small parts of the cranium such that the largest recorded value for any of these measurements was 42 mm (NAS). For measurements this small, a difference of one millimeter can return a high percentage error even though the range of the actual measurements can be small.

After removing measurements for individuals that had > 5% error, the calculated, population-level intraobserver error for all measurements in my dataset averaged  $1.09 \pm 1.2\%$  (min. = 0.0%, max. = 5.00%, median = 0.75%).

#### 4.3.2 Analyses:

Most statistical analyses were performed in RStudio version 1.0.136 (RStudio Team 2016) using R version 3.3.2 (R Core Team 2016) using APE (Paradis et al. 2004) corrplot (Wei et al. 2016), ggplot2 (Wickham 2009), Hmisc (Harrell 2006), and plyr (Wickham 2011), packages. Descriptive statistics for intra-observer error and quantitative comparisons were performed in Excel version 15.28.

##### 4.3.2.A Correlations:

I built correlation matrices with quantitative phenotypic data to analyze relationships within and among parts of the cranial skeleton. Prior to calculating correlations and constructing correlation matrices, I standardized the data. All linear measurements including those from the Howells data set, were scaled and centered to the mean, for each population, and for each sex within populations. I chose to use population-specific parameters for this step to preserve biological similarities within populations

and differences from other populations captured by raw measurement data. Within populations, measurements were also scaled and centered according to sex to preserve the relative sexual dimorphism within each population. Using population and sex-specific parameters to scale and center the data addresses the problem of size-related shape variation by minimizing the contribution of allometry to correlations (Goswami and Polly 2010). Following Goswami and Polly (2010), I did partition size out of my analyses, but by normalizing the data for relatively similarly-sized individuals separately, which minimizes the relative allometric contribution. This was determined to be the best option because it effectively minimizes relative allometric contribution within each dataset, population and sex specific, while preserving the differences between datasets and the variation within populations. Allometry poses real problems for correlations, both options- removing and keeping some form of allometric contribution, have the potential to create issues (see Goswami and Polly 2010 for more detail).

I used the Hmisc (Harrell 2006) package to calculate Pearson's correlation coefficient, and used corrplot (Wei et al. 2016) to construct correlation matrices for each sample (Table 1). The matrices include correlation coefficients for 33 cranial measurements (see Appendix 4). These measurements were chosen because they assess a particular aspect or trait within one of the regions of the cranium hypothesized to act as a module (Cheverud 1982, 1989, 1995; Lieberman et al. 2000a, b; Ackermann and Cheverud 2004; Bastir and Rosas 2006; Hallgrímsson et al. 2004; Goswami 2006, 2007), and arranged them in anatomical clusters, measurements of the facial skeleton are grouped, as are vault and basicranium measurements, and contained within these cranial regions are clusters of measurements of adjacent anatomical features. While some measurements may represent overlapping regions of the cranium because they measure different aspects of its shape and size, I tried to limit this. A Bonferroni correction was used to adjust the confidence intervals for the pairwise correlations in the matrices. I programmed my code so that any correlation coefficients that are insignificant would be removed from the matrices; none were insignificant.

#### 4.3.2.B Hypothesis 1 methods:

To test this hypothesis, I generated correlation matrices for the following samples: 1.) a sample representing the species level composed of all data (the Howells data and data for Early Period Native Californians), 2.) samples representing geographic regions, composed of all individuals from populations within each geographic region, including the Early Period Native Californian data with the Howells populations from the Americas for this geographic region, and 3.) samples of individual populations from one geographic region to look at the level of the population. I used the Americas as the geographic region to decompose into individual populations since these populations are from a range of environments across North and South America, and the addition of the Early Period Californian sample to this geographic region extends the time-depth to ca. 5000 BP. To assess whether sexual dimorphism could be driving patterns of correlation among samples, I also generated sex-specific

correlation matrices for the species-wide, geographic region-wide samples, and for individual populations within the Americas.

To provide a better, more easily discernable and effective representation of patterns of correlation, all weak correlations (ranging from -3 to 3) within the correlation matrices used in the test for  $H_1$  are shown in white and nearly-white colors in the figures. The intention and result of which was to place the focus on the most informative correlations and reduce the noise produced by weak ones.

#### 4.3.2.C Hypothesis 2 methods:

Correlations were generated for the complete data set inclusive of all Howells data and all Early Period Native Californian data, all Howells data, each geographic region, and each population, and sex-specific correlation matrices were also generated for each sample. If correlations between maximum cranial breadth and facial breadth are not positive and negative correlations between maximum cranial breadth and facial height are not observed, the null hypothesis is rejected.

#### 4.3.2.D Hypothesis 3 methods:

To test this hypothesis, I compared correlations within each sample between each of the three major measurements that assess cranial breadth within the three regions of the cranium– the face, neurocranium, and basicranium, which are maximum facial breadth (ZYB) (facial skeleton), maximum cranial breadth (XCB) (neurocranium), and biasterionic breadth (ASB) (basicranium). Correlations were for the complete data set inclusive of all Howells data and all Early Period Native Californian data, all Howells data, each geographic region, and each population, along with sex-specific correlation matrices, were also generated to test this hypothesis. The null hypothesis is rejected under two mutually exclusive conditions, if correlations between maximum width of the three regions of the skull are not high and significant, and if correlations between basicranial and neurocranial width are weaker than correlations between neurocranial width and facial breadth, and basicranial width and facial breadth.

### 4.4 Results:

#### 4.4.1 Hypothesis 1:

The first hypothesis explored the patterns of correlation below the level of the species, and, following the inverted pyramid scheme for the hierarchical levels of integration (Strait 2001), predicted that the patterns observed at the species level would persist as the samples were decomposed down to the geographic region, and then to the population level. Overall, there was variation among the patterns of correlation observed across all samples, but the amount of variation had a direct relationship to composition such that more differences were observed between populations than between geographic regions. In addition, individual populations

differed from the species-level more than the samples for geographic regions (Figure 2).

A few patterns were observed across all samples. Overall, stronger correlations in the face relative to other cranial regions were observed in all matrices. Within the neurocranium, all matrices demonstrated correlations stronger than  $\pm 0.3$  among the traits of the anterior frontal bone. This pattern was least perceptible in the Inuit (Howells' "Eskimo") population, although it may be due to the absence of one of the measurements in this region of the cranium, bregma radius (BRR), in this sample (Howells 1973, 1989, 1995). Another pattern observed across samples was the relationship (stronger than  $\pm 0.3$ ) between biauricular breadth of the neurocranium and the cheek region of the face (ZMB, JUB, ZYB). Correlations between the basicranium and neurocranium were weak for almost all samples, and there were no consistent patterns of correlation between these regions observed across samples. Although variation among cranial measurements was expected (Howells 1973, 1995), the lack of persistence observed for the relationships between measurements across samples was not.

The Americas sample was also decomposed into population-specific subsets, and then again into sex-specific subsets. Of these populations, the Early Period Native Californian sample exhibited the strongest correlations throughout the cranium. While the other populations from this region were relatively more similar to each other than to the Native Californian sample, the Santa Cruz Island and Peru samples had relatively stronger overall correlations compared to the rest of the Americas population samples. This population-level analysis also revealed that there was less variation between the sex-pooled and subsetted sex-specific regional samples than between the sex-pooled and sex-specific samples for individual populations.

Analyzing sex-pooled correlations comparatively with sex-specific subsets demonstrated the potential influence that sexual dimorphism can have on patterns of correlation within human crania. Patterns of sex-specific variation in correlations were demonstrated clearly in four of the geographic regions, however, the patterns that were observed differ. For the Asian and Australasian sample sets, correlations within and between phenotypic traits of the neurocranium were stronger in females, and the female sample from Australasia also demonstrated greater overall correlations with measurements of the face compared to the male sample. Whereas in the correlation matrix for the European regional sample, greater overall correlations with measurements of the face were observed in the male subset. Finally, the male subset of the Polynesia/Micronesia sample demonstrated stronger correlations throughout the cranium.

Consistent sexually-dimorphic patterns across populations were not observed. For two of the sex-specific subsets of the Americas' populations, correlations throughout the cranium were stronger overall in the female sample (Native California and Inuit (Howells' "Eskimo" population), while it was the male subset that had overall stronger correlations throughout the cranium for Santa Cruz Island population. For the Arikara population, correlations within and between the face were stronger in males, but for measurements of the neurocranium, correlations were relatively stronger in the female sample. Correlations in which measurements of basicranium were involved

were mostly negative for the female subset of this population, and mostly positive in the male subset. Overall, no consistent patterns of sexual dimorphism were observed at the population level that would imply a standard manner by which sexual dimorphism drives patterns of correlation in humans at the population level. However, the increasing amount of variation that was observed as samples were decomposed implies that sexual dimorphism can influence patterns of correlation, and that this potential influence is significantly higher at lower level samples, e.g., at the population level.

#### 4.4.2 Hypothesis 2:

Patterns of phenotypic correlations between the face and neurocranium expected under the hypothesis for human cranial integration proposed by Enlow and Hans (1996) were not observed in any of the samples tested (Figure 3). While negative correlations between cranial breadth and cranial height, cranial length, or facial height were observed in some populations and in some of the sex-specific samples of populations, none of these samples had negative correlations between cranial breadth and all three of the phenotypic traits. Maximum cranial breadth was observed to positively correlate with maximum facial breadth in all but two of the samples. Both samples that exhibited negative correlations were population and sex-specific samples (Dogon male (Africa) and Inuit (Howells' "Eskimo" female (Americas)). The positive correlation between breadth dimensions of the face and neurocranium predicted by this hypothesis was observed in all sex-pooled samples, at the species, geographic region, and population levels. However, this hypothesis also predicted negative correlations between maximum cranial breadth and neurocranial length, neurocranial height, and facial height, which was not observed in any of the sample sets. As a result, the hypothesis is rejected, because for all samples tested, the patterns of correlation observed did not fit the predicted pattern.

#### 4.4.3 Hypothesis 3:

The third hypothesis predicted that the correlations observed for measurements of maximum breadth between the skull's major developmental regions would be strong and statistically significant, and that the correlation between the neurocranium and the basicranium would be highest, suggesting the facial skeleton has a relatively greater degree of independence than the other regions of the cranium. Phenotypic correlations observed in the sample representing the level of the species, composed of the Howells data and Early Period Native Californian data, followed this pattern, as did the sex-specific subsets of this sample (Figure 4, Table 2). The same strength of correlations between the basicranium and neurocranium was observed for the sex-pooled and sex-specific samples. While the strength of the other two correlations varied, the differences were small ( $\leq 0.05$ ). However, all correlations were below 0.5., and the correlations between neurocranial and basicranial breadth were only slightly higher ( $r = 0.04 - 0.05$ ,  $p = < 0.0001$ ) than the correlations between the face and the neurocranium, while correlations between the face and basicranium were the lowest

( $r_{f:b} = 0.14 - 0.09 < r_{b:n}$ ). For the sample I tested that included all Howells data without the addition of the Early Period Native Californian data, the results were essentially the same.

At the regional level, patterns of correlation followed the pattern predicted by Hallgrímsson et al.'s (2007) hypothesis in all but three of the pooled-sex samples. Correlation patterns observed in the geographic region-level samples for all populations from the Americas did not fit the predicted pattern, but for the sex-pooled Americas sample,  $r_{b:n} = r_{f:n}$  ( $r = 0.5$ ,  $p = < 0.0001$ ), the same results were observed when the Native Californian data were excluded from the Americas sample. However, correlations between the basicranium and neurocranium were overall lower than those correlation between the face and the neurocranium. The Polynesia/Micronesia sample also did not fit the predicted pattern of correlations.

At the population level, correlations following the predicted pattern were observed in 14 of the 27 samples. When these 14 pooled-sex, population-level samples were decomposed into sex-specific samples, both sexes fit the predicted pattern in four of the populations (Table 3). Of the rest of the 14 populations, only the male subsetted data fit the predicted pattern in six samples, and only the female subsetted data fit the predicted pattern in two samples. Of the 13 sex-pooled population-level samples that did not fit the predicted pattern, six of the sex specific samples fit the pattern, and these samples were skewed towards females (4:2). Thus, correlations for eight of the populations were not observed to fit the predicted pattern regardless of whether the samples were composed of both sexes, or decomposed (subsetted) to represent a single sex.

The predicted pattern was met by populations following a few main patterns. All populations and sex-divided subsets of population-level data fit the pattern for the European and Australasian populations, with three female samples being the exception (Berg, Australia, Tolai). In the Americas populations, the sex-specific samples in which the pattern was observed were significantly skewed towards females (4:1). Of the Polynesia/Micronesia populations, the predicted pattern was observed only once (Easter Island). Sex-specific patterns among populations from the other geographic regions were not observed. The highest correlations between basicranial and neurocranial width was observed for Europe, but the greatest difference between the strength of correlations occurred in the Australasia sample ( $r_{b:n} = 0.51$ ,  $r_{b:f} = 0.23$ ,  $r_{f:n} = 0.36$ ,  $p = < 0.0001$  (pooled-sex);  $r_{b:n} = 0.51$ ,  $r_{b:f} = 0.22$ ,  $r_{f:n} = 0.27$ ,  $p = < 0.0001$  (male);  $r_{b:n} = 0.50$ ,  $r_{b:f} = 0.23$ ,  $r_{f:n} = 0.45$ ,  $p = < 0.0001$  (female), while the Africa sample had the smallest differences (range = 0.07, all Africa samples).

Although a number of the samples representing varying levels of sample composition were observed to follow the pattern predicted by Hallgrímsson et al.'s (2007) hypothesis, this hypothesis was rejected on the basis that it was not supported in all geographic region-wide, sex-pooled samples, and in less than half of the sex-pooled sample at the level of the population. This hypothesis predicted the correlation between width of the basicranium and neurocranium will be higher than correlations between facial and neurocranial breadth, and between facial and basicranial breadth across all mammals. At the least, the hypothesis was supported at the level of the

species with the caveat that this mechanism has not been observed at the below-species level in humans.

#### 4.4.4 Sexual dimorphism:

Revisiting the influence of sexual dimorphism on studies of integration, but through the lens of evaluating the second hypothesis, it is clear that sexual dimorphism has likely driven the patterns of correlation for some populations. Viewing the strength of correlations among populations, which were then subsetted into sex-specific samples indicated that for some of the populations, the overall (pooled-sex) results were driven by substantial differences in the strength of correlations between the sexes. For the sample for all populations from the Americas, and two populations (Teita (Africa) and Norse (Europe), the correlation between basicranial and neurocranial breadth was  $\geq 0.5$  ( $p = < 0.0001$ ) for the pooled-sex sample, but for only one of the sex-specific samples (male for the Norse, and female for the other two samples). This suggests that the pooled-sex results were skewed by sexual dimorphism in these samples. Without regard to the strength of individual correlations, correlation rankings observed for each sample differed for each sex for three of the populations within the Americas (Arikara, Inuit (Howells' "Eskimo" population), Santa Cruz Island), Australasia (Australia, Tasmania, Tolai), two of the European populations (Berg and Zalavar), and the Easter Island population from Polynesia/Micronesia. However, ranks of correlations were equal among the pooled and sex-specific samples for each of the regional samples and the sample comprising all populations. This suggests that sexual dimorphism does contribute to patterns of correlation at the level of the population, but that at higher levels, the amount of variation was washed out. This result has multiple implications for studies of cranial integration. That sexual dimorphism can be overwhelmed by other factors when you reach the population level means that some population-level variation is lost. This result also raises questions about what is biologically relevant or important to studies that seek to identify species-wide patterns of integration, especially when only a single or a few populations are analyzed and the results are applied at the species level.

#### 4.5 Discussion and conclusions:

This study compared the correlation of craniometric traits in modern human samples representing the level of the species and the sub-specific levels of geographic region and population, and finally, sex-specific subsets of each sample, and used hypothetical testing to model variation within and between samples. Predicted correlation patterns were based on theoretical principles of integration ( $H_1$ ) (Strait 2001), and previously established hypotheses for cranial integration attributed to shared function and development exclusive to humans ( $H_2$ ) (Enlow and Hans 1996), and predicted to apply across mammals ( $H_3$ ) (Hallgrímsson et al. 2007).

The overall objective of this study was to examine the potential influence of sample composition on patterns of human cranial integration. The above results suggest that sample composition influences patterns of correlation. The variation

between population-level patterns of correlation was muted when data for individual populations were subsumed into a single sample representing worldwide human variation, and to a slightly lesser extent, when populations were combined into geographically similar populations to represent the geographic region. However, relative to the other samples at the regional and population level, correlations for the Polynesia/Micronesia sample set, and, the Early Period Native Californian and Santa Cruz Island populations, respectively, differed significantly, and all also differed significantly from the species-wide sample. The biological variation observed between human populations is often associated geographic distance and variation in the environment (Stone et al. 2015; Howells 2007; Newman 1943) and research on human biological variation in the Americas demonstrated a direct relationship between environmental and biological similarity (Ross 2002). Because *Homo sapiens* are so geographically widespread, it is not surprising that patterns of correlation varied the most at the population level.

Across all samples, there was relatively more integration in the face relative to the neurocranium and basicranium, and little evidence of integration within the basicranium and between the basicranium and neurocranium, providing little evidence for the integrated neuro-basiscranial complex proposed by Lieberman et al. (2000a, b). Rather, my results support assertions that the basicranium is not an integrated unit (Bastir et al. 2006). In fact, Bastir et al. argue the basicranium should not be considered integrated regardless of correlations found among traits within the basicranium because this region of the cranium has more than one developmental component, and each has its own growth pattern (Bastir et al. 2006). The variation observed may arise from environmental pressures that influence cranial shape and perhaps development, especially if some of the environmental pressures are involved in epigenetics. Even still, Hallgrímsson et al. (2009) demonstrated that changes in phenotypic variance, its structure, and integration can be driven by a single mutation in mice.

These results suggest that samples of human craniometric data from certain populations could bias results, and should not be combined in analyses of correlation patterns unless many other populations are also incorporated to form a robust data set. Researchers analyzing individual populations should be cautious to apply their results to the species level, or first be sure the results are comparable to a reference sample that approximates the patterns of correlation expected at the species level. Furthermore, that the patterns of correlation among samples varied highlights the need to establish the range of variation between samples that should be accepted before a before testing hypotheses of integration.

Hallgrímsson et al.'s (2007) hypothesis was rejected below the species level. At both the regional and population levels, the pattern of correlation predicted by Hallgrímsson et al. (2007) was not observed across all samples. Martínez-Abadías et al. (2009) also observed patterns of correlation that supported Hallgrímsson et al.'s (2007) hypothesis.

Patterns of phenotypic correlations between dimensions of the face and neurocranium that would be expected under Enlow and Hans' (1996) hypothesis for morphological variation of the cranium in humans, whereby integration in human crania follows a pattern by which maximum cranial breadth positively correlates with facial

breadth, and negatively with facial height, neurocranial breadth, and neurocranial and height, were not observed. The results for the second hypothesis corroborate Martínez-Abadías et al.'s (2009) results based on analyses of phenotypic and genotypic data from a single population, and provide additional support to developmental models (Lieberman et al. 2000a; Bastir and Rosas 2004; Martínez-Abadías et al. 2009).

The differences observed between population-level samples of males and females were averaged out at the regional and species-wide levels. This suggests that there is a wide range of variation in the levels of sexual dimorphism within populations. In addition, it also suggests that the range of variation in levels of sexual dimorphism are too great to detect at the regional level. To detect these differences, it is necessary to analyze individual populations. While the use of pooled-sex samples composed of multiple populations could reduce population-specific noise, by design, it could also temper signals of biologically interesting and informative patterns within and between populations, and reduce the signal of patterns that reveal the variable ways the human crania respond to pressures among populations. As a result, the existence of and sources of biases are obscured, but could still influence results that are applied to the entire sample. Without the use of comparative analyses of individual populations to identify potential population-specific biases that drive the results observed in the entire sample, to figure out what is going on in various populations, researchers' abilities to choose appropriate reference samples that have the least potential to bias results, and to make appropriate conclusions from their results, is limited.

This study sought to analyze the variation in the patterns of correlation for samples of modern human crania with varying levels of composition because *Homo sapiens* are a biologically variable species in many respects, especially when it comes to the cranium (Howells 1973, 1989, 1995). With a nearly global distribution, humans occupy a wide range of environments, each with its own array of microevolutionary forces that altogether lead to different levels of variation within and between populations. Thus, patterns of correlation are potentially influenced by biologically-relevant, differential pressures. The variation in patterns observed in this study may arise from environmental pressures that influence cranial shape and perhaps development, especially if some of the environmental pressures are involved in epigenetics. Even still, Hallgrímsson et al. (2007) demonstrated that changes in phenotypic variance and its structure, and integration can be driven by a single mutation in mice. As such, sample composition must be carefully considered in studies of integration and modularity. Researchers could use what is known about the particular environmental-pressures that affect populations to better understand the evolutionary forces that drive variation in patterns of correlation. Doing so would promote a better understanding of the biology of particular populations and of human cranial variation and the ways the human cranium responds to evolutionary pressures within a particular environment, and thus may have implications on our understanding of the plasticity of *Homo sapiens* cranial skeleton.

#### 4.6 Acknowledgements:

This project would not have been possible without the support, encouragement, and advising of Leslea J. Hlusko. In addition, this project was also made possible by the following people and institutions who provided support, assistance, and in some cases, access to materials: C. Rainwater; S. Sholts, Department of Anthropology, National Museum of Natural History, Smithsonian Institution; T. White, and the Human Evolution Research Center; and Natasha Johnson and Benjamin W. Porter, Director, of the Phoebe A. Hearst Museum of Anthropology. Special thanks also go to colleagues in the Department of Integrative biology for their suggestions and support, especially L. Chang and P. Skipwith. And finally, many thanks to J.L. Reed for invaluable feedback and support. This research was supported in part by the Beim Scholarship through the Department of Integrative Biology, University of California, Berkeley.

#### 4.7 References:

- Ackermann RR. 2005. Ontogenetic integration of the hominoid face. *J Hum Evol* 48:175–197.
- Ackermann RR & Cheverud JM. 2004. Morphological integration in primate evolution. In: Pigliucci M & Preston K, editors. *Phenotypic integration*. Oxford: Oxford University Press. pp. 302–319.
- Bass WM. 1971. *Human osteology: A laboratory and field manual of the human skeleton*. Columbia, MO: Missouri Archaeological Society.
- Bastir M & Rosas A. 2004. Facial heights: Evolutionary relevance of postnatal ontogeny for facial orientation and skull morphology in humans and chimpanzees. *J Hum Evol* 47:359–381.
- Bastir M & Rosas A. 2005. Hierarchical nature of morphological integration and modularity in the human posterior face. *Am J Phys Anthropol* 128: 26–34.
- Bastir M & Rosas A. 2006. Correlated variation between the lateral basicranium and the face: A Geometric morphometric study in different human groups. *Arch Oral Biol* 51:814–824.
- Bastir M, Rosas A, & Kuroe K. 2004. Petrosal orientation and mandibular ramus breadth: evidence of a developmental integrated petroso-mandibular unit. *Am J Phys Anthropol* 123: 340–350.
- Brooks ST & Suchey JM. 1990. Skeletal age determination based on the os pubis: A Comparison of the Acsadi-Nemerskeri and Suchey-Brooks methods. *Hum Evol* 5:227–238.
- Buikstra JE & Ubelaker DH. 1994. *Standards for data collection from human skeletal remains: Proceedings of a seminar at the Field Museum of Natural History*. Fayetteville: Arkansas Archaeological Research Series No. 44. Fayetteville: Arkansas Archaeological Survey.
- Cheverud JM. 1982. Phenotypic, genetic, and environmental morphological integration in the cranium. *Evolution* 36:499–516.
- Cheverud JM. 1989. A comparative analysis of morphological variation patterns in the papionins. *Evolution* 43:1737–1747.
- Cheverud JM. 1995. Morphological integration in the saddle-back tamarin (*Saguinus fuscicollis*) cranium. *Am Nat* 145:63–89.
- Cheverud JM. 1996. Developmental integration and the evolution of pleiotropy. *Am Zool* 36 44–50.
- Enlow DH & Hans MG, eds. 1996. *Essentials of facial growth*. WB Saunders Company.
- Goswami A. 2006. Cranial modularity shifts during mammalian evolution. *Am Nat* 168:270–280.
- Goswami A. 2007. Cranial modularity and sequence heterochrony in mammals. *Evol Dev* 9:290–298.
- Goswami A & Polly PD. 2010. Methods for Studying Morphological Integration and Modularity. *Paleontological Society Papers* 16:213–244.
- Hallgrímsson B, Lieberman DE, Liu W, Ford-Hutchinson AF, & Jirik FR. 2007. Epigenetic interactions and the structure of phenotypic variation in the cranium. *Evol Dev* 9:76–91.

- Hallgrímsson B, Willmore K, Dorval C, & Cooper DM. 2004. Craniofacial variability and modularity in macaques and mice. *J Exp Zool B: Mol Dev Evol* 302:207–225.
- Hallgrímsson B, Jamniczky HA, Young NM, Rolian C, Parsons TE, Boughner JC, & Marcucio RS. 2009. Deciphering the palimpsest: Studying the relationship between morphological integration and phenotypic covariation. *Evol Biol* 36:355–376.
- Harrell FE. 2006. Hmisc package. Available online at [http:// biostat.mc.vanderbilt.edu/twiki/ bin/view/Main/Hmisc](http://biostat.mc.vanderbilt.edu/twiki/bin/view/Main/Hmisc).
- Hlusko LJ. 2004. Integrating the genotype and phenotype in hominid paleontology. *P Natl Acad Sci USA* 101: 2653–2657.
- Howells WW. 1973. Cranial Variation in Man. A Study by multivariate analysis of patterns of differences among recent human populations. *Peabody Mus Amer Arch Ethnol* 67.
- Howells WW. 1989. Skull shapes and the map. Craniometric analyses in the dispersion of modern Homo. *Peabody Mus Amer Arch Ethnol* 79.
- Howells WW. 1995. Who's Who in Skulls. Ethnic identification of crania from measurements. *Peabody Mus Amer Arch Ethnol* 82.
- Howells WW. 2007. History of craniometric studies, the view in 1975. In: Ubelaker, D., Smith, B., Standford, D. & Sturtevant, W. eds: *Handbook of North American Indians, Volume 3: Environment, Origins, and Populations*. United States Government Printing Office, Washington DC, pp. 497–503.
- Klingenberg CP. 2008. Morphological integration and developmental modularity. *Annu Rev Ecol Evol Syst* 39: 115–132.
- Klingenberg CP. 2009. Morphometric integration and modularity in configurations of landmarks: Tools for evaluating a-priori hypotheses. *Evol Dev* 11: 405–421.
- González-José R, Van der Molen S, González-Pérez E, & Hernández M. 2004. Patterns of phenotypic covariation and correlation in modern humans as viewed from morphological integration. *Am J Phys Anthropol* 123:69–77.
- Gonzalez PN, Oyhenart EE, & Hallgrímsson B. 2011. Effects of environmental perturbations during postnatal development on the phenotypic integration of the skull. *J Exp Zool B: Mol Dev Evol* 316: 547–561.
- Jernvall J. 2000. Linking development with generation of novelty in mammalian teeth. *Proc Natl Acad Sci USA* 97:2641–2645.
- Lieberman DE, Mowbray KM, & Pearson OM. 2000a. Basicranial influences on overall cranial shape. *J Hum Evol* 38:291–315.
- Lieberman DE, Ross CR, & Ravosa M. 2000b. The primate cranial base: Ontogeny, function and integration. *Ybk Phys Anthropol* 43:117–169.
- Lovejoy CO, Meindl RS, Pryzbeck TR, & Mensforth RP. 1985. Chronological metamorphosis of the auricular surface of the ilium: A New method for the determination of adult skeletal age at death. *Am J Phys Anthropol* 68:15–28.
- Lovejoy CO, Cohn MJ, & White TD. 1999. Morphological analysis of the mammalian postcranium: A Developmental perspective. *Proc Nat Acad Sci USA* 96:13247–13252.

- Martínez-Abadías N, Esparza M, Sjøvold T, González-José R, Santos M., & Hernández M. 2009. Heritability of human cranial dimensions: Comparing the evolvability of different cranial regions. *J Anat* 214:19–35.
- McCarthy RC & Lieberman DE. 2001. Posterior maxillary (PM) plane and anterior cranial architecture in primates. *Anat Rec* 264: 247–260.
- Meindl RS & Lovejoy CO. 1985. Ectocranial suture closure: A Revised method for the determination of skeletal age at death based on the lateral-anterior sutures. *Am J Phys Anthropol* 68:57–66.
- Newman M. 1943. A metric study of undeformed crania from Peru. *Am J Phys Anthropol* 1: 21–45.
- Olson EC & Miller RL. 1958. *Morphological Integration*. Chicago: University of Chicago Press.
- Ousley S. 2004. Threeskull 2.0.77 [Computer Program]
- Paradis E, Claude J, & Strimmer K. 2004. APE: Analyses of phylogenetics and evolution in R language. *Bioinformatics* 20:289–290.
- Phenice TW. 1969 A Newly Developed Visual Method of Sexing the Os Pubis. *Am J Phys Anthropol* 30:297–301.
- R Core Team 2016. R: A Language and environment for statistical computing. R Foundation for Statistical Computing, Vienna, Austria. URL <https://www.R-project.org/>.
- Relethford J. 1994. Craniometric Variation among Modern Human Populations. *Am J Phys Anthropol* 95: 53–62.
- Relethford J & Harpending H. 1994. Craniometric Variation, Genetic Theory, and Modern Human Origins. *Am J Phys Anthropol* 95: 249–270.
- Rosas A & Bastir M. 2002. Thin-plate spline analysis of allometry and sexual dimorphism in the human craniofacial complex. *Am J Phys Anthropol* 117:236–245.
- RStudio Team 2016. RStudio 1.0.136: Integrated Development for R. RStudio, Inc., Boston, MA URL <http://www.rstudio.com/>.
- Shea BT. 1985. On aspects of skull form in African apes and orangutans, with implications for hominoid evolution. *Am J Phys Anthropol* 68:329–342.
- Smith BH. 1984. Patterns of molar wear in hunter-gatherers and agriculturalists. *Am J Phys Anthropol* 63:39–56.
- Stone JH, Chew K, Ross AH, & Verano JW. 2015. Craniofacial plasticity in ancient Peru. *Anthropologischer Anzeiger* 72:169–183.
- Strait DS. 2001. Integration, phylogeny, and the hominid cranial base. *Am J Phys Anthropol* 114:273–297.
- Suchey J & Katz D. 1986. Skeletal age standards derived from an extensive multiracial sample of modern Americans. *Am J Phys Anthropol* 69:269.
- Wagner GP. 1996. Homology, natural kinds, and the evolution of modularity. *Am Zool* 36:36–43.
- Wei T, Simko V, & Wei MT. 2016. Package ‘corrplot’. *Statistician* 56:316–324.
- White TD, Black MT, & Folkens PA. 2011. *Human osteology*. San Diego, CA: Academic press.
- Wickham H. 2009. *ggplot2: Elegant graphics for data analysis*. Springer: New York.

Figure 1. The inverted pyramid following Strait (2001), modified to add sex.

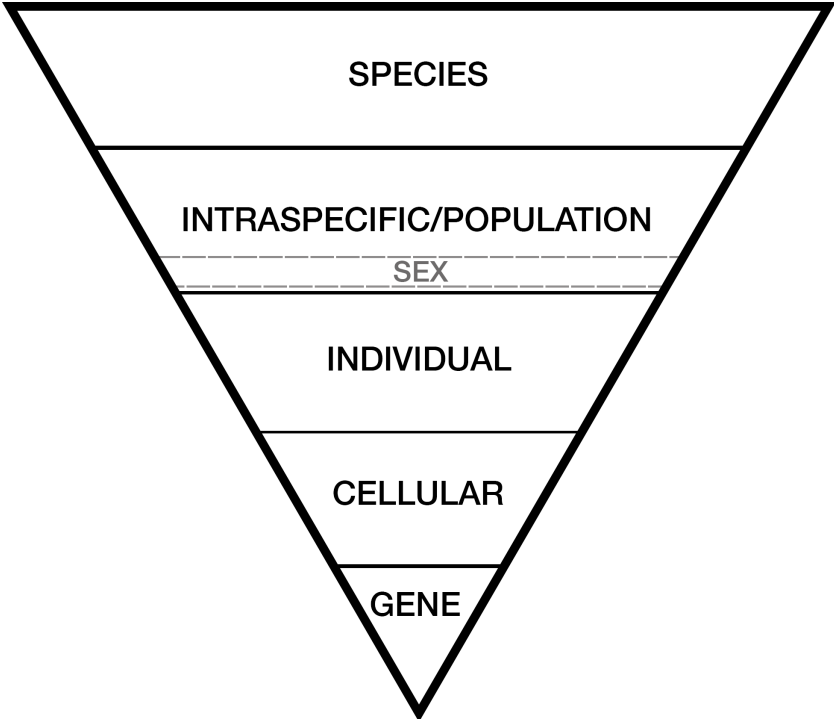
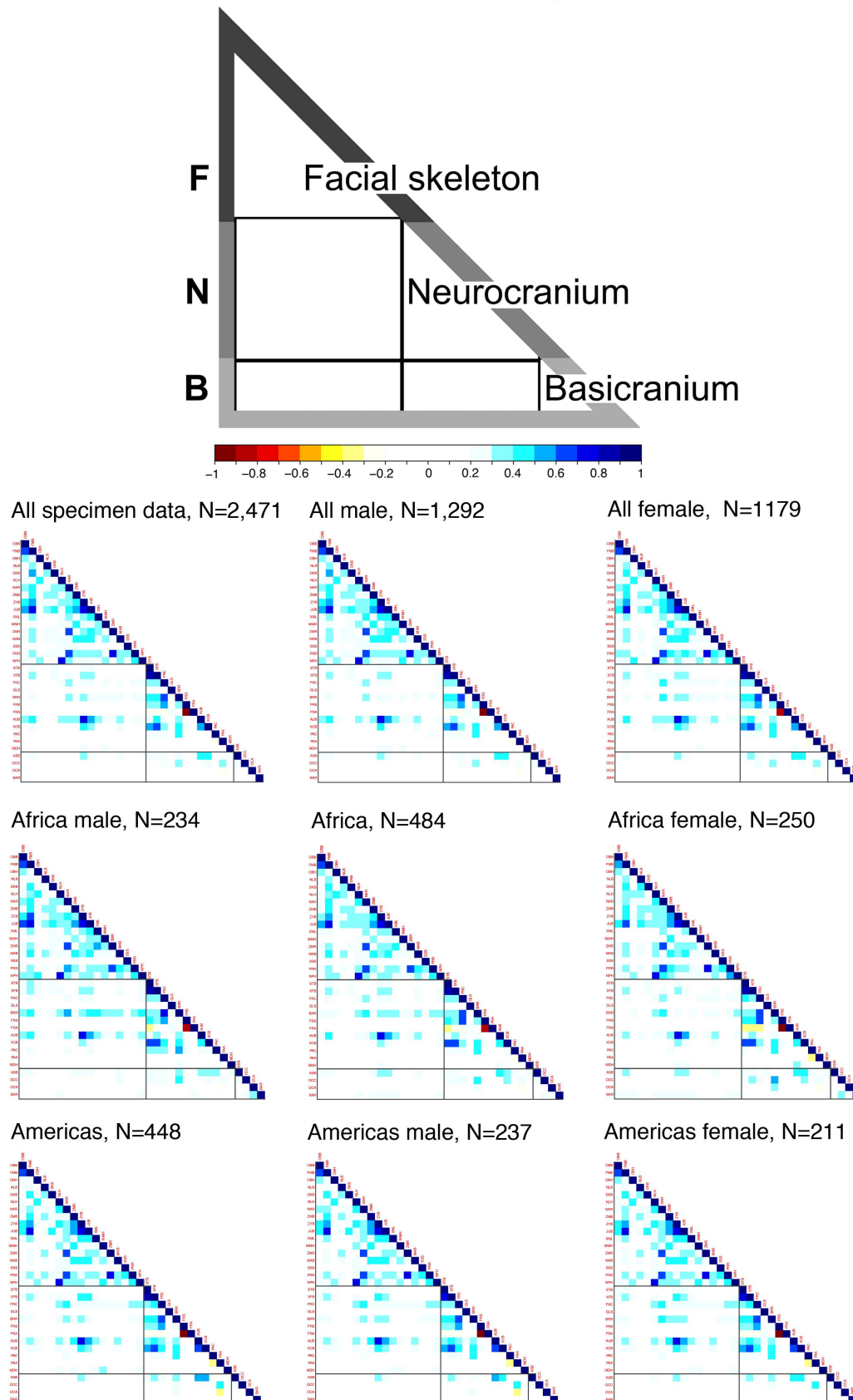
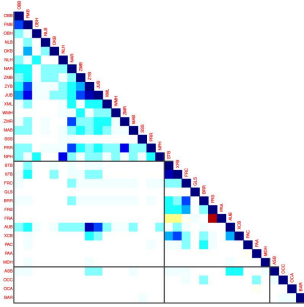


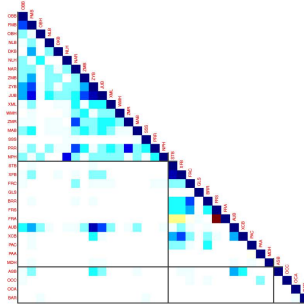
Figure 2. Correlation matrices for all samples, with legend at top.



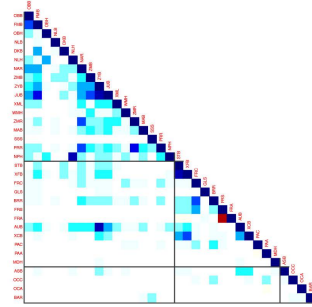
Asia, N=573



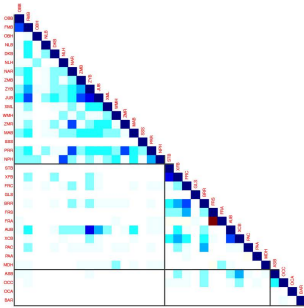
Asia male, N=317



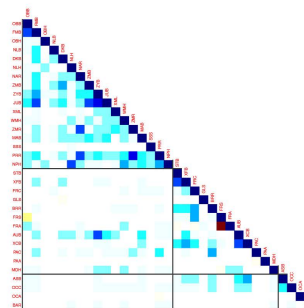
Asia female, N=256



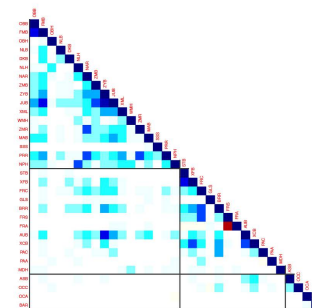
Australasia, N=298



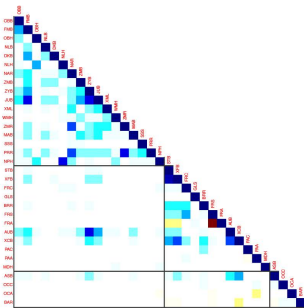
Australasia male, N=153



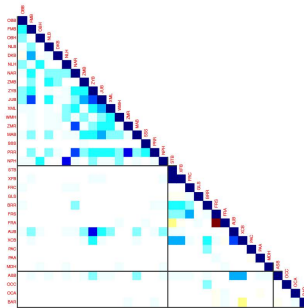
Australasia female, N=145



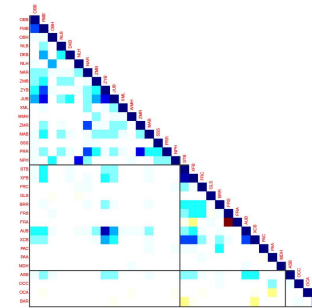
Europe, N=317



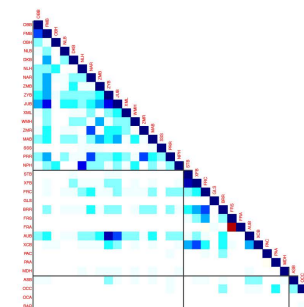
Europe male, N=164



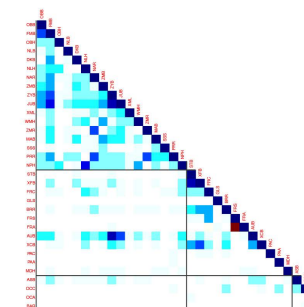
Europe female, N=153



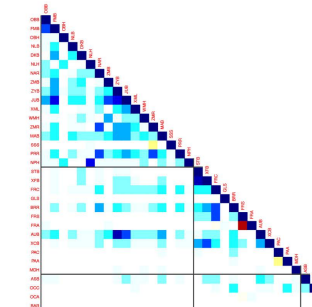
Polynesia/Micronesia,  
N=351



Polynesia/Micronesia  
male, N=187



Polynesian and  
Micronesia female,  
N=164



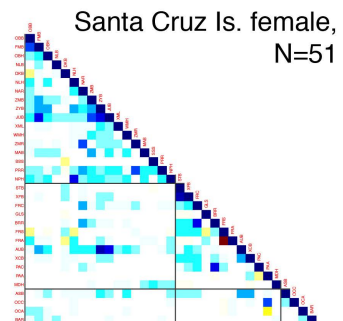
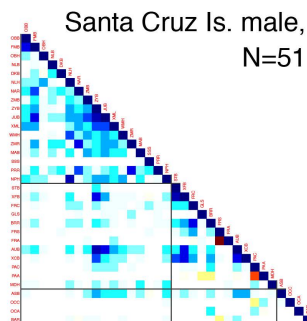
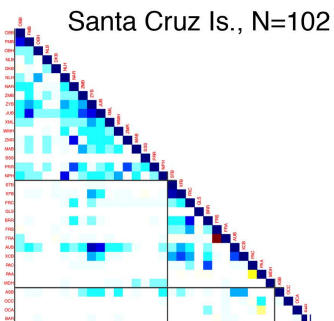
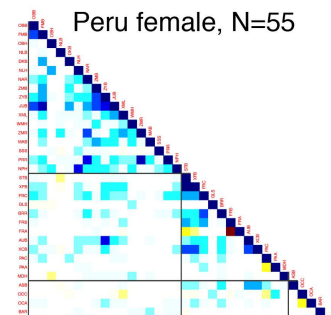
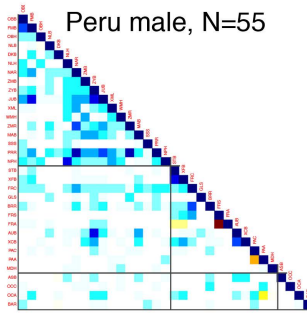
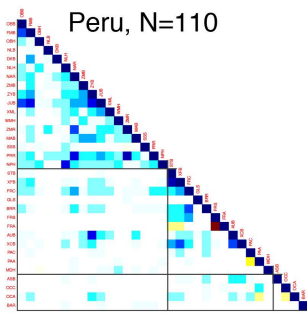
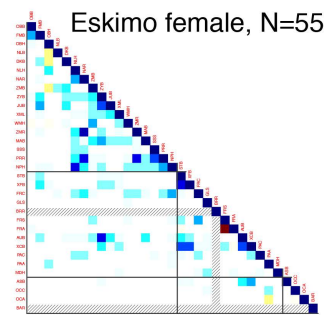
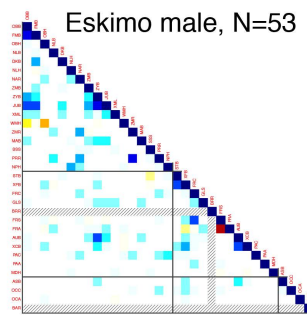
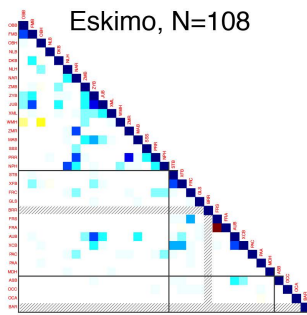
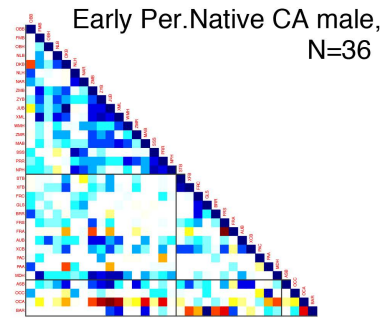
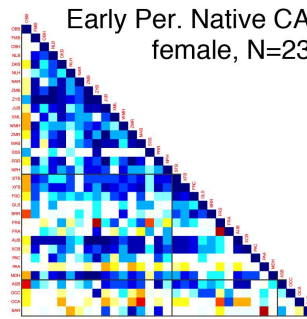
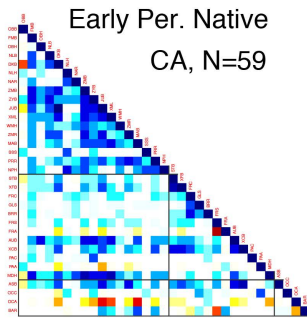
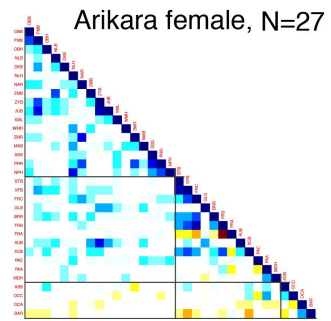
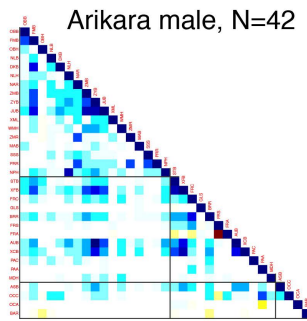
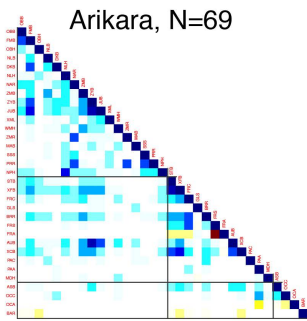
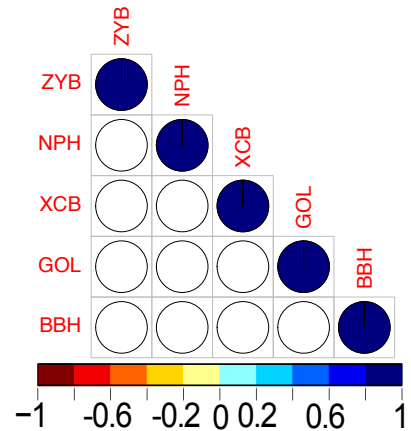


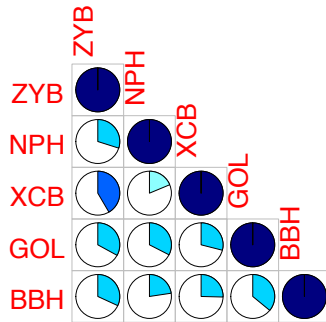
Figure 3. Correlations between measurements of maximum height, breadth, and length.

**Legend:** Shaded proportion of circles represent correlation. Cool colors indicate positive correlation, warm colors indicate negative correlation. For example, a correlation close to 1 will be represented as a circle nearly completely filled with dark blue. A correlation of 0.25 will be a circle that has a light blue fill in one quarter.

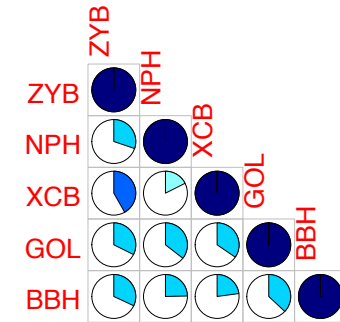
Cranial regions	Meas.	Dimension
Facial skeleton	ZYB	breadth
	NPH	length
Neurocranium	XCB	breadth
All	GOL	length
	BBH	height



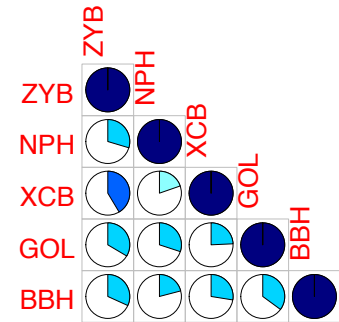
All data, N=2,471



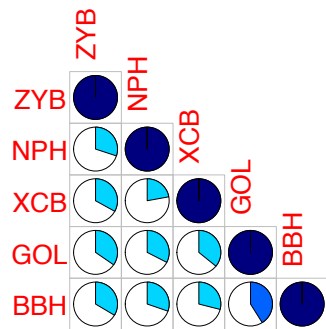
All female, N=1,179



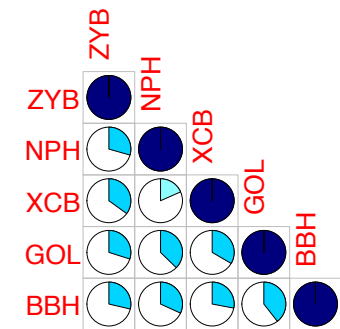
All male, N=1,292



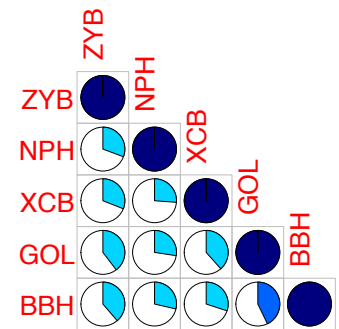
Africa, N=484



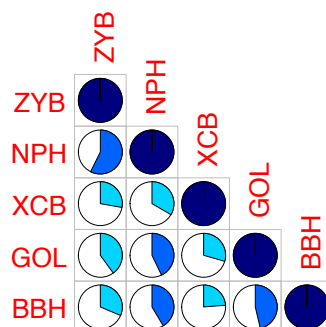
Africa female, N=250



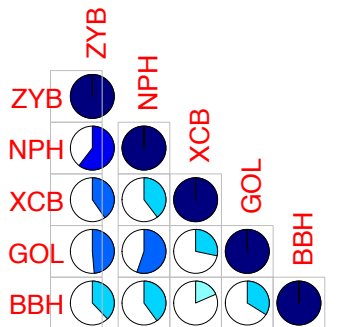
Africa male, N=234



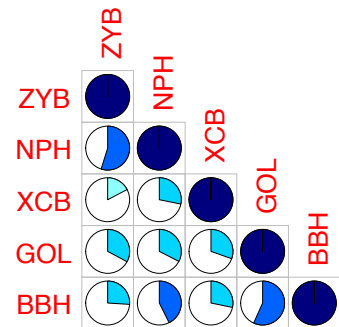
Bushman, N=90



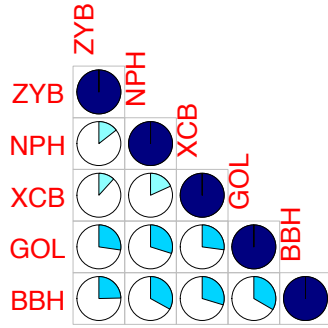
Bushman male, N=41



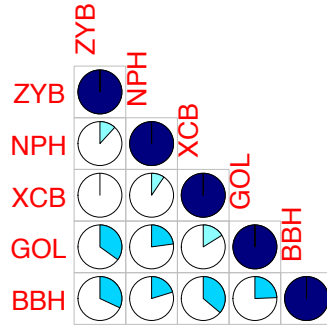
Bushman female, N=49



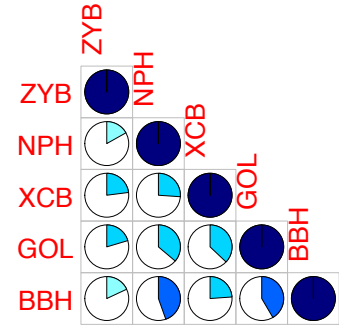
Dogon, N=99



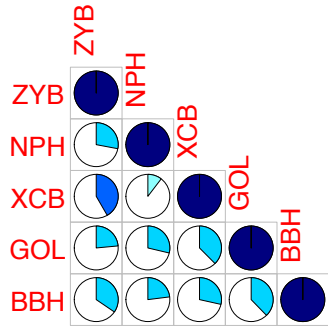
Dogon male, N=47



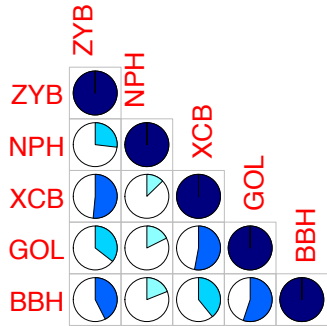
Dogon female, N=52



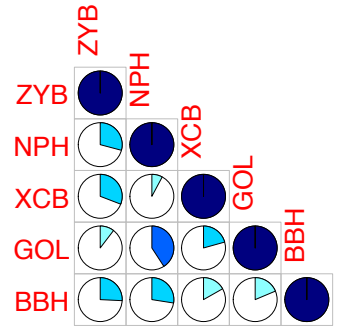
Egypt, N=111



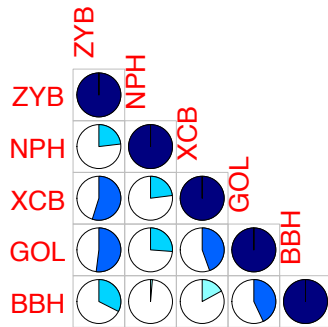
Egypt male, N=58



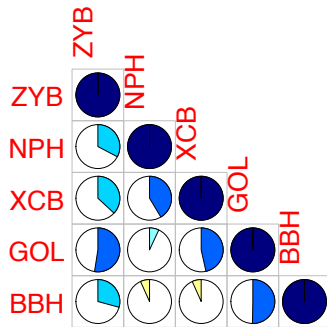
Egypt female, N=53



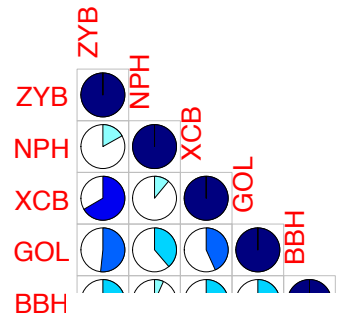
Teita, N=83



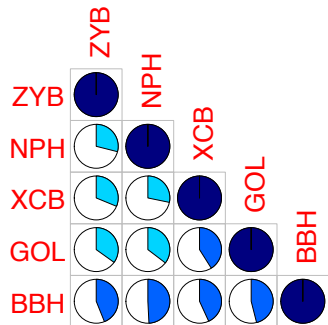
Teita male, N=33



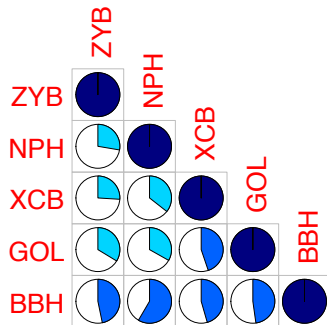
Teita female, N=50



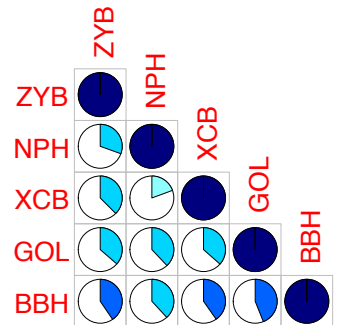
Zulu, N=101



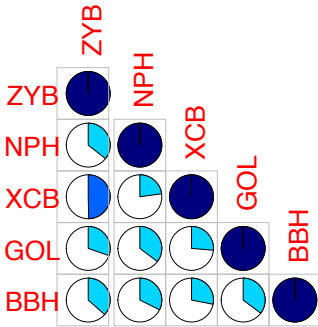
Zulu male, N=55



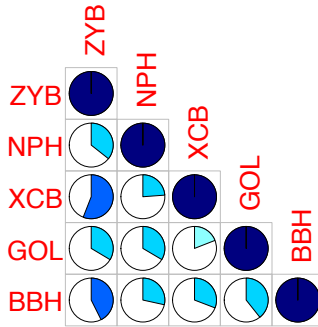
Zulu female, N=46



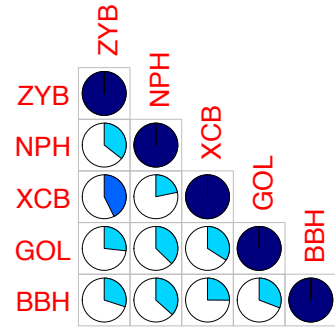
Americas, N=448



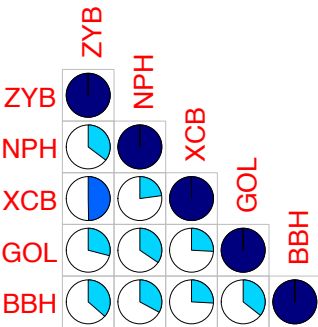
Americas males, N=237



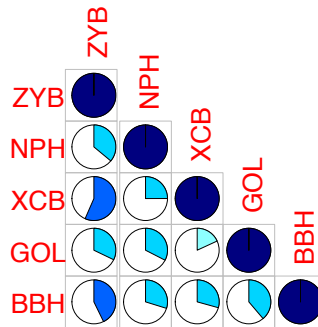
Americas females, N=211



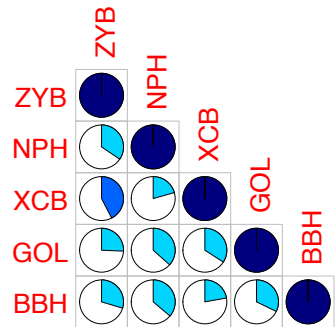
Americas, N=389



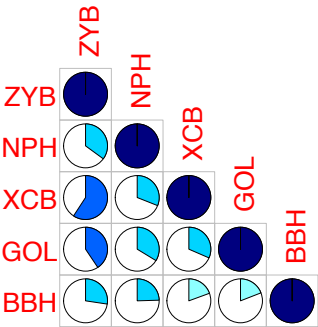
Americas male, N=201



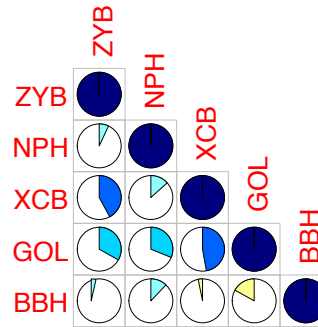
Americas female, N=188



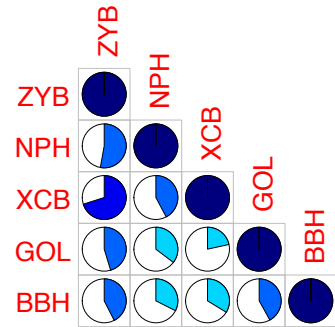
Arikara, N=69



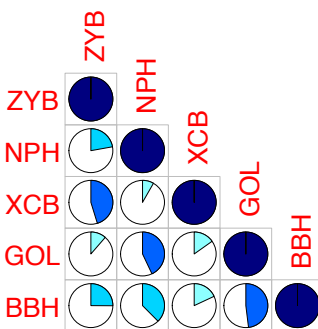
Arikara female, N=27



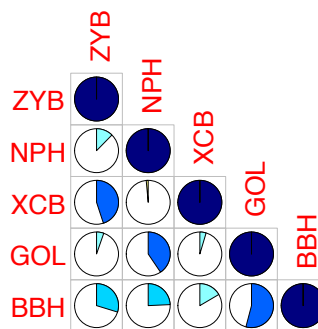
Arikara male, N=42



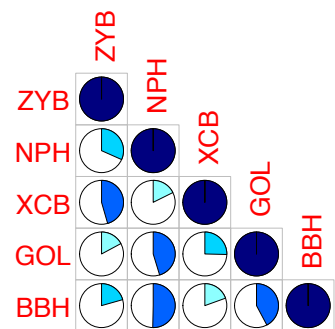
Eskimo, N=108



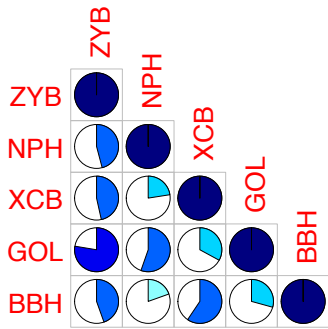
Eskimo male, N=53



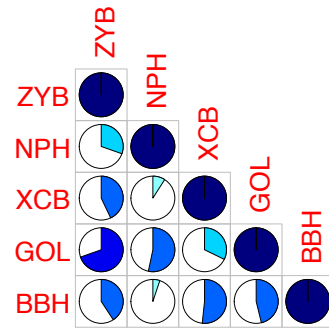
Eskimo female, N=55



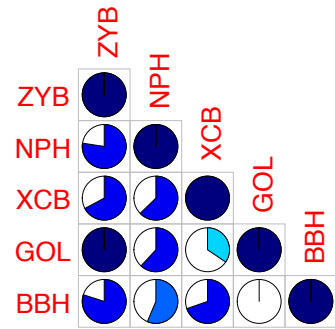
Early Per. CA N=59



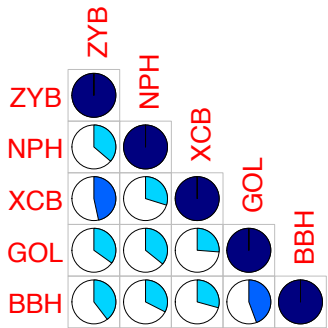
Early Per. CA males, N=36



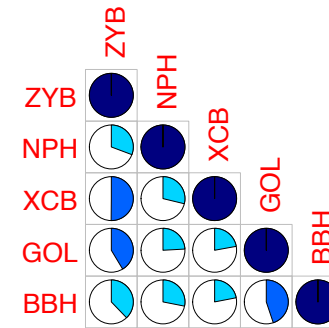
Early Per. CA females, N=23



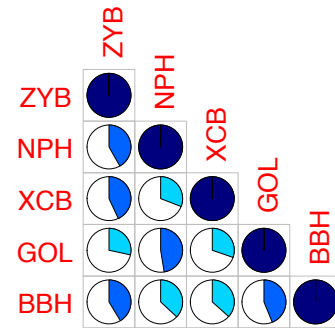
Peru, N=110



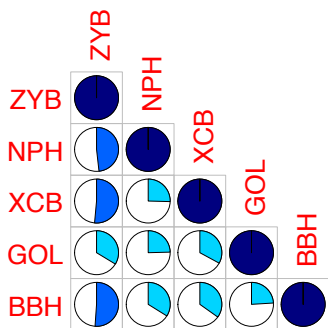
Peru male, N=55



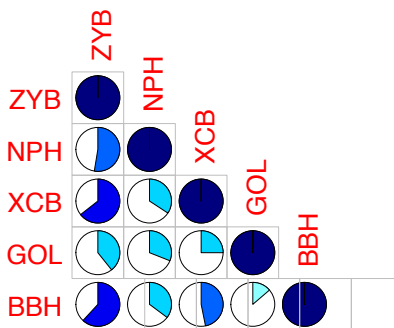
Peru female, N=55



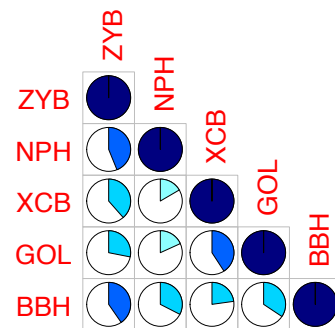
Santa Cruz Is., N=102



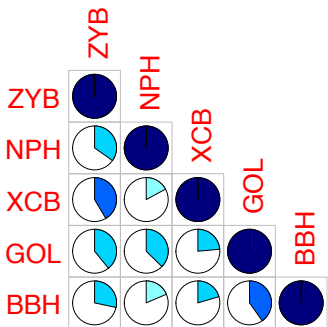
Santa Cruz Is. male, N=51



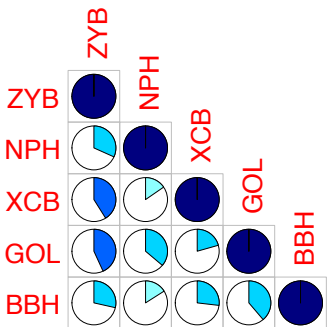
Santa Cruz Is. female, N=51



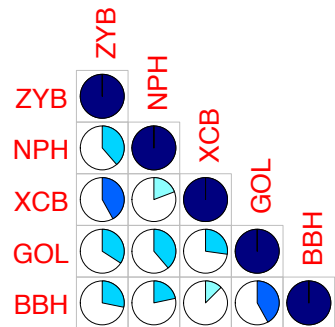
Asia, N=573



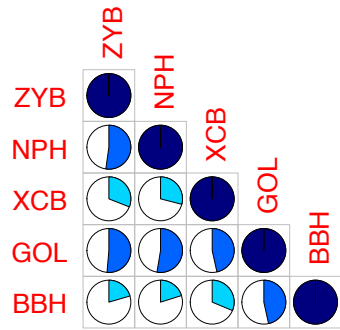
Asia male, N=317



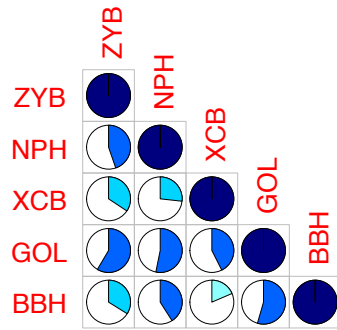
Asia female, N=256



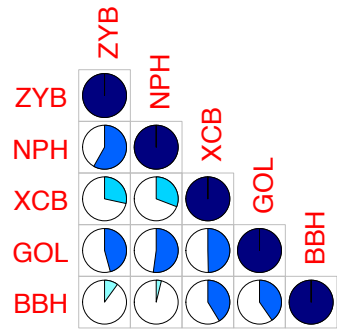
Ainu, N=86



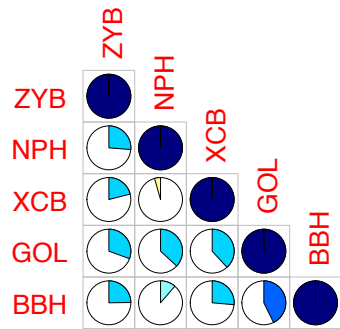
Ainu female, N=38



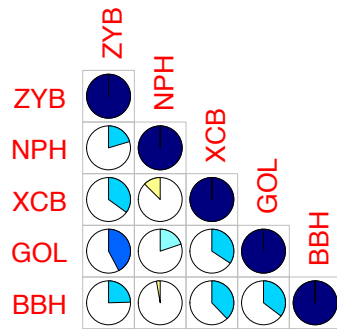
Ainu male, N=48



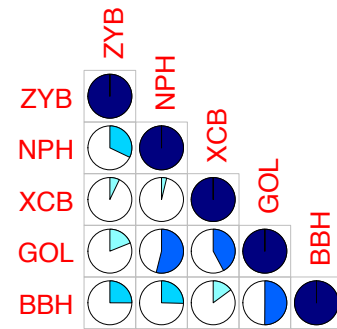
Andaman, N=70



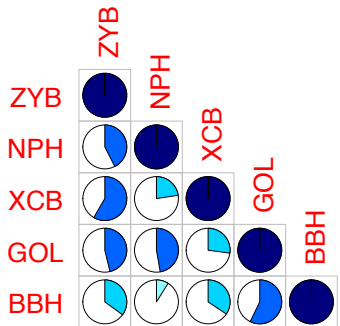
Andaman male, N=35



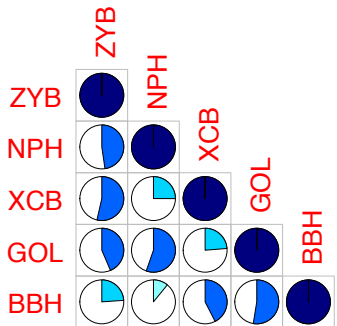
Andaman female, N=35



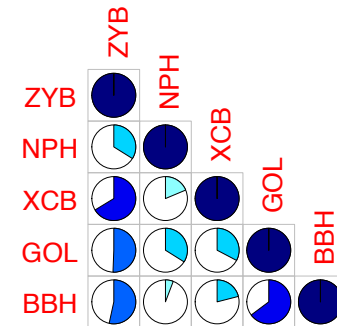
Atayal, N=47



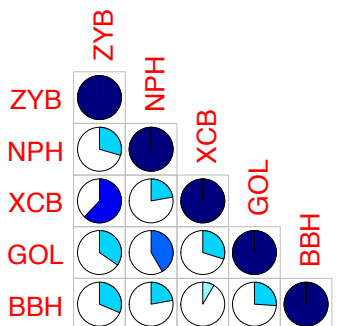
Atayal male, N=29



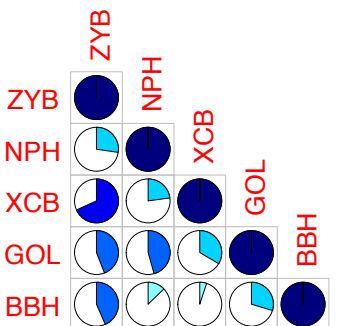
Atayal female, N=18



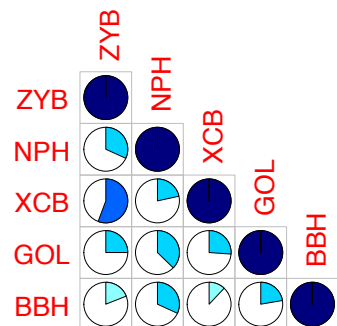
Buriat, N=109



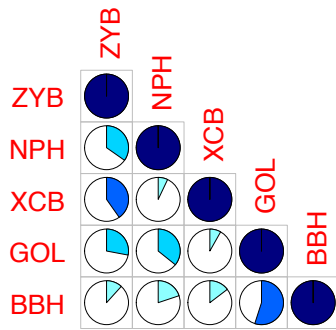
Buriat male, N=55



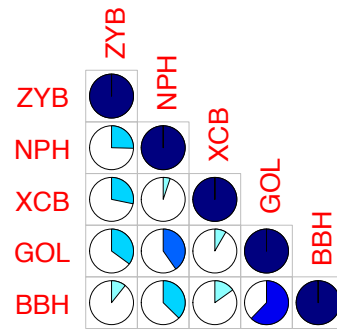
Buriat female, N=54



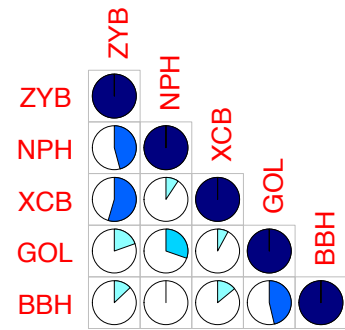
Hainan, N=83



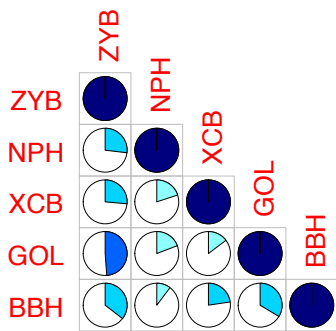
Hainan male, N=45



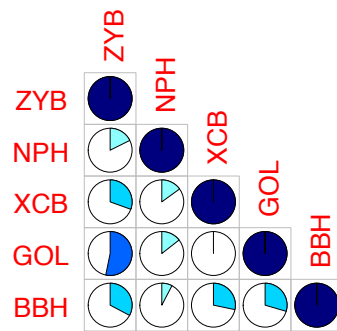
Hainan female, N=38



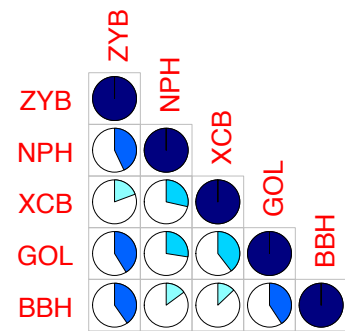
North Japan, N=87



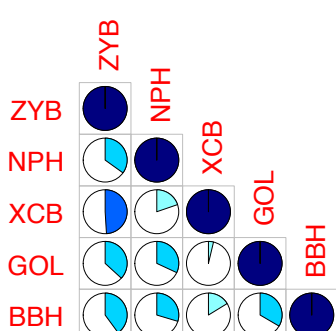
North Japan male, N=55



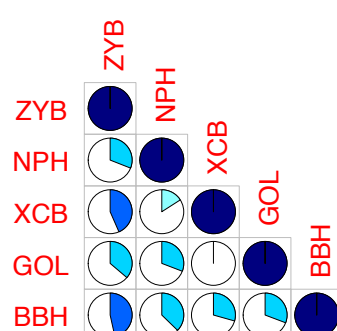
North Japan female, N=32



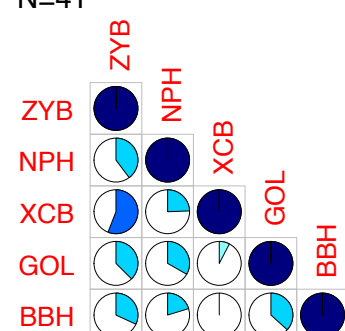
South Japan, N=91



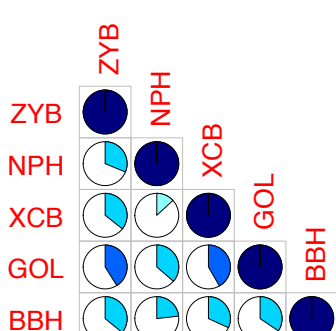
South Japan male, N=50



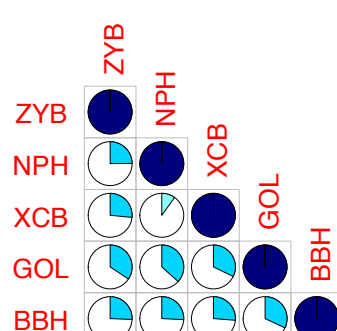
South Japan female, N=41



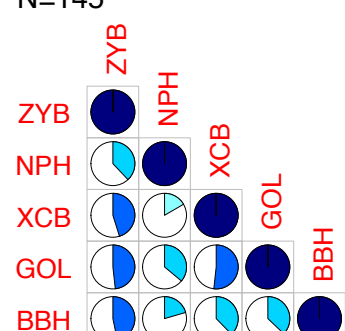
Australasia, N=298



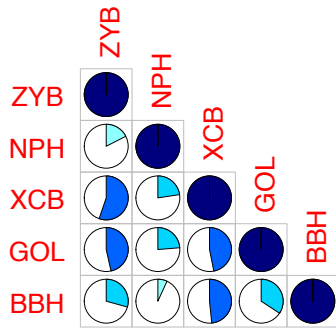
Australasia male, N=153



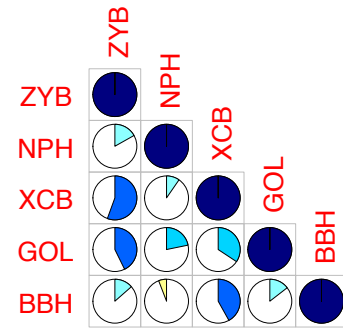
Australasia female, N=145



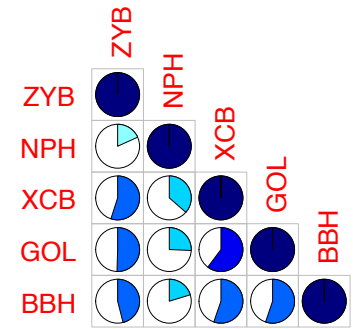
Australia, N=101



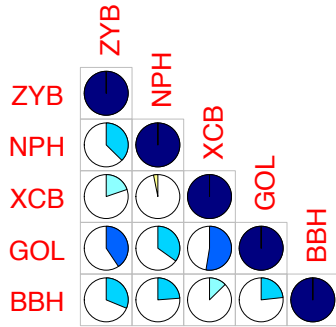
Australia male, N=52



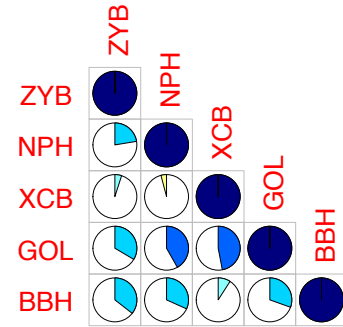
Australia female, N=49



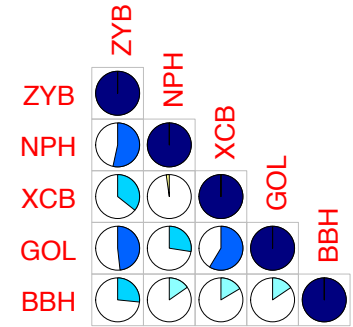
Tasmania, N=87



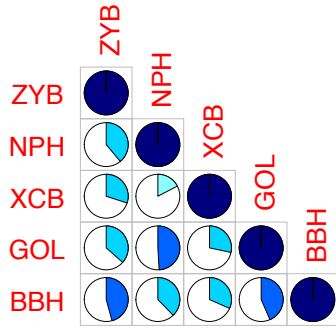
Tasmania male, N=45



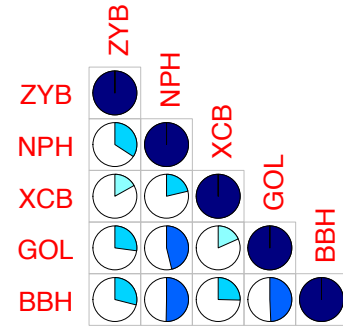
Tasmania female, N=42



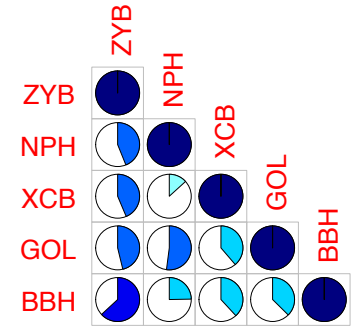
Tolai, N=110



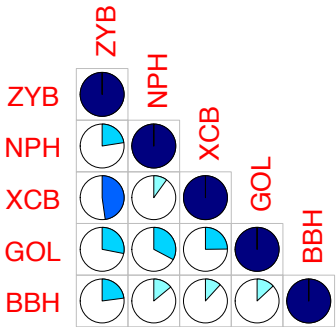
Tolai male, N=56



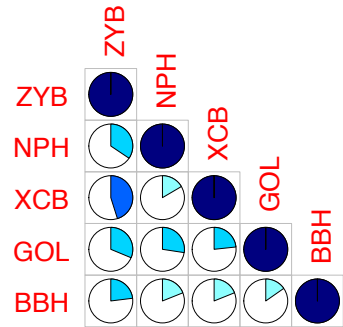
Tolai female, N=54



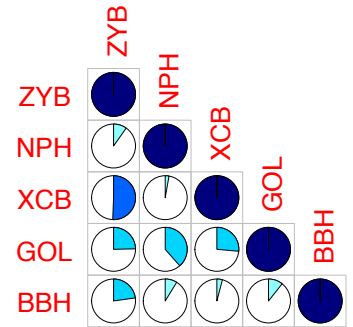
Europe, N=317



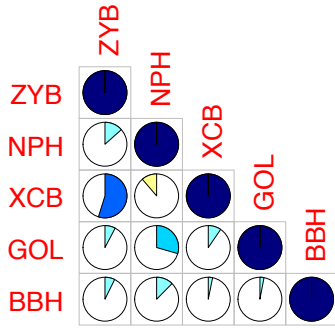
Europe male, N=164



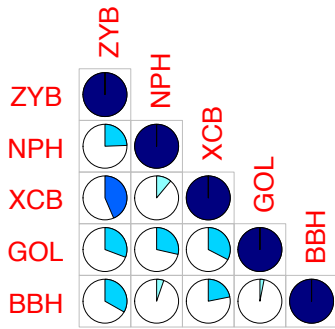
Europe female, N=153



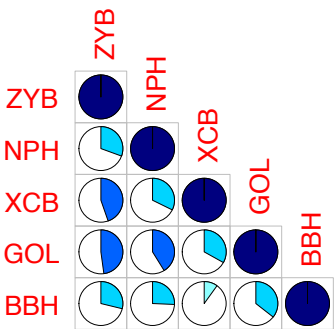
Berg, N=109



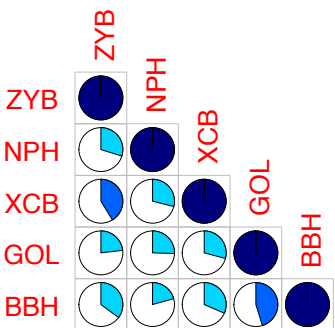
Norse, N=110



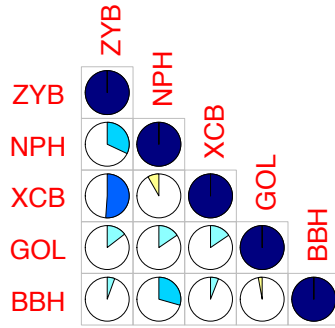
Zalavar, N=98



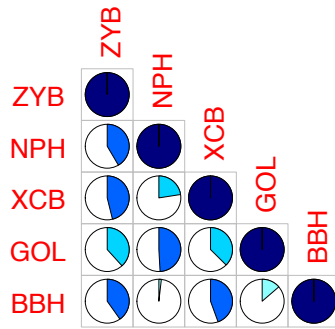
Poly/Micronesia, N=351



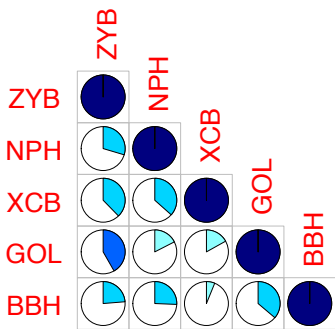
Berg male, N=56



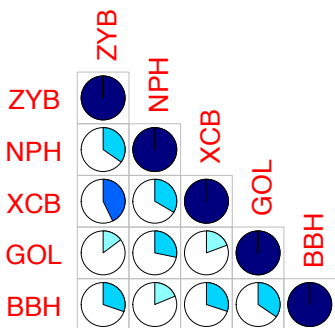
Norse male, N=55



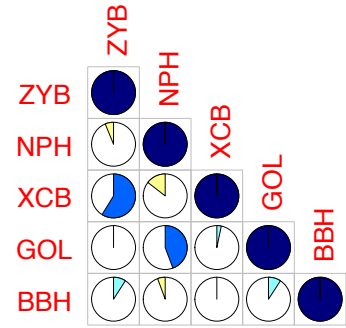
Zalavar male, N=53



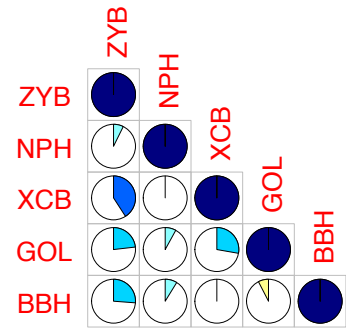
Poly/Micronesia male, N=187



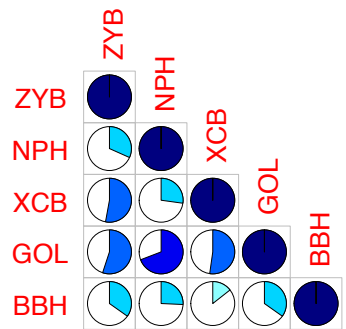
Berg female, N=53



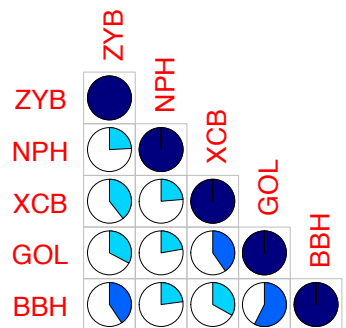
Norse female, N=55



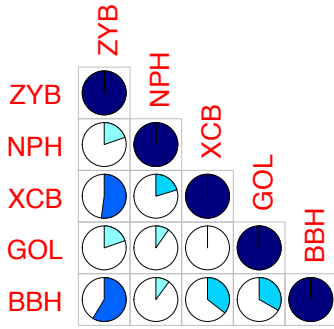
Zalavar female, N=45



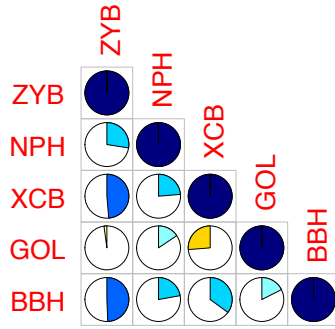
Poly/Micronesia female, N=164



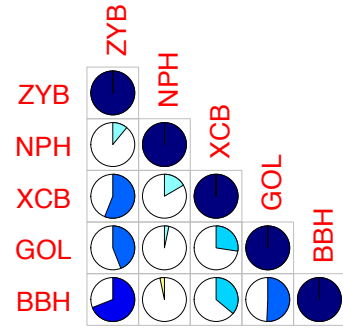
Guam, N=57



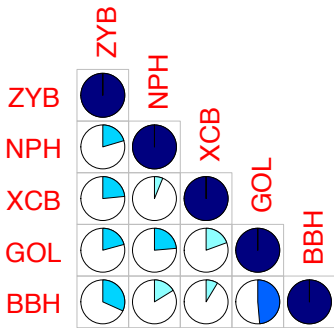
Guam male, N=30



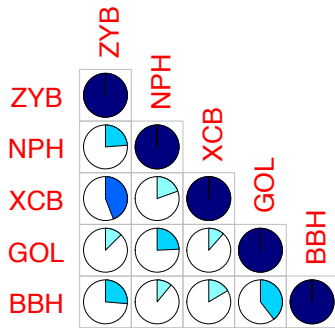
Guam female, N=27



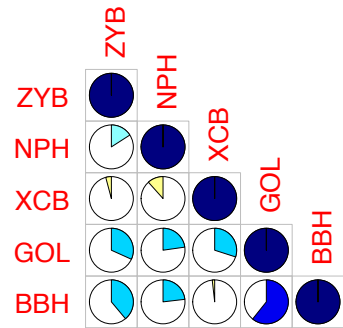
Easter Is., N=86



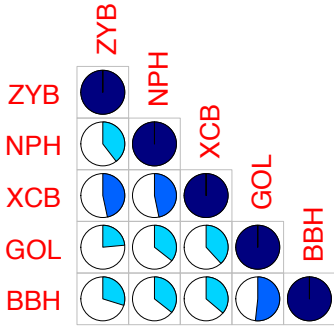
Easter Is. male, N=49



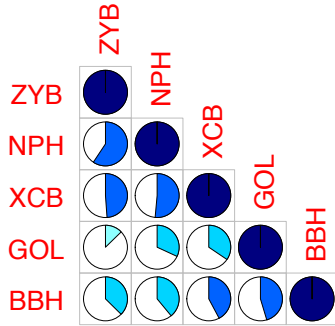
Easter Is. female, N=37



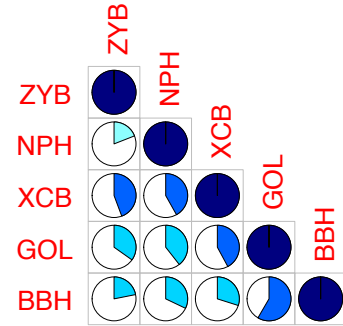
Mokapu, N=100



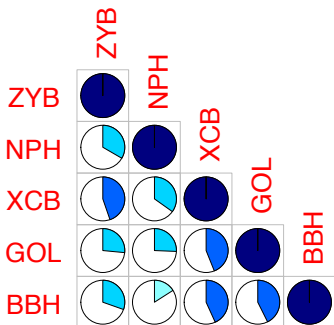
Mokapu male, N=51



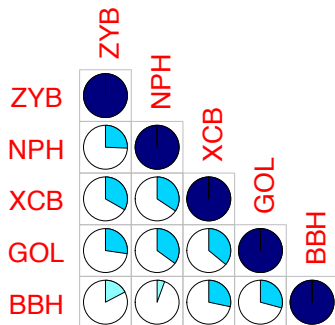
Mokapu female, N=49



Moriori, N=108



Moriori male, N=57



Moriori female, N=51

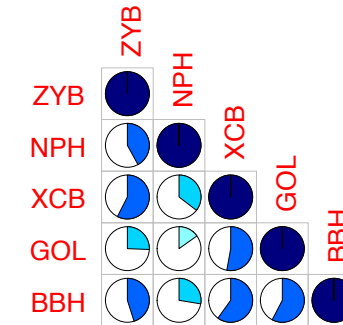
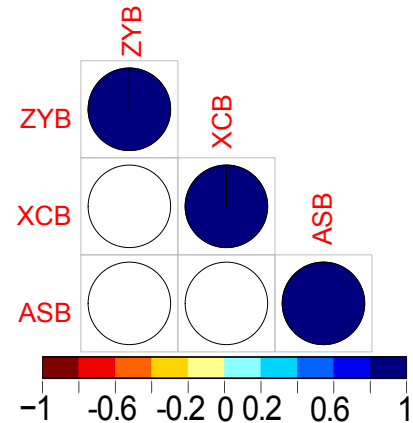


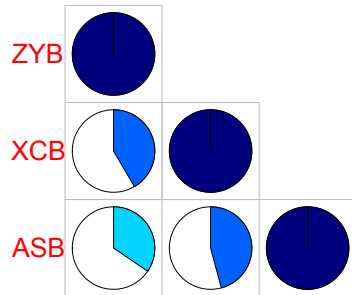
Figure 4. Correlations between measurements of maximum breadth.

**Legend:** Shaded proportion of circles represent correlation. Cool colors indicate positive correlation, warm colors indicate negative correlation. For example, a correlation close to 1 will be represented as a circle nearly completely filled with dark blue. A correlation of 0.25 will be a circle that has a light blue fill in one quarter.

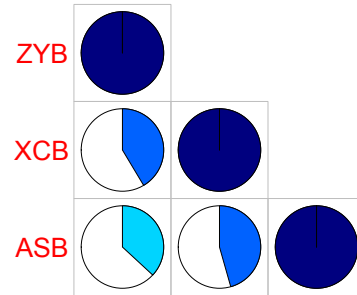


<u>Cranial region</u>	<u>Meas.</u>
Facial skeleton	ZYB
Neurocranium	XCB
Basicranium	ASB

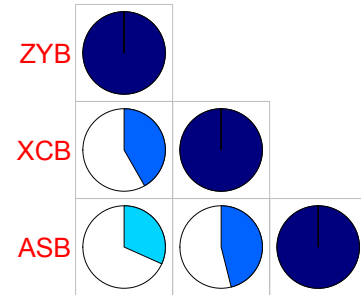
All data, N=2,471



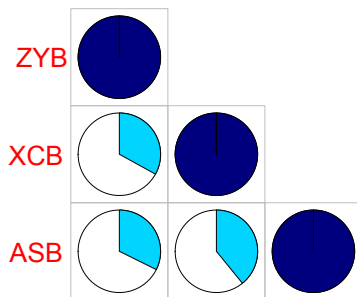
All male, N=1,292



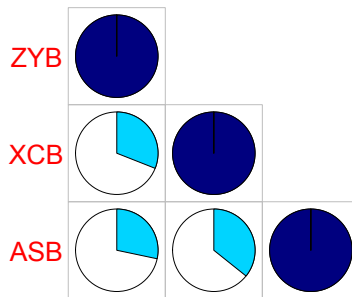
All female, N=1,179



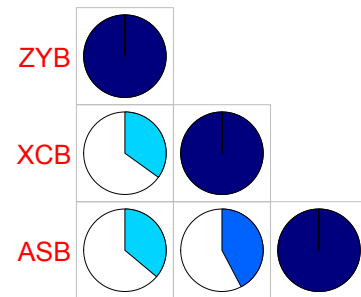
Africa, N=484



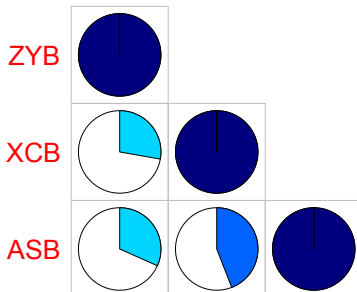
Africa male, N=234



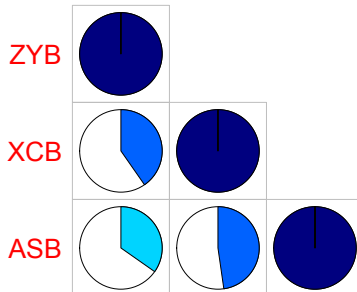
Africa female, N=250



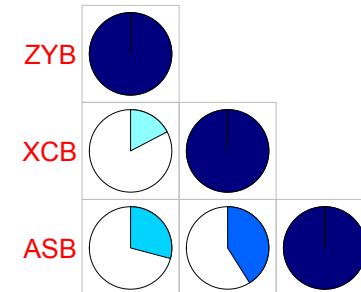
Bushman, N=90



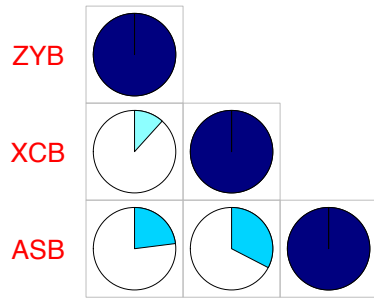
Bushman male, N=41



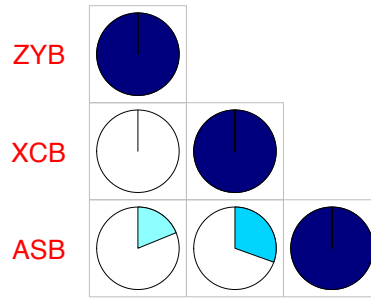
Bushman female, N=49



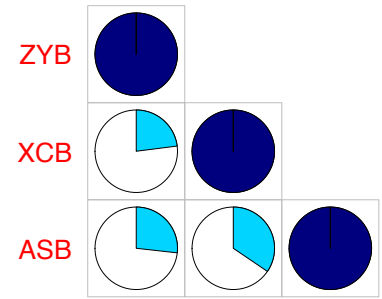
Dogon, N=99



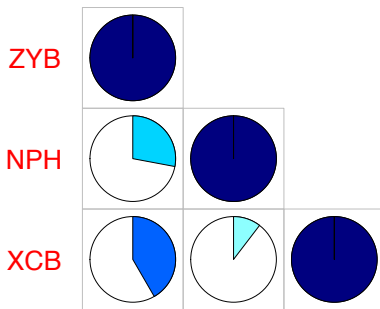
Dogon male, N=47



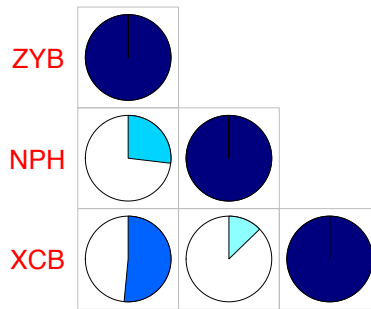
Dogon female, N=52



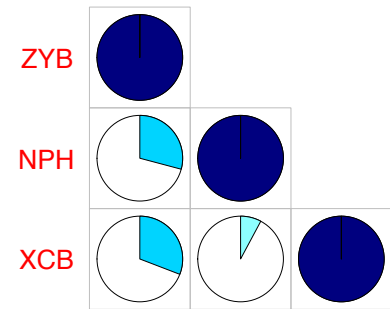
Egypt, N=111



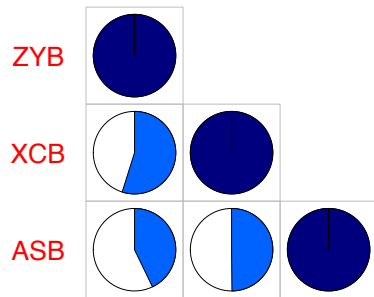
Egypt male, N=58



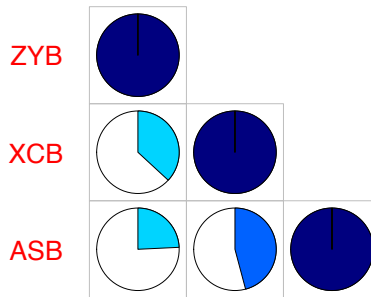
Egypt female, N=53



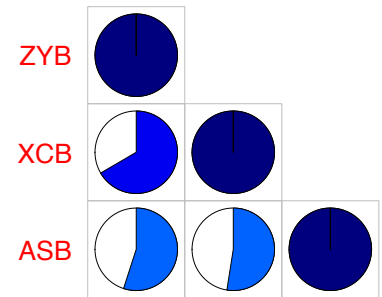
Teita, N=83



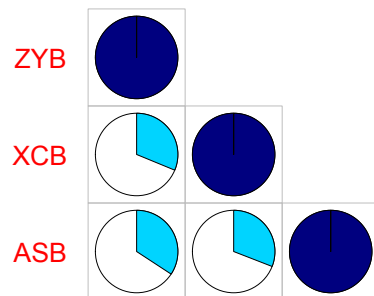
Teita male, N=33



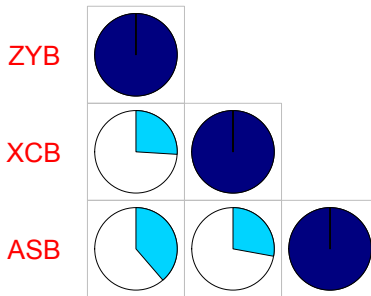
Teita female, N=50



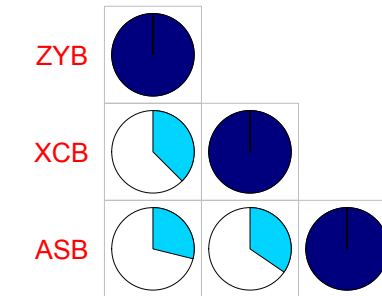
Zulu, N=101



Zulu male, N=55

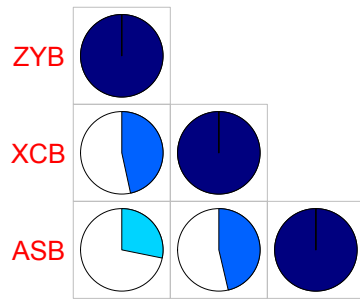


Zulu female, N=46

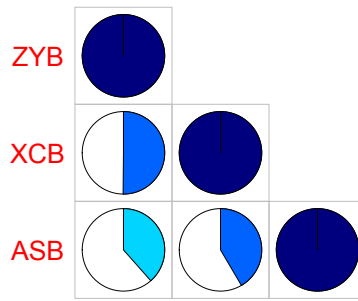




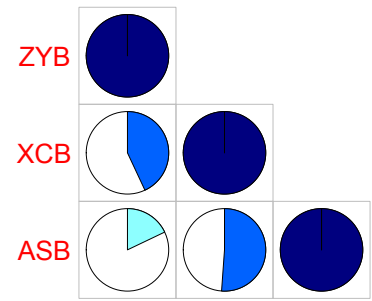
Peru, N=110



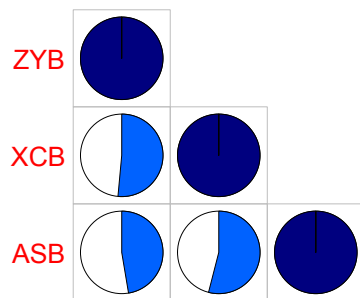
Peru male, N= 55



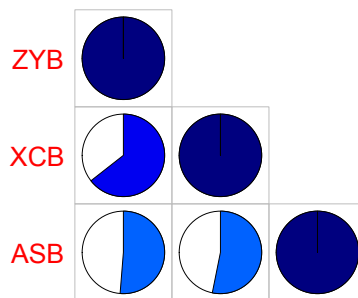
Peru female, N=55



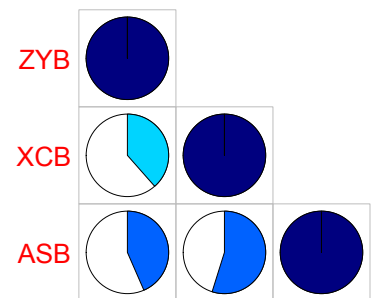
Santa Cruz Is., N=102



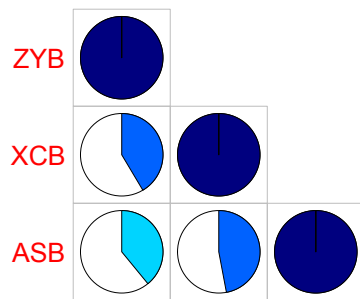
Santa Cruz Is. male, N=51



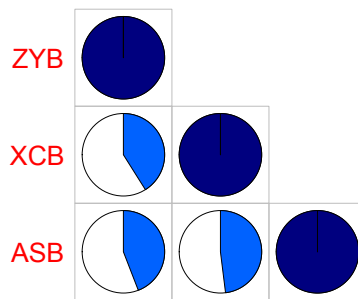
Santa Cruz Is. female, N=51



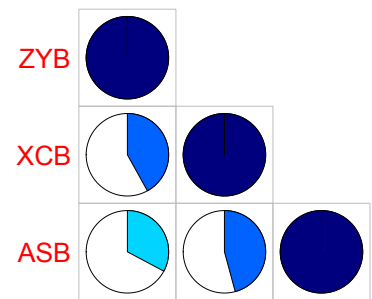
Asia, N=573



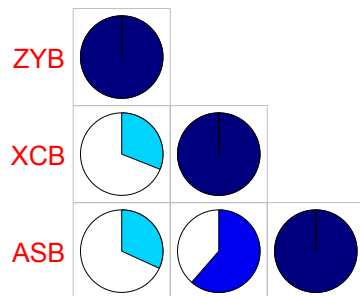
Asia male, N=317



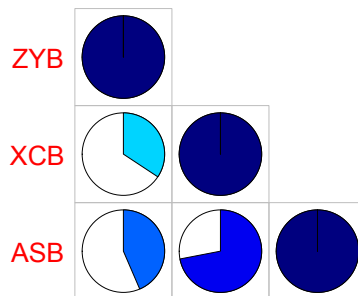
Asia female, N=256



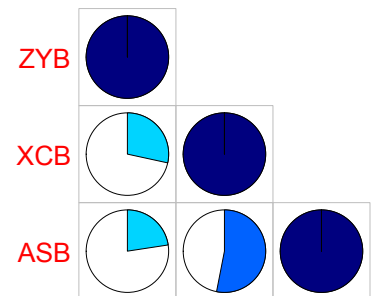
Ainu, N=86



Ainu female, N=38

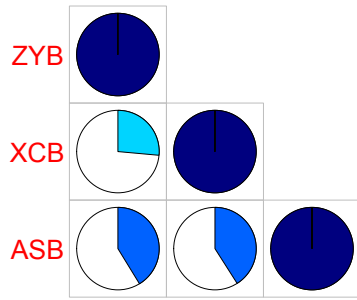


Ainu male, N=48

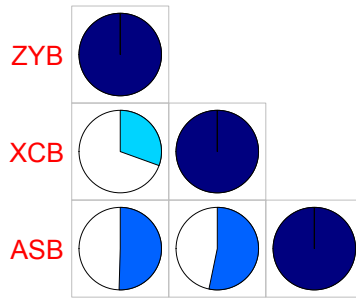




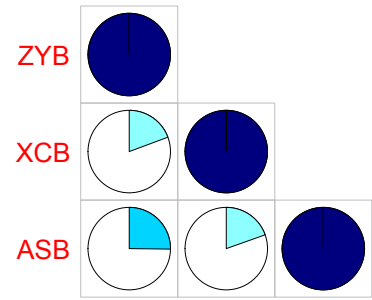
North Japan, N=87



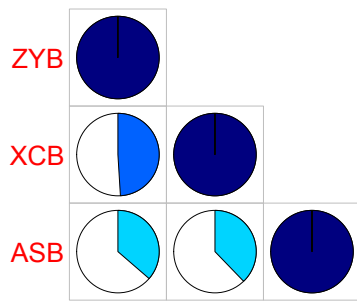
North Japan male, N=55



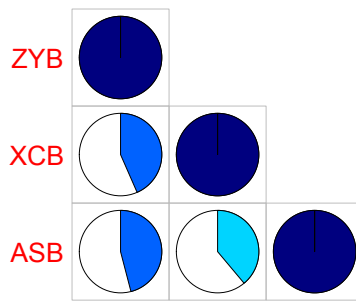
North Japan female, N=32



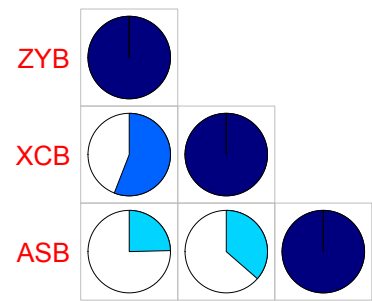
South Japan, N=91



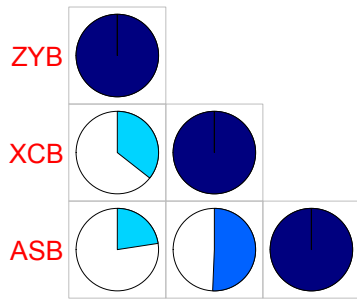
South Japan male, N=50



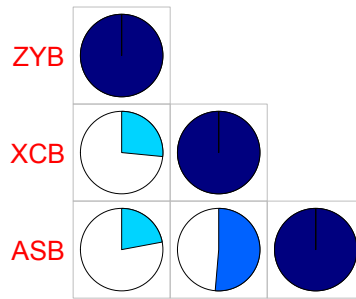
South Japan female, N=41



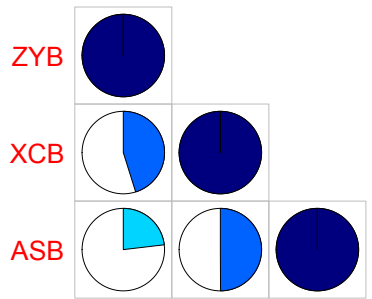
Australasia, N=298



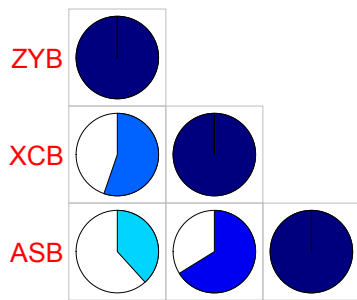
Australasia male, N=153



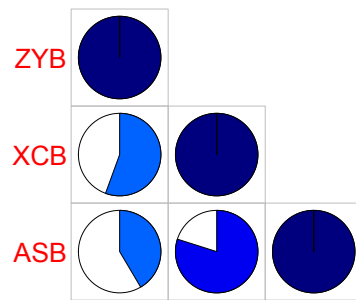
Australasia female, N=145



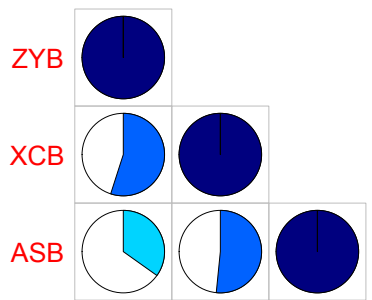
Australia, N=101



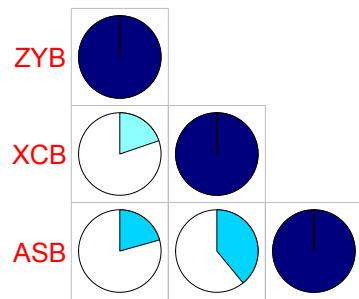
Australia male, N=52



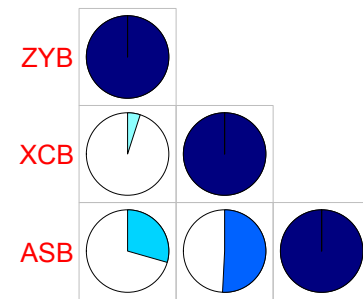
Australia female, N=49



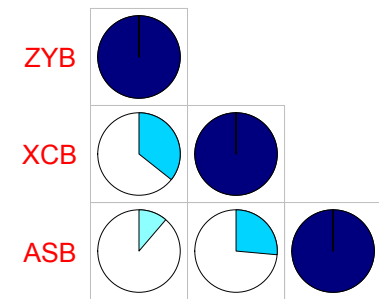
Tasmania, N=87



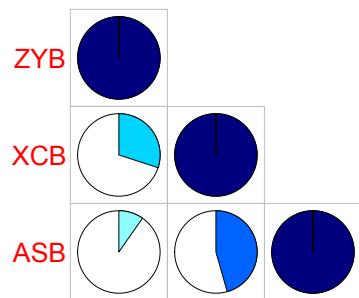
Tasmania male, N=45



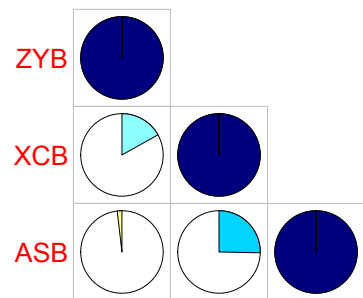
Tasmania female, N=42



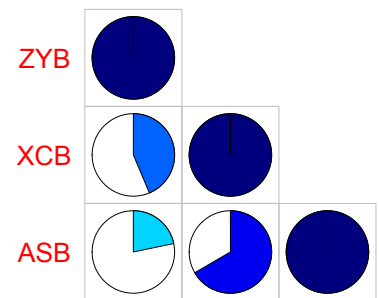
Tolai, N=110



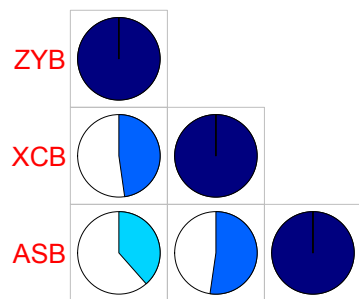
Tolai male, N=56



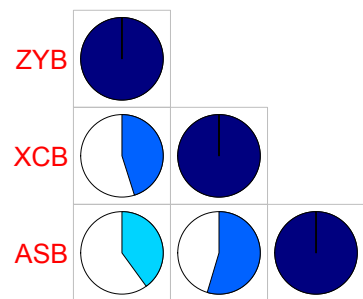
Tolai female, N=54



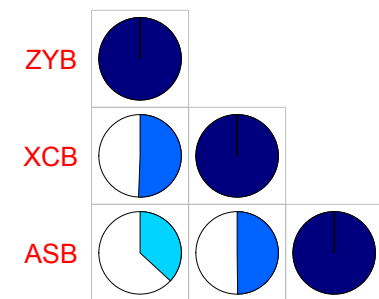
Europe, N=317



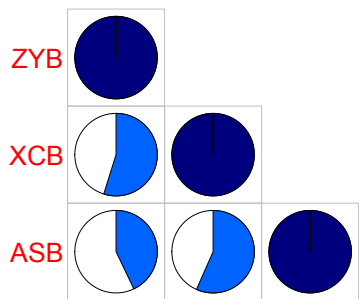
Europe male, N=164



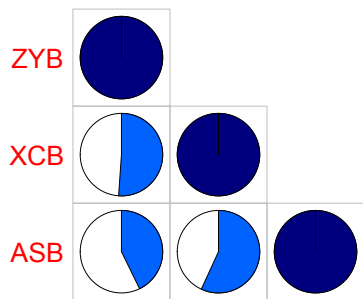
Europe female, N=153



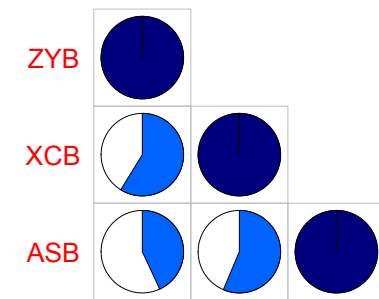
Berg, N=109



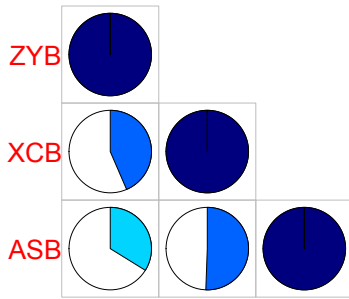
Berg male, N=56



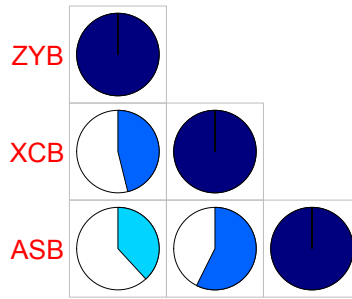
Berg female, N=53



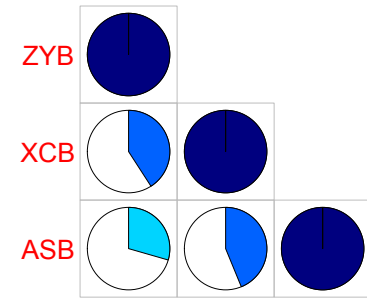
Norse, N=110



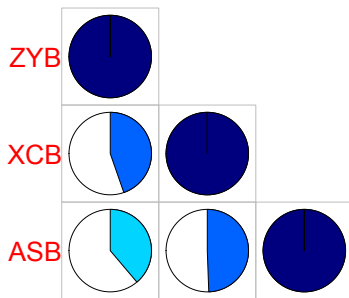
Norse male, N=55



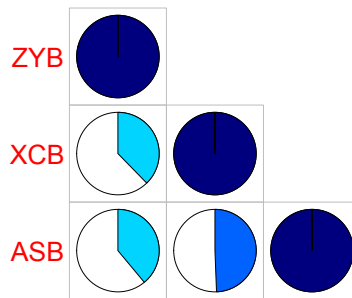
Norse female, N=55



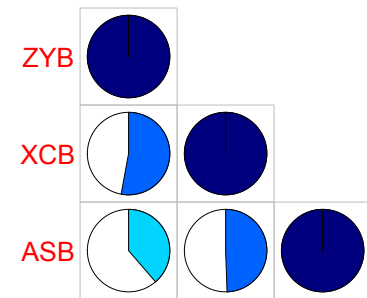
Zalavar, N=98



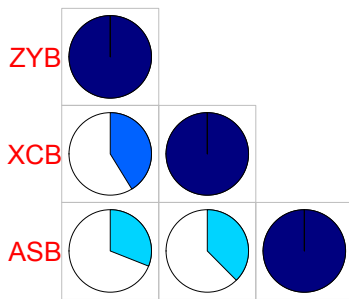
Zalavar male, N=53



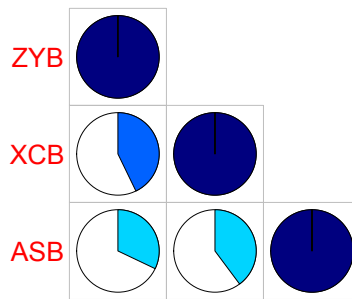
Zalavar female, N=45



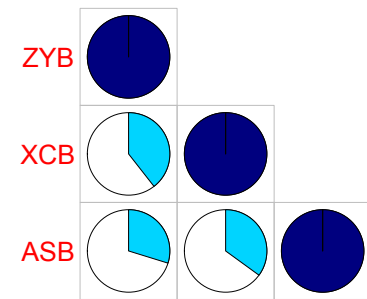
**Poly/Micronesia, N=351**



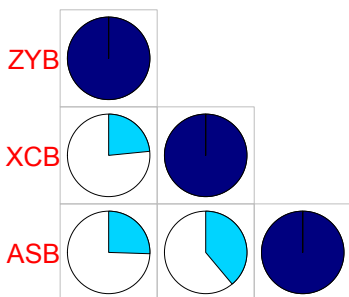
**Poly/Micronesia male, N=187**



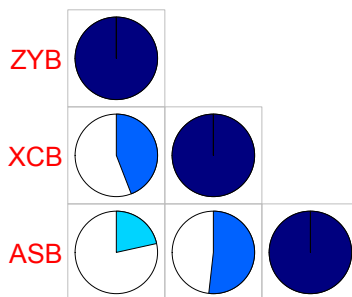
**Poly/Micronesia female, N=164**



Easter Is., N=86



Easter Is. male, N=49



Easter Is. female, N=37

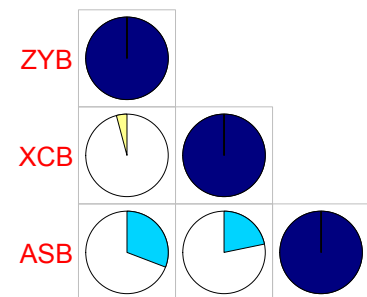




Table 1. Sample composition of the data sets.\*†

Level	Geo. region	Population	N=	Data set(s)	No. M	No. F
Species**	All	All	2,583	All	1,404	1,179
Geo.region	Africa	–	484	Howells	234	250
Population	–	Bushman	90	"	41	49
	–	Dogon	99	"	47	52
	–	Egypt	111	"	58	53
	–	Teita	83	"	33	50
	–	Zulu	101	"	55	46
Geo.region	Americas	–	448	All	237	211
Population	–	Arikara	69	Howells	42	27
	–	Eskimo	108	"	53	55
	–	Early Per. CA	59	Early Per. CA	36	23
	–	Peru	110	Howells	55	55
	–	Santa Cruz Is	102	"	51	51
Geo.region	Asia	–	665	"	409	256
Population	–	Ainu	86	"	48	38
	–	Andaman	70	"	35	35
	–	Anyang	42	"	42	–
	–	Atayal	47	"	29	18
	–	Buriat	109	"	55	54
	–	Hainan	83	"	45	38
	–	N. Japan	87	"	55	32
	–	Philippines	50	"	50	–
	–	S. Japan	91	"	50	41
Geo.region	Australasia	–	298	"	153	145
Population	–	Australia	101	"	52	49
	–	Tasmania	87	"	45	42
	–	Tolai	110	"	56	54
Geo.region	Europe	–	317	"	164	153
Population	–	Berg	109	"	56	53
	–	Norse	110	"	55	55
	–	Zalavar	98	"	53	45
Geo.region	Poly/Micronesia	–	361	"	197	164
Population	–	Easter Is.	86	"	49	37
	–	Guam	57	"	30	27
	–	Moriori	108	"	57	51
	–	Mokapu	100	"	51	49
	–	N. Maori	10	"	10	–
	–	S. Maori	10	"	10	–

\*Data sets used are the Howells data (1973;1989; 1995) and data for Early Period Native Californians collected by W.B.R. \*\*The Howells data is customarily used to represent modern human species-wide cranial variation, and it is, with the addition of the Early Period Native Californian data, used in this way. †Four populations (N=112) from the Howells data set were excluded from all analyses below the species level because they are composed of male individuals only. The complete Howells data set includes 2,524 individuals.

Table 2. Correlations between maximum cranial width of the facial skeleton, neurocranium, and basicranium used to test the third set of hypotheses.

		Legend		
		ZYB	XCB	ASB
Face		ZYB	-	
Neurocranium		XCB	F:N	-
Basicranium		ASB	F:B	B:N -
		All data		
		ZYB	XCB	ASB
All (M & F)	ZYB	-	0.42	0.35
	XCB	0.42	-	0.46
	ASB	0.35	0.46	-
Male	ZYB	-	0.41	0.37
	XCB	0.41	-	0.46
	ASB	0.37	0.46	-
Female	ZYB	-	0.42	0.32
	XCB	0.42	-	0.46
	ASB	0.32	0.46	-
		Africa		
		ZYB	XCB	ASB
All (M & F)	ZYB	-	0.33	0.32
	XCB	0.33	-	0.39
	ASB	0.32	0.39	-
Male	ZYB	-	0.31	0.28
	XCB	0.31	-	0.36
	ASB	0.28	0.36	-
Female	ZYB	-	0.35	0.36
	XCB	0.35	-	0.42
	ASB	0.36	0.42	-
		Americas		
		ZYB	XCB	ASB
All (M & F)	ZYB	-	0.50	0.37
	XCB	0.50	-	0.50
	ASB	0.37	0.50	-
Male	ZYB	-	0.41	0.39
	XCB	0.41	-	0.47
	ASB	0.39	0.47	-
Female	ZYB	-	0.42	0.33
	XCB	0.42	-	0.46
	ASB	0.33	0.46	-
		Asia		
		ZYB	XCB	ASB
All (M & F)	ZYB	-	0.41	0.39
	XCB	0.41	-	0.47
	ASB	0.39	0.47	-
Male	ZYB	-	0.41	0.44
	XCB	0.41	-	0.48
	ASB	0.44	0.48	-
Female	ZYB	-	0.42	0.33
	XCB	0.42	-	0.46
	ASB	0.33	0.46	-
		Australasia		
		ZYB	XCB	ASB
All (M & F)	ZYB	-	0.36	0.23
	XCB	0.36	-	0.51
	ASB	0.23	0.51	-
Male	ZYB	-	0.27	0.22
	XCB	0.27	-	0.51
	ASB	0.22	0.51	-
Female	ZYB	-	0.45	0.23
	XCB	0.45	-	0.50
	ASB	0.23	0.50	-
		Europe		
		ZYB	XCB	ASB
All (M & F)	ZYB	-	0.48	0.38
	XCB	0.48	-	0.52
	ASB	0.38	0.52	-
Male	ZYB	-	0.45	0.40
	XCB	0.45	-	0.55
	ASB	0.40	0.55	-
Female	ZYB	-	0.51	0.37
	XCB	0.51	-	0.50
	ASB	0.37	0.50	-
		POLY/Micronesia		
		ZYB	XCB	ASB
All (M & F)	ZYB	-	0.41	0.31
	XCB	0.41	-	0.38
	ASB	0.31	0.38	-
Male	ZYB	-	0.43	0.32
	XCB	0.43	-	0.40
	ASB	0.32	0.40	-
Female	ZYB	-	0.39	0.30
	XCB	0.39	-	0.35
	ASB	0.30	0.35	-

		Africa			Bushman			Dogon			Egypt			Tetra			Zulu					
		ZYB	XCB	ASB	ZYB	XCB	ASB	ZYB	XCB	ASB	ZYB	XCB	ASB	ZYB	XCB	ASB	ZYB	XCB	ASB			
<b>A F R I C A</b>	<b>All (M &amp; F)</b>	ZYB	-	0.33	0.32	-	0.28	0.32	-	0.12	0.23	-	0.42	0.32	-	0.55	0.43	-	0.31	0.34		
		XCB	0.33	-	0.39	0.28	-	0.44	0.12	-	0.33	0.42	-	0.40	0.55	-	0.50	0.31	-	0.31		
		ASB	0.32	0.39	-	0.32	0.44	-	0.23	0.33	-	0.32	0.40	-	0.43	0.50	-	0.34	0.31	-		
	<b>Male</b>	ZYB	-	0.31	0.28	-	0.40	0.35	-	-0.01	0.19	-	0.52	0.24	-	0.37	0.24	-	0.26	0.39		
		XCB	0.31	-	0.36	0.40	-	0.48	-0.01	-	0.30	0.52	-	0.33	0.37	-	0.46	0.26	-	0.28		
		ASB	0.28	0.36	-	0.35	0.48	-	0.19	0.30	-	0.24	0.33	-	0.24	0.46	-	0.39	0.28	-		
	<b>Female</b>	ZYB	-	0.35	0.36	-	0.17	0.29	-	0.23	0.27	-	0.31	0.40	-	0.67	0.55	-	0.38	0.29		
		XCB	0.35	-	0.42	0.17	-	0.41	0.23	-	0.34	0.31	-	0.48	0.67	-	0.52	0.38	-	0.35		
		ASB	0.36	0.42	-	0.29	0.41	-	0.27	0.34	-	0.40	0.48	-	0.55	0.52	-	0.29	0.35	-		
<b>A M E R I C A S</b>	<b>All (M &amp; F)</b>	<b>Americas</b>																				
		ZYB	XCB	ASB	ZYB	XCB	ASB	ZYB	XCB	ASB	ZYB	XCB	ASB	ZYB	XCB	ASB	ZYB	XCB	ASB	ZYB	XCB	ASB
		-	0.50	0.37	-	0.59	0.43	-	0.45	0.30	-	0.47	0.56	-	0.47	0.28	-	0.51	0.47	-	0.51	0.47
		0.50	-	0.50	0.59	-	0.48	0.45	-	0.38	0.47	-	0.81	0.47	-	0.46	0.51	-	0.54	0.51	-	0.54
		0.37	0.50	-	0.43	0.48	-	0.30	0.38	-	0.56	0.81	-	0.28	0.46	-	0.47	0.54	-	-	-	-
	<b>Male</b>	ZYB	-	0.56	0.45	-	0.70	0.52	-	0.45	0.33	-	0.43	0.72	-	0.50	0.38	-	0.64	0.51		
		XCB	0.56	-	0.46	0.70	-	0.54	0.45	-	0.23	0.43	-	0.78	0.50	-	0.42	0.64	-	0.53		
		ASB	0.45	0.46	-	0.52	0.54	-	0.33	0.23	-	0.72	0.78	-	0.38	0.42	-	0.51	0.53	-		
		<b>Peru</b>																				
		ZYB	XCB	ASB	ZYB	XCB	ASB	ZYB	XCB	ASB	ZYB	XCB	ASB	ZYB	XCB	ASB	ZYB	XCB	ASB	ZYB	XCB	ASB
	-	0.43	0.28	-	0.42	0.28	-	0.46	0.26	-	0.67	0.19	-	0.43	0.18	-	0.38	0.43	-	0.38	0.43	
	0.43	-	0.54	0.42	-	0.40	0.46	-	0.53	0.67	-	0.85	0.43	-	0.51	0.38	-	0.55	0.38	-	0.55	
	0.28	0.54	-	0.28	0.40	-	0.26	0.53	-	0.19	0.85	-	0.18	0.51	-	0.43	0.55	-	-	-	-	
	<b>Arkara</b>																					
	ZYB	XCB	ASB	ZYB	XCB	ASB	ZYB	XCB	ASB	ZYB	XCB	ASB	ZYB	XCB	ASB	ZYB	XCB	ASB	ZYB	XCB	ASB	
-	0.50	0.37	-	0.59	0.43	-	0.45	0.30	-	0.47	0.56	-	0.47	0.28	-	0.51	0.47	-	0.51	0.47		
0.50	-	0.50	0.59	-	0.48	0.45	-	0.38	0.47	-	0.81	0.47	-	0.46	0.51	-	0.54	0.51	-	0.54		
0.37	0.50	-	0.43	0.48	-	0.30	0.38	-	0.56	0.81	-	0.28	0.46	-	0.47	0.54	-	-	-	-		
<b>Eskimo</b>																						
ZYB	XCB	ASB	ZYB	XCB	ASB	ZYB	XCB	ASB	ZYB	XCB	ASB	ZYB	XCB	ASB	ZYB	XCB	ASB	ZYB	XCB	ASB		
-	0.56	0.45	-	0.70	0.52	-	0.45	0.33	-	0.43	0.72	-	0.50	0.38	-	0.64	0.51	-	0.64	0.51		
0.56	-	0.46	0.70	-	0.54	0.45	-	0.23	0.43	-	0.78	0.50	-	0.42	0.64	-	0.53	0.64	-	0.53		
0.45	0.46	-	0.52	0.54	-	0.33	0.23	-	0.72	0.78	-	0.38	0.42	-	0.51	0.53	-	-	-	-		
<b>Santa Cruz Is.</b>																						
ZYB	XCB	ASB	ZYB	XCB	ASB	ZYB	XCB	ASB	ZYB	XCB	ASB	ZYB	XCB	ASB	ZYB	XCB	ASB	ZYB	XCB	ASB		
-	0.50	0.37	-	0.59	0.43	-	0.45	0.30	-	0.47	0.56	-	0.47	0.28	-	0.51	0.47	-	0.51	0.47		
0.50	-	0.50	0.59	-	0.48	0.45	-	0.38	0.47	-	0.81	0.47	-	0.46	0.51	-	0.54	0.51	-	0.54		
0.37	0.50	-	0.43	0.48	-	0.30	0.38	-	0.56	0.81	-	0.28	0.46	-	0.47	0.54	-	-	-	-		
<b>Early Per. Native CA</b>																						
ZYB	XCB	ASB	ZYB	XCB	ASB	ZYB	XCB	ASB	ZYB	XCB	ASB	ZYB	XCB	ASB	ZYB	XCB	ASB	ZYB	XCB	ASB		
-	0.43	0.28	-	0.42	0.28	-	0.46	0.26	-	0.67	0.19	-	0.43	0.18	-	0.38	0.43	-	0.38	0.43		
0.43	-	0.54	0.42	-	0.40	0.46	-	0.53	0.67	-	0.85	0.43	-	0.51	0.38	-	0.55	0.38	-	0.55		
0.28	0.54	-	0.28	0.40	-	0.26	0.53	-	0.19	0.85	-	0.18	0.51	-	0.43	0.55	-	-	-	-		

		Asia			Ainu			Andaman			Atayal			Burai		
		ZYB	XCB	ASB	ZYB	XCB	ASB	ZYB	XCB	ASB	ZYB	XCB	ASB	ZYB	XCB	ASB
<b>All (M &amp; F)</b>	ZYB	-	0.41	0.39	-	0.31	0.32	-	0.58	0.55	-	0.21	0.24	-	0.62	0.41
	XCB	0.41	-	0.47	0.31	-	0.61	0.58	-	0.60	0.21	-	0.31	0.62	-	0.60
	ASB	0.39	0.47	-	0.32	0.61	-	0.55	0.60	-	0.24	0.31	-	0.41	0.60	-
<b>Male</b>	ZYB	-	0.41	0.44	-	0.28	0.23	-	0.54	0.60	-	0.35	0.24	-	0.68	0.52
	XCB	0.41	-	0.48	0.28	-	0.53	0.54	-	0.55	0.35	-	0.10	0.68	-	0.64
	ASB	0.44	0.48	-	0.23	0.53	-	0.60	0.55	-	0.24	0.10	-	0.52	0.64	-
<b>Female</b>	ZYB	-	0.42	0.33	-	0.34	0.44	-	0.66	0.46	-	0.07	0.24	-	0.56	0.29
	XCB	0.42	-	0.46	0.34	-	0.72	0.66	-	0.66	0.07	-	0.52	0.56	-	0.55
	ASB	0.33	0.46	-	0.44	0.72	-	0.46	0.66	-	0.24	0.52	-	0.29	0.55	-

A  
S  
I  
A

		Hainan			N Japan			S Japan		
		ZYB	XCB	ASB	ZYB	XCB	ASB	ZYB	XCB	ASB
<b>All (M &amp; F)</b>	ZYB	-	0.40	0.49	-	0.26	0.41	-	0.49	0.36
	XCB	0.40	-	0.38	0.26	-	0.41	0.49	-	0.38
	ASB	0.49	0.38	-	0.41	0.41	-	0.36	0.38	-
<b>Male</b>	ZYB	-	0.28	0.53	-	0.31	0.50	-	0.43	0.46
	XCB	0.28	-	0.51	0.31	-	0.53	0.43	-	0.39
	ASB	0.53	0.51	-	0.50	0.53	-	0.46	0.39	-
<b>Female</b>	ZYB	-	0.55	0.44	-	0.19	0.25	-	0.56	0.25
	XCB	0.55	-	0.24	0.19	-	0.20	0.56	-	0.36
	ASB	0.44	0.24	-	0.25	0.20	-	0.25	0.36	-

A  
S  
I  
A

			Australasia			Australia			Tasmania			Total		
			ZYB	XCB	ASB	ZYB	XCB	ASB	ZYB	XCB	ASB	ZYB	XCB	ASB
<b>A U S T R A L I A</b>	<b>All (M &amp; F)</b>	ZYB	-	0.36	0.23	-	0.55	0.38	-	0.20	0.21	-	0.30	0.10
		XCB	0.36	-	0.51	0.55	-	0.66	0.20	-	0.39	0.30	-	0.46
		ASB	0.23	0.51	-	0.38	0.66	-	0.21	0.39	-	0.10	0.46	-
	<b>Male</b>	ZYB	-	0.27	0.22	-	0.56	0.41	-	0.05	0.29	-	0.17	-0.02
		XCB	0.27	-	0.51	0.56	-	0.80	0.05	-	0.51	0.17	-	0.25
		ASB	0.22	0.51	-	0.41	0.80	-	0.29	0.51	-	-0.02	0.25	-
	<b>Female</b>	ZYB	-	0.45	0.23	-	0.55	0.35	-	0.36	0.11	-	0.44	0.22
		XCB	0.45	-	0.50	0.55	-	0.52	0.36	-	0.26	0.44	-	0.67
		ASB	0.23	0.50	-	0.35	0.52	-	0.11	0.26	-	0.22	0.67	-
			Europe			Berg			Norse			Zalavar		
			ZYB	XCB	ASB	ZYB	XCB	ASB	ZYB	XCB	ASB	ZYB	XCB	ASB
<b>E U R O P E</b>	<b>All (M &amp; F)</b>	ZYB	-	0.48	0.38	-	0.55	0.43	-	0.44	0.34	-	0.45	0.39
		XCB	0.48	-	0.52	0.55	-	0.57	0.44	-	0.51	0.45	-	0.49
		ASB	0.38	0.52	-	0.43	0.57	-	0.34	0.51	-	0.39	0.49	-
	<b>Male</b>	ZYB	-	0.45	0.40	-	0.51	0.43	-	0.46	0.38	-	0.38	0.39
		XCB	0.45	-	0.55	0.51	-	0.57	0.46	-	0.57	0.38	-	0.49
		ASB	0.40	0.55	-	0.43	0.57	-	0.38	0.57	-	0.39	0.49	-
	<b>Female</b>	ZYB	-	0.51	0.37	-	0.59	0.43	-	0.41	0.29	-	0.53	0.39
		XCB	0.51	-	0.50	0.59	-	0.56	0.41	-	0.44	0.53	-	0.49
		ASB	0.37	0.50	-	0.43	0.56	-	0.29	0.44	-	0.39	0.49	-

P M O L Y C R O N E N S E I S A I & A	Poly/Micronesia			Easter Is.			Guam			Mokapu			Morrri			
	ZYB	XCB	ASB	ZYB	XCB	ASB	ZYB	XCB	ASB	ZYB	XCB	ASB	ZYB	XCB	ASB	
All (M & F)	ZYB	-	0.41	0.31	-	0.23	0.26	-	0.52	0.31	-	0.47	0.47	-	0.45	0.21
	XCB	0.41	-	0.38	0.23	-	0.39	0.52	-	0.43	0.47	-	0.44	0.45	-	0.28
	ASB	0.31	0.38	-	0.26	0.39	-	0.31	0.43	-	0.47	0.44	-	0.21	0.28	-
Male	ZYB	-	0.43	0.32	-	0.44	0.22	-	0.49	0.29	-	0.49	0.43	-	0.33	0.33
	XCB	0.43	-	0.40	0.44	-	0.52	0.49	-	0.39	0.49	-	0.49	0.33	-	0.21
	ASB	0.32	0.40	-	0.22	0.52	-	0.29	0.39	-	0.43	0.49	-	0.33	0.21	-
Female	ZYB	-	0.39	0.30	-	-0.04	0.31	-	0.56	0.34	-	0.44	0.51	-	0.58	0.06
	XCB	0.39	-	0.35	-0.04	-	0.22	0.56	-	0.47	0.44	-	0.39	0.58	-	0.35
	ASB	0.30	0.35	-	0.31	0.22	-	0.34	0.47	-	0.51	0.39	-	0.06	0.35	-

Table 3. Summary of results for Hypothesis 3<sup>†</sup>

Level	Geo. Region	Population	All indiv.	Male	Female
Species <sup>1</sup>	All	All	x	x	x
Species <sup>2</sup>	"	All Howells	x	x	x
Geo.region	Africa	–	x	x	x
Population	–	Bushman	x	x	x
"	–	Dogon	x	x	x
"	–	Egypt			x
"	–	Teita		x	
"	–	Zulu	4		
Geo.region	Americas <sup>3</sup>	–	4		x
"	Americas <sup>3</sup>	–			x
Population	–	Arikara			
"	–	Eskimo			x
"	–	Native CA	x		x
"	–	Peru	x	x	x
"	–	Santa Cruz Is.			x
Geo.region	Asia	–	x	x	x
Population	–	Ainu	x	x	x
"	–	Andaman	x	x	
"	–	Atayal	x		x
"	–	Buriat			
"	–	Hainan			x
"	–	N. Japan	4	x	
"	–	S. Japan			
Geo.region	Australasia	–	x	x	x
Population	–	Australia	x	x	
"	–	Tasmania	x	x	
"	–	Tolai	x	x	x
Geo.region	Europe	–	x	x	x
Population	–	Berg	x	x	
"	–	Norse	x	x	x
"	–	Zalavar	x	x	x
Geo.region	Poly/Micronesia	–			
Population	–	Easter Is.	x	x	
"	–	Guam			
"	–	Moriori			
"	–	Mokapu	4		

<sup>†</sup>Data sets used are the Howells data (1973; 1989; 1995) and data for Early Period Native Californians collected by W.B.R. Four populations from the Howells data set were excluded from analyses in this study because they include data for male individuals only. The Howells data is customarily used to represent modern human species-wide cranial variation and is used here, with and without the addition of W.B.R.'s Native Californian data set. <sup>1</sup>This sample consists of all populations sampled in this study. <sup>2</sup>This species-level subset includes the Howells populations sampled in this study only. <sup>3</sup>This geographic-region level sample includes populations from the Americas from the Howells' data only, while the preceding sample also includes W.B.R.'s Native Californian data. To assess the influence of a single population-level sample at the region and species-wide levels, duplicate samples for the species-level and the Americas geographic region that excluded W.B.R.'s data were also analyzed. <sup>4</sup>For this sample,  $r_{b,n} = r_{n,f}$ .

## **Chapter 5**

### **Discussion and conclusions**

The first study (Chapter 2) has contributed to science the initial description and analysis of a recently discovered fossil cranium, which supported a taxonomic placement within *Homo sapiens*, augmenting the Late Pleistocene hominid fossil record, and adding to the current understanding of modern human origins. This study has demonstrated that by 60-32 ka there were *Homo sapiens* in northern Africa with cranial morphologies that fall within the range of variation observed in present-day humans, and which were indistinguishable from living people.

The morphological overlap observed between OH 83 and craniometrics of modern non-African humans has provided some additional support to previous observations that morphological variation ca. the Late Pleistocene was in part, influenced by adaptation to local environments, and/or other sources genetic in origin, gene flow and genetic drift (Lahr and Foley 1998), and which preceded the morphological variation between populations characteristic of recent and living modern humans. But, that said, the metric data for OH 83 do not specifically cluster with the Africans sampled by Howells (1973, 1989). The early fossils of *H. sapiens* demonstrate that the patterns of ancestry that characterize present-day human cranial variation were not present as of 160 ka (White et al. 2003). Perhaps these geographic clusters of cranial variation still had not coalesced by the time of OH 83, as this specimen does not cluster with the Africans sampled by Howells. The metric data alone are less convincing than the qualitative morphological data, due to the fragmentary nature of OH 83 and clear evidence of taphonomic distortion. As such, there are limited craniometric data available to adequately explore this possibility. Much further research on additional fossil material is needed to say anything more conclusive except that the standard linear metrics should not be considered in isolation.

Many aspects of the cranial vault bones are influenced by genetic effects (Susanne, 1977; Sherwood et al., 2008; 2011; Sherwood and Duren, 2013; Šešel et al., 2015), but little is known about the genetic architecture underlying the development of, or variation in, cranial features (Boas, 1912; 1928; Kohn, 1991; Sherwood and Duren, 2013; Šešel et al., 2015). OH 83 and each new hominid fossil cranium that is studied highlight the need to better understand the relationships between phenotypic traits of the cranium. Until we have a better grasp of the biological etiology of these morphologies, a cautious interpretation of the skeletal evidence is that the morphological variation of Middle and Late Pleistocene African hominid crania signifies population-level, rather than species-level differences. It is only through this and fieldwork producing additional hominid remains that will enable us to better resolve the transition from *H. erectus* to *H. sapiens*, and understand how population variation was patterned as our species evolved.

In the third chapter I presented original quantitative data I collected to document the cranial morphology of prehistoric Native Californian hunter gatherers estimated to have lived ca. 5000 BP (Early Period). Chapter three included comparative analyses of the craniometric variation among these Native Californians and modern humans from the W.W. Howells data (1973, 1989, 1995). For these analyses, I took two different

approaches to analyze variation comparatively between data sets, one using univariate analyses to make comparisons between the range of variation for individual craniometric measurements, while the second approach utilized correlations to quantitatively analyze interrelatedness between craniometric phenotypic data and evidence for morphological integration. Through these approaches, I fulfilled six main research objectives. The first approach was employed to fulfill two objectives, whereby I assessed the range of morphological variation among Early Period Native Californians as it compares to (1) the range of modern human variation assessed by Howells (1973, 1989, 1995) and (2) the range of Native American cranial variation represented in the Howells data (1973, 1989, 1995). The second approach was used to fulfill four additional objectives, including (3) examine correlation patterns in Early Period Native Californians, and use these results to assess comparatively (4) the complete Howells data set representing modern humans (Howells 1973, 1989, 1995), (5) a sample of populations sharing a common ancestry with the Native Californians, and (6) a sample representing populations with subsistence strategies similar to the Native Californians.

Through these analyses, I found that, when added to the Howells worldwide data set (1973, 1989, 1995), the Early Period Native Californians extend the range of variation for almost 25% of the measurements I analyzed. These measurements were extended primarily at the larger end of the range, but the magnitude by which the Native Californian data extended the range at either end was small. However, my data extended the range of variation for Native American populations for 53 measurements and the range was extended by much larger increments overall, and for four measurements, the range was extended at both the minimum and maximum ends. Native American populations are known to vary a lot. There are significant differences in time period, geographic location, and environment between the three Native American populations assessed by Howells. On this basis, a wide range of variation among them is expected. That the scope of the Early Period Native Californian data surpasses the range of craniometric variation for the Native Americans assessed by Howells for more than half of the measurements, the majority of which extend the maximum end of the range of variation, provides support to this characterization, demonstrates the wide range of cranial variation in northern Native Californians ca. 5000 BP, and supports qualitative observations that these individuals were robust.

Correlations in the Early Period Native American crania were generally high, while correlations in the Howells data, the Native American subset, and the hunter gatherer subset were drastically lower overall. The quantitative comparative analyses found that patterns of relatedness between traits in the Native Californian crania did not correspond more substantially to any one of the samples over the others, and all comparative samples were statistically significantly different from the Native Californian data.

It is possible that the Early Period Native Californian correlations were significantly different than the correlations for Howells Native Americans due to the wide range of variation among Native Americans, known to be highly polymorphic and have high levels of heterogeneity (González-José et al. 2001). At the least, these differences could be from the Early Period individuals varying significantly from the

Native American populations in the Howells data. The variation I observed between the Native Californian correlations and the correlations for the hunter-gatherers could be related to either the fact that all hunter gatherer populations, while reliant on similar subsistence strategies, do not fulfill their nutritional needs in the same way, or because this study did not include the mandible. It may also be due to the geographic, environmental, and ancestral differences between the Native Californians and the hunter gatherer populations. Differences aside, patterns of correlation suggesting integration within the craniofacial skeleton, and low correlations within the basicranium, were observed across samples sets.

This study demonstrated integration of the facial skeleton in humans across geographic regions, among populations with shared ancestry (Native American subset) among populations with similar subsistence strategies (hunter gatherers), and among humans including populations from ca. 5000 B.P. My results for this chapter also demonstrate that the study of other living and extinct Native American populations, using Howells measurement definitions so that this widely-used data set can be expanded may extend the range of variation further and provide other important perspectives on the range of variation in these indigenous groups. This research would apply to a number of fields of study including, but not limited to archaeology, human biology and evolution, and forensics.

In the third study (Chapter 4), I further explored variation in the patterns of correlation among modern human crania. Because *Homo sapiens* are a biologically highly variable species in many respects, especially when it comes to the cranium, I looked at how patterns of correlation vary based on sample composition. I compared patterns of correlation of samples of human crania representing the level of the species, and decomposing this sample representing modern human variation into samples for geographic regions, populations, and then sex-specific samples at each of those three levels. For these samples I tested whether evidence for integration persists at all levels as expected under theoretical assumptions of morphological integration (Strait 2001). I also tested a hypothesis of cranial integration among developmental regions hypothesized to be common to all mammals (Hallgrímsson et al. 2007), and a hypothesis for cranial integration patterns within humans (Enlow and Hans 1996). I used these hypotheses to investigate potential biases created by sample composition. In doing so, I sought to find out the following for a sample composed of multiple populations with diverse ancestries from different environments: (1) Will patterns of correlation potentially be influenced to demonstrate whether patterns depend on sample composition? (2) Is it scientifically rigorous to assume the results of analyzing such a sample can be applied at the species level? (3) Are there biases that can be created by subsuming multiple populations into one sample? and (4) Are the biases that arise when the individual populations are analyzed that create misleading noise?

The following results of this study corroborate results I found in the third chapter, as well as previous research. Across all samples, there was evidence for morphological integration within the face. These results support previous research that demonstrated integration within the mammalian facial skeleton, and that this integrated region behaves independently from the rest of the cranium (Cheverud 1982; 1989;

1995; Lieberman et al. 2000a,b; Ackermann and Cheverud 2004; Hallgrímsson et al. 2004; Goswami 2006). Across all samples I also observed that the basicranium demonstrated the least integration relative to the other cranial regions. Although fewer craniometric traits were included in the analysis of correlations within the basicranium, the measurements I included sufficiently describe the shape and dimensions of the majority of the basicranium. As such, it is unlikely that the lack of integration I observed within the basicranium was a result of not having included enough basicranial traits. This result supports previous assertions that the basicranium is not an integrated unit (Bastir 2008). Furthermore, the overall lack of high correlations between measurements of the neurocranium and basicranium I observed across all samples contradicts the hypothesis that these two regions are integrated and behave as a single cranial module (Lieberman et al. 2000a,b; Bastir and Rosas 2006; Hallgrímsson et al. 2007). Insofar as modularity, that the face exhibits such strong integration that was not observed in the other regions could be interpreted as evidence for a neuro-basicranial complex in humans. However, the weak correlations I observed among measurements of the neurocranium and basicranium into account does not merit this interpretation.

Phenotypic correlations between dimensions of the face and neurocranium expected under Enlow and Hans' (1996) hypothesis for craniofacial morphological variation of the human cranium were not observed. Similar results have been demonstrated for humans from Austria (Martínez-Abadías et al. 2009), both of which provide additional support for developmental models (Lieberman et al. 2000a; Bastir and Rosas, 2004; Martínez-Abadías et al. 2009), which Enlow and Hans' hypothesis (1996) contradict. Based on the other results of this study, Hallgrímsson et al.'s (2007) hypothesis was rejected below the species level, suggesting that the basicranial and neurocranial vault breadths are not more tightly integrated with each other than they are with facial breadth in all humans.

The range of variation in the levels of sexual dimorphism within different populations is wide, such that pooling populations into samples of geographic regions dilutes variation that can be detected in correlation matrices. While it is possible that larger sample sizes for individual populations could help to preserve signals of sexual dimorphism, this would only be the case if all or most of the populations within a geographic region demonstrate similar levels of sexual dimorphism. Regardless of population sample sizes, once populations are aggregated into a single regional sample signals of sexual dimorphism specific to populations would be diluted if each population has differing levels of sexual dimorphism because correlations essentially provide an average of the interrelatedness between traits for all individuals in the sample. This suggests that even though pooled-sex samples comprising multiple populations could help to reduce population-specific noise depending on the populations sampled, signals of biologically interesting and informative intraspecific patterns that could reveal more about the way morphological variation might be patterned in response to various environmental pressures could be diluted. As such, sample composition must be carefully considered in studies of integration and modularity. *Homo sapiens* are a biologically variable species in many respects, especially when it comes to the cranium (Howells 1973, 1989, 1995). With a nearly

global distribution, humans occupy a wide range of environments, each with its own array of microevolutionary forces that altogether leads to a varying extent of variation within and between populations, such that patterns of correlation are likely influenced to some extent by biologically-relevant differential pressures. Overall, my results demonstrated the effect of sample composition on patterns of correlation, whereby the greatest potential biases stem from the level at and below the population, as evidenced by the observations that variation in the patterns of correlation between populations was obfuscated by collapsing individual populations into a single sample representing worldwide human variation, and also, but less so, when populations were aggregated according to geographic region. Research on biological variation within humans has demonstrated the correlation between environmental and biological similarity (Ross 2002). Because *Homo sapiens* are so geographically widespread, it is not surprising that patterns of correlation varied the most at the population level. However, it also is a character of our species that would enable further research on this relationship insofar as it pertains to the human cranium. Future research could test hypotheses for cranial integration under samples representing various environmental variables to better understand which of these variables are biologically relevant to human cranial morphological integration. Further research also needs to be done in the theory of morphological integration, to inspire discussions on the appropriate interpretation of quantitative results and help further our understanding of the most appropriate data for this kind of research.

In the conventional research model for phylogenetic analyses and assessments of hominid fossil crania, traits, not biologically-informed morphological sets are analyzed (Hlusko 2004). Essentially, traits are treated as modular until they are proven integrated. Studies that have re-analyzed cladistics and phylogenetic data using sets of morphological characters have demonstrated that different results are observed when morphological integration is accounted for, and in some cases, have found these results are less ambiguous (Lovejoy et al. 1999; Strait 2001; Hlusko 2004). Better resolving the relationships between traits of the cranium, the underlying influence of these relationships, and by extension, population-level variation will ultimately help reveal how the hominid cranium develops and evolves.

## 5.2 References cited within Chapters 1 and 5

- Ackermann RR. 2002. Patterns of covariation in the hominoid craniofacial skeleton: Implications for paleoanthropological models. *J Hum Evol* 43:167–187.
- Ackermann RR. 2005. Ontogenetic integration of the hominoid face. *J Hum Evol* 48:175–197.
- Ackermann RR and Cheverud JM. 2004. Morphological integration in primate evolution. In: Pigliucci M, Preston K, editors. *Phenotypic integration*. Oxford: Oxford University Press. pp. 302-319.
- Barbujani G, Magagni A, Minch E, & Cavalli-Sforza LL. 1997. An apportionment of human DNA diversity. *Proc Natl Acad Sci USA* 94: 4516–4519.
- Bastir M & Rosas A. 2004. Facial heights: Evolutionary relevance of postnatal ontogeny for facial orientation and skull morphology in humans and chimpanzees. *J Hum Evol* 47:359–381.
- Bastir M & Rosas A. 2006. Correlated variation between the lateral basicranium and the face: A Geometric morphometric study in different human groups. *Arch Oral Biol* 51:814-824.
- Boas F. 1912. Changes in the bodily form of descendants of immigrants. *Am Anthropol* 14:530–562.
- Boas F. 1928. *Materials for the study of inheritance in man*. Vol 6. New York: Columbia University Press.
- Bräuer G & Leakey RE. 1986. The ES-11693 cranium from Eliye Springs, West Turkana, Kenya. *J Hum Evol* 15: 289–312.
- Cheverud JM. 1982. Phenotypic, genetic, and environmental morphological integration in the cranium. *Evolution* 36:499-516.
- Cheverud JM. 1989. A comparative analysis of morphological variation patterns in the papionins. *Evolution* 43:1737–1747.
- Cheverud JM. 1995. Morphological integration in the saddle-back tamarin (*Saguinus fuscicollis*) cranium. *Am Nat* 145:63–89.
- Day MH & Stringer CB. 1982. A reconsideration of the Omo Kibish remains and the *erectus*–*sapiens* transition. In: de Lumley MA, editor. *Homo erectus et la Place de l'Homme de Tautavel parmi les Hominidés Fossiles*. Première Congrès International de Paléontologie Humaine. UNESCO Colloque International du Centre National de la Recherche Scientifique Vol. 2, Prétirages, Nice:814–846.
- Enlow DH & Hans MG, eds. 1996. *Essentials of facial growth*. WB Saunders Company.
- González-José R, Ramírez-Rozzi F, Sardi M, Martínez-Abadías N, Hernández M, Pucciarelli H. 2005. Functional-craniology approach to the influence of economic strategy on skull morphology. *Am J Phys Anthropol* 128:757–771.
- González-José, R, Dahinten SL, Luis MA, Hernández M, & Pucciarelli HM. 2001. Craniometric variation and the settlement of the Americas: Testing hypotheses by means of R-matrix and matrix correlation analyses. *Am J Phys Anthropol* 116:154-165.
- Goswami A. 2006. Cranial modularity shifts during mammalian evolution. *Am Nat* 168:270-280.

- Haile-Selassie Y, Asfaw B, & White TD. 2004. Hominid cranial remains from upper Pleistocene deposits at Aduma, Middle Awash, Ethiopia. *Am J Phys Anthropol* 123:1–10.
- Hallgrímsson B, Lieberman DE, Liu W, Ford-Hutchinson AF, & Jirik FR. 2007. Epigenetic interactions and the structure of phenotypic variation in the cranium. *Evol Dev* 9:76–91.
- Hallgrímsson B, Willmore K, Dorval C, & Cooper DM. 2004. Craniofacial variability and modularity in macaques and mice. *J Exp Zool B: Mol Dev Evol* 302:207–225.
- Hlusko LJ. 2004. Integrating the genotype and phenotype in hominid paleontology. *P Natl Acad Sci USA* 101: 2653–2657.
- Howells WW. 1973. *Cranial Variation in Man. A Study by multivariate analysis of patterns of differences among recent human populations.* Peabody Mus Amer Arch Ethnol 67.
- Howells WW. 1989. Skull shapes and the map. Craniometric analyses in the dispersion of modern *Homo*. Peabody Mus Amer Arch Ethnol 79.
- Howells WW. 1995. Who's Who in Skulls. Ethnic identification of crania from measurements. Peabody Mus Amer Arch Ethnol 82.
- Kohn LAP. 1991. The Role of genetics in craniofacial morphology and growth. *Ann Rev Anthropol* 20:261–278.
- Lahr MM. 1996. *The evolution of modern human diversity: a study of cranial variation.* Vol. 18. Cambridge: Cambridge University Press.
- Lahr MM, Foley RA. 1998. Towards a theory of modern human origins: Geography, demography, and diversity in recent human evolution. *Am J Phys Anthropol Suppl* 27:137–176.
- Lieberman DE, McBratney BM, & Krovitz G. 2002. The evolution and development of cranial form in *Homo sapiens*. *PNAS* 3:1134–1139 doi:10.1073/pnas.022440799
- Lieberman DE, Mowbray KM, & Pearson OM 2000a. Basicranial influences on overall cranial shape. *J Hum Evol* 38:291–315.
- Lieberman DE, Ross CR, & Ravosa M 2000b. The primate cranial base: Ontogeny, function and integration. *Ybk Phys Anthropol* 43:117–169.
- Lovejoy CO, Cohn MJ, & White TD. 1999. Morphological analysis of the mammalian postcranium: A Developmental perspective. *Proc Natl Acad Sci USA* 96: 13247–13252.
- Martínez-Abadías N, Esparza M, Sjøvold T, González-José R, Santos M., & Hernández M. 2009. Heritability of human cranial dimensions: Comparing the evolvability of different cranial regions. *J Anat* 214:19–35.
- Olson EC, Miller RL. 1958. *Morphological Integration.* Chicago: University of Chicago Press.
- Pearson OM. 2008. Statistical and biological definitions of “anatomically modern” humans: suggestions for a unified approach to modern morphology. *Evol Anthropol* 17: 38–48.
- Pigliucci M & Preston KA, editors. 2004. *Phenotypic integration: studying the ecology and evolution of complex phenotypes.* Oxford, UK: Oxford University Press on Demand.

- Ross A. 2004: Regional isolation in the Balkan region: an analysis of craniofacial variation.
- Rosas A & Bastir M. 2002 Thin-plate spline analysis of allometry and sexual dimorphism in the human craniofacial complex. *Am J Phys Anthropol* 117: 236–245.
- Šešelj M, Duren DL, & Sherwood RJ. 2015. Heritability of the human craniofacial complex. *Anat Rec* 298:1535–47.
- Sherwood RJ & Duren DL. 2013. The genetics of morphology. In: Begun DR, editor. *A Companion to paleoanthropology*. Malden, MA: Wiley-Blackwell. p 306–320.
- Sherwood RJ, Duren DL, Demerath EW, Czerwinski SA, Siervogel RM, & Towne B. 2008. Quantitative genetics of modern human cranial variation. *J Hum Evol* 54:909–914.
- Sherwood RJ, Duren DL, Mahaney MC, Blangero J, Dyer TD, Cole SA, Czerwinski SA, Chumlea WC, Siervogel RM, Choh AC, Nahhas RW, Lee M, & Towne B. 2011. A genome-wide linkage scan for quantitative trait loci influencing the craniofacial complex in humans (*Homo sapiens sapiens*). *Anat Rec* 294(4):664–675.
- Strait DS. 2001. Integration, phylogeny, and the hominid cranial base. *Am J Phys Anthropol* 114:273–297.
- Stringer CB, Hublin JJ, & Vandermeersch B. 1984. The Origins of modern humans: A World survey of the fossil evidence. In: Smith FH and Spencer F, editors. *The Origins of modern humans: A World survey of the fossil evidence*. Liss: New York. p 51–135.
- Susanne C. 1977. Heritability of Anthropological Characters. *Hum Biol* 49(4): 573–580.
- Tattersall I & Schwartz JH. 2008. The morphological distinctiveness of *Homo sapiens* and its recognition in the fossil record: Clarifying the problem. *Evol Anthropol* 17: 49–54.
- White TD, Asfaw B, DeGusta D, Gilbert H, Richards GD, Suwa G, & Howell FC. 2003. Pleistocene *Homo sapiens* from Middle Awash, Ethiopia. *Nature* 423:742–747.
- Lewontin RC. 1972. The apportionment of human diversity. *Evol Biol* 6: 381–398.

Appendix 1. Mean and standard deviation of cranial measurements for modern sample.

Measurement	n =	Americas	Asia	Australasia	Europe	North Africa	Polynesia/Micronesia	Sub-Saharan Africa
STB	mean	106.28	111.75	101.97	116.47	111.41	108.69	108.14
	std dev	6.63	7.30	6.32	6.73	5.49	6.37	6.99
XFB	mean	112.39	115.36	108.76	118.74	113.51	112.43	111.16
	std dev	4.94	6.83	4.60	5.81	5.03	4.98	5.78
FRC	mean	108.51	109.47	107.59	109.84	110.11	113.25	108.18
	std dev	5.07	5.38	5.10	4.89	5.22	5.39	5.15
FMB	mean	96.08	96.02	99.46	96.92	93.97	98.08	97.45
	std dev	4.08	4.78	4.30	3.75	3.61	3.96	4.41

Craniometric data from Howells (1973, 1989).  
 Mean in mm, rounded to the nearest hundredth.

Appendix 2. Sample composition of the Howells data.

<b>Geo. region</b>	<b>Population</b>	<b>N=</b>	<b>No. M</b>	<b>No. F</b>
All	All	2,524	1,368	1,156
Africa	–	484	234	250
–	Bushman	90	41	49
–	Dogon	99	47	52
–	Egypt	111	58	53
–	Teita	83	33	50
–	Zulu	101	55	46
Americas	–	389	201	188
–	Arikara	69	42	27
–	Eskimo	108	53	55
–	Peru	110	55	55
–	Santa Cruz Is.	102	51	51
Asia	–	665	409	256
–	Ainu	86	48	38
–	Andaman	70	35	35
–	Anyang*	42	42	–
–	Atayal	47	29	18
–	Buriat	109	55	54
–	Hainan	83	45	38
–	N. Japan	87	55	32
–	Philippines*	50	50	–
–	S. Japan	91	50	41
Australasia	–	298	153	145
–	Australia	101	52	49
–	Tasmania	87	45	42
–	Tolai	110	56	54
Europe	–	317	164	153
–	Berg	109	56	53
–	Norse	110	55	55
–	Zalavar	98	53	45
Poly/Micronesia	–	361	197	164
–	Easter Is.	86	49	37
–	Guam	57	30	27
–	Moriori	108	57	51
–	Mokapu	100	51	49
–	N. Maori*	10	10	–
–	S. Maori*	10	10	–

Howells (1973, 1995). \*Populations only included in samples for all Howells data (Chapter 3) and all specimens (Chapter 4) due to skewed sex composition (males only).

Appendix 3. Craniometric measurements for Early Period Native Californians from the San Francisco Bay Area (ALA) and the Sacramento Valley (SJO).

Specimen ID	Sex	GOL	NOL	BNL	BBH	XCB	XFB	ZYB	AUB	ASB	BPL	NPH	NLH	JUB
ALA-208-109	M	NA	71.00	52.00	NA									
ALA-307-556	M	179.00	177.67	102.67	138.67	137.00	113.00	130.00	121.00	103.67	101.00	73.00	50.00	111.00
ALA-307-8257	M	NA	NA	NA	NA	142.33	116.67	NA	128.67	NA	NA	NA	NA	NA
ALA-307-8283	F	191.00	186.67	100.00	133.67	136.00	112.67	NA	109.00	101.33	94.33	63.00	47.33	108.50
ALA-307-8286	M	189.33	186.50	NA	NA	133.00	113.00	NA	117.33	108.67	NA	NA	54.67	110.33
ALA-307-8287	F	NA	120.00	106.67	NA	64.33	49.33	111.00						
ALA-307-8291	F	NA	NA	NA	NA	134.00	109.33	NA	NA	104.00	NA	NA	NA	NA
ALA-307-8292	M	NA	NA	NA	144.00	136.00	114.00	NA	124.00	108.00	NA	NA	NA	NA
ALA-307-8298	F	NA	NA	NA	NA	134.00	115.00	NA	118.50	98.50	NA	NA	NA	NA
ALA-307-8300	F	183.00	179.50	99.67	141.00	135.00	112.33	NA	120.00	107.33	96.67	63.33	45.00	114.67
ALA-307-8310	F	NA	NA	NA	NA	140.67	114.33	140.67	NA	109.00	NA	NA	NA	NA
ALA-307-8319	M	NA	NA	NA	111.67									
ALA-307-8320	M	NA	NA	NA	NA	135.00	110.67	NA	114.00	102.00	NA	NA	NA	NA
ALA-307-8321	M	NA	NA	NA	NA	149.33	119.67	NA	NA	114.33	NA	73.67	53.00	120.00
ALA-307-8345	M	NA	NA	NA	NA	NA	118.67	NA	NA	NA	NA	68.00	53.00	NA
ALA-328-10172	F	NA	NA	NA	136.00	130.00	119.50	NA	NA	105.00	NA	NA	NA	116.50
ALA-328-10250	M	NA	NA	109.33	141.00	135.00	109.67	139.00	127.00	111.33	99.50	66.50	49.50	117.00
ALA-328-10275	M	NA	NA	NA	149.00	150.00	116.50	NA	133.50	114.50	NA	NA	NA	119.50
ALA-328-10277	M	NA	NA	105.00	141.50	138.00	107.50	NA	125.00	107.00	100.00	74.00	51.50	117.00
ALA-328-10279	M	188.00	182.00	NA	NA	140.00	121.50	NA	126.00	110.00	NA	NA	NA	NA
ALA-328-10282	M	196.50	194.00	111.00	148.00	136.00	116.00	141.50	127.50	107.50	100.00	74.00	56.00	NA
ALA-328-10285	M	187.00	183.00	109.00	141.50	142.00	114.50	NA	127.50	116.50	NA	NA	46.50	118.00
ALA-328-10306	M	NA	NA	NA	NA	NA	113.00	NA	116.50	NA	NA	NA	NA	NA
ALA-328-10313	F	188.00	183.00	102.00	137.00	NA	112.50	NA	NA	104.00	98.50	65.00	44.00	NA
ALA-328-10322	F	179.00	NA	NA	NA	129.00	112.00	NA	120.00	108.00	NA	NA	NA	NA
ALA-328-10329	F	181.67	178.00	NA	NA	133.00	110.00	134.00	122.00	109.00	NA	59.33	45.33	112.33
ALA-328-10352	F	175.00	174.00	108.00	135.67	119.33	100.50	NA	111.67	101.00	NA	NA	NA	NA
ALA-328-8873	M	NA	NA	NA	NA	136.00	112.50	NA	129.50	109.00	NA	NA	NA	NA
ALA-328-8827	M	183.00	182.00	99.00	130.00	130.00	107.50	NA	126.00	104.50	95.00	70.00	49.00	114.50
ALA-328-9294	M	184.00	182.00	100.00	138.00	137.00	114.00	NA	130.00	112.50	89.00	66.00	51.50	NA

Specimen ID	Sex	NLB	MAB	MDH	OBH	OBB	DKB	NDS	WNB	SIS	ZMB	SSS	FMB	NAS
ALA-208-109	M	22.67	NA	NA	34.00	43.33	NA	NA	NA	NA	NA	NA	NA	NA
ALA-307-556	M	22.33	62.00	26.00	35.00	41.00	17.00	7.00	9.00	3.53	94.67	25.00	96.67	18.00
ALA-307-8257	M	NA	NA	NA	NA	NA	NA	NA	NA	NA	NA	NA	NA	NA
ALA-307-8283	F	NA	65.33	26.00	31.00	41.67	19.00	NA	NA	NA	90.67	25.00	NA	NA
ALA-307-8286	M	24.67	NA	25.00	34.33	45.00	18.00	NA	10.03	NA	97.33	28.67	96.67	15.33
ALA-307-8287	F	24.33	58.00	24.00	36.67	41.33	16.33	NA	NA	NA	95.00	25.00	89.00	NA
ALA-307-8291	F	NA	NA	NA	NA	NA	NA	NA	NA	NA	NA	NA	NA	NA
ALA-307-8292	M	NA	NA	NA	NA	NA	NA	NA	NA	NA	NA	NA	NA	NA
ALA-307-8298	F	NA	NA	NA	NA	NA	NA	NA	NA	NA	NA	NA	NA	NA
ALA-307-8300	F	24.33	59.00	31.33	33.67	39.67	21.00	NA	5.63	NA	101.00	21.00	95.67	14.00
ALA-307-8310	F	NA	NA	27.33	35.00	40.67	21.33	NA	NA	NA	NA	NA	NA	NA
ALA-307-8319	M	19.67	55.00	NA	NA	NA	NA	NA	NA	NA	100.67	28.00	NA	NA
ALA-307-8320	M	NA	NA	NA	NA	NA	NA	NA	NA	NA	NA	NA	96.50	NA
ALA-307-8321	M	NA	66.00	NA	33.67	43.50	NA	NA	NA	NA	102.00	29.33	96.33	19.33
ALA-307-8345	M	22.33	NA	NA	35.00	44.00	19.00	NA	NA	5.47	NA	NA	96.67	20.00
ALA-328-10172	F	27.00	NA	29.50	37.00	39.50	24.50	NA	10.80	NA	NA	NA	101.00	14.00
ALA-328-10250	M	26.00	65.67	27.67	35.67	40.67	21.33	NA	8.63	NA	97.33	20.00	96.33	NA
ALA-328-10275	M	26.50	74.00	NA	NA	40.50	NA	NA	NA	NA	106.00	NA	99.50	NA
ALA-328-10277	M	22.00	69.00	29.00	35.00	39.50	21.00	NA	11.05	NA	NA	NA	99.50	20.00
ALA-328-10279	M	NA	NA	NA	NA	NA	NA	NA	NA	NA	NA	NA	104.50	19.00
ALA-328-10282	M	27.50	69.00	36.50	35.00	41.50	24.00	8.00	NA	NA	111.00	28.50	103.50	22.00
ALA-328-10285	M	26.00	NA	29.50	33.50	38.50	25.50	NA	12.10	3.70	100.50	NA	102.50	NA
ALA-328-10306	M	NA	NA	NA	NA	NA	26.00	NA	NA	NA	NA	NA	100.50	16.00
ALA-328-10313	F	NA	NA	NA	32.00	43.00	NA	NA	NA	NA	NA	NA	103.00	19.00
ALA-328-10322	F	NA	NA	NA	NA	NA	26.00	NA	NA	NA	NA	NA	NA	NA
ALA-328-10329	F	22.67	NA	27.67	35.33	39.33	24.33	NA	NA	NA	95.33	22.33	96.33	NA
ALA-328-10352	F	NA	NA	NA	NA	NA	NA	NA	NA	NA	NA	NA	NA	NA
ALA-328-8873	M	NA	NA	35.50	NA	NA	NA	NA	NA	NA	NA	NA	NA	NA
ALA-328-8827	M	24.00	65.00	28.00	34.00	39.00	NA	9.00	6.85	NA	99.00	25.50	96.50	NA
ALA-328-9294	M	25.00	63.00	29.50	NA	NA	NA	NA	NA	NA	NA	NA	NA	NA

Specimen ID	Sex	EKB	DKS	IML	XML	WMH	GLS	STB	FRC	FRS	FRF	PAC	PAS	PAF
ALA-208-109	M	NA	NA	NA	NA	24.67	NA	NA	116.33	24.67	49.50	NA	NA	NA
ALA-307-556	M	92.33	18.00	34.67	48.00	25.33	2.00	115.00	107.33	19.00	49.00	114.67	NA	NA
ALA-307-8257	M	NA	NA	NA	NA	NA	NA	115.67	NA	NA	NA	122.50	26.00	69.00
ALA-307-8283	F	93.00	16.67	35.33	49.33	20.67	5.00	109.33	105.67	21.33	44.67	121.00	NA	NA
ALA-307-8286	M	92.00	21.33	32.00	48.67	23.00	3.00	105.67	109.50	23.00	48.50	116.00	22.50	NA
ALA-307-8287	F	88.33	18.33	NA	NA	19.67	3.00	NA	104.00	19.67	52.67	106.33	23.67	64.00
ALA-307-8291	F	NA	NA	NA	NA	NA	NA	109.00	NA	NA	NA	122.33	27.33	59.00
ALA-307-8292	M	NA	NA	NA	NA	NA	NA	113.33	NA	NA	NA	103.67	18.00	48.00
ALA-307-8298	F	NA	NA	NA	NA	NA	NA	110.50	102.00	21.00	48.67	111.67	25.67	54.00
ALA-307-8300	F	93.00	16.00	33.00	49.00	22.00	3.00	108.33	110.00	24.33	48.00	117.67	NA	56.00
ALA-307-8310	F	NA	NA	36.33	52.00	24.33	2.00	114.00	112.00	22.67	48.33	116.33	NA	55.50
ALA-307-8319	M	NA	NA	NA	NA	19.67	NA	NA	NA	NA	NA	NA	NA	NA
ALA-307-8320	M	NA	NA	NA	NA	NA	NA	106.67	NA	NA	NA	118.67	28.67	61.33
ALA-307-8321	M	96.00	19.50	NA	NA	26.00	NA	117.33	117.33	24.33	50.00	103.67	NA	56.33
ALA-307-8345	M	95.33	22.00	NA	NA	24.00	6.00	117.00	122.00	24.00	55.00	NA	NA	NA
ALA-328-10172	F	NA	NA	NA	NA	NA	NA	117.00	111.00	NA	NA	118.00	32.00	NA
ALA-328-10250	M	98.33	NA	37.00	54.00	24.67	NA	105.00	111.33	22.33	NA	120.00	NA	59.33
ALA-328-10275	M	95.50	NA	39.00	57.00	NA	NA	112.50	NA	NA	NA	116.50	NA	53.00
ALA-328-10277	M	95.00	NA	NA	NA	24.50	3.00	109.00	113.00	NA	NA	114.50	NA	NA
ALA-328-10279	M	NA	NA	NA	NA	NA	NA	119.00	118.00	27.00	58.00	127.00	30.00	59.00
ALA-328-10282	M	99.50	NA	NA	59.00	30.00	NA	112.50	115.00	23.50	53.00	119.00	23.50	62.50
ALA-328-10285	M	100.00	11.00	NA	NA	23.00	NA	114.00	113.00	21.50	55.00	126.50	31.00	61.00
ALA-328-10306	M	NA	NA	NA	NA	NA	4.00	109.00	113.00	23.50	NA	NA	NA	NA
ALA-328-10313	F	NA	NA	34.50	46.50	23.00	NA	111.00	107.00	24.50	NA	127.00	NA	NA
ALA-328-10322	F	NA	NA	NA	NA	NA	NA	104.00	NA	NA	NA	112.00	24.50	NA
ALA-328-10329	F	91.67	22.00	38.33	55.67	21.33	NA	109.00	108.33	27.00	NA	113.00	21.00	52.00
ALA-328-10352	F	NA	NA	NA	NA	NA	2.00	94.50	103.67	21.00	47.00	118.00	NA	NA
ALA-328-8873	M	NA	NA	38.00	57.50	27.00	NA	104.00	NA	NA	NA	109.00	NA	NA
ALA-328-8827	M	96.50	15.00	34.00	53.00	22.00	1.00	104.00	104.00	22.00	47.00	125.00	30.50	NA
ALA-328-9294	M	NA	NA	35.00	50.00	21.00	2.00	112.00	106.50	25.00	NA	133.00	NA	NA

Specimen ID	Sex	OCC	OCS	OCF	FOL	NAR	SSR	PRR	DKR	ZOR	FMR	EKR	ZMR	AVR
ALA-208-109	M	NA	NA	NA	NA	NA	NA	NA	NA	NA	NA	NA	NA	NA
ALA-307-556	M	100.00	28.67	49.50	37.33	91.00	97.33	107.00	82.00	77.33	70.00	68.33	72.33	88.00
ALA-307-8257	M	NA	NA	NA	NA	NA	NA	NA	NA	NA	78.33	NA	NA	NA
ALA-307-8283	F	103.67	NA	NA	36.33	90.33	93.00	97.00	82.67	76.33	72.67	69.00	68.00	79.00
ALA-307-8286	M	113.50	32.50	52.00	NA	95.67	100.33	NA	89.33	82.33	80.00	75.33	74.67	87.67
ALA-307-8287	F	NA	NA	NA	NA	84.00	90.33	97.00	78.67	73.00	71.33	67.00	68.00	77.00
ALA-307-8291	F	NA	NA	NA	NA	NA	NA	NA	NA	NA	NA	NA	NA	NA
ALA-307-8292	M	NA	NA	NA	NA	NA	NA	NA	NA	NA	70.00	NA	NA	NA
ALA-307-8298	F	NA	NA	NA	NA	87.00	NA	NA	NA	NA	71.00	NA	NA	NA
ALA-307-8300	F	100.00	29.50	43.50	38.00	89.67	92.67	100.00	82.33	78.67	76.67	72.33	72.00	81.33
ALA-307-8310	F	NA	NA	NA	NA	90.67	NA	NA	80.50	77.67	73.00	69.00	71.67	NA
ALA-307-8319	M	NA	NA	NA	NA	NA	NA	NA	NA	NA	NA	NA	NA	NA
ALA-307-8320	M	NA	NA	NA	NA	NA	NA	NA	NA	NA	73.00	NA	NA	NA
ALA-307-8321	M	NA	NA	NA	NA	96.33	110.67	119.33	87.00	84.00	73.33	77.33	77.67	102.00
ALA-307-8345	M	NA	NA	NA	NA	NA	NA	NA	NA	NA	NA	NA	NA	NA
ALA-328-10172	F	93.00	NA	NA	35.50	93.00	97.00	101.00	82.50	78.00	77.50	75.50	73.00	NA
ALA-328-10250	M	NA	NA	NA	NA	95.67	93.00	102.00	82.67	80.50	76.67	74.67	73.00	83.33
ALA-328-10275	M	106.50	NA	62.00	NA	NA	NA	NA	NA	NA	NA	NA	NA	96.50
ALA-328-10277	M	107.00	NA	NA	36.00	95.00	101.50	109.00	83.50	81.50	74.50	73.50	NA	90.00
ALA-328-10279	M	99.50	30.50	NA	NA	94.00	NA	NA	NA	NA	NA	NA	NA	NA
ALA-328-10282	M	111.50	39.50	64.50	NA	102.00	102.00	108.00	89.00	82.00	79.50	75.00	74.00	92.00
ALA-328-10285	M	94.00	27.00	48.50	38.00	96.50	NA	NA	84.00	83.00	80.50	76.00	78.00	NA
ALA-328-10306	M	NA	NA	NA	NA	100.50	NA	NA	91.50	NA	85.50	NA	NA	NA
ALA-328-10313	F	92.50	31.50	46.00	NA	NA	NA	NA	NA	NA	NA	NA	NA	NA
ALA-328-10322	F	100.50	29.50	NA	NA	NA	NA	NA	81.50	NA	NA	NA	NA	NA
ALA-328-10329	F	101.00	33.33	50.50	NA	93.33	94.67	98.00	85.67	78.00	75.00	70.00	70.33	NA
ALA-328-10352	F	86.00	NA	40.00	32.67	92.33	NA	NA	87.00	NA	70.00	NA	NA	NA
ALA-328-8873	M	NA	NA	NA	NA	NA	NA	NA	NA	79.50	79.50	NA	72.00	87.00
ALA-328-8827	M	95.50	27.50	48.50	34.50	91.00	93.00	100.00	80.00	76.00	72.00	69.50	67.50	81.00
ALA-328-9294	M	92.50	23.50	NA	40.00	92.00	89.00	94.50	86.00	75.00	NA	NA	69.50	78.50

Specimen ID	Sex	BRR	VRR	LAR	OSR	BAR	NAA	PRA	BAA	NBA	BBA	BRA	SSA	NFA
ALA-208-109	M	NA	NA	NA	NA	NA	NA	NA	NA	NA	NA	NA	NA	NA
ALA-307-556	M	113.00	117.33	106.00	44.33	NA	68.00	70.67	42.00	82.67	50.00	47.00	124.00	139.67
ALA-307-8257	M	127.33	131.00	114.67	NA	NA								
ALA-307-8283	F	114.00	121.33	113.00	44.33	19.33	66.33	76.00	38.00	81.00	51.33	48.00	122.00	NA
ALA-307-8286	M	121.33	125.33	115.00	45.67	NA	119.00	144.67						
ALA-307-8287	F	110.33	122.00	114.00	NA	124.33	149.00							
ALA-307-8291	F	120.33	122.67	103.33	NA	NA								
ALA-307-8292	M	119.33	125.67	119.33	NA	24.33	NA	NA						
ALA-307-8298	F	115.00	122.50	109.00	NA	NA								
ALA-307-8300	F	119.00	124.67	107.33	45.33	21.00	68.67	73.67	37.33	84.33	51.00	44.67	135.00	147.00
ALA-307-8310	F	112.67	120.33	109.67	NA	NA								
ALA-307-8319	M	NA	NA	NA	NA	NA	NA	NA	NA	NA	NA	NA	122.00	NA
ALA-307-8320	M	123.33	127.00	105.67	NA	NA								
ALA-307-8321	M	118.00	123.33	113.33	NA	120.33	136.33							
ALA-307-8345	M	NA	NA	NA	NA	NA	NA	NA	NA	NA	NA	NA	NA	135.00
ALA-328-10172	F	117.00	124.50	99.50	NA	NA	68.50	74.00	37.50	NA	53.00	NA	NA	149.00
ALA-328-10250	M	116.33	121.33	108.33	NA	25.33	63.50	79.50	36.50	79.67	51.00	50.00	135.50	137.00
ALA-328-10275	M	122.00	124.00	102.50	49.00	27.50	NA	NA						
ALA-328-10277	M	116.00	NA	108.00	45.00	NA	65.00	72.50	42.00	81.00	52.00	47.00	NA	136.00
ALA-328-10279	M	125.50	126.00	102.00	44.50	NA	140.00							
ALA-328-10282	M	124.50	127.00	112.00	45.50	24.50	62.00	78.00	41.00	82.00	50.00	48.00	126.00	134.00
ALA-328-10285	M	119.00	122.50	99.50	51.50	23.00	NA	NA	NA	79.00	51.50	49.00	NA	138.50
ALA-328-10306	M	122.00	NA	NA	NA	NA	NA	NA	NA	NA	NA	NA	NA	145.00
ALA-328-10313	F	NA	NA	NA	NA	NA	68.00	74.00	37.50	81.50	51.00	47.50	NA	139.00
ALA-328-10322	F	117.50	121.50	103.00	52.50	NA	NA							
ALA-328-10329	F	117.00	118.67	101.67	41.67	NA	129.67	143.00						
ALA-328-10352	F	112.33	113.67	96.00	44.67	23.33	NA	NA	NA	79.67	48.67	51.33	NA	NA
ALA-328-8873	M	114.00	NA	104.00	NA	NA								
ALA-328-8827	M	111.00	120.00	105.00	42.50	NA	65.50	72.00	42.00	79.00	52.00	49.00	126.00	140.00
ALA-328-9294	M	118.50	123.00	104.50	47.50	19.50	61.00	79.00	40.00	84.00	50.00	46.00	NA	NA

Specimen ID	Sex	DKA	NDA	SIA	FRA	PAA	OCA	RFA	RPA	ROA	BSA	SBA	SLA	TBA
ALA-208-109	M	NA	NA	NA	133.00	NA	NA	NA	NA	NA	NA	NA	NA	NA
ALA-307-556	M	128.00	101.00	103.67	141.00	135.67	120.00	62.33	63.00	70.33	172.00	104.00	87.00	137.33
ALA-307-8257	M	NA	NA	NA	NA	133.33	NA	NA	61.00	NA	NA	NA	NA	NA
ALA-307-8283	F	132.67	NA	NA	135.33	135.00	118.33	60.67	64.33	66.33	166.67	105.67	81.33	141.00
ALA-307-8286	M	123.00	113.00	116.67	134.00	137.00	121.00	59.00	58.67	76.67	NA	106.67	86.33	NA
ALA-307-8287	F	127.33	NA	NA	138.33	131.00	NA	63.00	56.33	NA	NA	109.33	NA	NA
ALA-307-8291	F	NA	NA	NA	NA	131.67	NA	NA	65.67	NA	NA	NA	NA	NA
ALA-307-8292	M	NA	NA	NA	NA	141.67	NA	NA	51.67	NA	NA	NA	NA	138.00
ALA-307-8298	F	NA	NA	NA	135.00	130.67	NA	59.00	60.00	NA	NA	104.00	NA	NA
ALA-307-8300	F	132.67	121.00	108.33	131.67	134.00	118.00	62.00	62.33	68.67	171.00	100.00	88.67	141.00
ALA-307-8310	F	NA	NA	NA	135.33	131.00	NA	65.67	63.33	NA	NA	104.67	NA	NA
ALA-307-8319	M	NA	NA	NA	NA	NA	NA	NA	NA	NA	NA	NA	NA	NA
ALA-307-8320	M	NA	NA	NA	NA	128.67	NA	NA	62.00	NA	NA	NA	NA	NA
ALA-307-8321	M	127.00	NA	NA	134.00	135.50	NA	65.67	53.33	NA	NA	109.33	NA	NA
ALA-307-8345	M	120.00	116.50	91.67	137.00	NA	NA	NA	NA	NA	NA	NA	NA	NA
ALA-328-10172	F	NA	NA	NA	NA	123.00	NA	NA	NA	68.00	160.00	98.50	NA	NA
ALA-328-10250	M	143.67	86.33	95.50	135.67	133.67	NA	62.33	64.33	NA	NA	104.33	NA	136.33
ALA-328-10275	M	86.50	NA	NA	NA	134.00	NA	NA	62.00	81.00	NA	NA	94.50	135.50
ALA-328-10277	M	140.00	NA	NA	NA	NA	NA	64.00	61.50	76.50	165.00	105.00	87.00	134.50
ALA-328-10279	M	NA	NA	NA	131.00	129.00	116.00	63.50	67.00	74.50	NA	93.00	91.00	NA
ALA-328-10282	M	130.00	113.00	NA	135.50	137.00	108.50	60.00	60.00	77.50	169.00	105.00	88.50	138.00
ALA-328-10285	M	146.50	101.50	117.00	138.50	128.00	120.50	62.00	70.00	68.50	NA	96.50	93.00	140.00
ALA-328-10306	M	NA	NA	NA	135.00	NA	NA	60.00	NA	NA	NA	NA	NA	NA
ALA-328-10313	F	NA	NA	NA	131.00	132.00	111.50	NA	NA	NA	NA	NA	NA	NA
ALA-328-10322	F	NA	NA	NA	NA	132.50	118.50	NA	60.50	72.50	NA	NA	96.00	NA
ALA-328-10329	F	111.67	NA	NA	126.67	138.67	113.00	60.67	61.67	77.33	NA	101.00	89.67	NA
ALA-328-10352	F	NA	NA	NA	135.67	131.67	125.67	60.00	68.67	65.00	NA	99.67	90.00	134.67
ALA-328-8873	M	NA	NA	NA	NA	NA	NA	NA	59.50	NA	NA	NA	NA	NA
ALA-328-8827	M	134.50	104.50	119.50	133.50	127.00	119.50	61.50	70.50	65.00	155.00	102.50	80.50	146.00
ALA-328-9294	M	NA	NA	NA	129.50	127.00	126.00	59.00	73.00	62.00	159.50	97.00	85.50	146.50

Specimen ID	Sex	LBI	LBI2	UFI	NLI	CRM	FFA	TFI*
ALA-208-109	M	NA	NA	NA	43.59	NA	NA	NA
ALA-307-556	M	76.54	77.11	56.15	44.67	151.56	150.67	38.46
ALA-307-8257	M	NA	NA	NA	NA	NA	NA	NA
ALA-307-8283	F	71.20	72.86	NA	NA	153.56	147.33	NA
ALA-307-8286	M	70.25	71.31	NA	45.12	NA	NA	NA
ALA-307-8287	F	NA	NA	NA	49.32	NA	NA	NA
ALA-307-8291	F	NA	NA	NA	NA	NA	NA	NA
ALA-307-8292	M	NA	NA	NA	NA	NA	NA	NA
ALA-307-8298	F	NA	NA	NA	NA	NA	NA	NA
ALA-307-8300	F	73.77	75.21	NA	54.07	153.00	153.00	NA
ALA-307-8310	F	NA	NA	NA	NA	NA	NA	NA
ALA-307-8319	M	NA	NA	NA	NA	NA	NA	NA
ALA-307-8320	M	NA	NA	NA	NA	NA	NA	NA
ALA-307-8321	M	NA	NA	NA	NA	NA	NA	NA
ALA-307-8345	M	NA	NA	NA	42.14	NA	NA	NA
ALA-328-10172	F	NA	NA	NA	NA	NA	NA	NA
ALA-328-10250	M	NA	NA	47.84	52.53	NA	143.17	35.61
ALA-328-10275	M	NA	NA	NA	NA	NA	NA	NA
ALA-328-10277	M	NA	NA	NA	42.72	NA	146.00	NA
ALA-328-10279	M	74.47	76.92	NA	NA	NA	NA	NA
ALA-328-10282	M	69.21	70.10	52.30	49.11	160.17	144.00	39.58
ALA-328-10285	M	75.94	77.60	NA	55.91	156.83	NA	NA
ALA-328-10306	M	NA	NA	NA	NA	NA	NA	NA
ALA-328-10313	F	NA	NA	NA	NA	NA	149.50	NA
ALA-328-10322	F	72.07	NA	NA	NA	NA	NA	NA
ALA-328-10329	F	73.21	74.72	44.28	50.00	NA	NA	33.83
ALA-328-10352	F	68.19	68.58	NA	NA	143.33	NA	NA
ALA-328-8873	M	NA	NA	NA	NA	NA	NA	NA
ALA-328-8827	M	71.04	71.43	NA	48.98	147.67	144.50	NA
ALA-328-9294	M	74.46	75.27	NA	48.54	153.00	145.00	NA

Specimen ID	Sex	GOL	NOL	BNL	BBH	XCB	XFB	ZYB	AUB	ASB	BPL	NPH	NLH	JUB
SJO-68-5827	M	185.33	183.00	107.00	143.50	136.00	119.33	NA	130.67	NA	100.00	70.67	54.00	NA
SJO-68-6472	M	181.33	178.33	98.33	143.33	137.00	116.33	126.33	120.33	105.67	91.67	63.00	46.33	111.00
SJO-56-7015	M	NA	NA	NA	NA	NA	120.50	NA	NA	NA	NA	NA	NA	NA
SJO-68-7285	M	184.00	182.00	100.67	142.33	146.67	127.33	147.33	128.33	120.00	97.33	63.33	47.33	136.00
SJO-68-7567	F	189.67	187.00	106.67	134.67	152.67	125.33	NA	136.33	115.67	107.67	66.00	50.33	140.00
SJO-68-7569	M	174.33	173.33	96.33	140.67	134.33	117.00	123.00	116.00	102.00	92.00	62.00	47.33	112.33
SJO-68-72327	F	NA	177.00	102.00	144.00	139.67	118.00	128.00	119.00	114.33	96.00	64.33	47.33	112.00
SJO-142-5661	M	188.33	184.67	NA	NA	146.00	124.00	NA	132.33	113.00	NA	NA	NA	NA
SJO-142-5666	F	NA	NA	NA	NA	137.67	118.67	NA	128.00	NA	NA	NA	NA	NA
SJO-142-5668	M	199.00	193.00	106.00	142.00	145.00	118.00	NA	NA	109.00	NA	NA	NA	NA
SJO-142-5675	M	NA	NA	NA	NA	138.00	114.50	130.50	116.00	NA	NA	60.00	45.00	115.50
SJO-142-5676	M	180.00	176.33	96.67	139.67	141.33	120.67	NA	125.00	112.50	NA	NA	47.67	NA
SJO-142-5677	M	NA	NA	NA	NA	143.33	NA	NA	132.67	119.67	NA	NA	NA	NA
SJO-142-5678	M	190.00	188.00	104.00	143.00	148.67	123.33	137.33	130.33	112.67	99.67	67.33	52.00	112.00
SJO-142-5679	M	NA	NA	NA	NA	152.00	131.00	135.00	130.67	120.00	NA	70.00	48.00	129.67
SJO-142-5800	F	NA	NA	NA	NA									
SJO-142-5801	M	NA	NA	NA	NA	135.00	113.00	NA	NA	NA	NA	NA	NA	NA
SJO-142-5806	M	NA	NA	NA	NA	150.67	115.00	NA	135.00	119.00	NA	NA	NA	NA
SJO-142-5808	F	179.33	NA	104.67	157.00	168.33	137.67	NA	150.50	128.67	NA	NA	NA	NA
SJO-142-5810	F	183.50	180.50	100.50	152.33	147.00	120.00	138.00	127.00	121.67	105.00	65.00	43.00	128.25
SJO-142-5813	M	NA	NA	NA	NA	NA	116.00	NA	134.00	111.00	NA	NA	55.00	NA
SJO-142-5814	F	186.00	182.50	NA	NA	140.67	116.33	NA	125.67	110.33	NA	70.33	49.67	NA
SJO-142-5815	F	201.00	NA	NA	NA	146.00	113.00	NA	130.50	123.50	NA	NA	NA	NA
SJO-142-5818	M	185.33	184.67	NA	NA	145.33	118.33	NA	134.33	116.67	NA	NA	NA	NA
SJO-142-5819	F	190.50	188.00	NA	144.00	144.33	116.33	NA	133.67	111.33	NA	NA	NA	NA
SJO-142-5820	M	189.67	185.00	104.33	146.00	NA	110.67	NA	NA	NA	98.33	69.00	51.67	121.33
SJO-142-5822	F	NA	NA	NA	NA	141.67	116.33	NA	123.00	110.67	NA	NA	NA	NA
SJO-142-5823	F	NA	NA	NA	NA	151.00	114.00	NA	129.00	122.00	NA	NA	NA	NA

Specimen ID	Sex	NLB	MAB	MDH	OBH	OBB	DKB	NDS	WNB	SIS	ZMB	SSS	FMB	NAS
SJO-68-5827	M	NA	63.00	NA	37.00	38.33	NA	NA	7.90	NA	NA	NA	NA	NA
SJO-68-6472	M	24.00	57.00	NA	36.00	36.00	24.00	NA	8.63	NA	95.67	18.33	97.00	15.00
SJO-56-7015	M	NA	NA	NA	NA	35.50	NA	NA	15.55	NA	NA	NA	NA	NA
SJO-68-7285	M	26.67	69.33	NA	NA	NA	33.67	11.00	15.05	3.15	102.67	22.67	99.67	NA
SJO-68-7567	F	27.33	73.00	35.00	NA	NA	34.33	10.67	15.50	NA	109.00	23.33	104.67	18.33
SJO-68-7569	M	23.33	59.33	26.00	33.00	36.33	21.50	NA	9.23	3.00	92.00	NA	94.33	13.33
SJO-68-72327	F	23.00	57.00	NA	33.00	36.33	22.00	11.67	7.73	NA	94.33	22.00	98.00	16.33
SJO-142-5661	M	NA	NA	NA	NA	45.67	22.50	NA	9.40	NA	NA	NA	NA	NA
SJO-142-5666	F	29.00	65.00	NA	NA	NA	NA	NA	NA	NA	NA	NA	NA	NA
SJO-142-5668	M	NA	NA	NA	NA	NA	NA							
SJO-142-5675	M	27.00	56.50	26.00	31.00	37.00	22.50	7.00	10.90	NA	NA	21.50	95.50	18.00
SJO-142-5676	M	28.67	60.67	29.33	36.00	40.67	26.00	NA	NA	NA	104.00	20.00	102.67	11.00
SJO-142-5677	M	NA	NA	NA	NA	NA	NA							
SJO-142-5678	M	24.00	54.50	28.33	35.33	40.33	22.00	8.33	11.55	4.13	99.33	24.00	96.67	15.00
SJO-142-5679	M	26.00	70.00	31.33	37.00	30.50	33.00	NA	14.20	NA	111.00	25.00	100.00	NA
SJO-142-5800	F	NA	NA	NA	NA	NA	NA							
SJO-142-5801	M	NA	NA	NA	NA	NA	NA							
SJO-142-5806	M	NA	NA	NA	NA	NA	NA							
SJO-142-5808	F	NA	82.00	NA	NA	NA	NA	NA	NA	NA	NA	NA	NA	NA
SJO-142-5810	F	25.67	65.33	28.00	34.67	38.00	24.67	6.00	13.85	NA	100.50	24.00	102.67	16.33
SJO-142-5813	M	27.00	NA	28.00	NA	NA	29.00	NA	NA	NA	NA	NA	NA	NA
SJO-142-5814	F	25.67	NA	30.33	35.67	38.00	NA	NA	NA	NA	106.33	NA	100.50	16.00
SJO-142-5815	F	NA	NA	NA	NA	NA	NA							
SJO-142-5818	M	NA	NA	32.33	NA	36.33	NA	NA	NA	NA	NA	NA	NA	NA
SJO-142-5819	F	NA	NA	NA	NA	NA	NA							
SJO-142-5820	M	NA	61.00	32.00	35.67	40.00	NA	NA	NA	NA	102.67	26.00	101.00	15.67
SJO-142-5822	F	NA	68.33	NA	NA	NA	NA	NA	NA	NA	NA	NA	NA	NA
SJO-142-5823	F	NA	NA	NA	NA	104.00	17.50							

Specimen ID	Sex	EKB	DKS	IML	XML	WMH	GLS	STB	FRC	FRS	FRF	PAC	PAS	PAF
SJO-68-5827	M	NA	NA	NA	NA	26.67	3.00	108.67	112.33	21.00	57.00	109.00	22.67	53.50
SJO-68-6472	M	90.67	14.00	34.67	53.00	23.00	4.00	114.33	113.33	21.33	51.50	117.00	26.67	NA
SJO-56-7015	M	NA	NA	NA	NA	21.50	3.00	120.50	109.33	19.00	43.50	103.33	25.00	NA
SJO-68-7285	M	90.50	NA	46.33	58.00	24.33	3.00	125.00	106.50	23.33	48.00	114.67	28.33	52.00
SJO-68-7567	F	96.00	9.00	42.33	59.50	22.67	3.00	117.33	109.67	29.00	44.00	120.00	31.67	57.50
SJO-68-7569	M	91.00	NA	34.33	48.00	21.33	NA	114.67	109.33	23.00	45.67	107.33	23.00	53.67
SJO-68-72327	F	89.00	14.00	35.50	52.33	24.67	3.00	116.67	116.33	25.33	52.50	113.33	24.67	61.33
SJO-142-5661	M	NA	NA	NA	NA	NA	4.00	119.33	122.50	27.50	NA	124.50	25.50	NA
SJO-142-5666	F	NA	NA	NA	NA	25.00	NA	110.33	NA	NA	NA	120.00	NA	65.00
SJO-142-5668	M	NA	NA	NA	NA	27.50	NA	106.00	119.00	25.00	50.50	NA	38.50	62.00
SJO-142-5675	M	NA	NA	NA	51.00	25.00	1.00	110.50	110.50	23.00	53.50	117.50	26.00	63.00
SJO-142-5676	M	96.67	19.67	NA	NA	23.67	NA	119.00	116.33	29.33	51.00	110.33	22.67	NA
SJO-142-5677	M	NA	NA	NA	NA	NA	7.00	104.00	117.00	24.50	48.00	113.50	33.00	47.00
SJO-142-5678	M	92.00	19.67	36.00	51.00	21.33	2.00	122.67	118.67	27.00	NA	119.00	NA	64.00
SJO-142-5679	M	90.00	12.00	41.00	54.00	27.00	2.00	126.00	113.00	32.00	40.00	114.00	40.00	60.00
SJO-142-5800	F	NA	NA	NA	NA	28.50	NA	NA	NA	NA	NA	NA	NA	NA
SJO-142-5801	M	NA	NA	NA	NA	NA	4.00	112.00	119.33	26.00	55.50	113.50	24.50	NA
SJO-142-5806	M	NA	NA	NA	NA	NA	7.00	114.33	126.67	27.50	NA	120.67	NA	NA
SJO-142-5808	F	NA	NA	46.00	60.67	27.00	5.00	136.50	128.33	28.00	53.33	115.67	30.33	59.50
SJO-142-5810	F	94.67	14.33	38.00	50.67	26.50	5.00	118.33	110.33	NA	48.00	122.33	31.00	57.33
SJO-142-5813	M	NA	NA	NA	NA	24.00	4.00	116.00	117.50	22.00	NA	119.00	25.00	65.50
SJO-142-5814	F	95.00	15.67	NA	NA	26.00	3.00	117.00	106.00	21.00	43.00	117.50	25.50	NA
SJO-142-5815	F	NA	NA	NA	NA	NA	NA	112.00	NA	NA	NA	117.00	29.00	NA
SJO-142-5818	M	NA	NA	36.33	NA	24.00	3.00	117.00	109.00	NA	45.50	105.00	21.33	58.67
SJO-142-5819	F	NA	NA	NA	NA	NA	4.00	116.67	111.33	21.00	50.33	115.00	25.00	56.00
SJO-142-5820	M	95.00	15.33	NA	NA	21.00	3.00	106.00	114.33	26.00	54.33	124.00	29.33	60.67
SJO-142-5822	F	NA	NA	NA	NA	NA	NA	NA	NA	NA	NA	108.33	18.50	57.50
SJO-142-5823	F	NA	NA	NA	NA	NA	3.00	117.00	112.00	22.00	50.00	99.00	21.67	46.50

Specimen ID	Sex	OCC	OCS	OCF	FOL	NAR	SSR	PRR	DKR	ZOR	FMR	EKR	ZMR	AVR
SJO-68-5827	M	103.00	30.67	54.67	44.50	NA	NA	NA	NA	NA	NA	NA	NA	NA
SJO-68-6472	M	101.00	27.00	42.00	39.33	85.33	85.67	95.33	70.67	72.33	73.33	65.33	67.33	77.33
SJO-56-7015	M	NA	NA	NA	NA	NA	NA	NA	NA	NA	NA	NA	NA	NA
SJO-68-7285	M	102.33	NA	NA	NA	86.67	97.50	103.50	75.67	84.50	73.00	78.50	79.00	85.00
SJO-68-7567	F	88.00	32.00	33.00	35.00	96.00	105.00	111.67	84.00	88.00	79.67	82.67	86.33	88.67
SJO-68-7569	M	105.67	28.33	49.33	37.33	84.33	89.67	94.33	72.67	73.00	72.00	68.67	69.33	78.67
SJO-68-72327	F	102.67	28.67	51.33	36.00	92.33	91.67	99.00	80.67	78.67	75.33	72.00	69.00	75.33
SJO-142-5661	M	108.33	28.67	54.67	NA	93.67	NA	NA	86.00	NA	NA	70.00	68.67	82.67
SJO-142-5666	F	NA	NA	NA	NA	NA	NA	NA	NA	NA	NA	NA	NA	NA
SJO-142-5668	M	82.00	17.00	26.50	42.50	101.00	NA	NA	NA	NA	NA	NA	NA	NA
SJO-142-5675	M	NA	NA	NA	NA	92.00	96.00	101.00	85.00	81.00	73.50	71.50	79.50	90.00
SJO-142-5676	M	103.67	27.33	47.67	39.33	88.33	93.00	NA	84.33	79.33	81.00	75.33	75.00	82.00
SJO-142-5677	M	NA	NA	NA	NA	100.33	NA	NA	NA	NA	81.67	NA	NA	NA
SJO-142-5678	M	107.67	29.67	52.67	40.33	94.00	95.00	100.33	85.67	78.00	76.33	72.33	72.67	NA
SJO-142-5679	M	NA	NA	NA	NA	88.67	100.00	111.00	83.00	86.00	71.00	79.00	81.00	91.50
SJO-142-5800	F	NA	NA	NA	NA	NA	NA	NA	NA	NA	NA	NA	NA	NA
SJO-142-5801	M	NA	NA	NA	NA	NA	NA	NA	NA	NA	NA	NA	NA	NA
SJO-142-5806	M	NA	NA	NA	NA	97.33	NA	NA	NA	NA	84.00	NA	NA	NA
SJO-142-5808	F	97.50	31.50	57.50	NA	92.00	NA	NA	NA	NA	NA	NA	NA	NA
SJO-142-5810	F	102.33	31.33	53.00	39.33	89.00	101.33	111.33	82.67	85.67	72.33	80.00	81.67	89.50
SJO-142-5813	M	NA	NA	NA	NA	NA	NA	NA	NA	NA	NA	NA	NA	NA
SJO-142-5814	F	103.67	34.50	52.50	NA	90.00	91.00	102.67	80.33	79.67	76.33	73.67	77.00	88.00
SJO-142-5815	F	104.00	30.00	NA	NA	NA	NA	NA	NA	NA	NA	NA	NA	NA
SJO-142-5818	M	103.67	39.67	46.50	NA	94.67	NA	NA	85.67	NA	77.00	76.00	72.67	NA
SJO-142-5819	F	NA	NA	NA	NA	NA	NA	NA	NA	NA	NA	NA	NA	NA
SJO-142-5820	M	98.00	27.67	42.33	39.67	NA	NA	NA	NA	NA	NA	NA	NA	NA
SJO-142-5822	F	NA	NA	NA	NA	NA	NA	NA	NA	NA	73.33	NA	NA	NA
SJO-142-5823	F	NA	NA	NA	NA	94.00	NA	NA	NA	NA	79.00	NA	NA	NA

Specimen ID	Sex	BRR	VRR	LAR	OSR	BAR	NAA	PRA	BAA	NBA	BBA	BRA	SSA	NFA
SJO-68-5827	M	NA	NA	NA	NA	NA	65	75.5	40	82	50.5	47.5	NA	NA
SJO-68-6472	M	119.67	126.00	111.33	48.33	24.00	65.33	76.33	38.67	85	52	43.33	138	146
SJO-56-7015	M	NA	NA	NA	NA	NA	NA	NA	NA	NA	NA	NA	NA	NA
SJO-68-7285	M	117.00	121.00	102.50	47.67	NA	68.67	74.33	37	86	49	45	132	146.7
SJO-68-7567	F	110.00	117.33	92.33	47.00	NA	73	71.33	36	77	52.33	50.33	133.7	141.3
SJO-68-7569	M	118.33	124.67	111.33	45.67	NA	67	74.67	38.33	86	51	43	132.3	148.3
SJO-68-72327	F	124.33	126.33	108.00	44.00	19.67	66	76.33	37.67	82	53.33	45	130	143.3
SJO-142-5661	M	133.00	133.67	113.67	46.67	NA								
SJO-142-5666	F	120.33	124.50	109.00	NA									
SJO-142-5668	M	127.00	132.50	103.00	47.50	15.00	NA	NA	NA	78	55	47	NA	NA
SJO-142-5675	M	118.00	121.50	105.00	NA	132	138.7							
SJO-142-5676	M	122.67	125.00	108.67	46.67	17.33	NA	NA	NA	81.67	55.33	43	138	156
SJO-142-5677	M	117.00	131.50	104.67	NA									
SJO-142-5678	M	127.00	132.00	115.67	49.67	16.33	67	74.33	38.67	79.33	54.67	46	128.3	145.7
SJO-142-5679	M	110.00	117.00	99.00	NA	133	146							
SJO-142-5800	F	NA	NA	NA	NA	NA	NA	NA	NA	NA	NA	NA	NA	NA
SJO-142-5801	M	NA	NA	NA	NA	NA	NA	NA	NA	NA	NA	NA	NA	NA
SJO-142-5806	M	127.50	131.50	110.00	NA									
SJO-142-5808	F	129.00	134.50	101.33	NA	NA	NA	NA	NA	84.33	54.33	41.67	NA	NA
SJO-142-5810	F	123.00	129.33	102.67	48.67	31.33	74	68.67	37	91	45.33	41	129	144
SJO-142-5813	M	NA	NA	NA	NA	NA	NA	NA	NA	NA	NA	NA	NA	NA
SJO-142-5814	F	116.33	121.00	107.00	53.00	NA	141.3	144.5						
SJO-142-5815	F	121.00	125.67	108.00	48.00	NA								
SJO-142-5818	M	112.67	113.67	94.33	48.33	NA								
SJO-142-5819	F	NA	NA	NA	NA	NA	NA	NA	NA	79.33	49.33	51.33	NA	NA
SJO-142-5820	M	NA	NA	NA	NA	NA	65.33	75	39.67	83.67	51	45.33	126	145.7
SJO-142-5822	F	121.67	122.50	109.67	NA									
SJO-142-5823	F	118.33	125.33	106.33	NA	142.5								

Specimen ID	Sex	DKA	NDA	SIA	FRA	PAA	OCA	RFA	RPA	ROA	BSA	SBA	SLA	TBA
SJO-68-5827	M	NA	NA	NA	139	134.7	118.3	NA						
SJO-68-6472	M	134	NA	NA	138.7	130.7	122.7	64.67	61	64.67	171	99	89	136.7
SJO-56-7015	M	NA	NA	120.5	141.3	128.5	NA							
SJO-68-7285	M	138	114	132.5	132.7	NA	107	63.33	63	76	179.5	102.5	88.67	129
SJO-68-7567	F	149	114.5	163	124	122.5	107.5	63.67	72	69.67	163.7	99	91	142.5
SJO-68-7569	M	147	NA	114.5	133.3	133.3	123.3	62.67	55.67	71	172.7	102.3	89.33	139
SJO-68-72327	F	134.7	85	102	132.7	132	123	63	58	71	167	99	92.33	143.7
SJO-142-5661	M	NA	NA	NA	131.5	135.5	125.3	63	60	72	NA	95.5	91	NA
SJO-142-5666	F	NA	NA	NA	NA	131	NA	NA	63	NA	NA	NA	NA	NA
SJO-142-5668	M	NA	NA	NA	133.5	125	131	62	80.5	51	NA	91	84	NA
SJO-142-5675	M	NA	116	NA	135	131.5	NA	62	63	NA	NA	100	NA	NA
SJO-142-5676	M	122.3	NA	NA	126	135	124.3	64.67	56.67	71	NA	98.67	93.33	149.3
SJO-142-5677	M	NA	NA	NA	133.5	118.5	NA	63.67	62	NA	NA	102.7	NA	NA
SJO-142-5678	M	122	105.7	107.3	130.3	132	122.3	63	58.33	68	156.7	100.7	90.67	152
SJO-142-5679	M	133	140	151	115	124	NA	67	68	NA	NA	99	NA	NA
SJO-142-5800	F	NA												
SJO-142-5801	M	NA	NA	NA	133	134	NA							
SJO-142-5806	M	NA	NA	NA	131.5	135	NA	66.5	60	NA	NA	98	NA	NA
SJO-142-5808	F	NA	NA	NA	131.7	125.3	113	68.67	59.67	NA	NA	90.33	NA	140.5
SJO-142-5810	F	137	129	172	137	127	116.3	60	66	75.5	178.5	95.67	91.75	128.3
SJO-142-5813	M	NA	NA	NA	138	133.5	NA							
SJO-142-5814	F	131.3	NA	NA	137	132.3	113	58.67	64.67	71.67	NA	102	90.67	NA
SJO-142-5815	F	NA	NA	NA	NA	128.3	118.5	NA	61	70.67	NA	NA	91	NA
SJO-142-5818	M	NA	NA	NA	145	138.5	104.7	63	60.33	87	NA	102	96.33	NA
SJO-142-5819	F	NA	NA	NA	138	133	NA							
SJO-142-5820	M	135	NA	NA	131	129.3	120.3	NA						
SJO-142-5822	F	NA	NA	NA	NA	142	NA	NA	55.33	NA	NA	NA	NA	NA
SJO-142-5823	F	NA	NA	NA	135.3	132	NA	63	52	NA	NA	106	NA	NA

Specimen ID	Sex	LBI	LBI2	UFI	NLI	CRM	FFA	TFI*
SJO-68-5827	M	73.38	74.32	NA	NA	154.9	147	NA
SJO-68-6472	M	75.55	76.82	49.87	51.8	153.9	150.3	36.68
SJO-56-7015	M	NA						
SJO-68-7285	M	79.71	80.59	42.99	56.34	157.7	154.7	32.13
SJO-68-7567	F	80.49	81.64	NA	54.3	159	150	NA
SJO-68-7569	M	77.06	77.5	50.41	49.3	149.8	153	38.48
SJO-68-72327	F	NA	78.91	50.26	48.59	NA	148	36.98
SJO-142-5661	M	77.52	79.06	NA	NA	NA	NA	NA
SJO-142-5666	F	NA						
SJO-142-5668	M	72.86	75.13	NA	NA	162	NA	NA
SJO-142-5675	M	NA	NA	45.98	60	NA	NA	34.48
SJO-142-5676	M	78.52	80.15	NA	60.14	153.7	NA	NA
SJO-142-5677	M	NA						
SJO-142-5678	M	78.25	79.08	49.03	46.15	160.6	146.3	37.86
SJO-142-5679	M	NA	NA	51.85	54.17	NA	NA	35.56
SJO-142-5800	F	NA						
SJO-142-5801	M	NA						
SJO-142-5806	M	NA						
SJO-142-5808	F	93.87	NA	NA	NA	168.2	NA	NA
SJO-142-5810	F	80.11	81.44	47.1	59.69	160.9	165	31.16
SJO-142-5813	M	NA	NA	NA	49.09	NA	NA	NA
SJO-142-5814	F	75.63	77.08	NA	51.68	NA	NA	NA
SJO-142-5815	F	72.64	NA	NA	NA	NA	NA	NA
SJO-142-5818	M	78.42	78.7	NA	NA	NA	NA	NA
SJO-142-5819	F	75.77	76.77	NA	NA	159.6	NA	NA
SJO-142-5820	M	NA	NA	NA	NA	NA	149	NA
SJO-142-5822	F	NA						
SJO-142-5823	F	NA						

#### Appendix 4. Cranial measurements included in correlation matrices.

Region*	Measure	Description
B	ASB	Breadth of occipital bone.
N	AUB	Breadth of cranial vault at root of the zygomatic process (minimum external breadth of zygomatic processes).
B	BAR	Relative degree of projection of basion from the transmeatal axis (ears).
N	BRR	Relative degree of projection of bregma from the transmeatal axis (ears).
F	DKB	Width of distance between the medial sides of the orbital margins.
F	FMB	Upper facial breadth (at orbital region).
N	FRA	Angulation of frontal bone along the anteroposterior axis. Higher angle reflects a flatter frontal bone (external profile).
N	FRC	Antero-posterior length of frontal bone.
N	FRS	Maximum curvature/prominence of the frontal bone.
N	GLS	Glabellar projection.
F	JUB	Breadth of cheek bones.
F	MAB	Maximum palate breadth.
N	MDH	Mastoid height.
F	NAR	Relative degree of projection of nasion from the transmeatal axis (ears).
F	NLB	Maximum breadth of nasal aperture.
F	NLH	Average height of nasal aperture.
F	NPH	Height of upper portion of face from nasion to prosthion (top of nasal bones to the tip of the maxilla).
F	OBB	Breadth of orbit.
F	OBH	Height of orbit.
B	OCA	Angulation of occipital bone along anteroposterior axis. The larger the angle, the flatter the occipital bone along the sagittal plane.
B	OCC	Antero-posterior length of the occipital bone.
N	PAA	Angulation of parietal bones along anteroposterior axis. A larger angle reflects flatter parietal bones along the sagittal taken at the sagittal suture.
N	PAC	Antero-posterior length of parietal bones.
F	PRR	Relative degree of projection of prosthion from the transmeatal axis (ears).
F	SSS	Projection of the face below the nose at subspinale.
N	STB	Breadth of the frontal bone at the origin of the temporal muscles.
F	WMH	Cheek height.
F	WNB	Minimum breadth of nasal bones.
N	XCB	Maximum breadth of the cranial vault.
N	XFB	Maximum breadth of anterior portion of cranial vault.
F	XML	Maximum cheek length.
F	ZMB	Breadth of midface.
F	ZMR	Relative degree of projection of the anterior cheekbones to the
F	ZYB	Maximum breadth of face at cheek bones.

All measurements follow Howells (1973, 1995) definitions. \*Cranial region abbreviations are as follows: F = facial skeleton, B = basicranium, N = neurocranium.

Appendix 5. Early Period Native Californian crania. (All in photo were measured for this study.)



Appendix 5.(continued)



Supplementary table 1. Measurement averages for validation study.\*

Specimen	—	gol	nol	bnl	bbh	xcb	xfb	zyb	aub	asb	nph	jub	fmb	fol	pac
SJO-68-7581	Scan					142.15	120.83					114.67	94.16		111.68
	Calipers					143.25	123.25					116.75	93.16		110.07
SJO-68-7582	Scan			109.64	150.49			147.02	129.73		76.49				104.02
	Calipers			110.25	151.25			147.75	131.25		78.05				104.88
SJO-68-7586	Scan				145.65			124.77				118.54	101.67		108.68
	Calipers				146.25			125.80				120.00	100.25		110.33
SJO-68-7590	Scan			100.84		132.20		132.92	116.02			117.43	99.12		109.71
	Calipers			99.80		133.80		134.25	117.25			115.49	97.75		112.50
SJO-68-7593	Scan				142.17		114.15	129.92	119.42		65.89		98.83	39.13	114.08
	Calipers				141.25		115.25	131.00	120.25		64.25		96.03	38.72	111.92
SJO-68-7596	Scan					145.33	119.64				71.71		105.24	38.42	
	Calipers					146.75	120.25				71.72		102.19	37.60	
SJO-68-7597	Scan					140.28	114.25	142.34			64.62	124.17	100.52		
	Calipers					141.25	113.25	144.25			62.75	126.25	98.14		
SJO-68-7598	Scan					142.26	118.51	132.26			64.41	114.93			107.42
	Calipers					143.50	119.25	133.25			64.86	114.90			107.00
SJO-68-7600	Scan	182.83	181.20			140.92	116.41	134.20	121.69	106.80	65.96	116.11	96.09		101.74
	Calipers	182.25	179.15			141.25	115.25	135.00	123.75	104.96	65.75	115.50	95.75		99.75
SJO-68-7601	Scan	185.53	182.44		142.15	147.53	118.26	150.02	136.41	116.23	73.11	127.94	109.47	45.23	102.44
	Calipers	185.75	181.75		143.50	148.50	118.00	150.50	137.50	116.00	72.98	128.83	109.50	44.40	104.22
SJO-68-7603	Scan					149.26	127.03	146.74			76.16	126.14	112.15		117.07
	Calipers					151.25	126.25	148.50			76.00	126.66	111.50		116.50

All measurements follow Howells definitions (1973) and are expressed in mm.

Supplementary table 2. Absolute error (AE) and absolute percentage error (APE) comparing measuring techniques.\*

Measurements	Measuring technique		AE	APE
	Scan	Calipers		
	Mean	Mean		
gol	184.18	184.00	0.18	0.10%
nol	181.82	180.45	1.37	0.76%
bnl	105.24	105.03	0.22	0.21%
bbh	145.12	145.56	0.44	0.31%
xcb	142.49	143.69	1.20	0.84%
xfb	118.64	118.84	0.21	0.18%
zyb	139.43	140.56	1.13	0.81%
aub	124.67	125.97	1.29	1.03%
asb	111.51	110.48	1.03	0.94%
nph	69.79	69.54	0.25	0.36%
jub	119.99	120.55	0.56	0.46%
fmf	101.92	100.47	1.44	0.44%
fol	40.92	40.24	0.69	1.70%
pac	108.18	108.75	0.57	0.53%
Average	120.99	121.01	0.76	0.69%

\*Following Fourie et al. 2001, we determined the absolute difference between the mean caliper measurements and the mean scan measurements for each linear measurement to calculate average measurement error (AE). We then calculated average percentage error (APE) as AE divided by the mean caliper measurement and multiplied by 100. All measurements follow Howells definitions (1973) and are expressed in mm.